



---

Publicly Accessible Penn Dissertations

---

2022

## Central Control Of Pain And Inflammation Through A Hunger Circuit

Michelle Lynne Klima  
*University of Pennsylvania*

Follow this and additional works at: <https://repository.upenn.edu/edissertations>

 Part of the [Allergy and Immunology Commons](#), [Biology Commons](#), [Immunology and Infectious Disease Commons](#), [Medical Immunology Commons](#), and the [Neuroscience and Neurobiology Commons](#)

---

### Recommended Citation

Klima, Michelle Lynne, "Central Control Of Pain And Inflammation Through A Hunger Circuit" (2022). *Publicly Accessible Penn Dissertations*. 5563.  
<https://repository.upenn.edu/edissertations/5563>

This paper is posted at ScholarlyCommons. <https://repository.upenn.edu/edissertations/5563>  
For more information, please contact [repository@pobox.upenn.edu](mailto:repository@pobox.upenn.edu).

---

# Central Control Of Pain And Inflammation Through A Hunger Circuit

## Abstract

Homeostasis is established through bidirectional communication between the periphery and the central nervous system. To maintain homeostasis, some biological drives can become prioritized over others. This changing balance between biological drives encourages peak performance and survival. However, when homeostasis is disturbed, chronic inflammatory diseases such as obesity, chronic pain, and arthritis can arise. We became interested in understanding if competing biological drives could be leveraged for therapeutic purposes. Food restriction inhibits inflammation; therefore, we explored how hunger and feeding neural circuits affect responses to noxious agents. Our first study investigated the role of hunger to alleviate pain behavior. We found that hunger significantly reduces time spent licking during the inflammatory phase of a formalin pain assay but leaves intact pain responses to acute threats. We next evaluated if hypothalamic hunger neurons are involved in this behavioral change. Stimulation of agouti-related protein expressing (AgRP) neurons significantly reduced formalin pain behavior. To determine the central nodes that mediate this effect, we systematically screened AgRP neuron projections for their ability to suppress pain. Only AgRP neurons projecting to the hindbrain parabrachial nucleus was able to reduce inflammatory pain behavior. Our second study investigated the role of hunger to influence inflammatory responses of an injury site. Using two models of localized inflammation, we found that food deprivation robustly reduces inflammation, pro-inflammatory cytokine levels, and associated temperature increases induced by injection of noxious stimuli [complete Freund's adjuvant (CFA) or formalin]. Activation of AgRP neurons recapitulated the effect of food deprivation on inflammation. We then evaluated the role of each AgRP axonal target structure to reduce inflammation. Interestingly, stimulation of AgRP neurons that project to the paraventricular nucleus of the hypothalamus or the parabrachial nucleus were sufficient to reduce CFA-induced inflammation. Finally, we identified the vagus nerve as a key pathway for the anti-inflammatory effect of hunger. We propose that hunger, through AgRP neurons, inhibits pro-inflammatory responses from the central nervous system and changes the output of efferent vagal fibers. This body of work reveals a central node for the reduction of pain and inflammation, highlighting a novel role for hypothalamic circuits to influence injury responses.

## Degree Type

Dissertation

## Degree Name

Doctor of Philosophy (PhD)

## Graduate Group

Neuroscience

## First Advisor

John N. Betley

## Keywords

AgRP, CFA, Formalin, Hunger, Inflammation, Pain

## Subject Categories

Allergy and Immunology | Biology | Immunology and Infectious Disease | Medical Immunology | Neuroscience and Neurobiology

**CENTRAL CONTROL OF PAIN AND INFLAMMATION THROUGH A HUNGER CIRCUIT**

Michelle L. Klima

A DISSERTATION

in

Neuroscience

Presented to the Faculties of the University of Pennsylvania

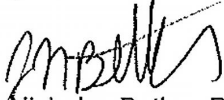
in

Partial Fulfillment of the Requirements for the

Degree of Doctor of Philosophy

2022

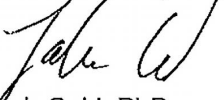
Supervisor of Dissertation



J. Nicholas Betley, PhD

Assistant Professor of Biology, University of Pennsylvania

Graduate Group Chairperson



Josh Gold, PhD

Professor of Neuroscience, University of Pennsylvania

Dissertation Committee

Marc Fuccillo, MD, PhD; Assistant Professor of Neuroscience, University of Pennsylvania

Ishmail Abdus-Saboor, PhD; Assistant Professor of Biological Sciences, Columbia University

Igor Brodsky, AB, Ph.D; Associate Professor of Microbiology, University of Pennsylvania

Christoph Thaiss, PhD; Assistant Professor of Microbiology, University of Pennsylvania

## ACKNOWLEDGMENT

I would like to thank Dr. Nick Betley, my advisor, and Dr. Amber Alhadeff for their support and mentorship throughout my graduate work. They taught me to persevere through years of negative data and develop new hypotheses to address unsolved questions. These skills will translate to any challenge I face in my next career and beyond. Thank you to my committee members: Marc Fucillo, Ishmail Abdus-Saboor, Igor Brodsky, and Christoph Thaiss; who have provided me with critical feedback and incredible support throughout the development and completion of my dissertation. I'd also like to thank the Betley lab members (past and present). Our lab has always had a fun and collaborative environment because of the incredible people who have joined throughout the years. I especially want to thank Kayla Kruger for being my right-hand researcher for most of my graduate work. I could not have measured so many mouse paws without your company!

I would like to thank my family for their unconditional love and support. My parents and brother have been my biggest cheerleaders for all my academic and personal pursuits. I could not be more grateful for their encouragement. My fiancé, Grant Grothusen, has been my rock throughout the final years of my PhD. Thank you for proofreading all my written materials and listening to me talk about mice for the last 4 years. I am incredibly grateful for the life we have created and excited for what comes next.

## ABSTRACT

### CENTRAL CONTROL OF PAIN AND INFLAMMATION THROUGH A HUNGER CIRCUIT

Michelle L. Klima

J. Nicholas Betley

Homeostasis is established through bidirectional communication between the periphery and the central nervous system. To maintain homeostasis, some biological drives can become prioritized over others. This changing balance between biological drives encourages peak performance and survival. However, when homeostasis is disturbed, chronic inflammatory diseases such as obesity, chronic pain, and arthritis can arise. We became interested in understanding if competing biological drives could be leveraged for therapeutic purposes. Food restriction inhibits inflammation; therefore, we explored how hunger and feeding neural circuits affect responses to noxious agents. Our first study investigated the role of hunger to alleviate pain behavior. We found that hunger significantly reduces time spent licking during the inflammatory phase of a formalin pain assay but leaves intact pain responses to acute threats. We next evaluated if hypothalamic hunger neurons are involved in this behavioral change. Stimulation of agouti-related protein expressing (AgRP) neurons significantly reduced formalin pain behavior. To determine the central nodes that mediate this effect, we systematically screened AgRP neuron projections for their ability to suppress pain. Only AgRP neurons projecting to the hindbrain parabrachial nucleus was able to reduce inflammatory pain behavior. Our second study investigated the role of hunger to influence inflammatory responses of an injury site. Using two models of localized inflammation, we found that food deprivation robustly reduces inflammation, pro-inflammatory cytokine levels, and associated temperature increases induced by injection of noxious stimuli [complete Freund's adjuvant (CFA) or formalin]. Activation of AgRP neurons recapitulated the effect of food deprivation on inflammation. We then evaluated the role of each AgRP axonal target structure to reduce inflammation. Interestingly, stimulation of AgRP neurons that project to the paraventricular nucleus of the hypothalamus or the parabrachial nucleus were sufficient to reduce CFA-induced

inflammation. Finally, we identified the vagus nerve as a key pathway for the anti-inflammatory effect of hunger. We propose that hunger, through AgRP neurons, inhibits pro-inflammatory responses from the central nervous system and changes the output of efferent vagal fibers. This body of work reveals a central node for the reduction of pain and inflammation, highlighting a novel role for hypothalamic circuits to influence injury responses.

## TABLE OF CONTENTS

<b>ACKNOWLEDGMENT .....</b>	<b>II</b>
<b>ABSTRACT .....</b>	<b>III</b>
<b>LIST OF TABLES.....</b>	<b>VIII</b>
<b>LIST OF ILLUSTRATIONS.....</b>	<b>IX</b>
<b>LIST OF ABBREVIATIONS.....</b>	<b>XII</b>
<b>CHAPTER 1: INTRODUCTION.....</b>	<b>1</b>
<b>The central nervous system contributes to the maintenance of physiological needs including hunger.....</b>	<b>2</b>
<b>Interoceptive cues can change behavior and physiology based on environmental and physical needs of the animal.....</b>	<b>3</b>
<b>Feeding behavior is maintained within the arcuate nucleus of the hypothalamus through a balance of AgRP and POMC activity.....</b>	<b>4</b>
<b>AgRP neuron activation, naturally by deprivation or experimentally, induces feeding behavior.....</b>	<b>5</b>
<b>AgRP neurons can initiate feeding through the deprioritization of other behaviors and biological drives.....</b>	<b>7</b>
<b>Frequent food restriction can improve health and longevity in many different species.....</b>	<b>8</b>
<b>Food restriction reduces inflammation likely contributing to the benefits of caloric deficit on longevity.....</b>	<b>9</b>
<b>CHAPTER 2: HUNGER REDUCES THE AFFECTIVE AND BEHAVIORAL COMPONENTS OF INFLAMMATORY PAIN.....</b>	<b>16</b>
<b>Summary.....</b>	<b>18</b>
<b>Introduction.....</b>	<b>19</b>
<b>Results .....</b>	<b>20</b>
Hunger Selectively Attenuates Responses to Inflammatory Pain.....	20
AgRP Neurons Specifically Inhibit Inflammatory Pain.....	22
AgRP→PBN Neurons Specifically Inhibit Inflammatory Pain.....	23
NPY Signaling in the lateral PBN Inhibits Inflammatory Pain.....	24
Acute Pain Reduces Food Seeking and Neural Activity in Hunger Circuits.....	25
<b>Discussion.....</b>	<b>26</b>

Bidirectional Behavioral Interaction Between Hunger and Pain.....	26
Neural and Molecular Mechanisms for the Inhibition of Pain.....	28
Conclusion .....	30
<b>Acknowledgments .....</b>	<b>54</b>
<b>References.....</b>	<b>55</b>
<b>STAR Methods.....</b>	<b>59</b>
<b>CHAPTER 3: HUNGER HAS A POTENT AND RELIABLE ANTI-INFLAMMATORY EFFECT ON INJURY-INDUCED INFLAMMATION. ....</b>	<b>74</b>
<b>Hunger reduces injury-induced inflammation.....</b>	<b>76</b>
<b>Hunger is a potent anti-inflammatory mechanism regardless of sex, age or weight.....</b>	<b>77</b>
<b>Hunger has a complex relationship with inflammation that cannot be recapitulated pharmacologically.....</b>	<b>78</b>
Glucocorticoids.....	79
Substance P.....	79
Opioids.....	80
Oxytocin .....	80
Leptin .....	81
Ghrelin.....	81
Serotonin.....	82
Microbiome.....	82
<b>Discussion.....</b>	<b>82</b>
<b>CHAPTER 4: AGOUTI-RELATED PROTEIN EXPRESSING NEURONS PROJECTING TO THE PARAVENTRICULAR HYPOTHALAMUS AND PARABRACHIAL NUCLEUS CAN REDUCE INJURY-INDUCED INFLAMMATION. ....</b>	<b>91</b>
<b>Activation of AgRP neurons reduces inflammation. ....</b>	<b>92</b>
<b>AgRP→PVH and AgRP→PBN subpopulations reduce inflammation. ....</b>	<b>93</b>
<b>No tested subpopulations within the pvh and pbn were able to reduce paw inflammation.</b>	<b>94</b>
<b>Discussion.....</b>	<b>95</b>
<b>CHAPTER 5: HUNGER USES THE EFFERENT PATHWAY OF THE VAGUS NERVE TO REDUCE PERIPHERAL INFLAMMATION.....</b>	<b>105</b>
<b>Subdiaphragmatic vagotomy disrupts the anti-inflammatory effect of hunger.....</b>	<b>106</b>
<b>Pharmacological blockade of all vagal output pathways disrupts the anti-inflammatory effect of hunger.....</b>	<b>107</b>
<b>Hunger influences CFA-induced inflammation through the efferent vagus nerve.....</b>	<b>108</b>

<b>Discussion</b> .....	<b>110</b>
<b>CHAPTER 6: METHODS FOR INFLAMMATION EXPERIMENTS</b> .....	<b>116</b>
<b>Collaborators</b> .....	<b>116</b>
<b>Acknowledgements</b> .....	<b>116</b>
<b>STAR Methods</b> .....	<b>117</b>
<b>CHAPTER 7: GENERAL DISCUSSION</b> .....	<b>135</b>
<b>Why does food deprivation influence pain and peripheral inflammation?</b> .....	<b>135</b>
<b>The insular cortex is poised to be the hub that integrates inflammation and hunger cues to prioritize feeding behaviors in formalin and CFA-models of inflammation.</b> .....	<b>137</b>
<b>Interoception and competing biological drives provide a unique entry point to develop therapeutics for chronic inflammatory diseases.</b> .....	<b>139</b>
<b>APPENDIX A: BRIEF REVIEW OF THE ANATOMY AND FUNCTIONS OF THE PVH</b> .....	<b>143</b>
<b>Anatomy of the PVH</b> .....	<b>143</b>
<b>Stress &amp; inflammation</b> .....	<b>144</b>
<b>Metabolism</b> .....	<b>145</b>
<b>APPENDIX B: BRIEF REVIEW OF THE ANATOMY AND FUNCTION OF THE SUB REGIONS OF THE PBN</b> .....	<b>149</b>
<b>Anatomy of the PBN</b> .....	<b>149</b>
The Medial PBN .....	149
The Kölliker Fuse nucleus.....	150
The Lateral PBN.....	150
<b>Molecular markers</b> .....	<b>151</b>
<b>BIBLIOGRAPHY</b> .....	<b>157</b>

## LIST OF TABLES

### CHAPTER 7

Table 7.1   Summary of key experimental findings to identify the pathway that hunger functions through to reduce inflammatory pain and inflammation. ....	140
---	-----

### APPENDIX B

Table B2.1   Subset of parabrachial nucleus genetic markers. ....	156
---	-----

## LIST OF ILLUSTRATIONS

### CHAPTER 1

Figure 1.1   The central autonomic network is composed of brain regions throughout the brainstem, midbrain, and cortex (adapted from Benarroch, 1993). .....	11
Figure 1.2   Chemogenetic and optogenetic activation of AgRP neurons induces rapid, reversible, and reliable food intake. ....	12
Figure 1.3   AgRP neuron architecture allows for interrogation of individual axon targets for any given behavior (adapted from Betley et al., 2013). ....	14
Figure 1.4   Food restriction can increase longevity in simple organisms and complex animals (adapted from Longo and Mattson, 2014). ....	15

### CHAPTER 2

Figure 2.1   Hunger Attenuates Response to Inflammatory Pain. ....	31
Figure 2.2   Hunger Attenuates Inflammation-Induced Sensitization to Mechanical and Thermal Pain. ....	33
Figure 2.3   Hunger Attenuates Negative Affective Components of Pain. ....	35
Figure 2.4   AgRP Neurons Mediate Suppression of Inflammatory Pain. ....	36
Figure 2.5   AgRP→PBN Neuron Activity Suppresses Inflammatory Pain. ....	38
Figure 2.6   Lateral PBN NPY Signaling Suppresses Inflammatory Pain. ....	40
Figure 2.7   Acute Pain Inhibits Feeding Behavior and Activity in AgRP Neurons. ....	42
Figure 2.S1, Related to Figure 2.1   Anti-Inflammatory and Opiate Drug Administration Reduce Responses to Inflammatory Phase and Thermal Pain, Respectively. ....	44
Figure 2.S2, Related to Figure 2.4   AgRP Neuron Activity Specifically Inhibits Inflammatory Phase Pain Response Without Off-Target Licking Effects. ....	45
Figure 2.S3, Related to Figure 2.4   AgRP→PBN Neurons Selectively Mediate Inflammatory Pain. ....	48
Figure 2.S4, Related to Figure 2.6   Peptidergic NPY signaling in the lateral PBN mediates inflammatory phase pain. ....	49
Figure 2.S5, Related to Figure 2.6   Glutamatergic Neurons in the IPBN Mediate Inflammatory Pain. ....	52
Figure 2.S6, Related to Figure 2.7   Acute Thermal but not Formalin-Induced Pain Suppresses AgRP Neuron Activity. ....	53

### CHAPTER 3

Figure 3.1   Hunger reduces paw inflammation induced by CFA and formalin. ....	84
Figure 3.2   Hunger reduces paw circumference induced by CFA and formalin. ....	85
Figure 3.3   Hunger reduces paw edema and inflammation associated increase in temperature. ....	86
Figure 3.4   Hunger reduces paw inflammation regardless of sex, age, or weight. ....	87
Figure 3.5   Hunger is comparable to non-steroidal anti-inflammatory drugs in reducing CFA-induced inflammation. ....	88
Figure 3.6   Pharmacological interrogation of systems known to influence immune responses failed to change the CFA-induced paw volume in ad libitum or food deprived conditions. ....	89

### CHAPTER 4

Figure 4.1   AgRP neuron activity reduces peripheral paw inflammation. ....	97
Figure 4.2   AgRP activity peaks after 4 hours of food deprivation, however, 18 hours of food deprivation maximally reduces CFA-induced edema. ....	99
Figure 4.3   AgRP→PVH and AgRP→PBN neuron activity suppresses CFA-induced paw inflammation. ....	100
Figure 4.4   Axon targets were confirmed through feeding assays, pain assays, and histology. ....	102
Figure 4.5   Manipulations of PVHOXT and PVHCRH neurons had no effect on CFA-induced paw volume. ....	103
Figure 4.6   Manipulations of PBN populations capable of reducing inflammatory pain had no effect on CFA-induced paw volume. ....	104

### CHAPTER 5

Figure 5.1   Mechanical destruction of both vagal pathways attenuates the suppression of CFA-induced paw inflammation during food deprivation. ....	111
Figure 5.2   Pharmacological blockade of anti-inflammatory vagal outputs attenuates the anti-inflammatory effect of hunger. ....	112
Figure 5.3   The afferent vagal pathway is not required for the anti-inflammatory effect of hunger. ....	114
Figure 5.4   Hunger is likely working through the efferent pathway to reduce inflammation. ....	115

**CHAPTER 7**

Figure 7.1 | AgRP neurons have various effects on behavior and physiology to prioritize food intake..... 141

Figure 7.2 | Proposed circuit for AgRP influence on inflammation through the insular cortex and out of the DMX (adapted from Livneh et al., 2017). ..... 142

**APPENDIX A**

Figure A1.1 | The PVH is composed of multiple subnuclei with varying functions related to autonomic and neuroendocrine systems. .... 146

Figure A1.2 | Examples of satiety inducing molecular markers in the PVH. .... 148

**APPENDIX B**

Figure B2.1 | Anatomy and functions of the parabrachial nucleus..... 153

Figure B2.2 | Examples of molecular markers in the PBN. .... 155

## LIST OF ABBREVIATIONS

5-HT – serotonin  
ACTH – adrenocorticotropin hormone  
AgRP – agouti-related protein expressing neurons  
ARC – arcuate nucleus  
BLA – basal lateral amygdala  
BNST – bed nucleus of the stria terminalis  
Bup – buprenorphine  
CAPS – capsaicin vagotomy  
CCK – cholecystokinin  
CeA – central amygdala  
CFA – complete Freund's adjuvant  
ChAT – choline acetyltransferase  
ChR2 – channelrhodopsin-2  
CNO – clozapine-n-oxide  
Cort – corticosterone  
CRF – corticotropin releasing factor  
CRH – corticotropin-releasing hormone  
DMX – dorsal motor nucleus  
DREADD – designer receptors activated by designer drugs  
GABA – gamma-aminobutyric acid  
HPA – hypothalamic-pituitary-adrenal  
i.p. – intraperitoneal  
LH – lateral hypothalamus  
IPBN – lateral PBN  
MLA – methyllycaconitine  
nAChR – nicotinic acetylcholine receptor  
Nal – naloxone  
NK1R – neurokinin 1 receptor

NPY – neuropeptide Y  
NPY – neuropeptide-y  
NSAID – non-steroidal anti-inflammatory drug  
NTS – nucleus tractus solitarius  
OXT – oxytocin  
PAG – periaqueductal gray  
PBN – parabrachial nucleus  
POMC – pro-opiomelanocortin neurons  
PVH – paraventricular hypothalamus  
PVT – paraventricular thalamus  
SEM – standard error of the mean  
SP – substance P  
TNF $\alpha$  – tumor necrosis factor alpha  
TRPV1 – transient receptor potential cation channel subfamily V member 1  
VGLUT2 – vesicular glutamate transferase 2  
VGX – subdiaphragmatic vagotomy

## CHAPTER 1: INTRODUCTION

Chronic inflammatory diseases pose a huge global health threat according to the World Health Organization. Over 40% of Americans are living with a chronic inflammatory condition and that number is expected to rise over the next 30 years (Pahwa et al., 2020). Chronic inflammatory diseases include a range of etiologies such as cardiovascular disease, allergies, arthritis and joint diseases, and pain diseases. Each type of disease poses its own economic and personal burden for the patient. Current treatments for chronic inflammatory diseases typically involve diet and activity changes as well as medication therapy. However, prognosis for many chronic inflammatory diseases is poor, leaving patients to suffer.

This dissertation focuses on two aspects of chronic inflammatory diseases: pain and inflammation. Pain and inflammation are natural responses to injury and immune threats that are critical for survival. However, both can become maladaptive and lead to chronic inflammatory disease (Pahwa et al., 2020). In 2010, it was estimated that 100 million Americans suffer from chronic pain and spend at least \$560 million dollars in healthcare each year (Gaskin and Pain, 2012). Chronic and maladaptive pain are a public health concern that can be tackled with proper medications; however, the current treatment options are causing other obstacles for their users. The most commonly used drug class for pain management are opioids, which have a very high abuse potential and pose their own threat to public health. In fact, one in four chronic pain patients using opioid treatments is also receiving medical attention for opioid abuse disorder (ASAM, 2016). Prescription opioids are fueling the opioid epidemic in the United States. In 2019, more than 50,000 Americans died from opioid-related use. The high incidence of opioid addiction makes it necessary to reduce the number of opioid prescriptions by finding alternate pain and inflammation management strategies that do not have an abuse potential.

The central nervous system plays a role in all physiological functions rendering it an effective therapeutic target for diseases that affect the whole body. The main goal of the central nervous system is to maintain homeostasis between all biological drives and physiological needs

to ensure survival. Under certain conditions it becomes necessary for one biological drive to be prioritized over another and adjust behavior and physiology accordingly. Using this theory of competing biological drives, we have shown that hunger can outcompete pain and inflammatory responses to an injury. This mechanism may be leveraged as a therapeutic target to manage conditions of chronic pain and inflammation that have been historically difficult to treat.

**The central nervous system contributes to the maintenance of physiological needs including hunger.**

All physiological functions of the body require coordination and communication between organs to create homeostasis for a proper balance between biological drives. The autonomic nervous system is a major homeostatic regulator as it innervates nearly all organs in the body to facilitate the management of many different functions. Typically, autonomic neurons sense biological factors from their target organs and send that signal to the central nervous system for integration; together these two processes are called the central autonomic network. The central nervous system then sends the signal to various brain regions which ultimately transmit a response through motor neurons back to the periphery to maintain whole-body homeostasis (Gibbons, 2019). Brain regions throughout the brainstem, midbrain and cortex contribute to the network including the nucleus tractus solitarius (NTS), the parabrachial nucleus (PBN), the periaqueductal gray (PAG), the hypothalamus, and the insular cortex (Figure 1.1, adapted from Benarroch, 1993). The central autonomic network contributes to pairing physiological needs with emotions, maintaining homeostasis among neuroendocrine and autonomic function, initiating stress responses, and facilitating viscerosensory behaviors such as breathing, circulation and vomiting (Benarroch, 1993). Disorders of these brain regions can cause disturbances in autonomic function. For instance, hypothalamic disorders can cause disruptions of healthy feeding behavior and energy metabolism leading to obesity or anorexic phenotypes (Carmel, 1980). The autonomic control of food intake is of particular relevance for the work outlined in this dissertation.

Food intake and energy expenditure are highly regulated processes to maintain homeostasis between nutrient requirements and energy stores. Despite uncontrollable factors such as food availability, emotions and social environments that influence individual meal sizes, overall energy homeostasis is preserved for each individual (Schwartz et al., 2000). The basic mechanism to maintain energy homeostasis is to balance anabolic and catabolic metabolism. This balance is key to creating appropriate body adiposity through suitable food intake and energy expenditure. Signals from body fat stores and gut hormones integrate in the central nervous system to activate the appropriate metabolic pathway and inhibit competing pathways. Leptin and insulin are adiposity signals released by body fat that directly activate the hypothalamus. When these adiposity signals are at low concentrations in the blood stream, they cause the anabolic pathway to be inhibited yet the catabolic pathway is activated. This creates a body state conducive to restoring fat reserves by reducing energy expenditure and increasing food consumption. Upon the ingestion of food, the digestive tract releases satiation signals that act in the NTS to rebalance the metabolic pathways and determine the appropriate amount of food to consume (Schwartz et al., 2000). Energy homeostasis pits different cell types, hypothalamic nuclei, and brainstem regions against one another to create a dynamic balance dependent on physiological, social, and environmental cues.

**Interoceptive cues can change behavior and physiology based on environmental and physical needs of the animal.**

Interoception is the ability of the body to sense its internal state and adjust physiology or behavior to maintain homeostasis across different biological needs (Quadt et al., 2018, Sherrington, 1906). Interoception requires bidirectional communication between the body and brain with hormones and neuropeptides. There are three main aspects of interoception: afferent signaling, central processing, and efferent signaling. Various receptor types ranging from chemoreceptors to mechanoreceptors detect changes in the periphery (Berntson and Khalsa, 2021). This information is sent to the central nervous system through humoral and neural pathways, especially through the

vagus nerve. These signals are then processed in the brainstem and transduced throughout homeostatic, emotional, and physiological processing centers (Berntson and Khalsa, 2021; Quadt et al., 2018). Ultimately, these signals converge in the cortex to integrate the components and determine appropriate changes in mood, physiology, and behavior to maintain peak performance. The signals for adjustments are then sent back to the body through efferent pathways, including the vagus nerve (Quadt et al., 2018).

The immune system works effectively through interoceptive cues to induce sickness behavior and physiological changes to create a healing environment. The immune system communicates threats to the central nervous system through the vagus nerve. Immune cells and vagal neurons have similar humoral and neuropeptide channels allowing for efficient and immediate communication (Goehler et al., 2000; Quadt et al., 2018). The immune interoceptive cues cause changes to behavior including fatigue and social isolation to reduce bodily harm and infection. Interestingly, immune signals also cause a reduction in consumption behaviors presumably to direct resources to the immune response instead of digestion (Quadt et al., 2018). This is a prime example of an interoceptive cue deprioritizing other biological drives. Immune challenges can minimize the necessity of food and water in order for the body to attend to the most salient need – the infection or injury. Understanding how biological drives out compete each other could be a powerful tool leveraged for management of chronic inflammatory diseases to return the body to homeostasis.

**Feeding behavior is maintained within the arcuate nucleus of the hypothalamus through a balance of AgRP and POMC activity.**

The brain integrates signals from the periphery and external environment to carry out behaviors to ensure survival. Of particular interest during my graduate work is feeding behavior. Feeding is a sophisticated behavior informed by energetic, nutritional, and environmental needs. The arcuate nucleus of the hypothalamus (ARC) has evolved to be especially poised for feeding through two primary cell populations: the anorexigenic pro-opiomelanocortin (POMC) neurons and

the orexigenic agouti related protein expressing (AgRP) neurons. AgRP and POMC neurons receive satiety and hunger signals from the periphery via neural, humoral, and endocrine signaling to influence feeding, energy expenditure and body weight. The two cell populations share inhibitory connections to keep orexigenic and anorexigenic signals in balance with each other. POMC neurons are activated by satiety signals and release alpha-melanocyte-stimulating hormone to activate melanocortin-4 receptors (Mc4r) to reduce food intake and increase energy expenditure. AgRP neurons, conversely, are activated by hunger signals and release AgRP, neuropeptide-Y (NPY), and gamma-Aminobutyric acid (GABA) to increase food intake (Hahn et al., 1998; Horvath et al., 1992, 1997). Both populations project to targets throughout the brain to initiate associated behavioral and physiological changes required to carry out the desired feeding phenotype.

AgRP and POMC neurons are necessary to maintain proper feeding behavior. In fact, ablation of AgRP neurons in adult animals will cause animals to experience irreversible starvation (Gropp et al., 2005; Luquet et al., 2005). Interestingly, this phenotype is not seen when AgRP is ablated during development suggesting there are compensatory mechanism at play during development to ensure feeding and survival (Luquet et al., 2005). Alternatively, ablation of POMC neurons in adult animals causes an increase in food intake and leads to obesity (Gropp et al., 2005). While there is a constant interplay between POMC and AgRP neurons, my thesis work specifically interrogates AgRP neurons.

**AgRP neuron activation, naturally by deprivation or experimentally, induces feeding behavior.**

It has been well established that AgRP neuron activity can be causally linked to food deprivation. AgRP mRNA is significantly higher in the ARC of mice food deprived compared to ad libitum fed controls. Further, co-expression of AgRP mRNA with NPY mRNA increases significantly when animals are food deprived (Hahn et al., 1998). Additionally, deprivation leads AgRP neurons to have more spontaneous neurotransmitter release than in the fed conditions. This increased plasticity suggests that AgRP neurons are more active during deprived states (Yang et al., 2011).

Consistent with the increased plasticity, AgRP neurons also produce more dendritic spines, have increased synaptic transmission, and thus increased excitability during food deprivation (Liu et al., 2011). Taken together these data show that food deprivation activates AgRP neurons.

AgRP neurons are sufficient to reproduce aspects of hunger in the absence of peripheral cues. Activation of AgRP neurons through chemogenetics (Krashes et al., 2011) or optogenetics (Aponte et al., 2011) causes an animal to voraciously eat under ad libitum conditions (Figure 1.2). Krashes et al. (2011) showed that animals expressing the excitatory designer receptors activated by designer drugs (DREADD, HM3D), will eat more chow than controls for at least 4 h after an activation of the synthetic receptors with an injection of clozapine-n-oxide (CNO) (Figure 1.2a). Aponte et al. (2011) also showed that AgRP activation leads to immediate food intake by using photostimulation on AgRP neurons expressing the light sensitive channel channelrhodopsin-2 (ChR2). They further showed that feeding is dependent on acute AgRP activation since there were no long-term feeding changes once the stimulation had ended (Figure 1.2c). Manipulating food intake through AgRP neuron activation is reliable and repeatable as we were able to produce similar food intake measurements with chemogenetic and optogenetic activation (Figure 1.2b, 1.2d). This rapid, reversible, and specific activation provides a model of feeding behavior without the off-target, chronic effects of hunger. Although hunger is a robust, complex body condition that involves multiple systems, we can manipulate a specific pathway to isolate aspects of feeding influenced solely by AgRP neurons.

AgRP neurons ramify to seven areas throughout the brain: bed nucleus of the stria terminalis (BNST), paraventricular hypothalamus (PVH), lateral hypothalamus (LH), paraventricular thalamus (PVT), central amygdala (CeA), PAG, and PBN (Figure 1.3a). Strikingly, AgRP projections have a one-to-one connection meaning there are no collateral axon projections to other targets; each AgRP axon communicates with one single brain region (Betley et al., 2013). This architecture allows for individual projection target activation of AgRP axons to understand functional differences between AgRP projection sites. Optogenetics is a robust tool to test each projection

region's role in a particular behavior. In this approach, optic fibers are placed over each target region in mice expressing ChR2 (Figure 1.3b). Betley et al. (2013) spearheaded this method and evaluated each projection target's role in food intake. They found that only four AgRP target regions induced immediate feeding, while the other three had no effect on feeding (Figure 1.3c). Stimulation of AgRP axon terminals in the BNST, PVH, LH and PVT significantly increased food intake, however the amounts of food consumed was different between each target. Stimulation of AgRP axon terminals in the PAG, PBN, and CeA had no effect on food intake (Betley et al., 2013). This difference in consumption suggests that each target structure plays a different role in encouraging feeding behavior.

**AgRP neurons can initiate feeding through the deprioritization of other behaviors and biological drives.**

It has been hypothesized that AgRP neurons can influence feeding through behavioral mechanisms other than just consumption. Interestingly, AgRP axons interact with structures that compose the central autonomic network (see Figure 1.1 and Figure 1.3a). This intimate connection with autonomic control centers suggests that AgRP neurons are able to influence more than just food intake. In fact, AgRP neurons have been shown to prioritize feeding by deprioritizing other competing need states. Animals have several homeostatic needs that are regulated by behavior to adapt for the current physiological and environmental condition. Some of these behaviors include sleep, hydration, feeding, reproduction, and predator evasion. In certain scenarios, one need state can become more dire than others. For instance, under extreme starvation it can become more important for an animal to risk predation to forage for food. In fact, AgRP neurons have been shown to influence adaptive behavior to reduce anxiety in response to high-risk situations to acquire food (Burnett et al., 2016; Jikomes et al., 2016). AgRP neurons can also deprioritize social interactions, water-seeking behavior, fertility, pain, and sleep (Alhadeff et al., 2018; Burnett et al., 2016; Goldstein et al., 2018; Padilla et al., 2017). Taken together, these data show that AgRP neurons can temper other need states to prioritize feeding.

## **Frequent food restriction can improve health and longevity in many different species.**

Food is essential for survival, however, evolutionarily food was less available than in modern society. Because of this, the body developed in a way to survive when food became scarce. Organs such as the liver and adipose tissue conserve energy from previous meals to enable survival in times with less energy consumption. Further, in fasted states, metabolic, endocrine, and nervous system functions adapt to allow for peak performance ultimately to acquire more food (Mattson et al., 2017). Today, high-caloric foods are readily available, and rates of obesity are rapidly increasing (Rakhra et al., 2020). The typical Western diet is composed of artificial foods high in fat, sugar, and sodium and minimal amounts of fruits and vegetables (Institute of Medicine, 2010). Many chronic inflammatory diseases are believed to be directly related to the excess caloric ingestion, including diabetes, cardiovascular disease, and some cancers (Rakhra et al., 2020). With this disordered eating in mind, changing feeding behavior to match our evolutionary physiology may be a cure for obesity-related diseases.

Food restriction has been recently hailed as a “miracle cure” for improved health and longer lifespan by improving cardiac function and maintaining a healthy body weight. Ultimately this leads to lower incidences of neurological, cardiac, and respiratory diseases, and cancer (Golbidi et al., 2017; Mattson et al., 2017). Recommended fasting diets range from multiple days with no food consumption, to daily caloric restrictions, to restricted feeding in specific hours of the day. Each method of restriction is being tested and validated using clinical and pre-clinical studies, however, rarely are two methods compared in the same study making it impossible to compare the effectiveness of each approach in a controlled manner (Mattson et al., 2017). However, restriction has been shown to increase lifespan in various model organisms. Bacteria, yeast, and worms survived significantly longer when raised in environments with no available nutrients (Figure 1.4a-1.4c, adapted from Longo and Mattson, 2014). Mice also lived significantly longer than ad libitum fed controls when maintained on a fasting schedule from a young age (Figure 1.4d, adapted from Longo and Mattson, 2014). There have been mixed results in preclinical work on the effectiveness

of restrictive diets on health. Factors such as age, genetic background, feeding method, and time course of the restriction can influence the success of each treatment approach (Mattson et al., 2017). Overall, caloric restriction seems to be a key factor in a healthy life, highlighting a need to better understand the mechanisms responsible for the beneficial effects of food restrictions.

**Food restriction reduces inflammation likely contributing to the benefits of caloric deficit on longevity.**

Food restriction inhibits inflammation. Fasting inhibits the activation of inflammasomes (Traba and Sack, 2017; Traba et al., 2015; Vandanmagsar et al., 2011), preventing the production and release of pro-inflammatory cytokines and reducing serum levels of tumor necrosis factor alpha (TNF $\alpha$ ), interleukin-1 $\beta$ , interleukin-18, brain-derived neurotrophic factor, and ceramides (Brandhorst et al., 2015; Johnson et al., 2007; Meydani et al., 2016; Youm et al., 2015). Food restriction also reduces oxidative stress, particularly in mononuclear cells and leukocytes (Dandona et al., 2001; Heilbronn and Ravussin, 2003; Johnson et al., 2007), alleviating inflammation. Beyond inflammatory pathways, food restriction can improve other indications of inflammation such as bone density (Brandhorst et al., 2015; Youm et al., 2013), cognitive impairment (Youm et al., 2013), respiration (Johnson et al., 2007), muscle (Mercken et al., 2013) and cardiac (Fontana et al., 2004) function, metabolism (Brandhorst et al., 2015), and neuroendocrine function (Heilbronn and Ravussin, 2003), sympathetic nerve output (Heilbronn and Ravussin, 2003), and cancer incidence (Brandhorst et al., 2015). These anti-inflammatory effects may contribute to the beneficial effects of food restriction on longevity, given the role of inflammation in the development of age-associated diseases (Franceschi and Campisi, 2014; Youm et al., 2013). Thus, a better understanding of how fasting reduces inflammation will be key to the prevention and treatment of inflammatory diseases.

Food deprivation leads to a series of complex physiological changes in both the central nervous system and the periphery. However, it is unclear if the mechanisms by which hunger affects inflammation are nucleated in the brain or in the periphery. For example, food deprivation influences peripheral hormone levels, gene expression, physiology, and metabolic factors that may

influence the immune system (Al-Hasani and Joost, 2005; Culbert et al., 2016; Wang et al., 2006). Alternately, it has also been shown that central manipulation of the *Sirtuin 1* gene in AgRP neurons can influence adaptive immune responses (Matarese et al., 2013). These hunger-activated AgRP neurons are known to drive feeding behavior (Hahn et al., 1998; Horvath et al., 1992, 1997; Sternson and Eiselt, 2015). Importantly, AgRP neuron activity also alleviates pain caused by an inflammatory chemical injury (Alhadeff et al., 2018). These data raise the possibility that AgRP neurons may contribute to the anti-inflammatory effects of hunger. The work in this dissertation investigates how hunger, through AgRP neurons, can influence pain and inflammation as a potential therapeutic mechanism for chronic inflammatory diseases.

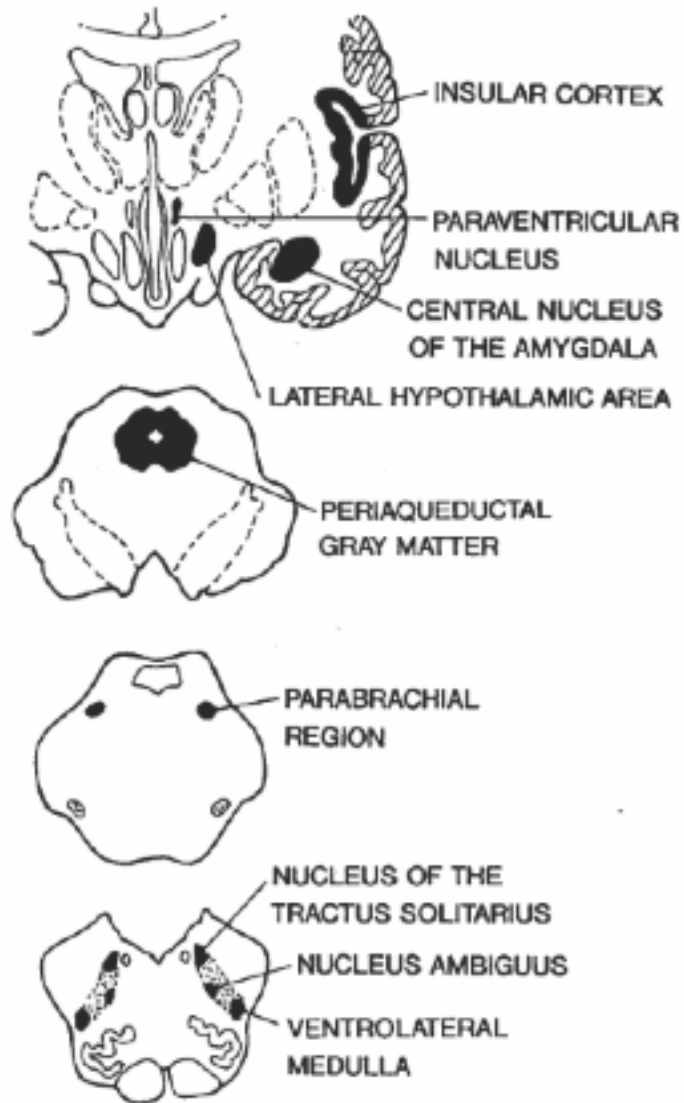


**Figure 1.1 | The central autonomic network is composed of brain regions throughout the brainstem, midbrain, and cortex (adapted from Benarroch, 1993).**

Diagram of a human brain with key central autonomic network regions labeled.

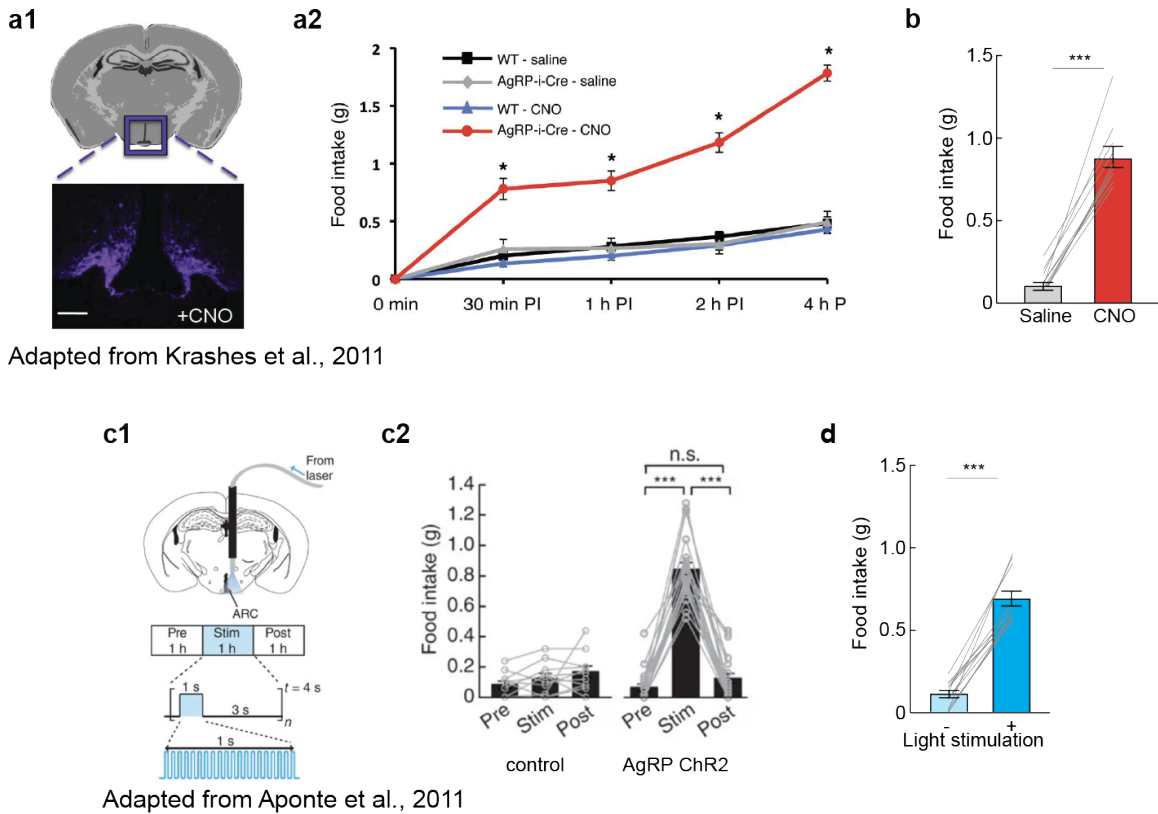
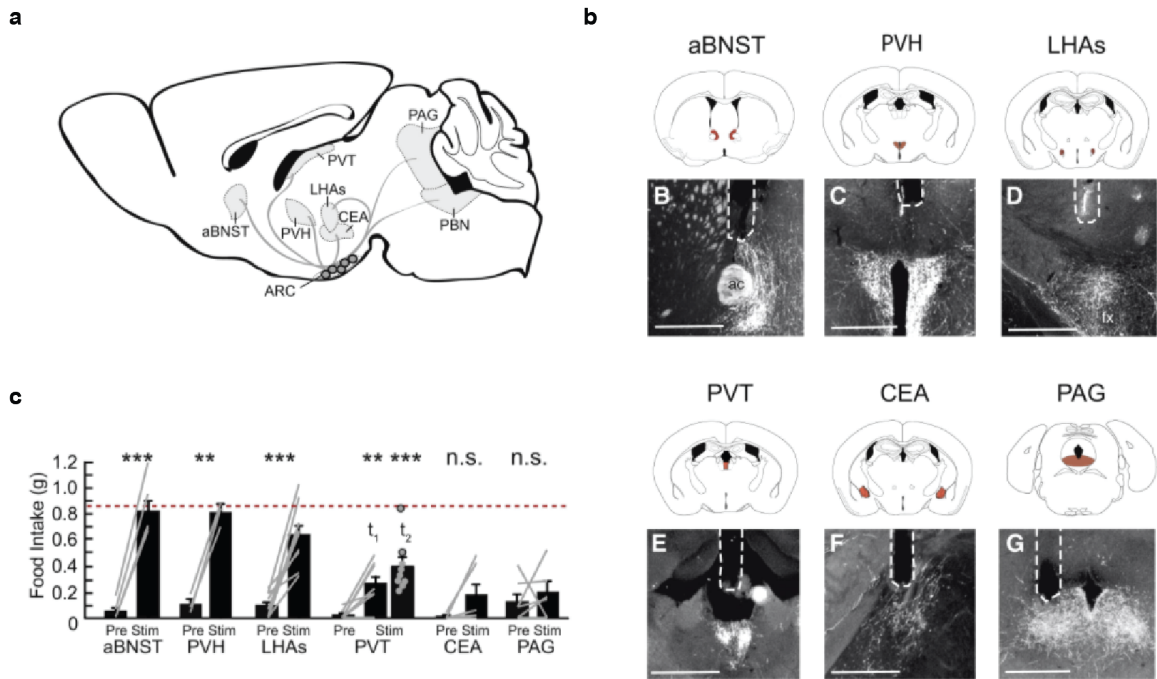


**Figure 1.2 | Chemogenetic and optogenetic activation of AgRP neurons induces rapid, reversible, and reliable food intake.**

(a) Krashes et al (2011) used chemogenetic activation of AgRP to initiate food intake. (a1) Schematic: Expression of the hM3D in AgRP neurons in the ARC. (a2) Food intake was significantly higher in HM3D mice treated CNO than control mice. (b) Our laboratory is able to recapitulate food intake using chemogenetic activation on AgRP neurons. Mice expressing HM3D had significantly higher food intake after CNO administration than saline. (c) Aponte et al (2011) used optogenetic stimulation of AgRP neurons to initiate food intake. (c1) Experimental design: An optical fiber was implanted above the ARC to allow for stimulation of AgRP neurons. Food intake was measured at 1 h increments before, during and after stimulation. (c2) Mice without ChR2 expression (control) had no significant difference in food intake across time points. Mice expressing ChR2 in AgRP neurons consumed significantly more food during stimulation than before or after. (d) Our lab is able to recapitulate food intake using optogenetics on AgRP

neurons. Mice expressing ChR2 in AgRP neurons consumed significantly more food with stimulation. Data expressed as mean  $\pm$  standard error of the mean (SEM): n.s.=not significant, \*= $p < 0.05$ , \*\*\*= $p < 0.001$ .



Adapted from Betley et al., 2013

**Figure 1.3 | AgRP neuron architecture allows for interrogation of individual axon targets for any given behavior (adapted from Betley et al., 2013).**

(a) AgRP neurons in the ARC ramify to 7 brain regions. (b) Fibers can be placed over each target region to activate axon terminals from AgRP neurons expressing ChR2. (c) Stimulation of ARC → aBNST, PVH, LH, and PVT causes a significant increase in food intake. Stimulation of ARC → CeA and PAG had no effect on food intake. Data expressed as mean ± SEM: n.s.=not significant, \*\*= $p < 0.01$ , \*\*\*= $p < 0.001$ .

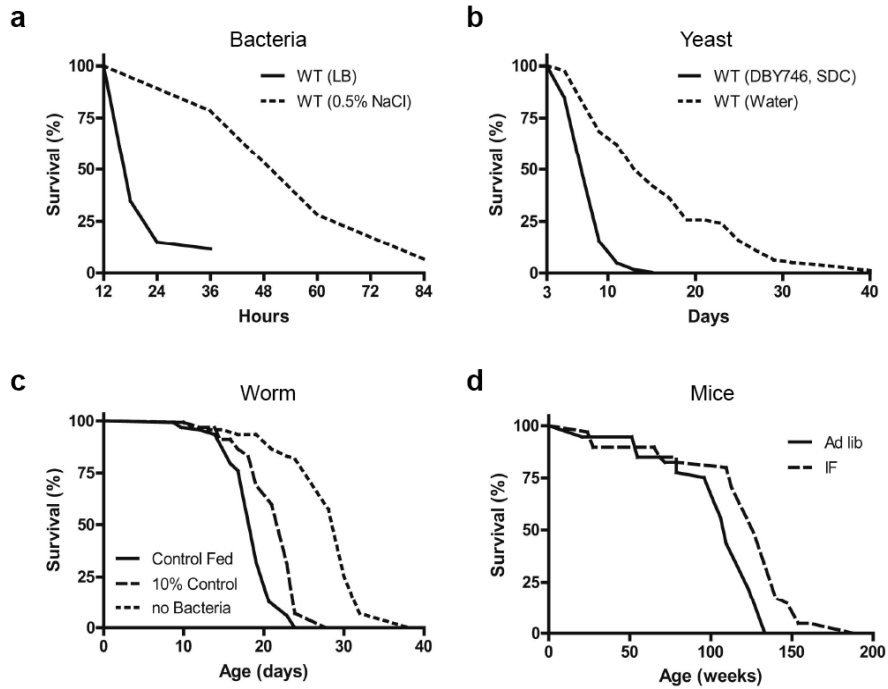


**Figure 1.4 | Food restriction can increase longevity in simple organisms and complex animals (adapted from Longo and Mattson, 2014).**

(a) Percent survival of *Escherichia coli* grown in either nutrient-rich Lyosgeny Broth (LB) or nutrient-free sodium chloride (NaCL) mediums (Gonidakis et al., 2010). (b) Percent survival of *Saccharomyces cerevisiae* grown in either nutrient-rich (DBY746, SDC) solution or nutrient-free water (Wei et al., 2008). (c) Percent survival of *Caenorhabditis elegans* living in a standard nutrient-rich environment (control fed), a 10% caloric nutrient environment (10% control), or in a nutrient-free environment (no bacteria) (Kaeberlein et al., 2006). (d) Percent survival of male C57BL/CJ mice maintained on an ad libitum or alternating day fasting diet (Goodrick et al., 1990)

## **CHAPTER 2: HUNGER REDUCES THE AFFECTIVE AND BEHAVIORAL COMPONENTS OF INFLAMMATORY PAIN.**

I worked in collaboration with Dr. Amber Alhadeff while she was a post-doctoral researcher in the Betley laboratory to complete the publication Alhadeff et al., 2018. As a listed author on the manuscript, I helped complete experiments, analyze data, and interpret the results. More specifically, I conducted formalin pain assays for: ad libitum fed v food deprived mice, AgRP axon mice, AgRP peptides in the PBN; performed the conditioned place aversion assay; and addressed reviewer concerns about the affective properties of PBN stimulation: open field assay [tail suspension test, hedonic feeding assay, conditioned place preference, conditioned place aversion (data not published)].

Running title: A Neural Circuit for the Suppression of Pain by a Competing Need State

Amber L. Alhadeff<sup>1</sup>, Zhenwei Su<sup>1</sup>, Elen Hernandez<sup>1</sup>, Michelle L. Klima<sup>1</sup>, Sophie Z. Phillips<sup>1</sup>, Ruby  
A. Holland<sup>2</sup>, Caiying Guo<sup>3</sup>, Adam W. Hantman<sup>3</sup>, Bart C. De Jonghe<sup>2</sup>, J. Nicholas Betley<sup>1\*</sup>

<sup>1</sup>Department of Biology, University of Pennsylvania, Philadelphia, PA 19104

<sup>2</sup>Department of Biobehavioral Health Sciences, University of Pennsylvania, Philadelphia, PA  
19104

<sup>3</sup>Janelia Research Campus, Howard Hughes Medical Institute, Ashburn, VA 20147

Key words: AgRP neurons; analgesia; calcium imaging; hunger; inflammation; neuropeptide Y;  
nociception; optogenetics; pain; parabrachial nucleus.

This work originally appeared in *Cell* (2018), 173(1):140-152.

## Summary

Hunger and pain are two competing signals that individuals must resolve to ensure survival. However, the neural processes that prioritize conflicting survival needs are poorly understood. We discovered that hunger attenuates behavioral responses and affective properties of inflammatory pain without altering acute nociceptive responses. This effect is centrally controlled, as activity in hunger-sensitive Agouti-Related Protein (AgRP)-expressing neurons abrogates inflammatory pain. Systematic analysis of AgRP projection subpopulations revealed that the neural processing of hunger and inflammatory pain converge in the hindbrain parabrachial nucleus (PBN). Strikingly, activity in AgRP→PBN neurons blocked the behavioral response to inflammatory pain as effectively as hunger or analgesics. The anti-nociceptive effect of hunger is mediated by Neuropeptide Y (NPY) signaling in the PBN. By investigating the intersection between hunger and pain, we have identified a neural circuit that mediates competing survival needs and uncovered NPY Y1 receptor signaling in the PBN as a target for pain suppression.

## Introduction

Survival depends on fulfilling salient needs in a changing environment. Formative behavioral observations highlighted the remarkable ability of individuals across species to adaptively respond to dynamic physiological and environmental challenges (Pavlov and Fol'bert, 1926; Tinbergen, 1951). Given these insights, it is surprising that the neural and molecular mechanisms governing the prioritization of adaptive behaviors remain elusive. While great strides have been made in understanding how individual need states such as hunger, thirst, fear and pain are signaled in the brain, relatively little is known about how the brain prioritizes such needs.

Pain is a natural response to injury, but long-term inflammation and associated pain can be maladaptive. While acute pain is reflexive in that it is triggered by activation of primary sensory neurons (i.e. nociceptors) in the periphery, inflammatory pain is mediated at least in part by central mechanisms (Coderre et al., 1990). From this perspective, targeting central nociceptive pathways may be an effective way to selectively reduce inflammatory pain while leaving intact adaptive responses to acute pain. Because persistent pain remains a major public health burden that is not well-controlled by current analgesics (Loeser, 2012), identifying endogenous mechanisms that specifically reduce the inflammatory response to injury may provide strategies for the design of effective pain therapies.

As a unique approach to identify neural circuits that regulate pain, we sought to explore competing need states that affect nociception. The response to pain is typically an adaptive mechanism that protects organisms against dangerous stimuli. However, as other physiological needs such as hunger increase, behavior must shift from avoiding bodily injury to fulfilling other immediate needs. Interactions between competing needs states have been reported; for example, acute stressors such as inescapable footshock, cold-water swims, or caloric deprivation can produce short-term analgesia (Bodnar et al., 1977; Bodnar et al., 1978b; Hamm and Lyeth, 1984; Hargraves and Hentall, 2005; LaGraize et al., 2004). Additionally, hunger has been shown to influence adaptive behavioral responses to fear and anxiety (Burnett et al., 2016; Jikomes et al., 2016; Padilla et al., 2016). We reasoned that individuals must prioritize the most acute threat to

survival and behave accordingly. To explore the behavioral, neural, and molecular mechanisms that rank survival needs, we examined the bidirectional interaction between hunger and different modalities of pain.

Here, we found that hunger selectively inhibits both the behavioral response and affective properties of inflammatory pain. Since neurons responsive to hunger are well-characterized (Sternson and Eisel, 2017), they provide an entry point to examine the neural circuit intersection of hunger and pain. We discovered that hypothalamic agouti-related protein-(AgRP) expressing neurons that project to the hindbrain parabrachial nucleus (PBN) selectively inhibit responses to inflammatory pain. The analgesic effect of hunger on inflammatory pain is mediated by neuropeptide Y (NPY) signaling on NPY Y1 receptors in the PBN. We further show that acute thermal, but not inflammatory, pain inhibits the activity of AgRP neurons, demonstrating that central mechanisms prioritize the most salient threat. Taken together, our data demonstrate that AgRP neurons mediate the interaction between hunger and pain and have uncovered PBN NPY Y1 receptor signaling as a target for analgesia.

## **Results**

### *Hunger Selectively Attenuates Responses to Inflammatory Pain.*

To understand how competing survival signals are prioritized, we first explored how 24 h food deprivation influences the behavioral response to pain induced by either chemical (formalin), thermal (52°C hotplate) or mechanical (Von Frey filament) insults (Figure 2.1A, 2.1H, and 2.1J) (Bodnar, 1978; Hamm and Lyeth, 1984; Hargraves and Hentall, 2005; LaGraize et al., 2004). Formalin paw injection is a reliable and widely used model of nociception with high face validity when tested with analgesic drugs (Hunskar and Hole, 1987). Formalin induces distinct acute (0-5 min) and long-term inflammatory (15-45 min) phases of pain (Dubuisson and Dennis, 1977), while responses to a hotplate or Von Frey filaments are acute and transient. We discovered that 24 h food deprivation attenuated the duration (Figure 2.1B-2.1D) and frequency (Figure 2.1E) of inflammatory phase paw licking after injection of a noxious chemical stimulus, similar to the effect of an anti-inflammatory painkiller (Hunskar and Hole, 1987) (Figure 2.S1A-2.S1E). Conversely,

food deprivation had no effect on the acute phase response to formalin injection (Figure 2.1F and 2.1G) or the response to acute thermal (Figure 2.1H and 2.1I) or mechanical (Figure 2.1J and 2.1K) pain, unlike an opioid painkiller (Figure 2.S1F-2.S1H). These data demonstrate that hunger selectively blocks inflammatory phase pain responses.

To determine whether hunger influences inflammation-induced sensitization to different modalities of pain, we next induced a persistent inflammatory response in the paw via injection of Complete Freund's Adjuvant (CFA) (Marchand et al., 2005). After paw injection of CFA, mice exhibit sensitization to both mechanical (Figure 2.2A, 2.2B, and 2.2E) and thermal (Figure 2.2G and 2.2H) stimuli. The sensitization to both of these stimuli is abolished in food restricted mice (Figure 2.2C, 2.2D, 2.2F and 2.2I), suggesting that hunger reduces inflammation-induced sensitization to thermal and mechanical pain. Taken together, these data suggest that hunger is a powerful suppressant of inflammatory pain response.

Pain results in both behavioral responses as well as negative affect, the latter of which has been modeled in rodents using classic conditioning paradigms (Deyama et al., 2007; Johansen and Fields, 2004). We first investigated how hunger influences the affective properties of pain by examining whether hunger attenuates a conditioned place avoidance normally associated with inflammatory pain (Figure 2.3A). We found that *ad libitum* fed mice exhibited a conditioned place avoidance of cues previously paired with formalin-induced inflammatory pain (Figure 2.3B-2.3D). This post-conditioning avoidance was abolished in animals that were food restricted during conditioning (Figure 2.3B-2.3D), a result that was independent of changes in locomotor activity (Figure 2.3E and 2.3F). This result is not likely due to a hunger-induced deficit in associative learning, given that food restricted mice learn to avoid contexts associated with other aversive stimuli as effectively as *ad libitum* fed mice (Figure 2.3G). Similar to the attenuation of a formalin conditioned place avoidance, we found that hunger also attenuated formalin-induced immobility (Figure 2.3H). Together, these data suggest that hunger attenuates measures of pain-induced negative affect, in addition to behavioral responses to inflammatory pain.

### *AgRP Neurons Specifically Inhibit Inflammatory Pain*

Formalin paw injection leads to paw inflammation in food deprived mice (Figure 2.S1I and 2.S1J), suggesting central mechanisms may mediate the interaction between hunger and inflammatory pain. Neural circuits activated by hunger are well-characterized (Sternson and Eiselt, 2017). In particular, neurons that co-express agouti-related protein (AgRP), gamma-aminobutyric acid (GABA), and Neuropeptide Y (NPY) (referred to as AgRP neurons) are critical regulators of food intake (Luquet et al., 2005). AgRP neuron inhibition in hungry mice reduces food intake (Krashes et al., 2011), while activation of AgRP neurons in sated mice robustly increases food intake (Aponte et al., 2011; Krashes et al., 2011). Photostimulation of mice expressing channelrhodopsin-2 (ChR2) in AgRP neurons (AgRP<sup>ChR2</sup>) dramatically reduced both formalin-induced inflammatory phase pain responses (Figure 2.4A-2.4D; Figure 2.S2A-2.S2C) and CFA-induced nociceptive sensitization (Figure 2.4E and 2.4F; Figure 2.S2F-2.S2H) relative to responses of GFP-expressing control mice (AgRP<sup>GFP</sup>). This effect was specific to inflammatory pain as activating AgRP neurons did not influence acute phase chemical or thermal pain responses (Figure 2.S2D, 2.S2E, 2.S2I, and 2.S2J) nor responses to control saline paw injections (Figure 2.S2K-2.S2M). Initiating AgRP neuron stimulation during an ongoing pain response inhibited paw licking within minutes (Figure 2.4G and 2.4H). This indicates that AgRP neuron activity rapidly mediates a behavioral switch and does not rely on long-term activity of AgRP neurons that may entrain a single behavioral state. To test whether AgRP neuron activity is sufficient to suppress inflammatory pain, we chemogenetically inhibited AgRP neurons during hunger. Food deprived mice expressing inhibitory Designer Receptors Exclusively Activated by Designer Drugs (DREADDs, hM4D) in AgRP neurons (AgRP<sup>hM4D+</sup>) significantly reduce food intake relative to littermate controls (AgRP<sup>hM4D-</sup>) following injection of the designer ligand clozapine-N-oxide (CNO, Figure 2.4I), as previously described (Krashes et al., 2011). Inhibition of AgRP neurons significantly reduced the protective effect of hunger on inflammatory pain (Figure 2.4J-2.4L). Thus, AgRP neuron activity during hunger is both necessary and sufficient to suppress inflammatory pain responses without affecting acute pain responses, recapitulating the behavioral interaction observed in hunger and identifying a neural mechanism for the suppression of inflammatory pain.

*AgRP→PBN Neurons Specifically Inhibit Inflammatory Pain.*

Given that hunger suppresses longer-term inflammatory pain responses, we next sought to identify brain regions where hunger and nociceptive information converge. Several brain regions innervated by AgRP neurons are also activated by formalin paw injection and implicated in nociception (Baulmann et al., 2000). To explore potential brain regions targeted by AgRP neurons that mediate inflammatory pain, we performed a formalin paw injection in *ad libitum* fed mice and quantified neurons directly under AgRP axons that expressed the immediate early gene Fos. The number of neurons expressing Fos protein was increased in the terminal projection fields of several AgRP neuron target regions following formalin paw injection compared to mice who received saline or no injection (Figure 2.5A and 2.5B; Figure 2.S3A).

Because the anatomical data suggested that multiple AgRP target regions may be involved in the transmission of inflammatory pain, we performed a systematic analysis of the function of each AgRP neuron projection subpopulation. Taking advantage of the one-to-one architecture of AgRP neuron projections (Figure 2.S3C) (Betley et al., 2013), we activated individual AgRP projection subpopulations in *ad libitum* fed mice and assessed behavioral responses to acute and inflammatory formalin-induced pain (Figure 2.5C; Figure 2.S3B). Although AgRP subpopulations that project to the bed nuclei of the stria terminalis (BNST), paraventricular thalamic nucleus (PVT), paraventricular hypothalamic nucleus (PVH), and the lateral hypothalamus (LH) are sufficient to evoke food intake (Figure 2.S3D) (Betley et al., 2013), we found that optogenetic activation of each of these discrete subpopulations does not reduce the behavioral response to acute or inflammatory formalin-induced pain (Figure 2.5D-2.5F; Figure 2.S3E). Other AgRP projection subpopulations, such as those that project to the periaqueductal grey (PAG), central nucleus of the amygdala (CeA), and parabrachial nucleus (PBN) are not sufficient to drive food intake when stimulated (Figure 2.S3D) (Betley et al., 2013), raising the hypothesis that these populations are involved in more nuanced aspects of feeding, such as the ability to suppress pain to facilitate food-seeking behavior. We found that activation of AgRP projections to the PBN virtually eliminates inflammatory phase pain responses (Figure 2.5D and 5E; Figure 2.S3E) without affecting responses to acute chemical (Figure 5F) or thermal (Figure 2.5G) pain. The suppression of inflammatory pain by AgRP→PBN

stimulation is not likely due to off target effects since prolonged stimulation does not reduce the acute response to formalin-induced pain (Figure 2.S3F) or locomotor activity (Figure 2.S3G and 2.S3H). Activating AgRP neurons that project to the CeA or the PAG had no effect on acute or inflammatory phase pain (Figure 2.5D-2.5F) nor did the delivery of light to AgRP<sup>GFP</sup>→PBN mice (Figure 2.S3I-2.S3K). This striking specificity of AgRP→PBN neuron function demonstrates that the PBN is a neural substrate for the interaction between hunger and inflammatory pain.

*NPY Signaling in the lateral PBN Inhibits Inflammatory Pain.*

To explore how AgRP→PBN signaling intersects with the neural representation of inflammatory pain, we first examined the anatomical overlap of AgRP projections and neurons activated by inflammatory pain. We find a dense AgRP axonal projection in the lateral PBN (IPBN) and a more medial projection to the locus coeruleus area (Figure 2.6A). AgRP axons projecting to the IPBN overlap with neurons activated by formalin paw injection (Figure 2.S4A), suggesting the activity in AgRP neurons projecting to the IPBN mediates inflammatory pain.

Because AgRP neuron activity is both necessary and sufficient to provide a protective effect against inflammatory pain during hunger (Figure 2.4), we next sought to determine the molecular signals in the PBN that mediate the suppression of pain during hunger. We first explored protein expression of the 3 main neurotransmitters of AgRP neurons: NPY, GABA, and AgRP. Expression of both NPY and the GABA synthetic enzyme GAD65 were increased in axon terminals of AgRP→IPBN neurons during hunger (Figure 2.6B and 2.6C), suggesting these molecules may mediate the interaction between hunger and pain in the IPBN. To test the functional relevance of these neurotransmitters, we performed microinjections of each neurotransmitter into the IPBN immediately before formalin paw injection. NPY signaling in the IPBN robustly and selectively attenuated inflammatory phase pain responses, without affecting acute pain responses or food intake (Figure 2.6D-2.6G, Figure 2.S4B). Conversely, neither GABA nor AgRP signaling in the IPBN (Figure 2.6E), nor NPY in the locus coeruleus area (Figure 2.S4C-2.S4F), had any effect on formalin-induced pain responses. Consistent with the kinetics of NPY signaling on behavior (Stanley and Leibowitz, 1985), the onset (Figure 2.S4G and 2.S4I) and offset (Figure 2.S4H and

2.S4I) of AgRP→PBN neuron activity during an ongoing inflammatory phase pain response triggered changes in nocifensive behavior within minutes.

To determine if NPY signaling in the IPBN functions in a physiologically relevant manner, we next assessed the role of endogenous NPY signaling during hunger. Strikingly, blocking NPY Y1 receptors (Atasoy et al., 2012) in the IPBN of food deprived mice reversed the analgesic effects of hunger (Figure 2.6H-2.6I) while antagonism of GABA receptors did not affect inflammatory pain (Figure 2.6H). Furthermore, blockade of Y1 receptors in the IPBN attenuated the suppression of inflammatory pain by AgRP→PBN neuron stimulation (Figure 2.6J and 2.6K), suggesting that AgRP neurons are the source of the analgesic NPY. This reduction in pain is likely mediated by glutamatergic neurons in the IPBN as inhibiting VGlut2-expressing, but not Gad2-expressing, neurons in the IPBN during the formalin assay reduced inflammatory pain (Figure 2.S5). Taken together, these data demonstrate that IPBN NPY signaling is both necessary and sufficient for the suppression of inflammatory pain.

#### *Acute Pain Reduces Food Seeking and Neural Activity in Hunger Circuits.*

Survival requires ranking and responding to the most critical need at a given time. Because hunger does not suppress the response to acute pain, we reasoned that neural mechanisms may exist to deprioritize hunger during threats to survival such as acute pain. Exposure to a 52°C hotplate increased the latency to feed in 24 h food deprived mice (Figure 2.7A). However, no change in food intake in hungry mice during inflammatory pain was observed (Figure 2.7B). To gain insight into the mechanisms through which acute pain inhibits feeding behavior, we next measured *in vivo* calcium dynamics in AgRP neurons as a proxy for neural activity (Figure 2.7C) (Gunaydin et al., 2014). Chow presentation significantly reduced the activity of AgRP neurons in hungry mice (Figure 2.S7A and 2.S7B), as previously reported (Betley et al., 2015; Chen et al., 2015; Mandelblat-Cerf et al., 2015). Consistent with the effects of pain on food intake, acute thermal pain, but not formalin injection, reduced the activity of AgRP neurons (Figure 2.7D-2.7G, Figure 2.S7C and 2.S7D). This suppression of AgRP neuron activity by acute thermal pain reached a magnitude comparable to ~50% of the suppression observed upon refeeding hungry mice (Figure

2.S7E). Together, these data suggest that acute thermal pain can influence behavior by suppressing activity in AgRP neuron circuits.

## **Discussion**

Here, we discovered a bidirectional interaction between hunger and pain and revealed a neural mechanism that processes competing survival signals. We demonstrated that hunger selectively attenuates the behavioral and affective responses to inflammatory pain. This effect is centrally mediated by a small subset of AgRP neurons that project to the PBN. The suppression of inflammatory pain by hunger requires NPY signaling through Y1 receptors. Conversely, acute but not inflammatory pain inhibited feeding behavior and reduced the endogenous activity of AgRP neurons during hunger. These findings demonstrate the utility of examining intersecting survival needs to reveal neural circuits that influence behavior, as we have identified a mechanism for the inhibition of inflammatory pain.

### *Bidirectional Behavioral Interaction Between Hunger and Pain*

It has been demonstrated that hunger can both increase and decrease responses to pain (Bodnar, 1978; Hamm and Lyeth, 1984; Hargraves and Hentall, 2005; LaGraize et al., 2004; Pollatos et al., 2012), suggesting that these two broadly tuned survival signals may interact in a hierarchical manner. We found that 24 h food deprivation consistently and dramatically attenuates responses to inflammatory pain, but has no effect on thermal pain, mechanical pain or the acute response to formalin paw injection. In comparison to previous studies, we observed two striking results. First, hunger had no effect on acute pain resulting from thermal, mechanical or chemical insult. While previous reports demonstrate that hunger modestly reduces (10-20%) acute pain (Bodnar et al., 1978a; Hamm and Lyeth, 1984; Hargraves and Hentall, 2005), the majority of the acute pain responses are left intact – an important ethological consideration to enhance survival. Second, we found that hunger selectively and almost completely abolished inflammatory pain responses, mimicking the effects of anti-inflammatory painkillers. This profound suppression, even without the distractor of food, suggests an analgesic effect of hunger and provides a behavioral

mechanism to facilitate food seeking following an injury. Taken together, our observations demonstrate that hunger has the ability to selectively inhibit long-term pain responses while leaving intact the adaptive ability to respond to acutely painful stimuli.

The robust suppression of inflammatory pain response by food deprivation prompted us to explore how hunger affects other dimensions of pain. Pain induces negative emotional responses, and it is thought that distinct neural systems regulate the sensory and affective components of pain (Johansen and Fields, 2004). Given that hunger is a complex motivational state that involves coordination of many distinct neural circuits (Andermann and Lowell, 2017; Grill, 2006), it is not surprising that hunger can interface with both the sensory and affective components of pain. Indeed, the affective components of pain were diminished by hunger, as hunger attenuated a place avoidance of cues previously associated with inflammatory pain. The ability of hunger to inhibit both the unpleasant aspects of pain in addition to behavioral responses to pain suggests an analgesic effect of hunger. These findings have implications not only for the treatment of pain disorders, but also for the treatment of affective disorders such as depression that are highly comorbid with conditions of chronic pain (Miller and Cano, 2009; Price, 2000).

Hunger attenuated inflammatory but not acute pain, but only acute pain was capable of inhibiting feeding behavior. Furthermore, acute thermal pain directly inhibited the activity of hunger-sensitive AgRP neurons, suggesting that pain is not simply a distractor from hunger. The transient reduction in AgRP neuron activity is consistent with our observation of short- but not long-term reductions in feeding behavior following painful stimuli. While other studies have reported robust reductions in endogenous AgRP neuron activity by food (Betley et al., 2015; Chen et al., 2015; Mandelblat-Cerf et al., 2015), our findings unexpectedly provide a feeding-independent mechanism that inhibits this neural population.

Together, our data show that acute pain inhibits hunger, and that hunger inhibits inflammatory pain. This hierarchical interaction between hunger and different modalities of pain suggests a prioritization of survival needs, whereby behavior addresses the most urgent environmental or physiological stimulus. Together, these observations are ethologically sound for

survival, as they describe a system that reliably responds to acute threat but allows for the suppression of longer-term pain when food seeking behavior is paramount for survival.

#### *Neural and Molecular Mechanisms for the Inhibition of Pain*

Activation of AgRP neurons suppressed inflammatory pain, revealing a common neural substrate for circuits that mediate hunger and pain. It is well established that AgRP neuron signaling influences complex behaviors that promote food seeking (Burnett et al., 2016; Dietrich et al., 2015; Krashes et al., 2011; Padilla et al., 2016). The ability of AgRP neuron activity to robustly inhibit inflammatory pain was surprising because analgesia is not an obvious priority for food seeking. However, facilitating feeding behavior following injury likely requires hard-wired neural circuitry to overcome obstacles such as pain. Interestingly, the AgRP neural network, which is composed of parallel projections that do not all drive food intake (Betley et al., 2013), provides an anatomical arrangement that allows distinct projections to inhibit neural processing of environmental signals that impede feeding.

To unravel the AgRP circuitry that inhibits inflammatory pain, we performed a systematic functional assessment of AgRP neuron subpopulations that revealed the striking specificity by which a tiny population of neurons can initiate behavioral switching. Indeed, activity in only ~300 AgRP neurons that project to the PBN (Betley et al., 2013) specifically eliminated inflammatory pain. The magnitude of suppression of inflammatory pain was comparable to morphine and was more robust than most anti-inflammatory or steroid analgesics (Hunskar and Hole, 1987). Given that activity in AgRP→PBN neurons is insufficient to drive food intake, the suppression of pain is not simply a consequence of being distracted by an ongoing hunger state. Rather, these neurons facilitate food seeking by reducing responses to competing aversive drives or stimuli that are processed in the PBN (Carter et al., 2013). Furthermore, this function of a feeding insufficient subpopulation highlights the importance of the distributed AgRP neuron circuitry – as this population of hunger-sensitive neurons has distinct subpopulations that interact with many systems in the brain to regulate other survival behaviors.

Manipulating AgRP→PBN neurons during an ongoing pain response causes changes in nocifensive behavior within minutes. This result suggests that peptidergic neurotransmission mediates the interaction between hunger and pain. Indeed, NPY signaling inhibited the behavioral response to inflammatory pain. We corroborated these data by showing that Y1R antagonism in the PBN selectively blocked the ability of hunger or AgRP→PBN stimulation to attenuate inflammatory pain. This occlusion of the dominant NPY receptor in the PBN (Alhadeff et al., 2015) demonstrates the necessity and sufficiency of NPY Y1 receptor signaling for the inhibition of inflammatory pain. Genetic (Naveilhan et al., 2001) and pharmacological (Solway et al., 2011) evidence demonstrate a role of NPY Y1 receptor in the dorsal horn of the spinal cord in mediating pain. Within the brain, it has been demonstrated that NPY signaling in the PAG and trigeminal nucleus also inhibits pain (Martins-Oliveira et al., 2016; Wang et al., 2001). Here, our findings uncover the PBN as an additional site of action for the analgesic effects of NPY, and are unique in that they selectively inhibit inflammatory pain.

GABA and AgRP signaling in the PBN have documented roles in energy balance control (Higgs and Cooper, 1996; Skibicka and Grill, 2009). Furthermore, GABA signaling from AgRP neurons projecting to the PBN is permissive for feeding (Wu et al., 2009), as it suppresses the visceral malaise associated with consumption of a large meal or toxic substance (Alhadeff et al., 2017; Campos et al., 2016; Carter et al., 2013; Essner et al., 2017). However, GABA and AgRP agonists microinjected into the PBN did not affect acute or inflammatory pain, highlighting NPY as the molecular mediator of pain in the PBN. While co-release of neurotransmitters is well-documented (Hnasko et al., 2010; Jonas et al., 1998), our findings dissociate distinct behavioral functions for co-transmitters released by a single neuron type.

Both hunger and pain are negative signals that individuals try to avoid (Betley et al., 2015; Johansen and Fields, 2004; Keys, 1946). The finding that hunger inhibits inflammatory pain raises the question of how one negative drive can inhibit another. Our neural circuit analysis provides insight into this paradox. Since AgRP→PBN neuron activity does not evoke food intake (Atasoy et al., 2012), it is unlikely that these neurons mediate the negative valence of hunger (Betley et al.,

2015). Our findings conclusively implicate AgRP→PBN signaling in mediating the response to pain. However, the distinct AgRP circuits that mediate the negative valence of hunger, and inhibit the negative valence of pain, remain compelling topics for future investigation.

### *Conclusion*

Our findings uncover a hierarchy of survival behaviors that prioritizes needs in a changing environment. Our behavioral observations provided a unique entry point to study circuits that inhibit pain. This unexpected ability to influence pain through activity in a distinct hypothalamic→hindbrain hunger circuit reveals an endogenous and ethologically relevant neural circuit mechanism for analgesia. Importantly, this neural circuit can be manipulated to inhibit potentially maladaptive inflammatory pain without compromising adaptive responses to painful stimuli that may acutely threaten survival. Through developing a mechanistic understanding of the influence of hunger on nociception, these experiments provide novel targets for the development of pain management therapies, of utmost importance in the search for non-addictive analgesics.

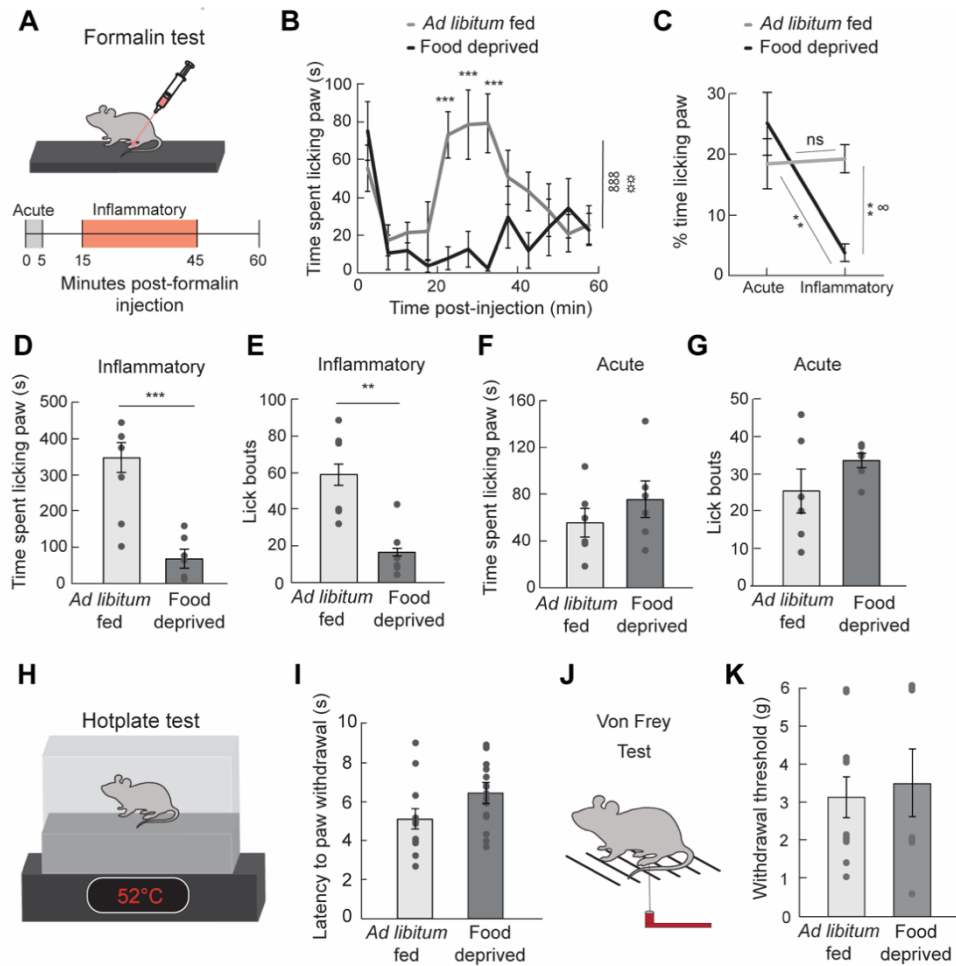


**Figure 2.1 | Hunger Attenuates Response to Inflammatory Pain.**

(A) Experimental design (formalin test): paw injection of 2% formalin was administered at 0 min; time spent licking paw was measured for 60 min and quantified during the acute phase (0-5 min) and the inflammatory phase (15-45 min). (B) Time spent licking paw following formalin injection displayed in 5 min time bins in *ad libitum* fed ( $n=6$ ) and 24 h food deprived ( $n=6$ ) mice (two-way repeated measures ANOVA,  $p<0.001$ ). (C) % time spent paw licking during acute and inflammatory phases of formalin test (two-way repeated measures ANOVA,  $p<0.05$ ). (D) Time spent paw licking during the inflammatory phase of formalin test in *ad libitum* fed and 24 h food deprived mice (unpaired t-test,  $p<0.001$ ). (E) Lick bouts during the inflammatory phase of formalin test in *ad libitum* fed and 24 h food deprived mice (unpaired t-test,  $p<0.01$ ). (F) Time spent paw licking during the acute phase of formalin test in *ad libitum* fed and 24 h food deprived mice (unpaired t-test,  $p=ns$ ).

(G) Lick bouts during the acute phase of formalin test in *ad libitum* fed and 24 h food deprived mice (unpaired t-test, p=ns). (H) Experimental design (hotplate test): Latency to withdraw paw from 52°C hotplate was measured. (I) Latency to withdraw paw in *ad libitum* fed (n=12) versus 24 h food deprived (n=14) mice during hotplate test (unpaired t-test, p=ns). (J) Experimental design (Von Frey): Paw withdrawal from Von Frey filaments was measured. (K) Withdrawal threshold (Von Frey filament at which mouse responded to >50% of trials) in *ad libitum* fed (n=11) versus 24 h food deprived (n=7) mice (unpaired t-test, p=ns). Data are expressed as mean ± SEM, ns p>0.05, t-tests and post-hoc comparisons: \*p<0.05, \*\*p<0.01, \*\*\*p<0.001; ANOVA interaction: ∞p<0.05, ∞∞∞p<0.001; ANOVA main effect of group: ☼☼p<0.01.

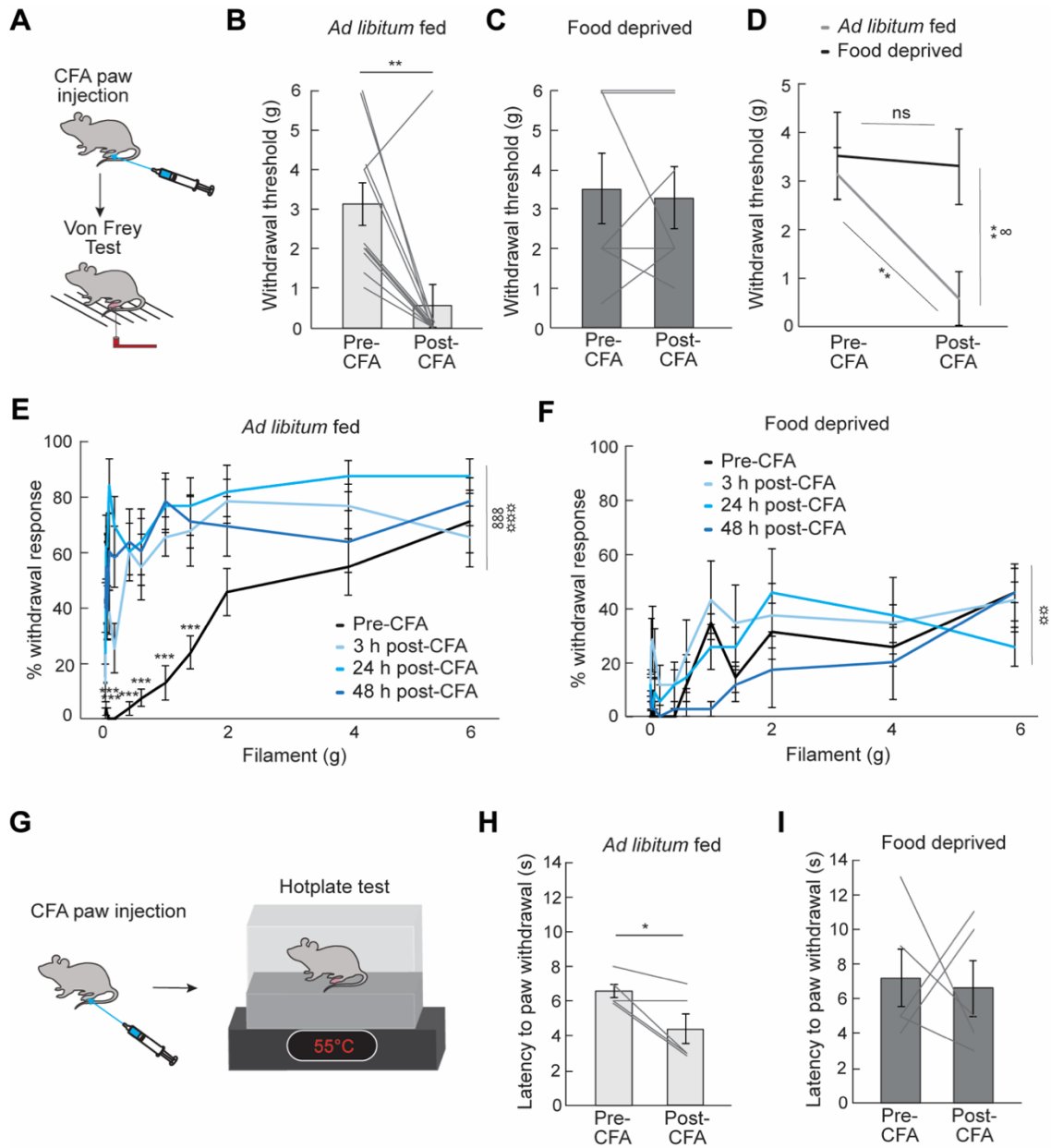


**Figure 2.2 | Hunger Attenuates Inflammation-Induced Sensitization to Mechanical and Thermal Pain.**

(A) Experimental design [Complete Freund's Adjuvant (CFA) and Von Frey Test]: CFA was injected in the plantar surface of the hindpaw after a baseline Von Frey test. Mice were subjected again to a Von Frey test 3 h, 24 h, and 48 h post-CFA injection. (B) Withdrawal threshold (Von Frey filament at which mouse responded to >50% of trials) in *ad libitum* fed mice (n=11) before and 24 h post-

CFA injection (paired t-test,  $p < 0.01$ ). (C) Withdrawal threshold in food restricted mice ( $n=7$ ) before and 24 h post-CFA injection (paired t-test,  $p=ns$ ). (D) Withdrawal threshold in *ad libitum* fed ( $n=11$ ) and food restricted mice ( $n=7$ ) before and 24 h post-CFA injection (two-way repeated measures ANOVA,  $p < 0.05$ ). (E) Percentage withdrawal from Von Frey filaments before and 3 h, 24 h, and 48 h post-CFA injection in *ad libitum* fed mice ( $n=11$ , two-way repeated measures ANOVA,  $p < 0.001$ ). (F) Percentage withdrawal from Von Frey filaments before and 3 h, 24 h, and 48 h post-CFA injection in food restricted mice ( $n=7$ , two-way repeated measures ANOVA,  $p=ns$ ). (G) Experimental design (CFA and hotplate test): mice were injected with CFA after a baseline hotplate test. Mice were subjected again to a hotplate test 3 h, 24 h, and 48 h post-CFA injection. (H) Latency to paw withdrawal from hotplate in *ad libitum* fed mice ( $n=5$ ) before and 48 h post-CFA injection (paired t-test,  $p < 0.05$ ). (I) Latency to paw withdrawal from hotplate in food restricted mice ( $n=10$ ) before and 48 h post-CFA injection (paired t-test,  $p=ns$ ). Data are expressed as mean  $\pm$  SEM,  $ns$   $p > 0.05$ , t-tests and post-hoc comparisons: \* $p < 0.05$ , \*\* $p < 0.01$ , \*\*\* $p < 0.001$ ; ANOVA interaction:  $\infty p < 0.05$ ,  $\infty\infty\infty p < 0.001$ ; ANOVA main effect of drug:  $\odot\odot p < 0.01$ ,  $\odot\odot\odot p < 0.001$ .

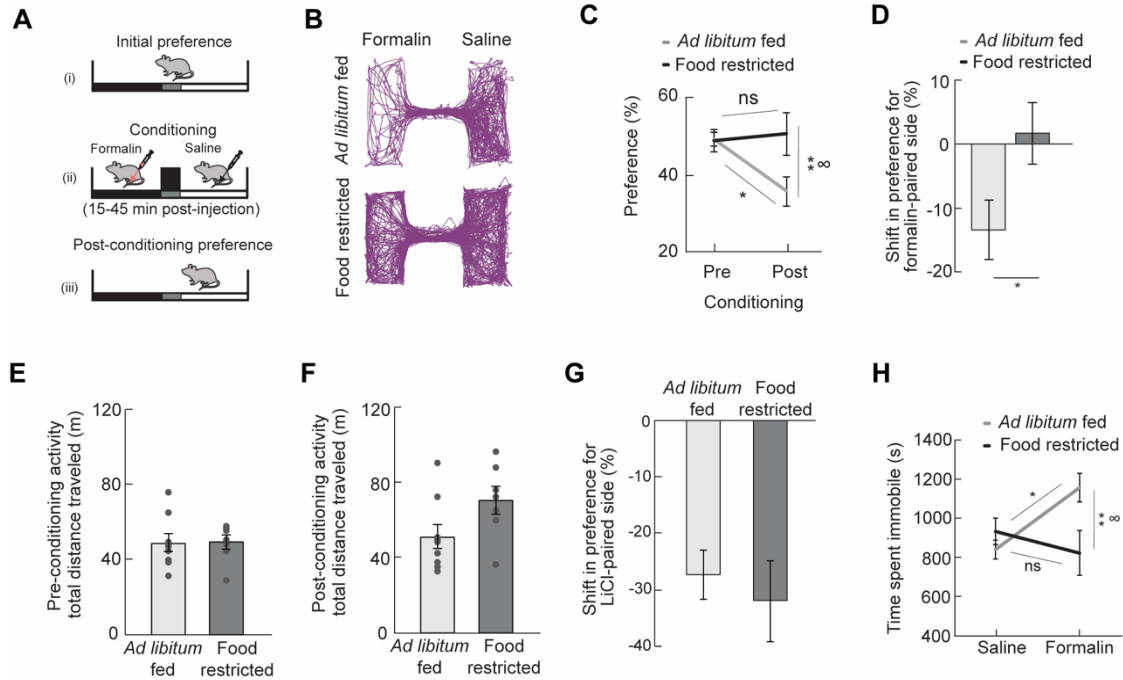


**Figure 2.3 | Hunger Attenuates Negative Affective Components of Pain.**

(A) Experimental design [conditioned place avoidance (CPA)]: one side of a two-sided chamber was paired with the inflammatory phase following formalin paw injection in either *ad libitum* fed or food restricted mice for 4 days and the post-conditioning preference was measured in replete animals. (B) Representative traces of locations of mice following formalin CPA. (C) Preference for formalin-paired side before and after conditioning in *ad libitum* fed ( $n=9$ ) and food restricted ( $n=7$ ) mice (two-way repeated measures ANOVA,  $p<0.05$ ). (D) Shift in preference for formalin-paired side in *ad libitum* fed and food restricted mice (unpaired t-test,  $p<0.05$ ). (E, F) Mice in *ad libitum* fed ( $n=9$ ) and food restricted ( $n=7$ ) groups exhibit similar locomotor activity both before (E) and after (F) CPA to inflammatory phase pain (unpaired t-tests,  $ps=ns$ ). (G) Shift in preference for lithium chloride-paired side in *ad libitum* fed and food restricted mice (unpaired t-test,  $p=ns$ ). (H) Time spent immobile in *ad libitum* fed and 24 h food deprived mice during inflammatory phase following formalin injection ( $n=7-10$ /group, two-way ANOVA,  $p<0.05$ ). Data are expressed as mean  $\pm$  SEM,  $ns$   $p>0.05$ , t-tests and post-hoc comparisons: \* $p<0.05$ , \*\* $p<0.01$ ; ANOVA interaction:  $\infty p<0.05$ .

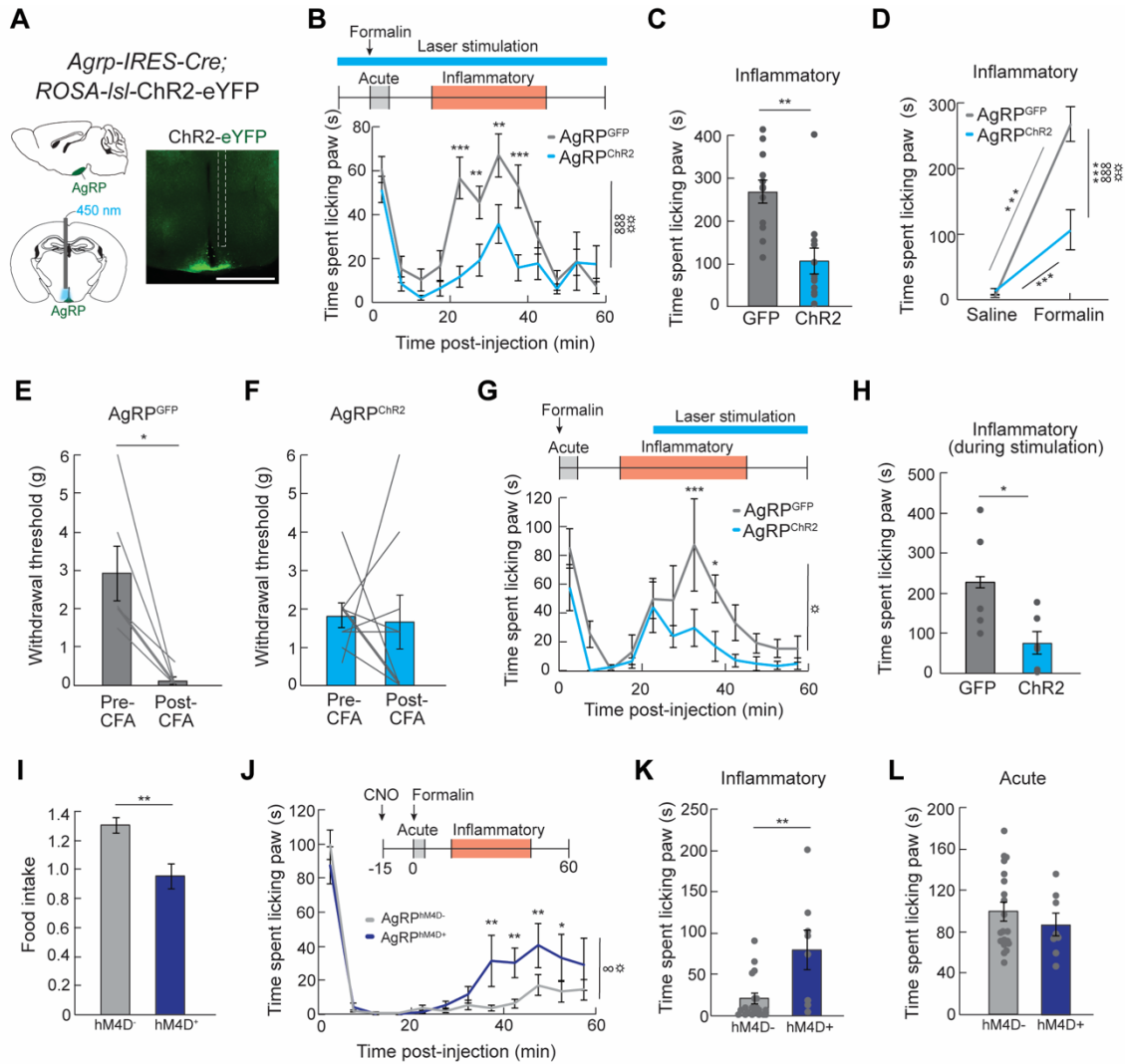


**Figure 2.4 | AgRP Neurons Mediate Suppression of Inflammatory Pain.**

(A) Schematic and representative image of ChR2 in *AgRP-IRES-Cre* mice implanted with an optical fiber (white dashed line indicates fiber track) above the ARC. Scale bar, 1 mm. (B) Top, experimental design: 450 nm light pulse delivery began 10 min before formalin administration and continued for the duration of the formalin test. Bottom, graph: Time spent paw licking in AgRP<sup>GFP</sup> (n=12) and AgRP<sup>ChR2</sup> (n=12) mice following formalin administration (two-way repeated measures ANOVA,  $p < 0.001$ ) (C) Inflammatory phase formalin-induced paw licking (time) in AgRP<sup>GFP</sup> and AgRP<sup>ChR2</sup> mice (unpaired t-test,  $p < 0.01$ ) (D) Time spent licking paw during inflammatory phase following saline or formalin injection in AgRP<sup>GFP</sup> and AgRP<sup>ChR2</sup> mice (two-way repeated measures

ANOVA,  $p < 0.001$ ). **(E)** Withdrawal threshold (Von Frey filament at which mouse responded to >50% of trials) in AgRP<sup>GFP</sup> mice ( $n=6$ ) before and 24 h post-CFA injection (paired t-test,  $p < 0.05$ ) **(F)** Withdrawal threshold in AgRP<sup>ChR2</sup> mice ( $n=9$ ) before and 24 h post-CFA injection (paired t-test,  $p=ns$ ) **(G)** Top, experimental design: 450 nm light pulses were delivered beginning 25 min post-formalin injection and lasting through the duration of the session. Bottom, graph: time spent paw licking in AgRP<sup>GFP</sup> ( $n=6$ ) and AgRP<sup>ChR2</sup> ( $n=6$ ) mice [two-way repeated measures ANOVA, main effect of stimulation (AgRP<sup>GFP</sup> vs. AgRP<sup>ChR2</sup>),  $p < 0.05$ ]. **(H)** Inflammatory phase formalin-induced paw licking (time) during laser stimulation (25-45 min) in AgRP<sup>GFP</sup> and AgRP<sup>ChR2</sup> mice (unpaired t-test,  $p < 0.05$ ). **(I)** Food intake in food deprived AgRP<sup>hM4D-</sup> ( $n=9$ ) and AgRP<sup>hM4D+</sup> ( $n=4$ ) mice 4 h following CNO injection (unpaired t-test,  $p < 0.01$ ). **(J)** Time spent paw licking in AgRP<sup>hM4D-</sup> ( $n=20$ ) and AgRP<sup>hM4D+</sup> ( $n=8$ ) mice following formalin injection (two-way repeated measures ANOVA,  $p < 0.05$ ). **(K)** Inflammatory phase formalin-induced paw licking (time) in AgRP<sup>hM4D-</sup> and AgRP<sup>hM4D+</sup> mice (unpaired t-test,  $p < 0.01$ ). **(L)** Acute phase formalin-induced paw licking (time) in AgRP<sup>hM4D-</sup> and AgRP<sup>hM4D+</sup> mice (unpaired t-test,  $p=ns$ ). Data are expressed as mean  $\pm$  SEM,  $ns$   $p > 0.05$ , t-tests and post-hoc comparisons: \* $p < 0.05$ , \*\* $p < 0.01$ , \*\*\* $p < 0.001$ ; ANOVA interaction:  $\infty p < 0.05$ ,  $\infty\infty\infty p < 0.001$ ; ANOVA main effect of group:  $\odot p < 0.05$ ,  $\odot\odot p < 0.01$ .

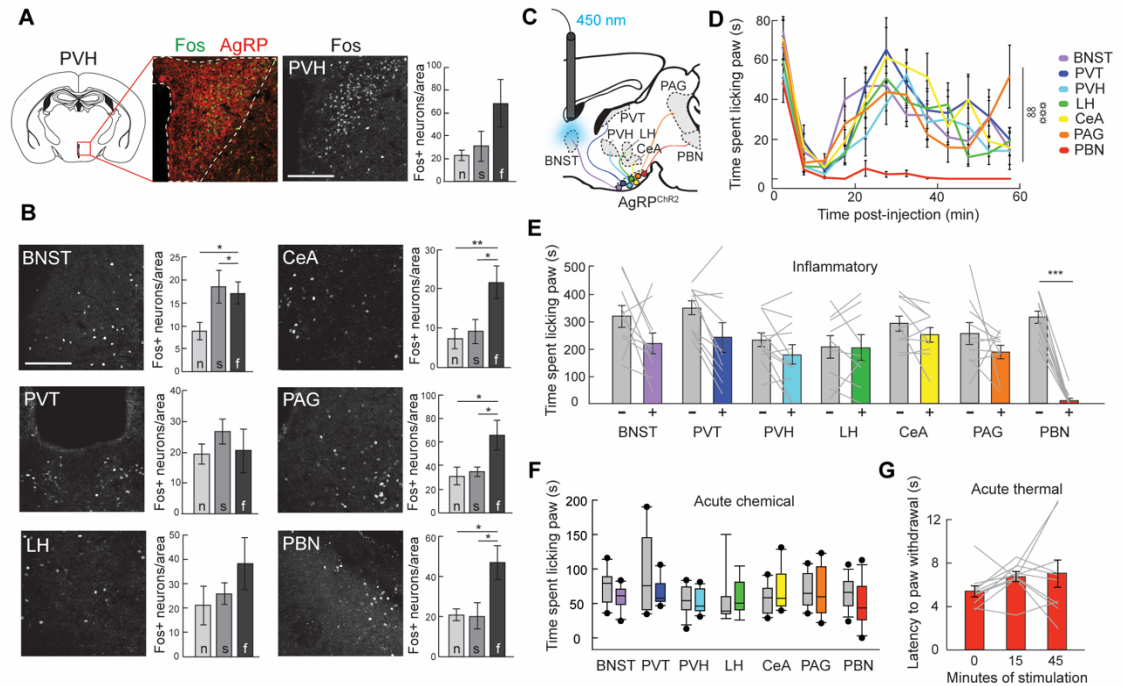


**Figure 2.5 | AgRP→PBN Neuron Activity Suppresses Inflammatory Pain.**

(A) Immediate early gene protein expression analysis was performed to detect changes in neural activity in AgRP neuron target regions following formalin paw injection. Fos+ neurons in each target region (PVH depicted here) were quantified per unilateral brain section under the area of dense AgRP axonal projections (red, outlined by white dashed line). Scale bar, 150  $\mu$ m. Graph depicts quantification of Fos+ neurons in the PVH under AgRP axons following no treatment (n), saline paw injection (s), or formalin paw injection (f). (B) Representative images and graphs depicting quantification of Fos+ neurons under AgRP axons following no treatment (n), saline paw injection (s), or formalin paw injection (f) (n=9, 2-4 images per mouse per target region, one-way ANOVA within brain region,  $p < 0.05$  for BNST, CeA, PAG, PBN). Scale bar, 150  $\mu$ m. (C) Diagram of the major AgRP neuron projection subpopulations analyzed. Delivery of light to individual axon target fields of AgRP neurons (BNST shown here) allows for selective activation of discrete AgRP neuron projection subpopulations. (D) Time spent paw licking following formalin injection during optogenetic stimulation of AgRP neuron projection subpopulations (n=9-12/target region, two-way repeated measures ANOVA,  $p < 0.01$ ). (E) Inflammatory phase formalin-induced paw licking (time)

with (+, colored boxes) and without (-, grey boxes) AgRP neuron stimulation of discrete projection subpopulations (paired t-tests with Bonferroni correction, all ps=ns except for PBN,  $p<0.001$ ). **(F)** Acute phase formalin-induced paw licking (time) with (colored boxes) and without (grey boxes) AgRP neuron stimulation of discrete projection subpopulations (paired t-tests with Bonferroni correction, all ps=ns). **(G)** Latency to paw withdrawal from 52°C hotplate in AgRP→PBN<sup>ChR2</sup> mice (n=12, one-way ANOVA, p=ns). Data are expressed as mean ± SEM, ns  $p>0.05$ , t-tests and post-hoc comparisons: \* $p<0.05$ , \*\* $p<0.01$ , \*\*\* $p<0.001$ ; ANOVA interaction:  $\infty\infty p<0.01$ ; ANOVA main effect of group: ☼☼☼ $p<0.001$ .

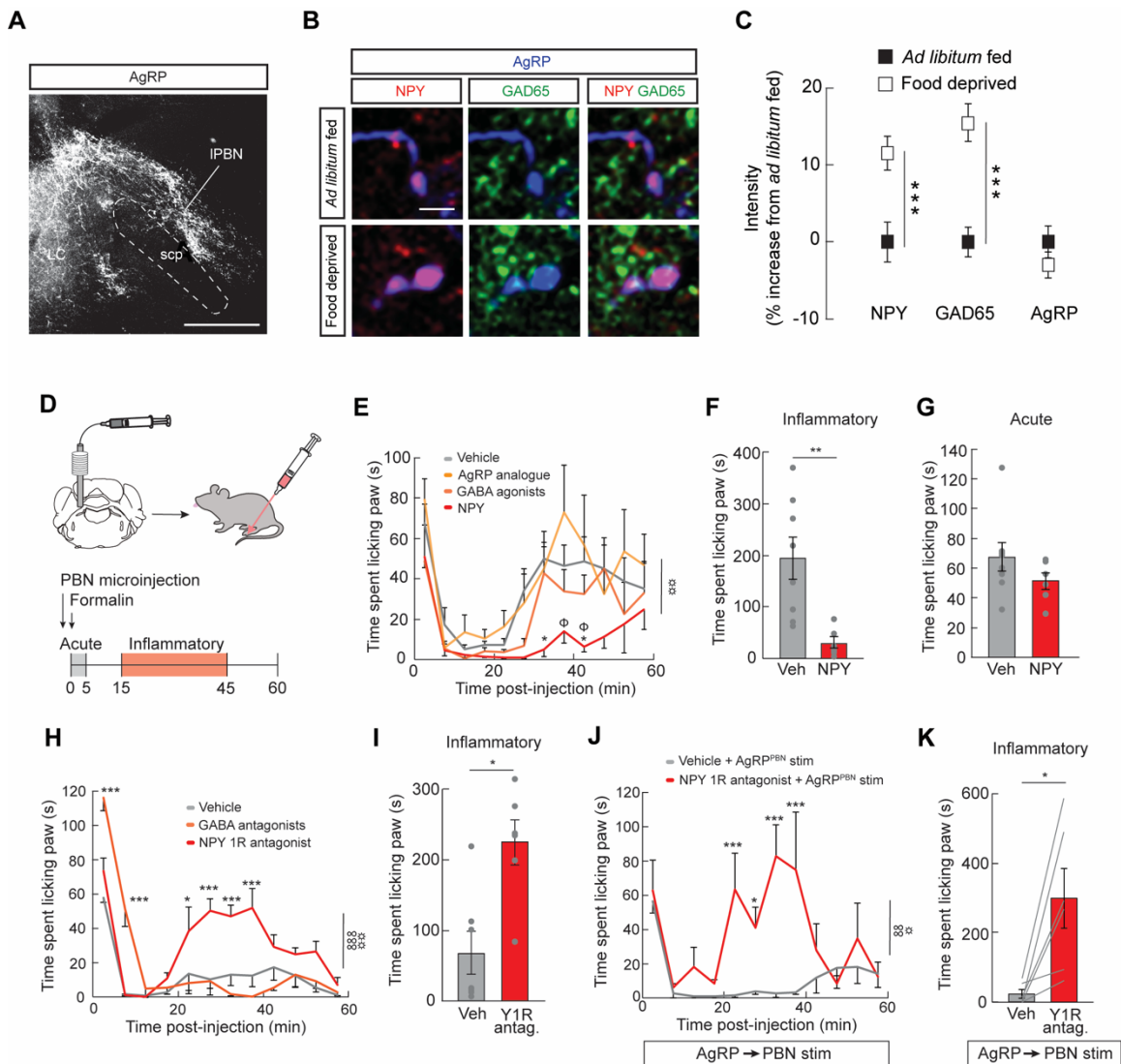


**Figure 2.6 | Lateral PBN NPY Signaling Suppresses Inflammatory Pain.**

(A) Representative image of AgRP fibers terminating in the lateral PBN (IPBN) and locus coeruleus area. LC, locus coeruleus; IPBN, lateral PBN; scp, superior cerebellar peduncle. Scale bar, 500  $\mu$ m. (B) Representative images of NPY (red), GAD65 (green) and AgRP (blue) immunofluorescence in AgRP $\rightarrow$ IPBN neuron boutons of *ad libitum* fed and 24 h food deprived mice. Scale bar, 5  $\mu$ m. (C) Average intensity of NPY, GAD65, and AgRP immunofluorescence in 24 h food deprived mice (n=3 mice, 256 boutons) relative to *ad libitum* fed controls (n=2 mice, 366 boutons) (unpaired t-tests,  $p$ s<0.001). (D) Experimental design: IPBN microinjections were

performed immediately before formalin paw injection. **(E)** Formalin-induced paw licking (time) in IPBN vehicle-, NPY-, GABA agonists-, and AgRP analogue-microinjected mice (n=6-8/group, two-way ANOVA, main effect of drug  $p<0.01$ ). Post-hoc comparisons: \* $p<0.05$  vehicle vs. NPY;  $\Phi p<0.05$  NPY vs. AgRP analogue. **(F)** Inflammatory phase formalin-induced paw licking (time) in IPBN vehicle- and NPY-microinjected mice (unpaired t-test,  $p<0.01$ ). **(G)** Acute phase formalin-induced paw licking (time) in IPBN vehicle- and NPY-microinjected mice (unpaired t-test,  $p=ns$ ). **(H)** Formalin-induced paw licking (time) in IPBN vehicle-, Y1 receptor (Y1R) antagonist-, and GABA receptor antagonist-microinjected mice (n=6-7/group, two-way repeated measures ANOVA,  $p<0.001$ ). **(I)** Inflammatory phase formalin-induced paw licking (time) in IPBN vehicle- and Y1R antagonist-microinjected mice (unpaired t-test,  $p<0.05$ ). **(J)** Formalin-induced paw licking (time) in IPBN vehicle- and Y1 receptor (Y1R) antagonist-microinjected mice with AgRP→PBN neuron stimulation (n=6, two-way repeated measures ANOVA,  $p<0.01$ ). **(K)** Inflammatory phase formalin-induced paw licking (time) in IPBN vehicle- and Y1R antagonist-microinjected mice with AgRP→PBN neuron stimulation (unpaired t-test,  $p<0.05$ ). Data are expressed as mean  $\pm$  SEM, ns  $p>0.05$ , t-tests and post-hoc comparisons: \* $p<0.05$ , \*\* $p<0.01$ , \*\*\* $p<0.001$ ; ANOVA interaction:  $\infty\infty p<0.01$ ,  $\infty\infty\infty p<0.001$ ; ANOVA main effect of drug:  $\odot p<0.05$ ,  $\odot\odot p<0.01$ ,  $\odot\odot\odot p<0.001$ .

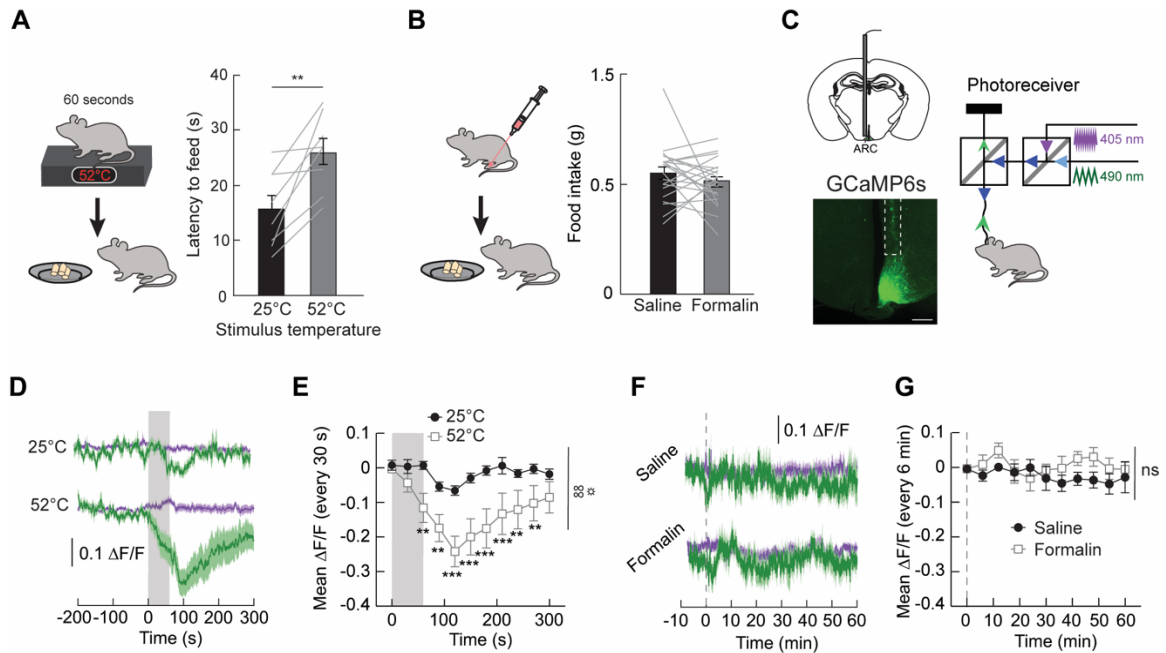


**Figure 2.7 | Acute Pain Inhibits Feeding Behavior and Activity in AgRP Neurons.**

(A) Left, experimental design: latency to feed (first bite) was measured following 60 s exposure to a 52°C hotplate. Right, graph: latency to feed after 60 s exposure to either a 25°C or 52°C plate ( $n=8$ , paired t-test,  $p<0.01$ ). (B) Left, experimental design: 1 h food intake was measured after formalin paw injection. Right, graph: 1 h food intake in food deprived mice after paw injection of saline or formalin ( $n=21$ , paired t-test,  $p=ns$ ). (C) Left, schematic and representative image of expression of the calcium indicator GCaMP6s in AgRP neurons. Scale bar, 500  $\mu\text{m}$ . Right, configuration for monitoring calcium dynamics *in vivo* using GCaMP6s expressed in AgRP neurons. The 490 nm excitation activates the calcium-dependent GCaMP6s signal and the 405 nm excitation activates the calcium-independent (*isosbestic*) GCaMP6s fluorescence. (D) Calcium-dependent (mean, dark green; SEM, green shading) and calcium-independent (mean, dark purple; SEM, purple shading) change in fluorescence ( $\Delta F/F$ ) in AgRP neurons following exposure to 25°C or 52°C plate ( $n=10$ ). Grey shaded region indicates time exposed to hotplate. (E) Quantification of change in fluorescence (30 s time bins) in mice following exposure to 25°C or 52°C plate ( $n=10$ , two-way repeated measures ANOVA,  $p<0.01$ ). (F) Calcium-dependent (mean, dark green; SEM,

green shading) and calcium-independent (mean, dark purple; SEM, purple shading) change in fluorescence ( $\Delta F/F$ ) in AgRP neurons following saline or formalin paw injection (n=8). Dashed line indicates time of paw injection. **(G)** Quantification of change in fluorescence (6 min time bins) in mice following saline or formalin paw injection (n=8, two-way repeated measures ANOVA, p=ns). Data are expressed as mean  $\pm$  SEM, ns  $p > 0.05$ , t-tests and post-hoc comparisons: \*\* $p < 0.01$ , \*\*\* $p < 0.001$ ; ANOVA interaction:  $\infty p < 0.01$ ; ANOVA main effect of group:  $\odot p < 0.05$ .

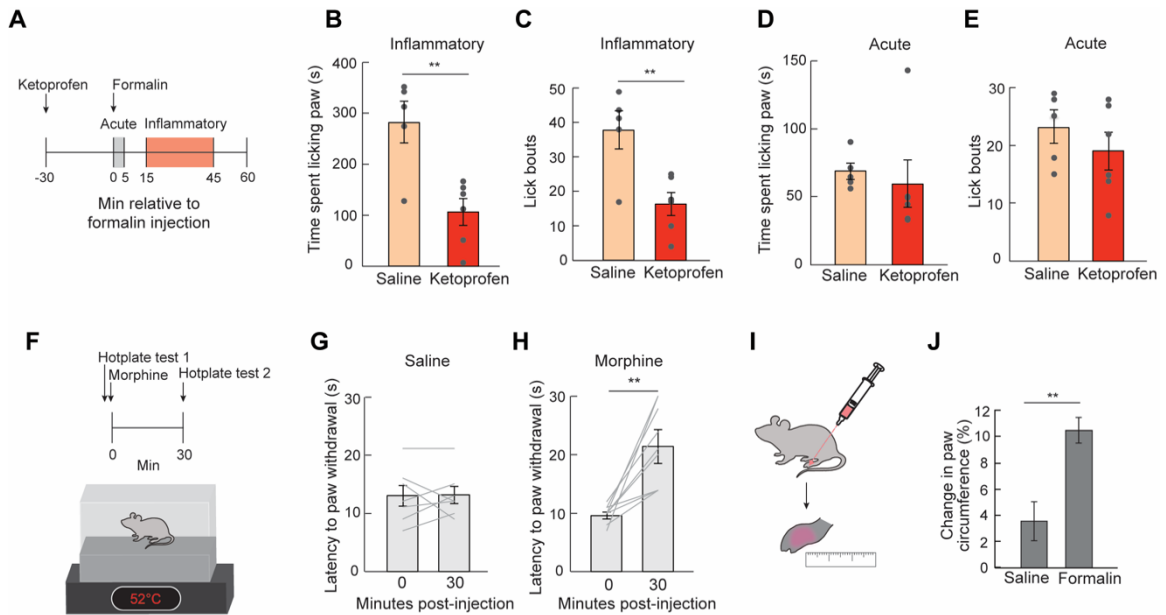


**Figure 2.S1, Related to Figure 2.1 | Anti-Inflammatory and Opiate Drug Administration Reduce Responses to Inflammatory Phase and Thermal Pain, Respectively.**

(A) Experimental timeline for effects of an anti-inflammatory analgesic (ketoprofen) on the formalin test. (B) Inflammatory phase formalin-induced paw licking (time) in i.p. saline- (n=5) and ketoprofen- (n=6) treated mice (unpaired t-test,  $p < 0.01$ ). (C) Inflammatory phase formalin-induced lick bouts in saline- and ketoprofen-treated mice (unpaired t-test,  $p < 0.01$ ). (D) Acute phase formalin-induced paw licking (time) in saline- and ketoprofen-treated mice (unpaired t-test,  $p = ns$ ). (E) Acute phase formalin-induced lick bouts in saline- and ketoprofen-treated mice (unpaired t-test,  $p = ns$ ). (F) Experimental timeline for effects of morphine on the hotplate test. (G) Latency to paw withdrawal from 52°C hotplate before and 30 min post i.p. saline injection (paired t-test,  $p = ns$ ). (H) Latency to paw withdrawal from hotplate before and 30 min post i.p. morphine injection (paired t-test,  $p < 0.01$ ). (I) Experimental design: 24 h food deprived mice were injected with saline or formalin in their hindpaw and change in paw circumference was measured 30 min post-injection. (J) Change in paw circumference in food deprived saline- (n=6) and formalin- (n=9) injected mice (unpaired t-test,  $p < 0.01$ ). Data are expressed as mean  $\pm$  SEM, ns  $p > 0.05$ , t-tests: \*\* $p < 0.01$ .

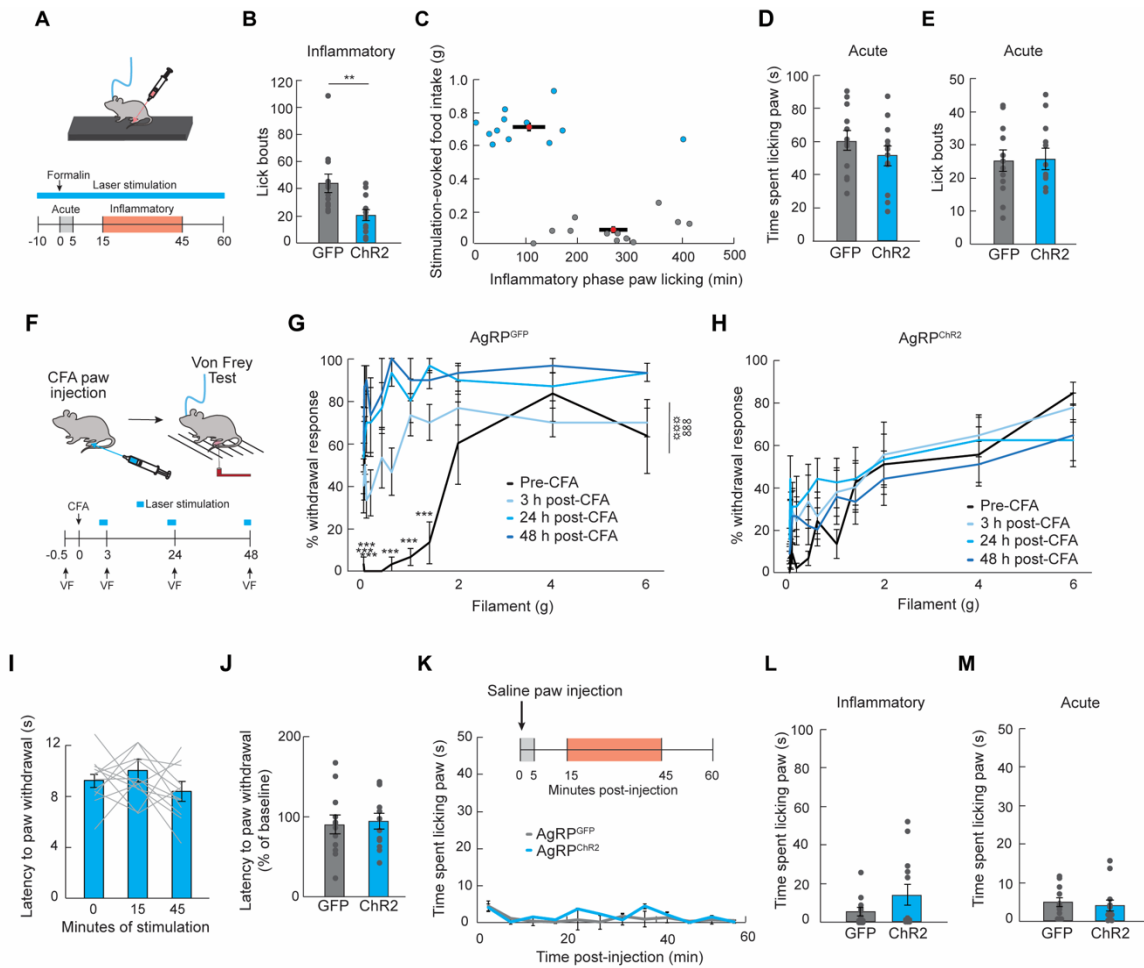


**Figure 2.S2, Related to Figure 2.4 | AgRP Neuron Activity Specifically Inhibits Inflammatory Phase Pain Response Without Off-Target Licking Effects.**

**(A)** Experimental design: Laser light pulses delivered to AgRP neurons of AgRP<sup>GFP</sup> and AgRP<sup>ChR2</sup> mice began 10 min before formalin injection and continued while formalin-induced paw licking was quantified. **(B)** Inflammatory phase formalin-induced lick bouts in AgRP<sup>GFP</sup> and AgRP<sup>ChR2</sup> mice (unpaired t-test, p<0.01). **(C)** Laser stimulation-induced food intake (y-axis) correlates with inflammatory phase paw licking (x-axis); AgRP<sup>GFP</sup> (grey circles, n=12), AgRP<sup>ChR2</sup> (blue circles, n=12), red circles are group averages (Pearson regression, R=0.60, p<0.01). **(D)** Time spent paw licking during acute phase of formalin test in AgRP<sup>GFP</sup> and AgRP<sup>ChR2</sup> mice (unpaired t-test, p=ns) **(E)** Acute phase formalin-induced lick bouts in AgRP<sup>GFP</sup> and AgRP<sup>ChR2</sup> mice (unpaired t-test, p=ns). **(F)** Experimental design: AgRP<sup>GFP</sup> and AgRP<sup>ChR2</sup> mice were injected with Complete Freund's

Adjuvant (CFA) after a baseline Von Frey test. Mice underwent additional Von Frey tests at 3h, 24 h, and 48 h post-CFA injection, with 1 h of laser stimulation before each test. **(G)** Percentage withdrawal from Von Frey Filaments before and 3 h, 24 h, and 48 h post-CFA injection in AgRP<sup>GFP</sup> mice (n=6, two-way repeated measures ANOVA, p<0.001). **(H)** Percentage withdrawal from Von Frey Filaments before and 3 h, 24 h, and 48 h post-CFA injection in AgRP<sup>Chr2</sup> mice (n=9, two-way repeated measures ANOVA, p=ns). **(I)** Latency to withdraw paw from hotplate during AgRP neuron stimulation in AgRP<sup>Chr2</sup> mice (n=12, repeated-measures one-way ANOVA, p=ns). **(J)** Normalized latency to withdraw paw from hotplate in AgRP<sup>GFP</sup> and AgRP<sup>Chr2</sup> mice after 45 min of laser stimulation (unpaired t-test, p=ns). **(K)** Time spent licking paw in AgRP<sup>GFP</sup> (n=12) and AgRP<sup>Chr2</sup> (n=12) mice with laser stimulation following saline paw injection (two-way repeated measures ANOVA, p=ns). **(L)** Inflammatory phase paw licking (time) in AgRP<sup>GFP</sup> and AgRP<sup>Chr2</sup> mice during laser stimulation following saline paw injection (unpaired t-tests, p=ns). **(M)** Acute phase paw licking (time) in AgRP<sup>GFP</sup> and AgRP<sup>Chr2</sup> mice during laser stimulation following saline paw injection (unpaired t-tests, p=ns). Data are expressed as mean ± SEM, ns p>0.05, t-tests and post-hoc comparisons: \*p<0.05, \*\*p<0.01, \*\*\*p<0.001; ANOVA interaction: ∞p<0.05, ∞∞∞p<0.001; ANOVA main effect of drug: ☼☼☼p<0.001.

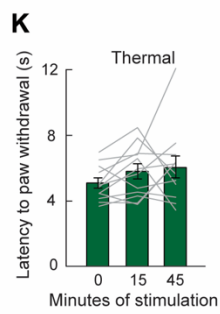
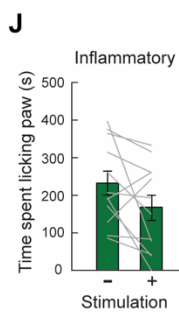
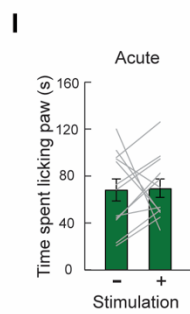
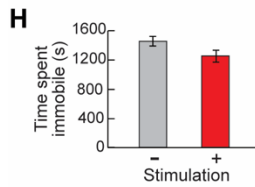
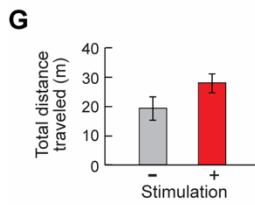
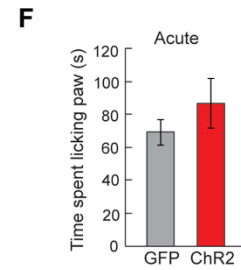
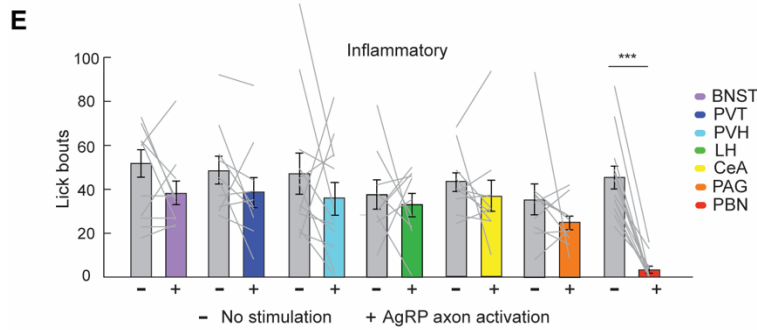
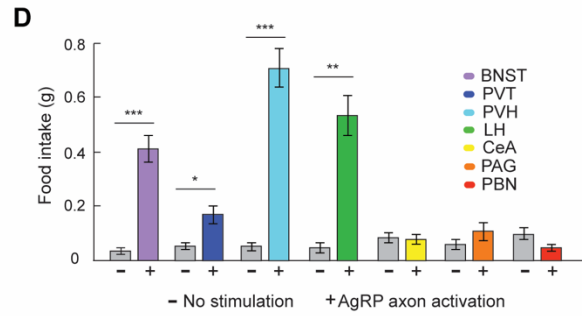
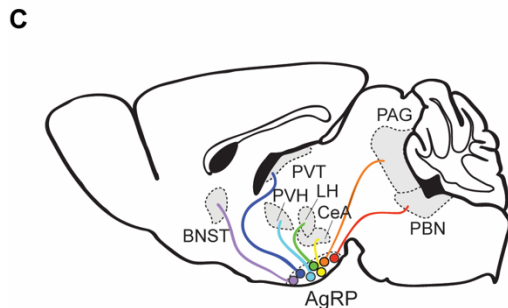
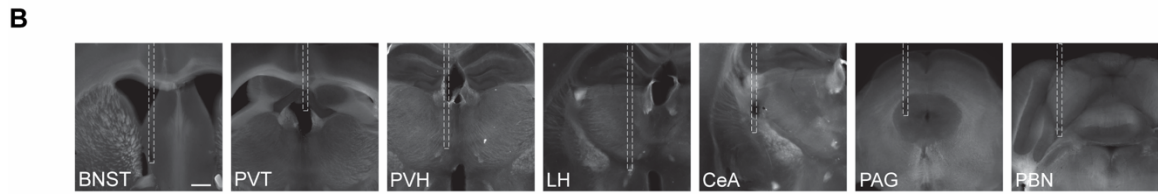
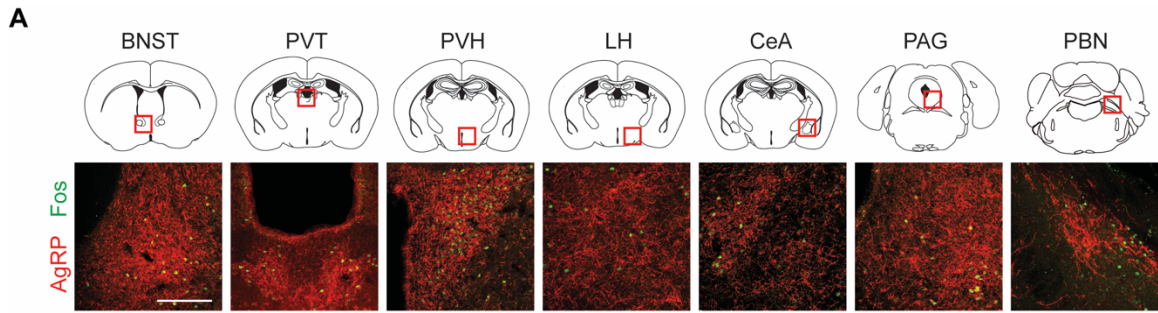


**Figure 2.S3, Related to Figure 2.4 | AgRP→PBN Neurons Selectively Mediate Inflammatory Pain.**

(A) Schematics of target brain regions and representative images of formalin-induced Fos underlying AgRP axon projections in the BNST, PVT, PVH, LH, CeA, PAG, and PBN. Scale bar, 150  $\mu$ m. (B) Representative images of fiber placements (indicated in white dotted lines). Scale bar, 1 mm. (C) Diagram of the major AgRP neuron projection subpopulations analyzed. (D) Food intake (1 h) in *ad libitum* fed mice with (+, colored bars) and without (-, grey bars) laser stimulation of AgRP axons (n=9-12/target region, paired t-test with Bonferroni correction, BNST and PVH  $p < 0.001$ ; LH  $p < 0.01$ , PVT  $p < 0.05$ ; CeA, PAG, PBN  $p = ns$ ). (E) Inflammatory phase formalin-induced lick bouts with (+, colored bars) and without (-, grey bars) AgRP neuron stimulation of discrete AgRP projection subpopulations (n=9-12/target region, paired t-tests with Bonferroni correction, all  $p = ns$  except for PBN,  $p < 0.001$ ). (F) Acute phase formalin-induced paw licking (time) in AgRP→PBN<sup>ChR2</sup> mice (n=5) following 40 min of laser stimulation compared to stimulation of AgRP→PBN<sup>GFP</sup> mice (n=12) (unpaired t-test,  $p = ns$ ). (G) Total distance traveled in AgRP→PBN<sup>ChR2</sup> mice (n=5) with and without 30 min laser stimulation (unpaired t-test,  $p = ns$ ). (H) Time spent immobile in AgRP→PBN<sup>ChR2</sup> mice (n=5) with and without 30 min laser stimulation (unpaired t-test,  $p = ns$ ). (I) Acute phase formalin-induced paw licking (time) during light pulse delivery in AgRP→PBN<sup>GFP</sup> mice (n=12, paired t-test,  $p = ns$ ). (J) Inflammatory phase formalin-induced paw licking (time) during light pulse delivery in AgRP→PBN<sup>GFP</sup> mice (n=12, paired t-test,  $p = ns$ ). (K) Latency to paw withdrawal from 52°C hotplate during light pulse delivery in AgRP→PBN<sup>GFP</sup> mice (n=12, one-way ANOVA,  $p = ns$ ). Data are expressed as mean  $\pm$  SEM, ns  $p > 0.05$ , \* $p < 0.05$ , \*\* $p < 0.01$ , \*\*\* $p < 0.001$ .

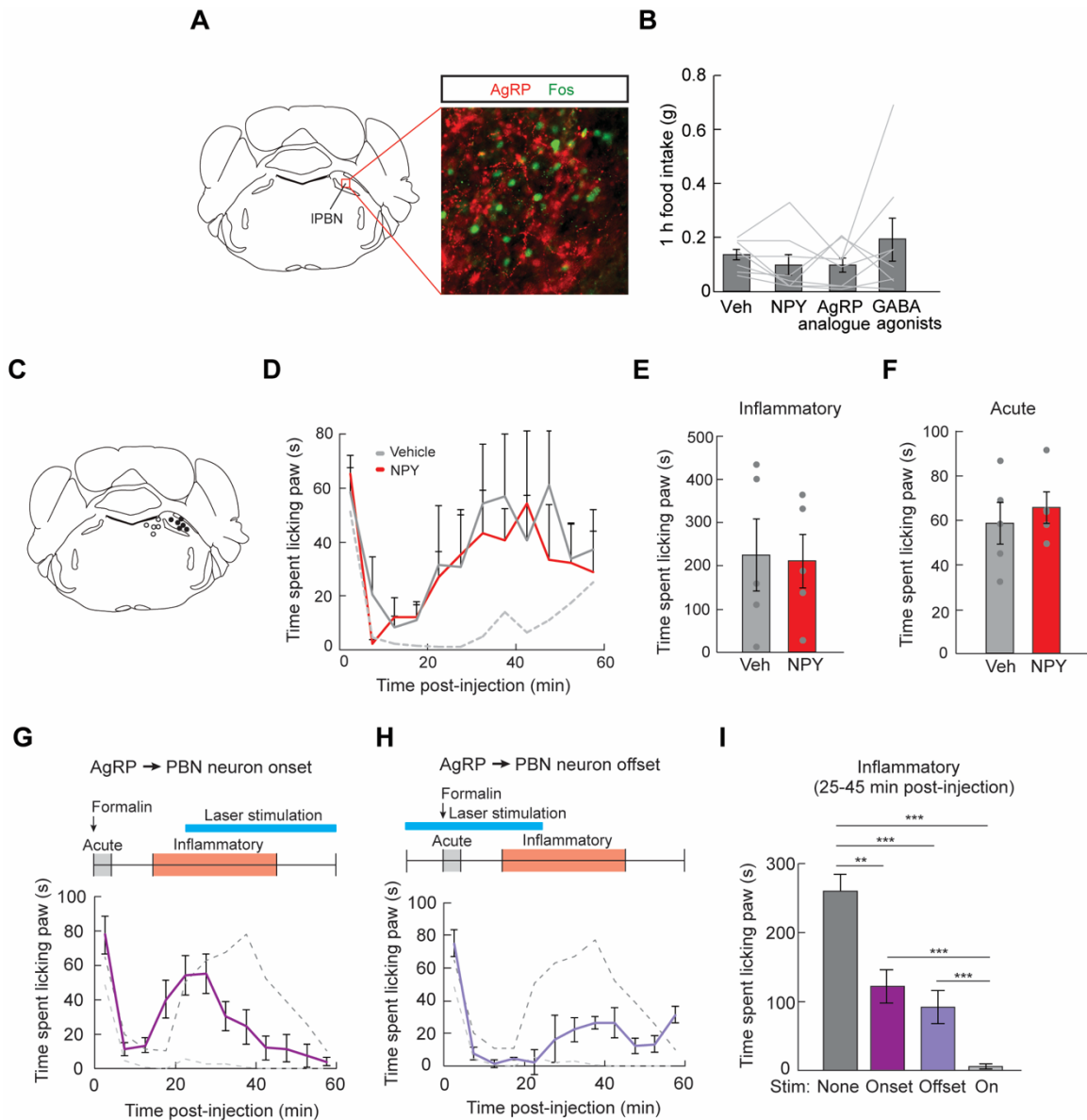


**Figure 2.S4, Related to Figure 2.6 | Peptidergic NPY signaling in the lateral PBN mediates inflammatory phase pain.**

(A) Schematic and representative image demonstrating formalin-induced Fos and AgRP axons in the lateral PBN (IPBN). (B) Food intake (1 h) following PBN microinjection of vehicle, NPY, an AgRP analogue, or GABA agonists (n=8, one-way repeated measures ANOVA, p=ns). (C) Schematic showing center of injection sites for mice injected with NPY in the IPBN (closed circles) or the locus coeruleus (LC) area (open circles). (D) Time spent licking paw in LC vehicle- (n=5) or

NPY (n=5) -injected mice (two-way repeated measures ANOVA, p=ns). (E) Inflammatory phase paw licking (time) in LC vehicle- (n=5) or NPY (n=5) -injected mice (unpaired t-tests, p=ns). (F) Acute phase paw licking (time) in LC vehicle- (n=5) or NPY (n=5) -injected mice (unpaired t-tests, p=ns). (G) Top, Experimental design: Laser stimulation was initiated 25 min post-formalin injection and lasted for the duration of the test. Bottom, graph: formalin-induced paw licking (time) with the onset of AgRP→PBN neuron activity in AgRP→PBN<sup>ChR2</sup> mice (n=12); traces of pain responses with and without AgRP→PBN<sup>ChR2</sup> stimulation for the entire session are indicated in dotted lines for reference. (H) Top, Experimental design: Laser stimulation was initiated 10 min before formalin injection and terminated 25 min post-injection. Bottom, graph: formalin-induced paw licking (time) with the offset of AgRP→PBN neuron activity in AgRP→PBN<sup>ChR2</sup> mice (n=7); traces of pain responses with and without AgRP→PBN<sup>ChR2</sup> stimulation for the entire session are indicated in dotted lines for reference. (I) Time spent responding to inflammatory pain following the onset or offset of laser stimulation (25-45 min post-injection). Inflammatory phase pain responses after the onset (magenta) and offset (purple) of AgRP→PBN<sup>ChR2</sup> stimulation are compared to the inflammatory responses with and without AgRP→PBN<sup>ChR2</sup> stimulation (unpaired t-tests with Bonferroni correction, stimulation vs. onset/offset vs. no stimulation, all ps<0.01). Data are expressed as mean ± SEM, ns p>0.05, t-tests: \*\*p<0.01, \*\*\*p<0.001

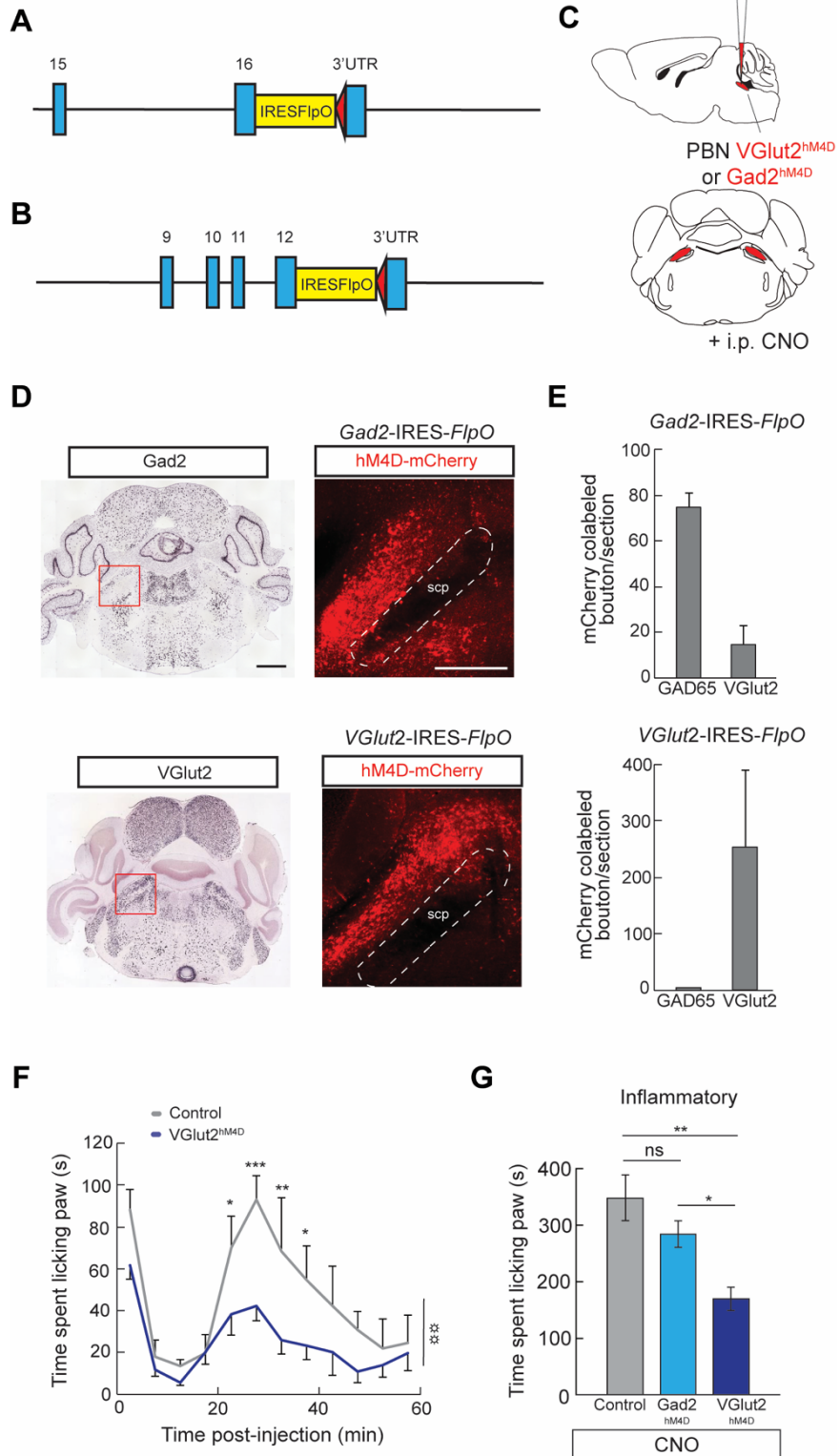


**Figure 2.S5, Related to Figure 2.6 | Glutamatergic Neurons in the IPBN Mediate Inflammatory Pain.**

(A) Genomic structure of genetically modified *Gad2* allele. (B) Genomic structure of genetically modified *VGlut2* allele. (C) Strategy for expressing hM4D in *Gad2* and *VGlut2* PBN neurons: A FlpO-dependent rAAV expressing Cre was combined with a Cre-dependent rAAV expressing hM4D as in (Li et al., 2013), allowing for the expression of hM4D in *Gad2*<sup>+</sup> and *VGlut2*<sup>+</sup> IPBN neurons. These neurons were inhibited by i.p. injection of clozapine-N-oxide (CNO) as previously demonstrated (Mu et al., 2017). (D) Left, *in situ* hybridization for *Gad2* and *VGlut2* mRNA in the PBN [images from Allen Brain Explorer, <http://mouse.brain-map.org>, (Lein et al., 2007)]. Red boxes indicated region of images to the right. Scale bar, 1 mm. Right, representative images of hM4D-mCherry expression (red) in the IPBN of experimental mice. Quantification of IPBN sections revealed an average of  $98.2 \pm 6.4$  and  $194.8 \pm 35.9$  hM4D-expressing neurons (per unilateral section) in *Gad2-IRES-FlpO* (n=6) and *VGlut2-IRES-FlpO* mice, respectively. Scale bar, 500  $\mu$ m. scp, superior cerebellar peduncle. (E) Quantification of GAD65<sup>+</sup> or *VGlut2*<sup>+</sup> boutons colabeled with mCherry in *Gad2-IRES-FlpO* (top) and *VGlut2-IRES-FlpO* (bottom) mice. (F) Time spent licking paw in control (n=5) and *VGlut2*<sup>hM4D</sup> (n=6) neurons after injection of CNO (two-way repeated measures ANOVA, main effect of group,  $p < 0.01$ ). (G) Inflammatory phase paw licking in control (n=5), *Gad2*<sup>hM4D</sup> (n=6) *Vglut2*<sup>hM4D</sup> (n=6) mice following CNO injection. Data are expressed as mean  $\pm$  SEM, ns  $p > 0.05$ , t-tests and post-hoc comparisons: \* $p < 0.05$ , \*\* $p < 0.01$ , \*\*\* $p < 0.001$ ; ANOVA main effect of group:  $\odot\odot\odot p < 0.01$ .

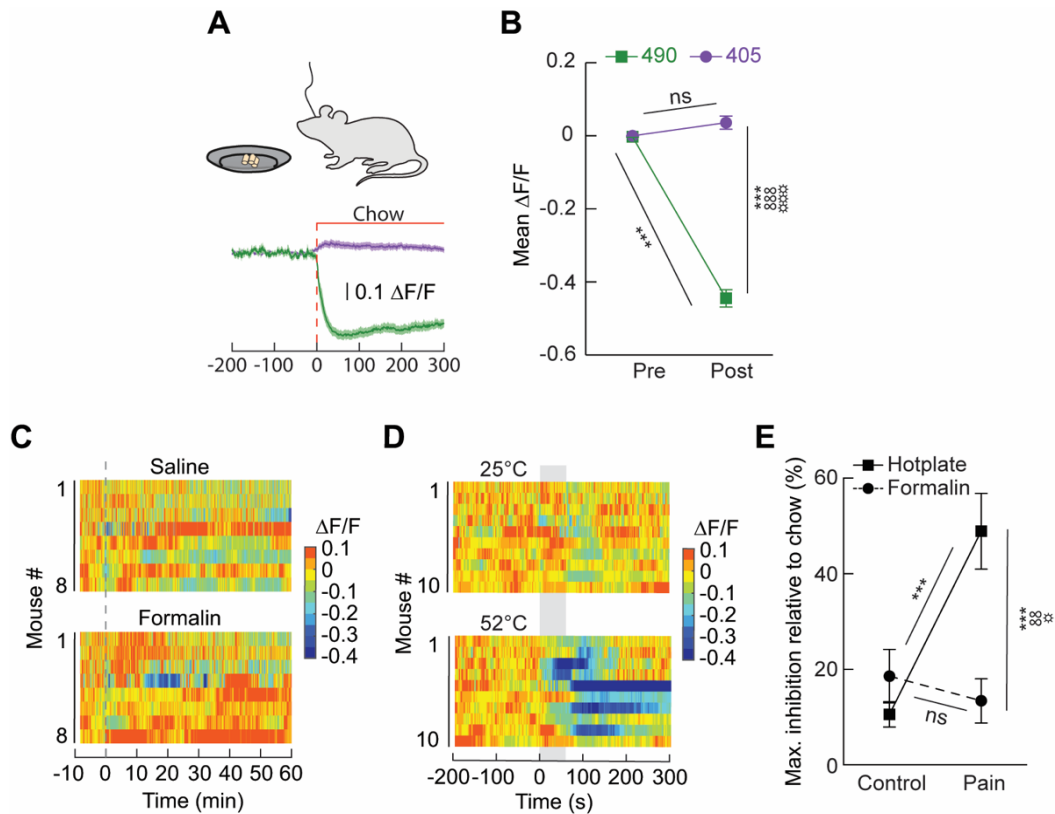


**Figure 2.S6, Related to Figure 2.7 | Acute Thermal but not Formalin-Induced Pain**

**Suppresses AgRP Neuron Activity.**

(A) Calcium-dependent (mean, dark green; SEM, green shading) and calcium-independent (mean, dark purple; SEM, purple shading) change in fluorescence ( $\Delta F/F$ ) in AgRP neurons of food restricted mice ( $n=10$ ) before and after chow refeeding. (B) Mean change in GCaMP6s signal ( $\Delta F/F$ ) before and after chow presentation (two-way repeated measures ANOVA,  $p<0.001$ ). (C) GCaMP6s fluorescence changes ( $\Delta F/F$ ) of AgRP neurons in individual mice with saline or formalin paw injection. (D) GCaMP6s fluorescence changes ( $\Delta F/F$ ) in AgRP neurons of individual mice with 60 s exposure to 25°C or 52°C plate. (E) Maximum change in AgRP neuron calcium dynamics with formalin or hotplate exposure relative to activity change observed following chow presentation ( $n=10$  25°C/52°C plate,  $n=8$  saline/formalin injection; two-way repeated-measures ANOVA,  $p<0.01$ ). Data are expressed as mean  $\pm$  SEM, ns  $p>0.05$ , t-tests and post-hoc comparisons: \*\*\* $p<0.001$ ; ANOVA interaction:  $\infty\infty p<0.01$ ,  $\infty\infty\infty p<0.001$ ; ANOVA

main effect of pre vs. post chow presentation (Figure S6B) or ANOVA main effect of condition (Figure S6E): ☉ $p<0.05$ , ☉☉☉ $p<0.001$ .

### **Acknowledgments**

This research was funded by the University of Pennsylvania School of Arts and Sciences (J.N.B.), AHA 17SDG33400158 (J.N.B.), the Whitehall Foundation (J.N.B), NIH-1R01DK1114104 (J.N.B), NIH-2T32DK7314-36 (A.L.A), NIH-F32DK112561-01 (A.L.A.) and NIH-R01DK112812 (B.C.D.). We thank S. Pulido, B. Jannuzi, O. Park, C. Shin, K. Patel, I. Cogdell, R. Ly, O. Green and P. Ehmann for experimental assistance, and S. Sternson, H. Grill, M. Schmidt and A. Chen for comments on the manuscript.

## References

- Alhadeff, A.L., Golub, D., Hayes, M.R., and Grill, H.J. (2015). Peptide YY signaling in the lateral parabrachial nucleus increases food intake through the Y1 receptor. *American journal of physiology Endocrinology and metabolism* 309, E759-766.
- Alhadeff, A.L., Holland, R.A., Zheng, H., Rinaman, L., Grill, H.J., and De Jonghe, B.C. (2017). Excitatory Hindbrain-Forebrain Communication Is Required for Cisplatin-Induced Anorexia and Weight Loss. *J Neurosci* 37, 362-370.
- Andermann, M.L., and Lowell, B.B. (2017). Toward a Wiring Diagram Understanding of Appetite Control. *Neuron* 95, 757-778.
- Aponte, Y., Atasoy, D., and Sternson, S.M. (2011). AGRP neurons are sufficient to orchestrate feeding behavior rapidly and without training. *Nature neuroscience* 14, 351-355.
- Atasoy, D., Betley, J.N., Su, H.H., and Sternson, S.M. (2012). Deconstruction of a neural circuit for hunger. *Nature* 488, 172-177.
- Baulmann, J., Spitznagel, H., Herdegen, T., Unger, T., and Culman, J. (2000). Tachykinin receptor inhibition and c-Fos expression in the rat brain following formalin-induced pain. *Neuroscience* 95, 813-820.
- Betley, J.N., Cao, Z.F., Ritola, K.D., and Sternson, S.M. (2013). Parallel, redundant circuit organization for homeostatic control of feeding behavior. *Cell* 155, 1337-1350.
- Betley, J.N., Wright, C.V., Kawaguchi, Y., Erdelyi, F., Szabo, G., Jessell, T.M., and Kaltschmidt, J.A. (2009). Stringent specificity in the construction of a GABAergic presynaptic inhibitory circuit. *Cell* 139, 161-174.
- Betley, J.N., Xu, S., Cao, Z.F., Gong, R., Magnus, C.J., Yu, Y., and Sternson, S.M. (2015). Neurons for hunger and thirst transmit a negative-valence teaching signal. *Nature* 521, 180-185.
- Bodnar, R., Kelly, D., Spiaggia, A., Glusman, M. (1978). Biphasic alterations of nociceptive thresholds induced by food deprivation. *Physiological Psychology* 6, 391-395.
- Bodnar, R.J., Kelly, D.D., Spiaggia, A., and Glusman, M. (1977). Analgesia Produced by Cold-Water Stress - Effect of Naloxone. *Federation proceedings* 36, 1010-1010.
- Bodnar, R.J., Kelly, D.D., Spiaggia, A., and Glusman, M. (1978a). Biphasic Alterations of Nociceptive Thresholds Induced by Food-Deprivation. *Physiological Psychology* 6, 391-395.
- Bodnar, R.J., Kelly, D.D., Steiner, S.S., and Glusman, M. (1978b). Stress-produced analgesia and morphine-produced analgesia: lack of cross-tolerance. *Pharmacology, biochemistry, and behavior* 8, 661-666.
- Burnett, C.J., Li, C., Webber, E., Tsaousidou, E., Xue, S.Y., Bruning, J.C., and Krashes, M.J. (2016). Hunger-Driven Motivational State Competition. *Neuron* 92, 187-201.
- Campos, C.A., Bowen, A.J., Schwartz, M.W., and Palmiter, R.D. (2016). Parabrachial CGRP Neurons Control Meal Termination. *Cell metabolism* 23, 811-820.
- Carey, L.M., Gutierrez, T., Deng, L., Lee, W.H., Mackie, K., and Hohmann, A.G. (2017). Inflammatory and Neuropathic Nociception is Preserved in GPR55 Knockout Mice. *Sci Rep* 7, 944.

- Carter, M.E., Soden, M.E., Zweifel, L.S., and Palmiter, R.D. (2013). Genetic identification of a neural circuit that suppresses appetite. *Nature* 503, 111-114.
- Chen, Y., Lin, Y.C., Kuo, T.W., and Knight, Z.A. (2015). Sensory detection of food rapidly modulates arcuate feeding circuits. *Cell* 160, 829-841.
- Coderre, T.J., Vaccarino, A.L., and Melzack, R. (1990). Central nervous system plasticity in the tonic pain response to subcutaneous formalin injection. *Brain Res* 535, 155-158.
- Deyama, S., Yamamoto, J., Machida, T., Tanimoto, S., Nakagawa, T., Kaneko, S., Satoh, M., and Minami, M. (2007). Inhibition of glutamatergic transmission by morphine in the basolateral amygdaloid nucleus reduces pain-induced aversion. *Neurosci Res* 59, 199-204.
- Dietrich, M.O., Zimmer, M.R., Bober, J., and Horvath, T.L. (2015). Hypothalamic AgRP neurons drive stereotypic behaviors beyond feeding. *Cell* 160, 1222-1232.
- Dubuisson, D., and Dennis, S.G. (1977). The formalin test: a quantitative study of the analgesic effects of morphine, meperidine, and brain stem stimulation in rats and cats. *Pain* 4, 161-174.
- Essner, R.A., Smith, A.G., Jamnik, A.A., Ryba, A.R., Trutner, Z.D., and Carter, M.E. (2017). AgRP Neurons Can Increase Food Intake during Conditions of Appetite Suppression and Inhibit Anorexigenic Parabrachial Neurons. *J Neurosci* 37, 8678-8687.
- Grill, H.J. (2006). Distributed neural control of energy balance: contributions from hindbrain and hypothalamus. *Obesity* 14 Suppl 5, 216S-221S.
- Gunaydin, L.A., Grosenick, L., Finkelstein, J.C., Kauvar, I.V., Fenno, L.E., Adhikari, A., Lammel, S., Mirzabekov, J.J., Airan, R.D., Zalocusky, K.A., et al. (2014). Natural neural projection dynamics underlying social behavior. *Cell* 157, 1535-1551.
- Hamm, R.J., and Lyeth, B.G. (1984). Nociceptive thresholds following food restriction and return to free-feeding. *Physiol Behav* 33, 499-501.
- Hargraves, W.A., and Hentall, I.D. (2005). Analgesic effects of dietary caloric restriction in adult mice. *Pain* 114, 455-461.
- Higgs, S., and Cooper, S.J. (1996). Hyperphagia induced by direct administration of midazolam into the parabrachial nucleus of the rat. *Eur J Pharmacol* 313, 1-9.
- Hnasko, T.S., Chuhma, N., Zhang, H., Goh, G.Y., Sulzer, D., Palmiter, R.D., Rayport, S., and Edwards, R.H. (2010). Vesicular glutamate transport promotes dopamine storage and glutamate corelease in vivo. *Neuron* 65, 643-656.
- Hunziker, S., and Hole, K. (1987). The formalin test in mice: dissociation between inflammatory and non-inflammatory pain. *Pain* 30, 103-114.
- Jikomes, N., Ramesh, R.N., Mandelblat-Cerf, Y., and Andermann, M.L. (2016). Preemptive Stimulation of AgRP Neurons in Fed Mice Enables Conditioned Food Seeking under Threat. *Curr Biol* 26, 2500-2507.
- Johansen, J.P., and Fields, H.L. (2004). Glutamatergic activation of anterior cingulate cortex produces an aversive teaching signal. *Nat Neurosci* 7, 398-403.
- Jonas, P., Bischofberger, J., and Sandkuhler, J. (1998). Corelease of two fast neurotransmitters at a central synapse. *Science* 281, 419-424.

- Keys, A. (1946). Experimental Human Starvation - General and Metabolic Results of a Loss of One 4th the Body Weight in 6 Months. *Fed Proc* 5, 55-55.
- Krashes, M.J., Koda, S., Ye, C., Rogan, S.C., Adams, A.C., Cusher, D.S., Maratos-Flier, E., Roth, B.L., and Lowell, B.B. (2011). Rapid, reversible activation of AgRP neurons drives feeding behavior in mice. *J Clin Invest* 121, 1424-1428.
- LaGraize, S.C., Borzan, J., Rinker, M.M., Kopp, J.L., and Fuchs, P.N. (2004). Behavioral evidence for competing motivational drives of nociception and hunger. *Neurosci Lett* 372, 30-34.
- Lein, E.S., Hawrylycz, M.J., Ao, N., Ayres, M., Bensinger, A., Bernard, A., Boe, A.F., Boguski, M.S., Brockway, K.S., Byrnes, E.J., et al. (2007). Genome-wide atlas of gene expression in the adult mouse brain. *Nature* 445, 168-176.
- Lerner, T.N., Shilyansky, C., Davidson, T.J., Evans, K.E., Beier, K.T., Zalocusky, K.A., Crow, A.K., Malenka, R.C., Luo, L., Tomer, R., et al. (2015). Intact-Brain Analyses Reveal Distinct Information Carried by SNc Dopamine Subcircuits. *Cell* 162, 635-647.
- Li, H., Penzo, M.A., Taniguchi, H., Kopec, C.D., Huang, Z.J., and Li, B. (2013). Experience-dependent modification of a central amygdala fear circuit. *Nat Neurosci* 16, 332-339.
- Liu, P., Jenkins, N.A., and Copeland, N.G. (2003). A highly efficient recombineering-based method for generating conditional knockout mutations. *Genome research* 13, 476-484.
- Loeser, J.D. (2012). Relieving pain in America. *Clin J Pain* 28, 185-186.
- Luquet, S., Perez, F.A., Hnasko, T.S., and Palmiter, R.D. (2005). NPY/AgRP neurons are essential for feeding in adult mice but can be ablated in neonates. *Science* 310, 683-685.
- Madisen, L., Mao, T., Koch, H., Zhuo, J.M., Berenyi, A., Fujisawa, S., Hsu, Y.W., Garcia, A.J., 3rd, Gu, X., Zanella, S., et al. (2012). A toolbox of Cre-dependent optogenetic transgenic mice for light-induced activation and silencing. *Nature neuroscience* 15, 793-802.
- Mandelblat-Cerf, Y., Ramesh, R.N., Burgess, C.R., Patella, P., Yang, Z., Lowell, B.B., and Andermann, M.L. (2015). Arcuate hypothalamic AgRP and putative POMC neurons show opposite changes in spiking across multiple timescales. *eLife* 4.
- Marchand, F., Perretti, M., and McMahon, S.B. (2005). Role of the immune system in chronic pain. *Nat Rev Neurosci* 6, 521-532.
- Martins-Oliveira, M., Akerman, S., Tavares, I., and Goadsby, P.J. (2016). Neuropeptide Y inhibits the trigeminovascular pathway through NPY Y1 receptor: implications for migraine. *Pain* 157, 1666-1673.
- Miller, L.R., and Cano, A. (2009). Comorbid chronic pain and depression: who is at risk? *J Pain* 10, 619-627.
- Mu, D., Deng, J., Liu, K.F., Wu, Z.Y., Shi, Y.F., Guo, W.M., Mao, Q.Q., Liu, X.J., Li, H., and Sun, Y.G. (2017). A central neural circuit for itch sensation. *Science* 357, 695-699.
- Naveilhan, P., Hassani, H., Lucas, G., Blakeman, K.H., Hao, J.X., Xu, X.J., Wiesenfeld-Hallin, Z., Thoren, P., and Ernfor, P. (2001). Reduced antinociception and plasma extravasation in mice lacking a neuropeptide Y receptor. *Nature* 409, 513-517.

- Padilla, S.L., Qiu, J., Soden, M.E., Sanz, E., Nestor, C.C., Barker, F.D., Quintana, A., Zweifel, L.S., Ronnekleiv, O.K., Kelly, M.J., et al. (2016). Agouti-related peptide neural circuits mediate adaptive behaviors in the starved state. *Nat Neurosci* 19, 734-741.
- Pavlov, I.P., and Fol'bert, G.V. (1926). Die höchste Nerventätigkeit (das Verhalten) von Tieren. Eine zwanzigjährige Prüfung der objektiven Forschung ; Bedingte Reflexe. Sammlung von Artikeln, Berichten, Vorlesungen und Reden, 3. Aufl., übers. von G. Volbroth. edn (München,: J. F. Bergmann).
- Penzo, M.A., Robert, V., Tucciarone, J., De Bundel, D., Wang, M., Van Aelst, L., Darvas, M., Parada, L.F., Palmiter, R.D., He, M., et al. (2015). The paraventricular thalamus controls a central amygdala fear circuit. *Nature* 519, 455-459.
- Pollatos, O., Herbert, B.M., Fustos, J., Weimer, K., Enck, P., and Zipfel, S. (2012). Food Deprivation Sensitizes Pain Perception. *J Psychophysiol* 26, 1-9.
- Price, D.D. (2000). Psychological and neural mechanisms of the affective dimension of pain. *Science* 288, 1769-1772.
- Skibicka, K.P., and Grill, H.J. (2009). Hypothalamic and hindbrain melanocortin receptors contribute to the feeding, thermogenic, and cardiovascular action of melanocortins. *Endocrinology* 150, 5351-5361.
- Solway, B., Bose, S.C., Corder, G., Donahue, R.R., and Taylor, B.K. (2011). Tonic inhibition of chronic pain by neuropeptide Y. *Proc Natl Acad Sci U S A* 108, 7224-7229.
- Stanley, B.G., and Leibowitz, S.F. (1985). Neuropeptide Y injected in the paraventricular hypothalamus: a powerful stimulant of feeding behavior. *Proc Natl Acad Sci U S A* 82, 3940-3943.
- Sternson, S.M., and Eiselt, A.K. (2017). Three Pillars for the Neural Control of Appetite. *Annu Rev Physiol* 79, 401-423.
- Su, Z., Alhadeff, A.L., and Betley, J.N. (2017). Nutritive, Post-ingestive Signals Are the Primary Regulators of AgRP Neuron Activity. *Cell reports* 21, 2724-2736.
- Tinbergen, N. (1951). *The study of instinct* (Oxford Eng.: Clarendon Press).
- Tong, Q., Ye, C.P., Jones, J.E., Elmquist, J.K., and Lowell, B.B. (2008). Synaptic release of GABA by AgRP neurons is required for normal regulation of energy balance. *Nature neuroscience* 11, 998-1000.
- Wang, J.Z., Lundeberg, T., and Yu, L.C. (2001). Anti-nociceptive effect of neuropeptide Y in periaqueductal grey in rats with inflammation. *Brain research* 893, 264-267.
- Wu, Q., Boyle, M.P., and Palmiter, R.D. (2009). Loss of GABAergic signaling by AgRP neurons to the parabrachial nucleus leads to starvation. *Cell* 137, 1225-1234.
- Zhu, H., Aryal, D.K., Olsen, R.H., Urban, D.J., Swearingen, A., Forbes, S., Roth, B.L., and Hochgeschwender, U. (2016). Cre dependent DREADD (designer receptors exclusively activated by designer drugs) mice. *Genesis*.

## STAR Methods

### CONTACT FOR REAGENT AND RESOURCE SHARING

Further information and requests for resources and reagents should be directed to and will be fulfilled by the Lead Contact, J. Nicholas Betley. ([jnbetley@sas.upenn.edu](mailto:jnbetley@sas.upenn.edu)).

### EXPERIMENTAL MODEL AND SUBJECT DETAILS

Mice were group housed on a 12 h light/12 h dark cycle with *ad libitum* access to food (Purina Rodent Chow, 5001) and water unless otherwise noted. Group housed adult male and female mice (at least 8 weeks old) were used for experimentation. *Agpr-IRES-Cre* (Jackson Labs 012899, *Agpr<sup>tm1(cre)Lowl/J</sup>*) (Tong et al., 2008), *Ai32* (Jackson Labs 012569, *B6;129S-Gt(ROSA)26Sor<sup>tm32(CAG-COP4\*H134R/EYFP)Hze/J</sup>*) (Madisen et al., 2012), *R26-LSL-Gi-DREADD* (Jackson Labs 026219, *B6N.129-Gt(ROSA)26Sor<sup>tm1(CAG-CHRM4\*,-mCitrine)/Ute/J</sup>*) (Zhu et al., 2016), *VGlut2-IRES-FlpO* and *Gad2-IRES-FlpO* generated as described in Method Details, and *C57BL/6J* mice were used for experimentation. Genotyping was performed using primers and conditions provided by Jackson Labs or custom primers for *Gad2-IRES-FlpO* and *VGlut2-IRES-FlpO* mice as described in Method Details. All mice were habituated to handling and experimental conditions prior to experiments. For within-subject behavioral analyses, all mice received all experimental conditions. For between-subject analyses, mice were randomly assigned to experimental condition. We performed experiments in both male and female subjects, and did not observe any trends or significant sex differences. Thus, to ensure our studies were appropriately powered and to minimize the number of subjects who had to undergo pain assays, we combined males and females for analyses in all experiments. All procedures were approved by the University of Pennsylvania Institutional Animal Care and Use Committee.

### METHOD DETAILS

**Recombinant Adeno-Associated Virus (rAAV) Constructs and Production:** The following Cre- or FlpO-dependent rAAV vectors were used: AAV1.CAGGS.Flex.ChR2-tdTomato.WPRE.SV40

(titer: 1.38e13 GC/ml), AAVrh10.CAGGS.flex.ChR2.tdTomato.WPRE.SV40 (titer: 1.23e13 GC/ml), AAV1rh.CAG.Flex.eGFP.WPRE.bGH (titer: 1.708e13 GC/ml), AAV1.Syn.Flex.GCaMP6s.WPRE.SV40 (titer: 4.216e13 GC/ml), AAV-fDIO-Cre-GFP (titer: 2.91e13 GC/ml), pAAV-hSyn-DIO-hM4D(Gi)-mCherry (titer: 4.3e12 GC/ml). All viruses were produced by the University of Pennsylvania Vector Core, except for the latter which was purchased from Addgene (ID 44362). CAG, promoter containing a cytomegalovirus enhancer; the promoter, first exon and first intron of the chicken beta actin gene; and the splice acceptor of rabbit beta-globin gene. Syn, human Synapsin 1 promoter. FLEX, Cre-dependent flip-excision switch. WPRE, woodchuck hepatitis virus response element. bGH, bovine growth hormone polyadenylation signal. ChR2, channelrhodopsin-2. GCaMP, Genetically encoded calcium indicator resulting from a fusion of GFP, M13 and Calmodulin. DIO, Double-floxed inverted orientation. hM4, human M4 muscarinic receptor.

#### **Generation of FlpO mice:**

*VGlut2-IRES-FlpO mouse generation:* Targeting vector construction: The targeting vector was constructed using a recombineering technique previously described (Liu et al., 2003). A 8,572 bp genomic DNA fragment containing exon 9-12 of the VGlut2 gene was retrieved from BAC clone RP23-228J18 to a vector containing the DT gene, a negative selection marker. A cassette of IRES-FlpO-loxP2272-ACE-Cre POII NeoR-loxP2272 was inserted between stop codon TAA and 3' UTR. The length of the 5' homologous arm is 5,519 bp and that for the 3' arm is 3,049 bp. ES cell targeting and screening: The targeting vector was electroporated into F1 hybrid of 129S6 x C57BL/6J ES cells derived by the Janelia Transgenic Facility. The G418 resistant ES clones were screened by nested PCR using primers outside the construct paired with primers inside the inserted cassette. The primer sequences were as follows: 5' arm forward primers: VGlut2 Scr F1 (5'-CAGCTCCTTTGAGAATGGCA-3') and VGlut2 Scr F2 (5'-CCTGACAGTTTCAAACGTGG-3'). Reverse primers: IRES R1 (5'-AGGAACTGCTTCCTTCACGA-3') and IRES R2 (5'-CCTAGGAATGCTCGTCAAGA-3'). 3' arm forward primers: ACE F3 (5'-ACAGCACCATTGTCCACTTG-3') and ACE F4, (5'-GCTGGTAAGGGATATTTGCC-3'); Reverse

primers: VGlut2 Scr R3 (5'-ACATTGGTGCCACTTAGCTG-3') and VGlut2 Scr R4 (5'-GCATGTGAGCTACCTTAAGC-3'). *Generation of chimera and F1 genotyping:* The PCR positive ES clones were expanded for generation of chimeric mice. The ES cells were aggregated with 8-cell embryos of CD-1 strain. The chimeras were mated with wildtype C57BL/6J females and the neo cassette was automatically removed in F1 pups. The F1 pups were genotyped by PCR using primers flanking the insertion site and a primer in IRES for the 5' arm. The primer set VGlut2 gt F P1 (5'-TGCTACCTCACAGGAGAATG-3') and IRES P3 (5'-GCTTCGGCCAGTAACGTTAG-3'). The PCR products are 186 bp for the mutant allele. The primer set for the 3' arm is VGlut2 P2 (5'-TGACAACTGCCACAGATTG-3') and FlpO gt F P4 (5'-CTGGACTACCTGAGCAGCTA-3'). The generated PCR products are 294 bp for the mutant allele. The primer set VGlut2 P1 (5'-TGCTACCTCACAGGAGAATG-3') and Vglut2 P2 (5'-TGACAACTGCCACAGATTG-3') is designed to detect the wildtype allele for homozygote genotyping. The correct targeting was further confirmed by obtaining homozygotes from chimera x F1 heterozygous females mating. The mouse lines from two independent ES cell clones were homozygosity tested and bred for experiments. *Genotyping PCR:* The template DNA was obtained by digesting an ear piece in 50 µl proteinase K buffer (50 mM Tris pH 8.8, 1 mM EDTA pH 8.0, 0.5% Tween-20 and proteinase K 0.6 mg/ml). The reaction was incubated at 55°C overnight and heat inactivated at 100°C for 10 minutes. 0.5 µl of the template was used in 12 µl PCR reaction. The reaction was carried out with an initial denature cycle of 94°C for 3 min, followed by 35 cycles of 94°C 30 s, 55°C 30 s and 72°C 30 s and ended with one cycle of 72°C for 5 min.

*Gad2-IRES-FlpO mouse generation:* Targeting vector construction: The targeting vector was constructed using a recombineering technique previously described (Liu et al., 2003). A 10,389 bp genomic DNA fragment containing exon 16 of the Gad2 gene was retrieved from BAC clone RP23-27D24 to a vector containing the DT gene, a negative selection marker. A cassette of IRES-FlpO-loxP2272-ACE-Cre POII NeoR-loxp2272 was inserted between stop codon TAA and 3' UTR. The length of the 5' homologous arm is 3,195 bp and that for the 3' arm is 7,193 bp. *ES cell targeting and screening:* The targeting vector was electroporated into F1 hybrid of 129S6 x C57BL/6J ES

cells derived by the Janelia Transgenic Facility. The G418 resistant ES clones were screened by nested PCR using primers outside the construct paired with primers inside the inserted cassette. The primer sequences were as follows: 5' arm forward primers: Gad2 Scr F1 (5'-CAATTGCTGAGCTGAAGTGC-3') and Gad2 Scr F2 (5'-CAAGCAGTCAGCAGATTCCA-3'). Reverse primers: IRES R1 (5'-AGGAACTGCTTCCTTCACGA-3') and IRES R2 (5'-CCTAGGAATGCTCGTCAAGA-3'). 3' arm forward primers: ACE F3 (5'-ACAGCACCATTGTCCACTTG -3') and ACE F4 (5'-GCTGGTAAGGGATATTTGCC-3'); Reverse primers: Gad2 Scr R3 (5'-GGCTTGATTCTCAGAGGAA-3') and Gad2 Scr R4 (5'-GCACAACAGTTGGACCTTAG-3'). *Generation of chimera and F1 genotyping:* The PCR positive ES clones were expanded for generation of chimeric mice. The ES cells were aggregated with 8-cell embryos of CD-1 strain. The chimeras were mated with wildtype C57BL/6J females and the neo cassette was automatically removed in F1 pups. The F1 pups were genotyped by PCR using primers flanking the insertion site and a primer in IRES for the 5' arm. The primer set Gad2 gt F P1 (5'-TATGGGACCACAATGGTCAG-3') and IRES P3 (5'-GCTTCGGCCAGTAACGTTAG-3'). The PCR products are 212 bp for the mutant allele. The primer set for the 3' arm is Gad2 P1 (5'-TATGGGACCACAATGGTCAG-3'), Gad2 P2 (5'-TGCTGGGATTAAAGGCATGC-3') and FlpO gt F P4 (5'-CATCAACAGGCGGATCTGAT-3'). The generated PCR products are 261 bp for the mutant allele and 325 bp for wildtype allele. The correct targeting was further confirmed by obtaining homozygotes from chimera x F1 heterozygous females mating. The mouse lines from three independent ES cell clones were homozygosity tested and were bred for experiments. *Genotyping PCR:* Genotyping PCR was performed as for *VGlut2-IRES-FlpO* mice.

**Viral Injections, Fiber Optic and Cannula Placement:** Bilateral viral injections and unilateral implantation of ferrule-capped optical fibers (200  $\mu\text{m}$  core, NA 0.37 for optogenetic stimulation; 400  $\mu\text{m}$  core, NA 0.48 for fiber photometry, Doric) were performed as previously described (Betley et al., 2013). For somatic stimulation of AgRP neurons, *AgRP-IRES-Cre* mice were crossed with *Ai32* mice to express ChR2 in AgRP neurons. Mice were anesthetized with isoflurane (1.5-3%), given ketoprofen (5 mg/kg) and bupivacaine (2 mg/kg) analgesia and placed into a stereotaxic device

(Stoelting). An optical fiber was placed over the arcuate hypothalamic nucleus (ARC) at bregma -1.35 mm, midline  $\pm 0.25$  mm, skull surface -5.8 mm. For axonal stimulation of AgRP neurons, a rAAV encoding Cre-dependent ChR2 was bilaterally injected into the ARC of *AgRP-IRES-Cre* mice using the aforementioned ARC injection coordinates (150 nl per site, bilaterally). Optical fibers were unilaterally implanted according to the following coordinates. BNST: bregma +0.85 mm, midline  $\pm 0.82$  mm, skull surface -3.8 mm; PVH: bregma -0.5 mm, midline  $\pm 0.2$  mm, skull surface -5.4 mm; PVT: bregma -1.0 mm, midline  $\pm 0.0$  mm, skull surface -2.7 mm; LH: bregma -1.0 mm, midline  $\pm 0.9$  mm, skull surface -5.4 mm; CeA: bregma -1.15 mm, midline  $\pm 2.4$  mm, skull surface -4.25 mm; ARC: bregma -1.35 mm, midline  $\pm 0.25$  mm, skull surface -5.8 mm; PAG: bregma -4.4 mm, midline  $\pm 0.6$  mm, skull surface -2.8 mm; lateral PBN: bregma -5.8 mm, midline  $\pm 1.2$  mm, skull surface -3.7 mm. Fibers were secured to the skull with bone screws and dental cement. For pharmacological experiments, mice were implanted with unilateral 26 gauge guide cannulae (Plastics One, Roanoke, VA) above the lateral PBN (according to the above coordinates) which were secured to the skull with bone screws and dental cement (Alhadeff et al., 2015). For chemogenetic inhibition of lateral PBN neurons, VGlut2-IRES-FlpO and Gad2-IRES-FlpO mice were bilaterally injected (200 nl/hemisphere) in the lateral PBN with a FlpO-dependent rAAV encoding Cre, and a Cre-dependent rAAV encoding inhibitory Designer Receptors Exclusively Activated by Designer Drugs (DREADDs, hM4D). For fiber photometry, a rAAV encoding Cre-dependent GCaMP6s was bilaterally injected into the ARC of *AgRP-IRES-Cre* mice using the following coordinates: bregma -1.35 mm; midline  $\pm 0.25$  mm; skull surface -6.15 mm and -6.3 mm (250 nl per site, bilaterally), and an optical fiber was implanted over the ARC using the following coordinates: bregma -1.35 mm; midline  $\pm 0.25$  mm; skull surface -6.0 mm. Mice were given at least 3 weeks for recovery and transgene expression. Fiber and cannula placements were verified post-mortem.

**General Experimental Design:** For each experiment, our subject numbers were determined by our pilot studies, laboratory publications, and power analyses [power=0.8, significance level=0.05, effect sizes=10-30%]. For within-subject behavioral and fiber photometry analyses, all mice received all experimental conditions. For between-subject analyses, mice were randomly assigned

to experimental condition. For all behavioral and fiber photometry experiments, experiments were performed in at least two cohorts to ensure replicability of results, by at least 2 researchers who were blinded to experimental conditions. For histological experiments, protein intensities and neuron counts were quantified by 4 research assistants who were blinded to experimental condition. For all behavioral and fiber photometry experiments, virus expression, fiber placements, and/or cannula placements were verified post-mortem, and any mice with viral expression or implants outside of the area of interest were excluded from all analyses.

***In Vivo Photostimulation:*** Photostimulation was performed as previously described (Betley et al., 2013), with 10 ms pulses at 20 Hz for 1 s, repeated every 4 s. The output beam from a diode laser (450 nm, Opto Engine) was controlled by a microcontroller (Arduino Uno) running a pulse generation script. The laser was coupled to a multimode optical fiber (200  $\mu\text{m}$  core, NA 0.37, Doric) with a 1.25 mm OD zirconium ferrule (Kientech) and mating sleeve that allowed delivery of light to the brain by coupling to the implanted ferrule-capped optical fiber in the mouse. Power was set to ensure delivery of at least 2  $\text{mW}/\text{mm}^2$  to AgRP soma and at least 5  $\text{mW}/\text{mm}^2$  to the center of the AgRP neuron projection fields.

**Food Deprivation/Restriction:** For 24 h food deprivation, mice were placed in a cage with alpha dry bedding and *ad libitum* access to water, but no food, 24 h prior to experimentation. For chronic food restriction, mice were weighed at the same time each day and given chow once daily (1.5–3.0 g) after experimentation to maintain 85-90% of their starting body weight.

**Food Intake Experiments:**

*Effects of AgRP neuron stimulation on food intake:* Mice were allowed to habituate for at least one hour to a chamber with a lined floor and *ad libitum* access to chow and water. Following the habituation period, food intake was measured for 1 h to establish a pre-stimulation baseline. Photostimulation was performed during the next hour. After each hour, food intake was measured.

For somatic AgRP neuron stimulation, only mice that consumed >0.6 g of chow were included in experiments. Food intake evoked by stimulation of each AgRP neuron projection subpopulation was measured and reported in Figure S3D.

*Effects of AgRP neuron inhibition on food intake:* Mice were habituated to an empty home cage with a lined floor. Mice were food deprived for 24 h, intraperitoneally (i.p.) injected with saline or clozapine-N-oxide (CNO, 2.5 mg/kg, Tocris), and placed into their cage with *ad libitum* access to chow and water. Chow intake was measured 4 h post-injection, accounting for crumbs.

*Effects of hotplate exposure on latency to feed:* 24 h food deprived mice were individually placed in a home cage with a lined floor and access to water. After a 10 min habituation period, mice were exposed to a cast iron plate at either 25°C or 52°C for 1 min and immediately placed back into the cage with food and water. Latency to consume food was measured.

*Effects of formalin injection on food intake:* 24 h food deprived mice were individually placed in a home cage with a lined floor and access to water. After a 10 min habituation period, mice were injected subcutaneously in the dorsal hindpaw with saline or 2% formalin (20 µl, Sigma HT50-1-2) and returned to their cage with food. Food intake was recorded 1 h post-injection.

**Inflammatory Pain Measurements (Formalin Test):** Mice were placed in a clear enclosure for a 10 min habituation period. Mice were subcutaneously injected in the dorsal hindpaw with saline or 2% formalin (20 µl). Mice were monitored for time spent licking paw, and number of lick bouts, for 1 h post-injection by researchers blinded to experimental condition. All sessions were video-recorded. The time spent paw licking was grouped into 5 min bins (Hunskaar and Hole, 1987) and recorded for 1 h. Additionally, acute (0-5 min) and inflammatory (15-45 min) phase pain responses were quantified.

*Effects of ketoprofen on formalin test:* The non-steroidal anti-inflammatory drug ketoprofen (30 mg/kg) or saline was administered subcutaneously 30 min before formalin injection.

*Effects of food deprivation on formalin test:* Food was removed 24 h prior to formalin injection. *Ad libitum* fed mice served as controls.

*Effects of formalin on paw inflammation:* 24 h food deprived mice were lightly anesthetized and paw circumference was measured immediately before saline or formalin paw injection. Paw circumference was measured again 30 min post-injection.

*Optogenetic AgRP neuron stimulation:* To assess the effects of AgRP neuron stimulation on acute and inflammatory phase pain responses to formalin, mice received optogenetic stimulation of AgRP neurons or individual projection subpopulations beginning 10 min prior to formalin injection and lasting throughout the formalin test. To assess the ability of AgRP neuron stimulation to affect an ongoing inflammatory pain response, stimulation of AgRP neurons or AgRP→PBN neurons was initiated 25 min post-formalin injection and lasted for the duration of the formalin test. To assess whether the offset of AgRP→PBN neuron activity results in a reinstatement of inflammatory phase pain response, laser stimulation was given 10 min prior to formalin injection and terminated 25 min post-formalin injection. To test whether prolonged AgRP→PBN neuron stimulation affects the ability to paw lick, mice were stimulated for 40 min and formalin-induced acute phase pain was measured.

*Chemogenetic AgRP neuron inhibition:* To assess the necessity of AgRP neuron activity for the inhibition of inflammatory pain by hunger, mice were 24 h food deprived and i.p. injected with CNO (2.5 mg/kg) 15 min before formalin injection.

*Chemogenetic inhibition of lateral PBN VGlut2 and Gad2 neurons:* To determine whether lateral PBN glutamatergic (VGlut2-expressing) or GABAergic (Gad2-expressing) neurons mediate inflammatory pain responses, VGlut2<sup>hM4D</sup>, Gad2<sup>hM4D</sup>, and control mice were i.p. injected with CNO (2.5 mg/kg) 15 min before formalin injection.

**Thermal Pain Measurements (Hotplate Test):** A cast iron plate with plexiglass walls was placed on a hotplate and heated to 52°C. Mice were placed on the hotplate and latency to withdraw paw was recorded by researchers blinded to experimental condition. All sessions were video-recorded.

*Effects of morphine on hotplate test:* Mice underwent a baseline hotplate test and were subsequently i.p. injected with saline or morphine (10 mg/kg). Mice were tested again on the hotplate 30 min post-injection.

*Effects of food deprivation on hotplate test:* Food was removed 24 h prior to hotplate test. *Ad libitum* fed mice served as controls.

*Optogenetic AgRP neuron stimulation during hotplate test:* To assess the effects of AgRP neuron stimulation on acute thermal pain response, mice were placed in a plexiglass chamber, attached to patch fibers, and allowed to habituate for 30 min. Mice underwent a baseline hotplate test, and 5 min later laser stimulation was initiated. Mice were tested again on the hotplate following 15 and 45 min of stimulation of AgRP neurons or control light delivery to GFP-expressing mice. A separate experiment was performed to assess the role of AgRP→PBN neurons on acute thermal pain by delivering light to the PBN of mice expressing either ChR2 or GFP in AgRP neurons, using identical experimental procedures.

**Mechanical Pain Measurements (Von Frey Test):** Mice were habituated for 30 min in small plexiglass chambers atop mesh flooring. Twelve Von Frey filaments (ranging from 0.008 g to 6 g) were used. Starting with the smallest Von Frey filament and continuing in ascending order, each filament was applied to the plantar surface of the hind paw until the filament bent. Each filament was tested 5 times. The number of withdrawal responses was recorded for each filament, and the percentage withdrawal responses for each filament was calculated (# of withdrawal trials/total trials). Withdrawal threshold was determined as the filament at which the mouse responded with a

paw withdrawal to >50% of trials. To test the effects of hunger on mechanical pain, mice were 24 h food deprived and then subjected to the Von Frey test.

**Inflammation-Induced Sensitization:** Complete Freund's Adjuvant (CFA, Sigma) was diluted 1:1 in saline and injected (20  $\mu$ l) into the plantar surface of the paw after a baseline Von Frey or hotplate test. Given that we and others observe a more robust CFA-induced sensitization to thermal pain at 55°C (Carey et al., 2017), we used this temperature for CFA-induced thermal sensitization. Von Frey or hotplate tests were repeated 3 h, 24 h, and 48 h post-CFA injection.

*Effects of hunger on inflammation-induced sensitization:* Mice were 24 h food deprived and subjected to Von Frey or hotplate tests as described above. Mice were provided enough food in one daily aliquot to maintain 85-90% BW through the rest of testing (up to 48 h post-CFA injection).

*Effects of AgRP neuron stimulation on inflammation-induced sensitization:* Optogenetic AgRP neuron stimulation was performed for 1 h before each of the post-CFA Von Frey tests (3 h, 24 h, and 48 h post-CFA injection).

**Conditioned Place Avoidance:** Two-sided apparatus were used with distinct visual (black vs. white walls), textural (flooring: plastic vs. soft textural side of Kimtech bench-top protector), and olfactory (almond vs. peppermint extract) cues. A neutral middle zone to shuttle between sides was maintained and the chamber was equipped with an overhead camera to track mouse position. *Ad libitum* fed mice were habituated to the apparatus and a pre-conditioning preference was determined via AnyMaze software. Mice were then separated into two groups: food restricted (85-90% of initial body weight) or *ad libitum* fed. Conditioning, which consisted of a saline paw injection (20  $\mu$ l) on the less preferred side or a 2% formalin paw injection (20  $\mu$ l) on the preferred side was performed twice daily for four days. To isolate conditioning to the inflammatory phase of formalin

pain, mice were placed in the apparatus 15 min post-injection. After conditioning, all mice were given *ad libitum* access to food. The next day, mice were given access to both sides of the apparatus and their position and activity were tracked. The percentage occupancy, shifts in occupancy, and total distance traveled in the formalin-paired side during the post-conditioning test were calculated. To control for any associative learning deficits during hunger, the same conditioned place avoidance paradigm was used, except that mice were given i.p. saline on the less preferred side and i.p. lithium chloride (125 mg/kg) on the preferred side during conditioning.

#### **Locomotor Activity Assays:**

*Effects of food deprivation of formalin-induced immobility:* Mice were habituated to 10" x 10" x 10" plexiglass chambers. Food was removed from mice 24 h prior to 2% formalin injection, and mice were placed in chambers and video-recorded during the inflammatory phase following formalin injection (15-45 min post-injection). Videos were analyzed with AnyMaze software (Stoelting) for time spent immobile, which was defined as not changing position in the X-Y grid for at least 8 s.

*Effects of AgRP → PBN neuron stimulation on locomotor activity:* Mice were habituated to 10" x 10" x 10" plexiglass chambers. AgRP → PBN neurons were optogenetically stimulated for 30 min and behavior was video-recorded. Videos were analyzed with AnyMaze software (Stoelting) for total distance traveled and time spent immobile, which was defined as not changing position in the X-Y grid for at least 8 s.

**Immunohistochemistry and Imaging:** Mice were transcardially perfused with 0.1 M phosphate buffered saline (PBS) followed by 4% paraformaldehyde (PFA). Brains were removed and post-fixed for 4 h in PFA and then washed overnight in PBS. Coronal brain sections were cut (30-200  $\mu$ m sections) on a vibratome or cryostat and stored in PBS. Brain sections were incubated overnight at 4°C with primary antibodies diluted in PBS, 1% BSA and 0.1% Triton X-100. Antibodies used: goat anti-AgRP (1:2,500, Neuromics, GT15023), rabbit anti-cFos (1:5,000, Cell Signaling, 2250),

guinea pig anti-RFP (1:10,000) (Betley et al., 2013), rabbit anti-GFP (1:5,000, Invitrogen, A-11122), rabbit anti-NPY (1:1,500, Immunostar, 22940), rat anti-GAD65 (1:2,000) (Betley et al., 2009), guinea pig anti-VGlut2 (1:2,000, SYSY, 135404). Sections were washed 3 times and incubated with species appropriate and minimally cross-reactive fluorophore-conjugated secondary antibodies (1:500, Jackson ImmunoResearch) for 2 h at room temperature. Sections were washed twice with PBS and mounted and coverslipped with Fluorogel. Epifluorescence images were taken on a Leica stereoscope to verify fiber placements, cannula placements, and obtain low magnification images. Confocal micrographs were taken on a Leica STED laser scanning microscope using a 20X, 0.75 NA objective for quantification of Fos immunoreactivity under AgRP axons; a 40X, 1.3 NA objective for quantification of protein expression in AgRP→PBN terminals; and a 63X or 100X, 1.4 NA objective for protein colocalization of mCherry, VGlut2, and GAD65 in PBN axon terminals.

#### **Quantification of Protein Expression:**

*Immediate early gene protein expression analysis:* To quantify the number of neurons expressing Fos protein under AgRP axons, mice received no treatment (n=3) or a 20  $\mu$ l subcutaneous injection of formalin (5%, n=3) or saline (n=3) in the dorsal hindpaw. Two hours later, mice were perfused and brains were processed for immunohistochemistry. First, images of Fos and AgRP from a formalin-treated mouse were obtained in each of the major AgRP projection target regions. Identical image acquisition settings were maintained for all subsequent imaging of Fos and AgRP in experimental and control mice. To quantify the number of Fos-expressing neurons in each AgRP neuron target region, single optical sections (pinhole = 1 airy unit, 2-4 sections/mouse/AgRP target region) were used and the AgRP neuron staining was used to define the region for quantification (see Figure 4A).

*Quantification of synaptic protein expression:* *Ad libitum* fed (n=2) and 24 h food deprived (n=3) mice were perfused and PBN brain sections were processed for NPY, the GABA synthetic enzyme GAD65, and AgRP immunoreactivity. Confocal images were obtained first from a food deprived

mouse so that the intensities of NPY, GAD65, and AgRP were in the linear range. Image acquisition settings were maintained for all subsequent imaging and 2 PBN images per mouse were obtained. For intensity quantifications, single confocal sections (pinhole = 1 airy unit) were used and the intensities of NPY, GAD65, and AgRP were calculated using the histogram function on Adobe Photoshop.

*Colocalization of hM4D, Vglut2, and GAD65 in IPBN neurons:* To determine the specificity of expression of hM4D in the *Gad2-IRES-FlpO* and *Vglut2-IRES-FlpO* knock-in lines, staining was performed against mCherry, Vglut2 and GAD65 in coronal sections from at least 2 mice/line used for experimentation. For quantification, single confocal sections (pinhole = 1 airy unit) were used and the number of Vglut2+ or GAD65+ structures that expressed hM4D-mCherry were counted.

**Pharmacology:** For all experiments, mice were habituated to handling and infusion procedures. Drugs were diluted from frozen aliquots before each experiment and microinjected (100 nl) with a Hamilton syringe attached to an internal cannula (Plastics One) and microliter syringe pump (PHD Ultra, Harvard Apparatus) into the PBN of mice immediately before a formalin test (see above) or food intake measurements.

*Effects of IPBN NPY, GABA agonists, and AgRP analogue on formalin-induced inflammatory pain:* Neuropeptide Y [NPY, Tocris, 0.1 µg], GABA<sub>A</sub> and GABA<sub>B</sub> receptor agonists [muscimol, Tocris, 25 ng and baclofen, Tocris, 25 ng], an AgRP analogue [melanocortin 4 receptor antagonist; SHU9119, 25 pmol] or vehicle [artificial cerebrospinal fluid (aCSF)] was microinjected into the lateral PBN immediately before paw injection of formalin.

*Effects of IPBN NPY, GABA agonists, and AgRP analogue on food intake:* The aforementioned drugs were infused in the IPBN during the light cycle and food intake was recorded 1 h post-injection.

*Effects of locus coeruleus NPY on formalin-induced inflammatory pain:* Since AgRP axons terminate both in the IPBN and the locus coeruleus, NPY or vehicle was infused in the locus coeruleus area (directly medial from IPBN) immediately before formalin paw injection.

*Effects of IPBN NPY Y1 receptor antagonist on the inhibition of inflammatory pain by hunger:* Microinjections of the selective NPY Y1 receptor antagonist BIBO 3304 [Tocris, 3  $\mu$ g], GABA<sub>A</sub> and GABA<sub>B</sub> antagonists [saclofen, 100 ng, Sigma, and bicuculline, 10 ng, Sigma] or vehicle (50% DMSO in aCSF) were infused into the IPBN of 24 h food deprived mice.

*Effects of IPBN NPY Y1 receptor antagonist on the inhibition of inflammatory pain by AgRP→PBN stimulation:* To test whether the protective effects of AgRP→PBN neuron stimulation on inflammatory pain are mediated by NPY, we performed an experiment similar to that in (Atasoy et al., 2012). Mice expressing Chr2 in AgRP neurons were injected in the IPBN with vehicle or the Y1 receptor antagonist BIBO 3304. An optic fiber was then inserted through the PBN cannula and a formalin paw injection was administered. AgRP→PBN stimulation occurred throughout the duration of the formalin test.

**Fiber Photometry:** Food-restricted (85-90% body weight) mice in their home cage were attached to a patch fiber (400  $\mu$ m core, NA 0.48, Doric) and connected to 405 nm and 490 nm LEDs (Thor Labs, M405F1, M470F3) modulated by a real-time amplifier [Tucker-Davis Technology (TDT), Alachua, FL, RZ5P] and focused onto a femtowatt photoreceiver (Newport, Model 2151) (Figure 6C) (Gunaydin et al., 2014). Changes in calcium-dependent GcaMP6s fluorescence (490 nm) signal were compared with calcium-independent GCaMP6s fluorescence (405 nm), providing internal control for movement and bleaching artifacts (Lerner et al., 2015; Su et al., 2017). Fluorescence measurements (1 Hz) were extracted from Synapse software (TDT), processed in MatLab (GraphPad), and expressed as  $\Delta F/F$ , where the denominator represents average baseline fluorescence.

*Effects of acute thermal pain on AgRP neuron activity:* Food restricted (85-90% BW) mice were connected to the fiber photometry setup for a 5 min baseline period in their home cage. Mice were then placed on a 25°C or 52°C plate for 1 min, after which they returned to their cage. GCaMP6s fluorescence was monitored for 10 min following hotplate exposure.

*Effects of acute and inflammatory formalin-induced pain on AgRP neuron activity:* Food restricted (85-90% BW) mice were connected to the fiber photometry setup for a 5 min baseline period in their home cage. Mice were injected in the dorsal hindpaw with 2% formalin or saline (20 µl) and returned to their cage. GCaMP6s fluorescence was monitored for 1 h post-formalin injection.

## **QUANTIFICATION AND STATISTICAL ANALYSES**

Data were expressed as means ± SEMs in figures and text. Paired or unpaired two-tailed t-tests with or without Bonferroni corrections and Pearson regressions were performed as appropriate. One-way, two-way, and repeated measures ANOVA were used to make comparisons across more than two groups using SigmaPlot or STATISTICA. Test, statistics, significance levels, and sample sizes for each experiment are listed in Supplementary Tables 1 and 2. ns p>0.05, t-tests and post-hoc comparisons: \*p<0.05, \*\*p<0.01, \*\*\*p<0.001; interaction: ∞p<0.05, ∞∞p<0.01, ∞∞∞p<0.001; main effect (group, condition or drug): ☼<0.05, ☼☼p<0.01, ☼☼☼p<0.001.

### **CHAPTER 3: HUNGER HAS A POTENT AND RELIABLE ANTI-INFLAMMATORY EFFECT ON INJURY-INDUCED INFLAMMATION.**

Thus far, we have shown that food deprivation, through AgRP neurons, can reduce inflammatory pain behavior. We had two hypotheses about how hunger could be influencing pain: 1. Hunger could be reducing the perception of pain at the level of the central nervous system or 2. Hunger could be causing changes at the injury site to prevent pain signals from reaching the central nervous system. While the work in this dissertation does not directly answer the question of how hunger influences pain, we became interested in understanding what was happening at the paw after injection of a noxious chemical during hunger. Can hunger have a targeted effect on injury-induced inflammatory responses?

Hunger can reduce pain behavior exclusively during the inflammatory phase of pain (Alhadeff et al., 2018). This specificity led us to question hunger's influence on the underlying inflammatory response to these nocifensive agents. In our previous work, we primarily interrogated hunger's influence on the pain response to formalin, yet we did show that hunger could influence the pain response to complete Freund's adjuvant (CFA) as well. We started our interrogation of hunger and inflammation using both inflammatory models from our original pain study: formalin and CFA paw injections. As our experiments continued, we focused on CFA because the infection triggers a much larger and more sustained inflammatory response (Ren and Dubner, 1999). To gain an understanding of the inflammatory response to CFA we measured edema levels, temperature, and inflammatory cell counts at the injury site.

CFA is a mixture of mycobacteria and paraffin oil that can be injected in an animal to create an inflammatory response that induces swelling/edema, heat, redness, and pain (Ren and Dubner, 1999). Historically CFA has been used to model chronic inflammatory and autoimmune diseases such as arthritis, encephalomyelitis, thyroiditis, and myasthenia gravis (Billiau and Matthys, 2001). Autoimmune diseases are defined as chronic disruption of the immune system resulting in immune reactions to the body's own organs, tissues, and cells (National Institute of Health, 2005). Ultimately

this causes production of antibodies to natural proteins in the body. CFA can be used as an arthritic model by injection into a joint. Initially, the joint becomes swollen and painful, while overtime the bones become damaged (Jacobson et al., 1999; Ratkay et al., 1993). After full initiation of the adjuvant-induced arthritis, mice produce high levels of antibodies against collagen leading to an autoimmune response to the collagen rich joints (Ratkay et al., 1993). CFA is also used as a local inflammatory agent to test inflammatory pain responses (Walker et al., 1999). CFA induces hyperalgesia and allodynia within 2 hours of injection for at least one week (Ren and Dubner, 1999). Immediately after CFA exposure the innate immune system is triggered to release pro-inflammatory cytokines and chemokines, especially tumor necrosis factor alpha (TNF $\alpha$ ), interferon gamma, interleukin-12 and interleukin-6 (Billiau and Matthys, 2001).

It is known that food restriction can suppress systemic inflammation by reducing pro-inflammatory markers and inhibiting pro-inflammatory signaling pathways (Brandhorst et al., 2015; Meydani et al., 2016; Traba et al., 2015; Vandanmagsar et al., 2011). Previous work investigating the role of food restriction on inflammation have evaluated phenotypes of aging-induced inflammation, genetic inflammatory disorders, and obesity-induced inflammation (Brandhorst et al., 2015; Fontana et al., 2004; Heilbronn and Ravussin, 2003; Li et al., 2021b; Mercken et al., 2013; Vandanmagsar et al., 2011; Youm et al., 2015). Food restriction's ability to combat an acute inflammatory event, like an injury, has been under studied.

Our model evaluates CFA 24 h after introduction to the mouse's dorsal footpad – capturing the initial immune response to the bacterial infection. At this time point, we are evaluating synovitis created from the infiltration of immune cells to the injection site, not long-term arthritic changes which occur between three and seven days after injection (Oliveira et al., 2007). We chose to look at CFA on a short-term scale to understand how food deprivation and the central nervous system influence targeted inflammatory events. The arthritic model causes global changes that leads to an autoimmune reaction to collagen throughout the body. Our work adds pertinent information about the intimate relationship the central nervous system has with immune responses to specific injuries.

### **Hunger reduces injury-induced inflammation.**

To assess injury-induced edema, we measured paw volume after the introduction of a chemical stimuli using a plethysmometer which uses volume displacement as a proxy for size. Briefly, the paw is submerged in a saline solution and volume displacement is detected (Figure 3.1a). All measurements were calculated as a percent increase from the original paw volume prior to the injury. We observed a 40% increase in paw volume 1 hour after a formalin paw injection (Figure 3.1b, 3.1c) and a 100% increase in paw volume 24 hours after a CFA paw injection (Figure 3.1d) in ad libitum fed mice. Interestingly, 24-hour food deprivation attenuated the injury-induced inflammatory response resulting from both formalin and CFA paw injections by approximately 50% (Figure 3.1c, 3.1d). Importantly, food deprivation had no effect on paw volume after saline paw injections showing that the reduction in paw size is not a consequence of dehydration or weight loss from food deprivation (Figure 3.1c, 3.1d). To corroborate our plethysmometer findings, we also measured paw circumference before and after the chemical injuries. We observed a 20% increase in paw circumference 1 hour after a formalin paw injection and a 40% increase in paw circumference 24 hours after a CFA injection. Again, 24-hour food deprivation reduced paw circumference by approximately 50% (Figure 3.2a-c). This effect on inflammation is sustained, as chronic food restriction has the ability to reduce CFA paw inflammation for up to 1 week (168 hours, Figure 3.2d).

Local inflammation is characterized by increases in swelling (edema), redness, temperature, and cytokine/chemokine infiltration (Medzhitov, 2008; Nathan, 2002). Thus far, we have discovered that food deprivation can reduce edema and wanted to evaluate hunger's influence on these other characteristics of inflammation. Using an infrared camera, we were able to specifically measure paw temperature across conditions (Figure 3.3a). 24 hours after a CFA paw injection, paw temperature increased by about 4°C from baseline paw temperatures (Figure 3.3b). Food deprivation reduced paw temperature by about 3°C returning the temperature to near baseline values (Figure 3.3b). Because food deprivation has a profound effect on inflammation, we

next looked at whether food deprivation has an effect on the cytokine response to injury. TNF $\alpha$  is a proinflammatory cytokine released by macrophages in early in the response to an immune challenge (Billiau and Matthys, 2001). To understand food deprivation's influence on cytokine levels, we measured TNF $\alpha$  levels at the injury site. We found a significant reduction in TNF $\alpha$  levels in food deprived mice compared to ad libitum fed controls (Figure 3.3c).

To evaluate structural changes in the paw, we performed histology on paws injected with CFA either in *ad libitum* or food deprived conditions. We observed that the reduction in CFA-induced paw volume caused by hunger is directly related to the levels of edema (Figure 3.3d) as defined by the comparison of vacuole sizes and frequency between ad libitum fed and food deprived groups. There were no differences in histopathological changes at the injury site (Oliveira et al., 2007) as defined by qualitative suppurative inflammation scores and CD45+ cell staining in the paw (Figure 3.3e, 3.3f). Because of this lack of cellular changes, we next explored the possibility that hunger irreversibly reduces inflammation. We measured paws of animals before, during and after 24h food deprivation and found that while hunger dramatically reduces paw volume after CFA injection, refeeding the animals reversed the effect of food deprivation (Figure 3.3g). Together with our paw histology findings showing no histopathological changes in food deprivation, this suggests that hunger has an acute effect on inflammation and the signals produced must be maintained for the ongoing suppression of inflammation.

### **Hunger is a potent anti-inflammatory mechanism regardless of sex, age or weight.**

To assess whether biological variables influence the ability of hunger to suppress inflammation, we evaluated the effect of food deprivation on CFA-induced inflammation in animals of different sex, age, and body weight. Across experimental cohorts, we consistently found that food deprivation reduced paw volume after an injection of CFA (Figure 3.4a). Given that there are sex differences in immune responses (Doyle and Murphy, 2017; Klein and Flanagan, 2016; Kovats et al., 2009), we examined how hunger influences inflammation in male and female mice. As previously reported, we observed that female mice had a larger paw volume after a CFA injection

(Cook and Nickerson, 2005; Doyle and Murphy, 2017), however, food deprivation reduces the inflammation in both male and female mice (Figure 3.4b). The immune system can also be influenced by age (Shaw et al., 2013; Taniguchi and Karin, 2018) or body weight (Vandanmagsar et al., 2011; Wellen and Hotamisligil, 2005). We therefore quantified paw volume after CFA injection in mice at varying ages and body weights. Although age influences the inflammatory response to CFA, hunger reduced CFA-induced inflammation to the same extent across all age and body weight groups (Figure 3.4c, 3.4d). Overall, we found that hunger can reliably and reproducibly reduce CFA-induced edema by about 50% regardless of sex, age, and body weight.

Because hunger is a highly reliable, reproducible, and potent mechanism to attenuate injury-induced inflammation, we next compared food deprivation to standard inflammation treatments. Ad libitum fed and food deprived mice were given vehicle or a non-steroidal anti-inflammatory drug (NSAID). As expected, both food deprivation and NSAID administration reduced paw size (Figure 3.5a, 3.5c). However, compared to typical doses of NSAIDs, we found that food deprivation has a larger anti-inflammatory effect. Indeed, food deprivation reduced CFA-induced paw volume 20% more than administration of ketoprofen or ketorolac (Figure 3.5e, 3.5d)

**Hunger has a complex relationship with inflammation that cannot be recapitulated pharmacologically.**

Thus far we have identified hunger as a potent anti-inflammatory mechanism for injury-induced inflammation. However, we do not know the mechanism by which hunger is reducing inflammation. We started to answer this question by systemically activating and inhibiting different pharmacological systems and measuring paw volume. A reduction in paw size while mice are ad libitum fed could identify a pathway that hunger is utilizing to reduce paw inflammation. Alternatively, a failure to reduce paw size in food deprived mice could identify a pathway necessary for hunger's influence on inflammation. Together, these experiments could identify a system or pathway that hunger is acting through to influence inflammation.

### *Glucocorticoids*

The hypothalamic-pituitary-adrenal (HPA) axis is a neuroendocrine pathway that can initiate anti-inflammatory signaling in order to maintain balance during immune reactions (Pavlov et al., 2003a). Cytokines are able to cross the blood brain barrier making them capable of interacting with all stages of the HPA axis. The HPA axis primarily releases glucocorticoids to inhibit pro-inflammatory pathways and prevent long term gene transcription for an inflammatory environment (Rivest, 2001). When activated, the PVH of the hypothalamus secretes corticotrophin-releasing hormone (CRH) which produces adrenocorticotropin hormone (ACTH) in the anterior pituitary gland. Finally, ACTH stimulates the release of glucocorticoids from the adrenal glands leading to an anti-inflammatory regulation of the immune system (Webster et al., 2002) To evaluate the role of glucocorticoids in the anti-inflammatory effect of hunger, we introduced the glucocorticoid agonist corticosterone (ort) in ad libitum mice and the antagonist RU486 in food deprived mice. Activation of the glucocorticoid system with cort during satiety had no effect on paw volume (Figure 3.6a). Inhibition of the glucocorticoid system with RU486 during food deprivation also had no effect on paw volume (Figure 3.6b). Systemic interrogation of the glucocorticoid system did not have a significant effect on paw volume, so we used behavioral stress as an organic activator of the glucocorticoid system. Rodent restraint stress increases corticosterone blood circulation within 10 minutes (Hare et al., 2014). Mice were maintained in restraint tubes for 1 hour between paw measurements. We found that there was no difference in paw volume before or after restraint stress (Figure 3.6c)

### *Substance P*

Substance P (SP) is a tachykinin neuropeptide found in central, peripheral and immune systems making it an excellent candidate for cross-communication between the brain and immune system. SP has a high affinity for neurokinin 1 receptors (NK1Rs) which are present on many immune cell types including dendritic cells, macrophages, neutrophils, and T-cells. Nerves release SP on to lymphatic tissues to produce a proinflammatory environment and typically relay pain information (Suvas, 2017). SP signaling directs guided proinflammatory responses specifically to

bacterial infected areas allowing effective and efficient bacterial clearance (Pascual, 2004). Since SP is a proinflammatory molecule, we tested the role of SP on paw volume by blocking NK1Rs in satiety and stimulating NK1Rs with SP in food deprivation. We found no significant difference in paw volume between mice treated with saline and a NK1R antagonist under ad libitum fed conditions (Figure 3.6d). Similarly, we found no difference in paw volume between mice treated with saline and SP under food deprived conditions (Figure 3.6e).

### *Opioids*

Opioid receptors increase in the central nervous system after CFA injections suggesting a relationship between inflammation and opioid signaling (Besse et al., 1992; Millan et al., 1988; Nahin and Byers, 1994). However, there is a controversy over whether opioids participate in fueling a pro or anti-inflammatory response (Eisenstein, 2019). Despite this, we thought it was important to understand if opioids influence paw volume. We tested activation of opioid receptors in satiety and antagonism of opioid receptors in food deprivation. Ad libitum fed mice treated with buprenorphine to activate the opioid system had no differences in paw volume compared to saline controls (Figure 3.6f). Food deprived mice treated with naloxone to block opioid signaling had no difference in paw volume compared to saline controls (Figure 3.6g).

### *Oxytocin*

Oxytocin (OXT) has been used to treat a variety of conditions ranging from mood and personality disorders to digestion and metabolic issues to autonomic and immune function (Hurlemann and Grinevich, 2018). A key hormone for early development, OXT is a protective molecule allowing for adaptation to stressors and prepping the body for future traumas (Carter et al., 2020, Kingsbury and Bilbo, 2019). Because of this protective function, OXT is believed to have anti-inflammatory effects. In fact, it has been shown that higher levels of oxytocin can increase wound healing after surgery (Gouin et al., 2010, Carter et al., 2020). OXT can also reduce inflammatory markers through degranulation of mast cells after a heart attack (Xiong et al., 2020). However, OXT is also important for body fluid regulation and too high levels of oxytocin can lead to pulmonary edema (Ferguson et al., 2008; Mansour et al., 2021). OXT and vasopressin work in

tandem to maintain body fluids and immune responses, usually having opposite effects of each other. We tested if OXT had an influence on paw volume of food deprived mice. We found that both saline and oxytocin treated mice had similar reductions in paw size during food deprivation (Figure 3.6h).

#### *Leptin*

Leptin is a potent pro-inflammatory molecule that has become of particular interest in the interaction between obesity and inflammatory diseases (Abella et al., 2017). Leptin is a hormone secreted by adipose tissue that primarily serves to regulate energy expenditure and calorie consumption (Rosenbaum and Leibel, 2014). However, adipose tissue positively correlates with levels of circulating leptin and could be the contributing mechanism of chronic inflammation in obese individuals (Lago et al., 2009). Leptin production is triggered by cytokine release when there is an acute threat. Acute leptin levels lead to proinflammatory immune responses, while chronic leptin levels cause leptin resistance and dampened overall immune function (Abella et al., 2017; Wrann et al., 2012). Because of leptin's influence on inflammation and association with feeding, we evaluated if leptin has a role in the anti-inflammatory effect of hunger. Mice treated with leptin had no difference in paw volume to saline controls when food deprived (Figure 3.6i).

#### *Ghrelin*

During food deprivation many different chemical compounds are released to trigger the physiological effects of hunger. One key "hunger hormone" is ghrelin. Ghrelin is well known to induce feeding behavior. In fact, ghrelin initiates feeding through activation of AgRP neurons in the hypothalamus (Nakazato et al., 2001). However, ghrelin is involved in many more physiological functions besides feeding. Ghrelin has been implicated in energy expenditure, sympathetic nerve activity, and metabolism among other functions (Pradhan et al., 2013). We therefore tested if ghrelin has an influence on inflammation. Systemic treatment of ad libitum fed mice with ghrelin was not significantly different than saline treated mice and therefore had no effect on paw inflammation (Figure 3.6j).

### *Serotonin*

Serotonin (5-HT) is a hormone that coordinates many physiological functions from mood and behavior to inflammation and immunity throughout the body and central nervous system (Berger et al., 2009). The majority of 5-HT is in the periphery produced by enterochromaffin cells of the gut and carried throughout the body on platelets (Maurer-Spurej et al., 2004; Gershon and Tack, 2007; Jonnakuty and Gragnoli, 2008). Many types of immune cells have 5-HT receptors and can affect innate immune responses to injury and toxins by influencing immune cell signaling (Ahern, 2011; Baganz and Blakely, 2012). Since 5-HT is believed to activate the immune response (Konig et al. 1992; Mossner and Lesch, 1998; Gordon and Barnes, 2003), we hypothesized that systemic 5-HT administration in food deprived mice would block the anti-inflammatory effect of hunger. However, we found that mice treated with 5-HT had no difference in paw volume compared to controls (Figure 3.6k).

### *Microbiome*

The gut is filled with bacteria that can elicit anti-inflammatory and proinflammatory effects based on the strain of bacteria, diet, and genetics of the host organism. An unhealthy microbiome has been linked to a variety of autoimmune disorders such as rheumatoid arthritis, Crohn's disease, and asthma (Wang et al., 2020). A healthy microbiome has bacteria that release anti-inflammatory metabolic compounds such as butyrate which inhibits the production of proinflammatory cytokines in innate immune responses (Klampfer et al., 2003; Lührs et al., 2009). We evaluated the role of the microbiome in CFA inflammation by using antibiotics to deplete all gut bacteria in our mice as previously described (Virtue et al, 2019). We found that saline and antibiotic treated mice had the same paw volume in ad libitum fed and food deprived conditions (Figure 3.6l).

## **Discussion**

Hunger has a potent effect on inflammation. We robustly and reliably found food deprivation to attenuate paw volume by about 50%. Food deprivation also reduced other aspects of inflammation including temperature and pro-inflammatory cytokine levels. We attempted to

identify a pharmacological pathway that food deprivation was working through to reduce inflammation but were unsuccessful. Each tested system has been broadly implicated in inflammation before, however, we failed to see any change in paw inflammation in our manipulations. The negative data here highlights the complexity of the immune system. One hypothesis for the failure to influence inflammation with our pharmacological challenges could be the compensatory nature of pharmacological systems. In fact, there has been a push in the field to develop multi-target pharmacological treatment for a variety of diseases and indications because the body can adapt with one player missing (Anastasio, 2017). The immune system is such a critical component of survival, that it is not surprising that there is redundancy among its pathways. There may be a balance between these systems evaluated that we are unable to capture with manipulation of any given one. An alternative hypothesis is that hunger is causing a change in the neural control of inflammation. We know that feeding behavior is coordinated by the central nervous system and hunger is mediated by AgRP neurons in the hypothalamus (Hahn et al., 1998; Horvath et al., 1992, 1997; Cowley et al., 2003; Liu et al., 2012; Takahashi and Cone, 2005; Yang et al., 2011; Su et al, 2017). Because of this, we next sought to evaluate the role of AgRP neurons in the anti-inflammatory effect of hunger.

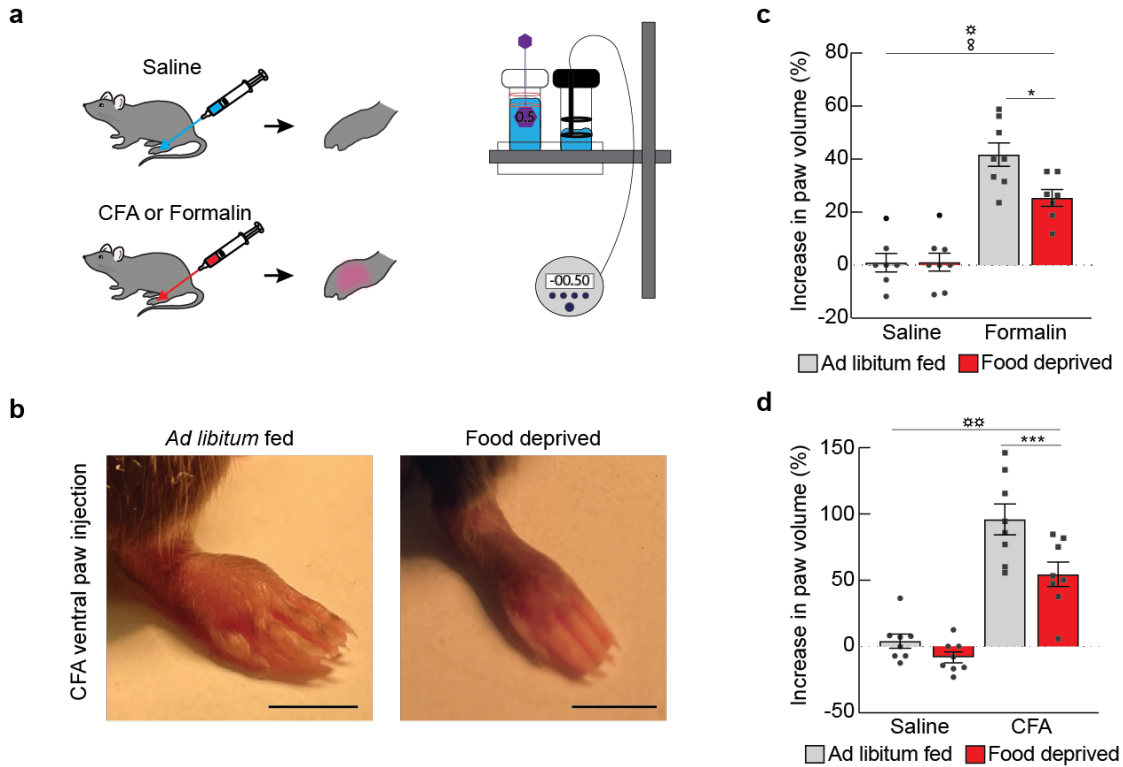


**Figure 3.1 | Hunger reduces paw inflammation induced by CFA and formalin.**

(a) Experimental design: Mice were injected with saline, CFA, or formalin and paw volume was measured using a plethysmometer at various time points post-injection. (b) Images of paws 24 h after CFA injection followed by ad libitum access or 24 h food deprivation. Scale bar, 5 mm. (c) Increase in paw volume of ad libitum (n=8) and 24 h food deprived (n=8) mice 1 h after a saline or formalin injection (two-way ANOVA, main effect of ad libitum v food deprived p=0.029). (d) Increase in paw volume of ad libitum (n=8) and 24 h food deprived (n=8) mice 24 h after a saline or CFA injection (two-way ANOVA, main effect of ad libitum v food deprived p=0.003). Data are expressed as mean  $\pm$  SEM; post-hoc comparisons: \*p<0.05, \*\*\*p<0.001; two-way ANOVA interaction:  $\infty$ p<0.05; ANOVA main effect:  $\odot$ p<0.05,  $\odot\odot$ p<0.01.

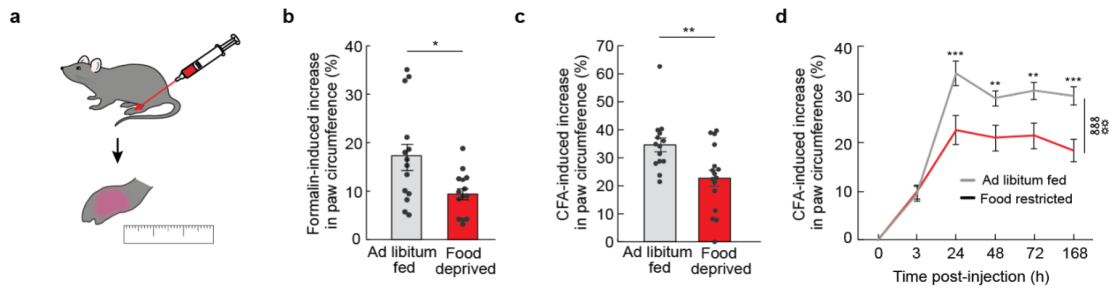


**Figure 3.2 | Hunger reduces paw circumference induced by CFA and formalin.**

(a) Experimental design: Mice were injected with saline, formalin or CFA and paw circumference was measured. (b) Increase in paw circumference of ad libitum (n=14) and 24 h food deprived (n=14) mice 1 h after formalin injection (unpaired t-test,  $p=0.014$ ). (c) Increase in paw circumference of ad libitum (n=15) and 24 h food deprived (n=16) mice 24 h after CFA injection (unpaired t-test,  $p=0.005$ ). (d) Increase in paw circumference in ad libitum fed (n=14) and food restricted (n=16) mice maintained at ~90% body weight following paw injection of CFA over 1 week (two-way repeated measures ANOVA, main effect of state  $p<0.001$ ). Data are expressed as mean  $\pm$  SEM; t-test and post hoc comparisons: \* $p<0.05$ , \*\* $p<0.01$ , \*\*\* $p<0.001$ ; two-way ANOVA interaction:  $\infty\infty\infty p<0.001$ ; ANOVA main effect:  $\odot\odot p<0.01$ .

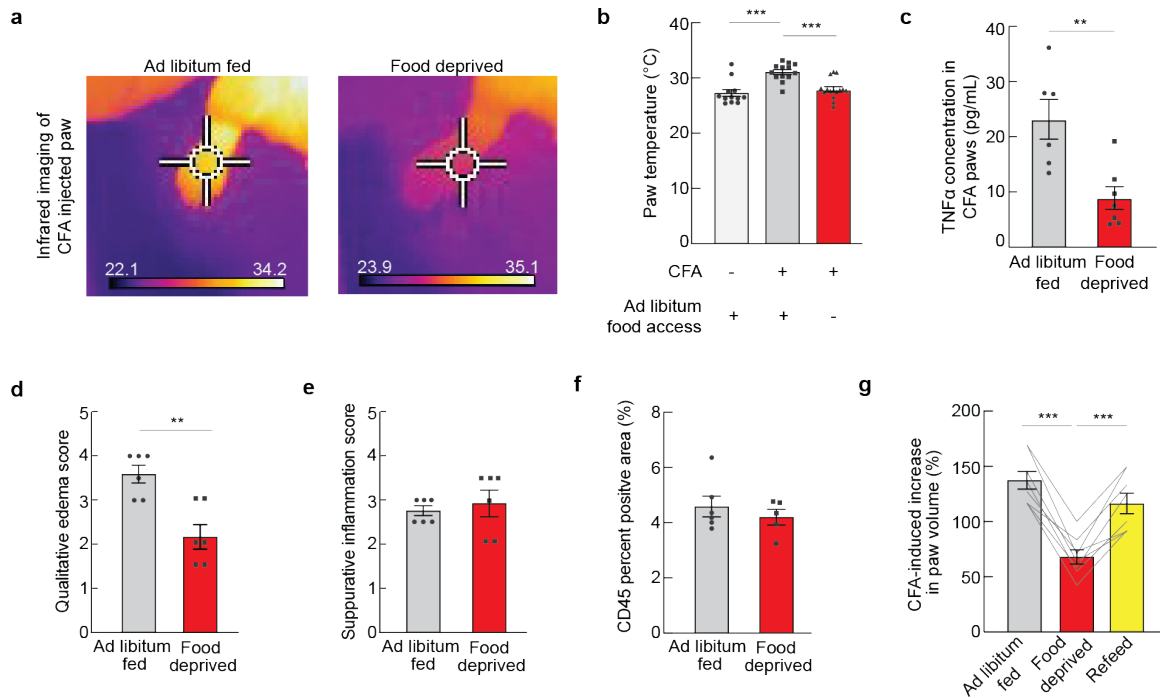


**Figure 3.3 | Hunger reduces paw edema and inflammation associated increase in temperature.**

(a) Infrared images of paws 24 h after injection with CFA in ad libitum fed and 24 h food deprived conditions. (b) Paw temperature of mice without a CFA injection (n=13), 24 h after a CFA injection in ad libitum fed (n=12) and 24 h food deprived states (n=15) (one-way ANOVA,  $p < 0.001$ ). (c) Concentration of TNF $\alpha$  detected in paws 24 h after CFA injection in ad libitum (n=6) or food deprived (n=7) mice (unpaired t-test,  $p = 0.004$ ). (d) Qualitative edema score from paw histology analysis of ad libitum fed (n=6) and 24 h food deprived (n=6) mice 24 h after a CFA injection (unpaired t-test,  $p = 0.002$ ). (e) Qualitative suppurative inflammation score from paw histology analysis of ad libitum fed (n=6) and 24 h food deprived (n=6) mice 24 h after a CFA injection (unpaired t-test,  $p = 0.641$ ). (f) CD45+ area in ad libitum fed (n=6) and 24 h food deprived (n=5) mice 24 h after a CFA injection (unpaired t-test,  $p = 0.430$ ). (g) Increase in paw volume of mice (n=8) 24 h after a CFA injection in ad libitum fed, 24 h food deprived and refeed states (one-way repeated measures ANOVA,  $p < 0.001$ ). Data are expressed as mean  $\pm$  SEM, t-test and post-hoc comparison: \*\* $p < 0.01$ , \*\*\* $p < 0.001$ .

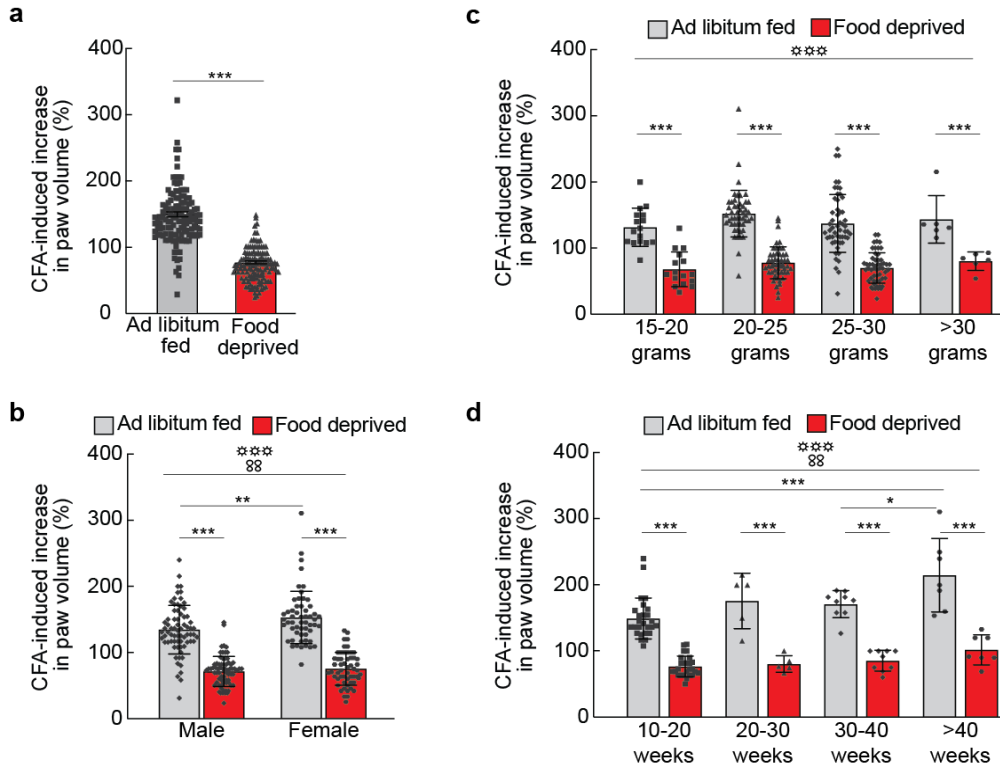


**Figure 3.4 | Hunger reduces paw inflammation regardless of sex, age, or weight.**

(a) Composite graphs showing the increase in paw volume of all mice tested in this figure across age, sex, and weight ( $n=126$ ) 24 h after a CFA paw injection in ad libitum fed state followed by a subsequent 24 h food deprivation (paired t-test,  $p<0.001$ ). (b) Increase in paw volume of male ( $n=71$ ) and female ( $n=55$ ) mice 24 h after a CFA paw injection during ad libitum fed state subsequently followed by 24 h food deprivation (two-way ANOVA, main effect of ad libitum v food deprived  $p<0.001$ ). (c) Increase in paw volume of 15-20 ( $n=16$ ), 20-25 ( $n=50$ ), 25-30 ( $n=54$ ), and >30 ( $n=6$ ) g mice 24 h after a CFA paw injection during ad libitum fed state subsequently followed by 24 h food deprivation (two-way ANOVA, main effect of ad libitum v food deprived  $p<0.001$ ). (d) Increase in paw volume of 10-20 ( $n=16$ ), 20-30 ( $n=50$ ), 30-40 ( $n=54$ ), and >40 ( $n=7$ ) week old mice 24 h after a CFA injection during ad libitum fed subsequently followed by 24 h food deprivation (two-way ANOVA, main effect of ad libitum v food deprived  $p<0.001$ ). Data are expressed as mean  $\pm$  SEM; t-tests and post-hoc comparisons: \* $p<0.05$ , \*\* $p<0.01$ , \*\*\* $p<0.001$ ; two-way ANOVA interaction:  $\infty p<0.01$ ; ANOVA main effect:  $\odot\odot\odot p<0.001$ .

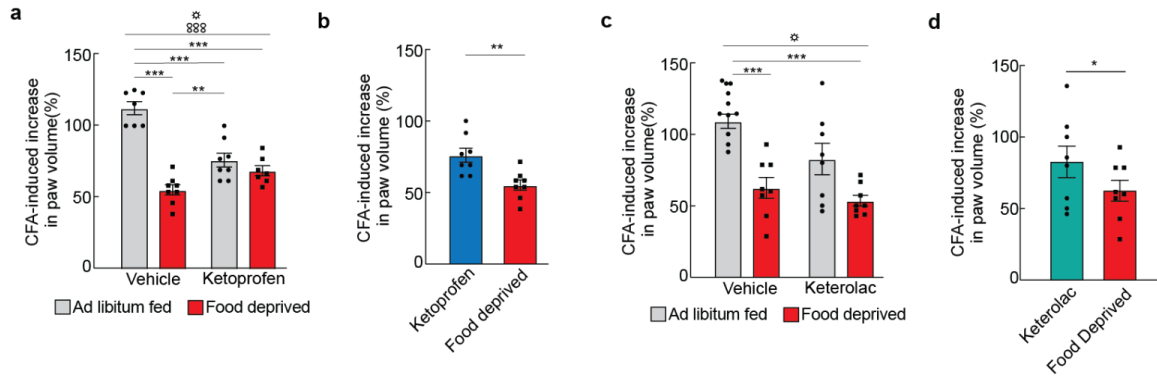


**Figure 3.5 | Hunger is comparable to non-steroidal anti-inflammatory drugs in reducing CFA-induced inflammation.**

(a) Increase in paw volume of mice 24 h after a CFA injection measured 1 h following administration of vehicle in ad libitum fed (n=7) and 24 h food deprived (n=8) states or 30 mg/kg ketoprofen in ad libitum (n=8) or 24 h food deprived (n=7) states (two-way ANOVA, main effect of injection  $p < 0.001$ ).

(b) Increase in paw volume of mice (n=8) 24 h after a CFA injection in ad libitum fed mice treated with 30 mg/kg ketoprofen or 24 h food deprived mice treated with vehicle (paired t-test,  $p = 0.003$ ).

(c) Increase in paw volume of mice 24 h after a CFA injection measured 1 h following administration of vehicle in ad libitum fed (n=8) and 24 h food deprived state (n=8) or 30mg/kg ketorolac in ad libitum fed (n=8) and food deprived (n=8) states (two-way ANOVA, main effect of injection  $p = 0.023$ ).

(d) Increase in paw volume of mice (n=8) 24 h after a CFA injection measured 1 h following treatment with 30 mg/kg ketorolac in the ad libitum fed state and vehicle in the 24 h food deprived state (paired t-test,  $p = 0.011$ ) Data are expressed as mean  $\pm$  SEM; t-tests and post-hoc comparisons: \* $p < 0.05$ , \*\* $p < 0.01$ , \*\*\* $p < 0.001$ ; two-way ANOVA interaction:  $\infty\infty\infty p < 0.001$ ; ANOVA main effect:  $\odot p < 0.05$ .

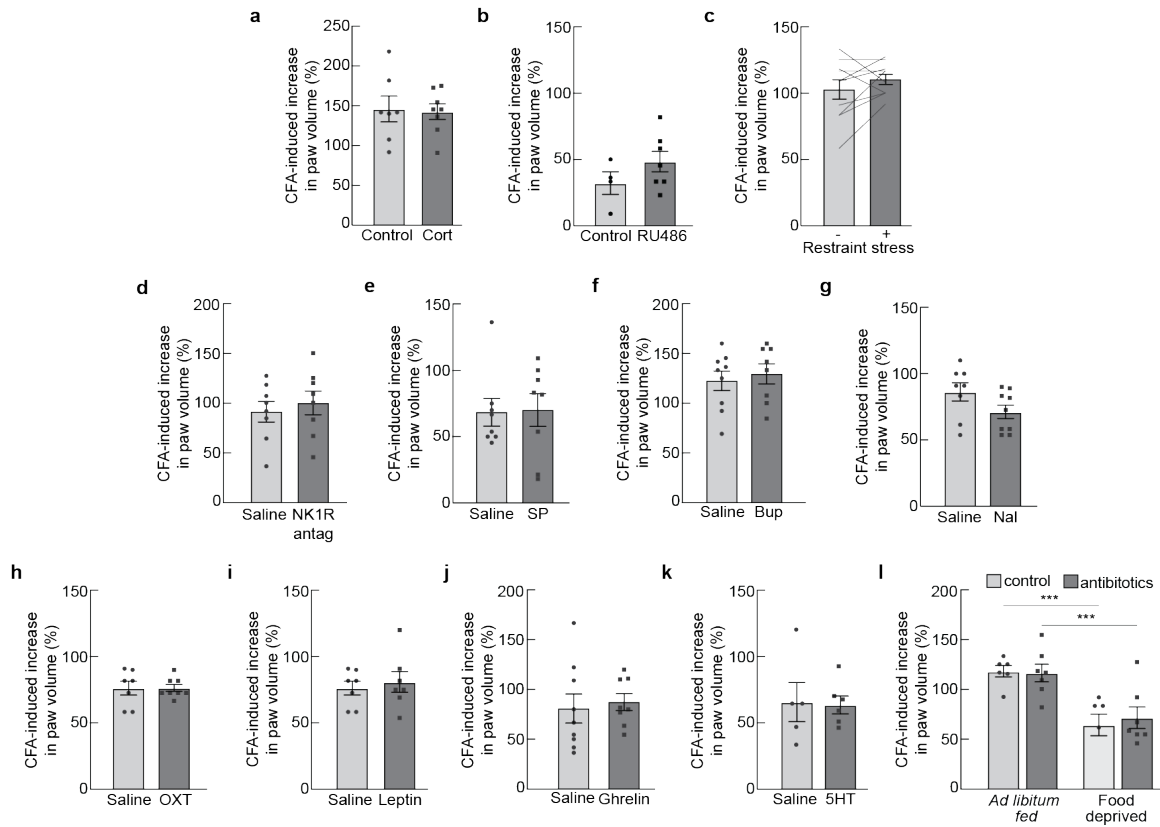


**Figure 3.6 | Pharmacological interrogation of systems known to influence immune responses failed to change the CFA-induced paw volume in ad libitum or food deprived conditions.**

(a) Increase in paw volume of mice 1 h after treatment with control (n=7) or 10mg/kg corticosterone (Cort) (unpaired t-test, p=0.850). (b) Increase in paw volume of mice 1 h after treatment with control (n=4) or 25mg/kg RU486 (n=7) during food deprivation (unpaired t-test, p=0.217). (c) Increase in paw volume of mice (n=10) before and after 1 h of restraint stress (paired t-test, p=0.242). (d) Increase in paw volume of mice 1 h after treatment with saline (n=8) or the 5mg/kg NK1R antagonist L-733-060 (n=8) (unpaired t-test, p=0.590). (e) Increase in paw volume of mice 1 h after treatment with saline (n=8) or 5µg/kg Substance P (SP) (n=8) (unpaired t-test, p=0.920). (f) Increase in paw volume of mice 1 h after treatment with saline (n=9) or 0.1mg/kg buprenorphine (Bup) (n=8) (unpaired t-test, p=0.628). (g) Increase in paw volume of mice 1 h after treatment with saline (n=8) or 10mg/kg naloxone (Nal) (n=9) during food deprivation (unpaired t-test, p=0.596). (h) Increase in

paw volume of mice 1 h after treatment with saline (n=7) or 1mg/kg oxytocin (n=8) during food deprivation (unpaired t-test, p=0.983). (i) Increase in paw volume of mice 1 h after treatment with saline (n=7) or 1mg/kg leptin (n=7) (unpaired t-test, p=0.636). (j) Increase in paw volume of mice 1 h after treatment with saline (n=9) or 1mg/kg ghrelin (n=8) (unpaired t-test, p=0.716). (k) Increase in paw volume of mice 1 h after treatment with saline (n=5) or 1mg/kg serotonin (5-HT) (n=6) during food deprivation (unpaired t-test, p=0.891). (l) Increase in paw volume of mice chronically treated with saline (n=6) or antibiotics (n=7) during ad libitum and food deprived states (two-way ANOVA, main effect of treatment p=0.821). Data are expressed as mean  $\pm$  SEM; t-tests and post-hoc comparisons: \*\*\*p<0.001

#### **CHAPTER 4: AGOUTI-RELATED PROTEIN EXPRESSING NEURONS PROJECTING TO THE PARAVENTRICULAR HYPOTHALAMUS AND PARABRACHIAL NUCLEUS CAN REDUCE INJURY-INDUCED INFLAMMATION.**

Is the anti-inflammatory response to hunger mediated by the brain? We next explored the possibility that neural circuits activated by food deprivation attenuate inflammatory responses to injury. Hunger is a full body experience causing disturbances in many systems that likely cannot be fully captured through AgRP neuronal manipulations, however, AgRP neuronal activity can recapitulate many phenotypes of a hungry animal. First, we can look at physiology. AgRP neuron activity is directly related to food deprivation. AgRP neuron activation significantly increases as an animal becomes food deprived and significantly decrease when sated (Cowley et al., 2003; Liu et al., 2012; Takahashi and Cone, 2005; Yang et al., 2011). AgRP neurons are interoceptive neurons that continually sense circulating nutrients and hormones to determine the right amount of activity for the appropriate feeding behavior. In fact, AgRP neurons rapidly change their activity levels in response to the calories consumed and subsequent satiation signals released for a given meal (Su et al., 2017). Activation of AgRP neurons also influences metabolism through changes in adiposity and insulin resistance (Pei et al., 2019; Steculorum et al., 2016). Next, we can look at behavior. Feeding behavior requires food seeking, detection, and consumption. AgRP neurons encourage food seeking by facilitating the pairing of contextual food cues with successful food consumption (Wang et al., 2021). AgRP neurons also participate in food detection as they reduce activity upon the presentation of sensory food cues (Betley et al., 2015; Su et al., 2017). Lastly, AgRP neurons are both necessary and sufficient to food consumption. Activation of AgRP neurons induces immediate food intake (Aponte et al., 2011; Krashes et al., 2011), while ablation causes anorexia (Gropp et al., 2005; Luquet et al., 2005). Aside from these obvious features of food intake, AgRP neurons also facilitate in dampening other biological drives and motivational states including sleep, anxiety, fear, and pain to prioritize feeding behaviors (Burnett et al., 2016; Goldstein et al., 2018; Alhadeff et al., 2018). Taken together, all these data highlight AgRP neurons as a manipulatable pathway to produce many features of hunger. AgRP neurons are of particular relevance for our

inflammation studies because of their ability to inhibit formalin- and CFA-induced inflammatory pain (Alhadeff et al., 2018). Because AgRP neurons recapitulate many facets of hunger and have been implicated in inflammatory pain responses, we investigated how activation of AgRP neurons influences CFA-induced inflammation.

### **Activation of AgRP neurons reduces inflammation.**

AgRP neurons makeup about 10,000 neurons in the ARC (Betley et al., 2013). To test their role in inflammation, we activated these neurons for 1 h, 24 h after a CFA paw injection. We expressed excitatory DREADDs in AgRP neurons and activated them with an intraperitoneal (i.p.) injection of CNO (Figure 4.1a). As expected (Krashes et al., 2011), chemogenetic activation of AgRP neurons caused ad libitum fed animals to robustly increase food intake compared to controls (Figure 4.1b). Chemogenetic activation of AgRP neurons led to an attenuation in CFA-induced paw volume (Figure 4.1c) while CNO in control mice had no effect on paw volume (Figure 4.1d). For a complementary approach to activate AgRP neurons, we engineered mice to express the light-sensitive ion channel, ChR2 exclusively in AgRP neurons and activated them with delivery of light (Figure 4.1e). As expected (Aponte et al., 2011), optogenetic activation of AgRP neurons increased food intake (Figure 4.1f). Optogenetic activation of AgRP neurons attenuated CFA-induced paw size (Figure 4.1g, 4.1h). Importantly, activating AgRP neurons also reduced the CFA-induced increase in temperature, suggesting that the neural circuits activated by hunger are sufficient to recapitulate hunger's suppression of both indications of inflammation (Figure 4.1i, 4.1j).

How does AgRP neuron signaling reduce peripheral paw inflammation? To explore the possibility that this central circuit mediates a rapid change in peripheral cytokines that influence inflammation, we next measured circulating levels of inflammatory cytokines following formalin paw injection (Figure 4.1k). We found a significant reduction in levels of TNF $\alpha$  (Figure 4.1l) following AgRP neuron stimulation. These data suggest that AgRP neuron activity may ultimately signal the periphery to decrease levels of inflammatory cytokines during food deprivation that can lead to reduction in inflammation.

Interestingly, activation of AgRP neurons was unable to reduce CFA-induced paw volume to the same extent as food deprivation. To understand AgRP neuron activity during food deprivation, we used fiber photometry to monitor calcium signaling of AgRP neurons while undergoing food deprivation. We engineered mice to express a genetically encoded calcium indicator in AgRP neurons and monitored neural activity of AgRP neurons in response to a food pellet at increasing hours of deprivation (Figure 4.2a, 4.2b). AgRP neurons reach peak activation after 4 hours of food deprivation (Figure 4.2c, 4.2d). However, paw volume does not reach its peak attenuation until after 18 hours of food deprivation (Figure 4.2e). In fact, after 4 hours of food deprivation, paw volume appears to be attenuated to the same degree as AgRP chemogenetic and optogenetic activation (Figure 4.1). This suggests that AgRP neurons are only one piece of the complicated relationship between food deprivation and injury-induced edema. From here, we sought to identify the pathway by which AgRP neurons are partially reducing CFA-induced paw volume.

#### **AgRP→PVH and AgRP→PBN subpopulations reduce inflammation.**

Hypothalamic AgRP hunger neurons project to multiple targets throughout the brain from the ARC (Betley et al., 2013; Broberger et al., 1998). Because AgRP neurons form anatomical subpopulations that do not collateralize (Betley et al., 2013), we were able to individually stimulate each axon projection to explore where hunger information is transmitted to suppress inflammation. We performed a systematic analysis of the major AgRP neuron projection subpopulations by activating individual projections in ad libitum fed mice and measuring CFA-induced changes in paw volume (Figure 4.3a). We found that activation of AgRP projection subpopulations in the PVH and PBN reduced paw volume after CFA (Figure 4.3b). In contrast, activation of projection subpopulations to the BNST, PVT, LH, CeA, and PAG had no effect on paw volume (Figure 4.3b). This reduction is dependent on the expression of ChR2, as light stimulation of control mice had no effect (Figure 4.3c). Interestingly, we found a difference in these two axonal populations to influence paw temperature. AgRP→PVH stimulation reduced CFA-induced paw temperature, however

AgRP→PBN stimulation did not change paw temperature (Figure 4.3d-4.3g). Further, neither population was able to reduce TNF $\alpha$  levels at the paw (Figure 4.h). We verified activation of each brain region through feeding assay, pain assays, and histology (Alhadeff et al., 2018; Betley et al., 2013) (Figure 4.4). The PVH and PBN are dense, complex structures with many cell types and functions. We next wanted to identify the subpopulation within each structure that AgRP is inhibiting to reduce paw inflammation.

**No tested subpopulations within the pvh and pbn were able to reduce paw inflammation.**

The PVH and PBN are dense brain regions with numerous cell types participating in many behavioral and physiological functions (see Appendix 1 and 2). We sought to identify the subpopulation of neurons within the PVH and PBN mediating the reduction in inflammation during AgRP inhibition of each structure. We started investigating the PVH by testing two major neuron populations previously implicated in regulating the immune system and inflammation: OXT and CRH neurons. OXT is a critical hormone in maintaining resilience to stressors, including inflammation, and typically inhibits proinflammatory cytokines (Carter et al., 2020) Manipulation of PVH<sup>OXT</sup> neurons had no effect on inflammation as both chemogenetic activation (HM3D) and inhibition (HM4D) did not change paw size in ad libitum (Figure 4.5a) or food deprived (Figure 4.5b) mice. We then tested activation of the central corticosterone system since glucocorticoids are believed to regulate the immune system (Rivest, 2001; Webster et al., 2002). Optogenetic (Figure 4.5c) and chemogenetic (Figure 4.5d) activation of PVH<sup>CRH</sup> neurons had no effect on inflammation in ad libitum fed mice. During food deprivation, chemogenetic activation of PVH<sup>CRH</sup> also had no effect on inflammation compared to controls (Figure 4.5e).

We have already implicated the PBN to regulate behavioral pain responses associated with inflammatory agents, we therefore started our interrogation of the PBN by looking at the populations that influenced pain behavior (Alhadeff et al., 2018). Chemogenetic inhibition of vesicular glutamate transporter 2 expressing (VGLUT2) neurons in the PBN reduced pain behavior during the formalin pain assay, however, PBN<sup>VGLUT2</sup> inhibition was unable to reduce paw

inflammation (Figure 4.6a). To specifically test if PBN neurons reducing inflammation are the same as PBN neurons attenuating pain behavior, we took advantage of mutant TRAP mice (*Fos<sup>CreERT2</sup>*) (Corder et al., 2019). We expressed inhibitory DREADDs (HM4D) into the PBN of TRAP mice followed by the induction of activity-dependent DNA recombination during a formalin pain assay (Figure 4.6b). This allowed for HM4D expression exclusively in neurons within the PBN that were activated during the 1 h formalin pain assay. Chemogenetic inhibition of PBN pain neurons failed to cause a change in paw volume (Figure 4.6c).

## Discussion

How does food deprivation, and AgRP→PVH and PBN signaling, ultimately result in reduced inflammation? The central control of inflammation is in part mediated by the HPA axis (Waldburger and Firestein, 2010). This system originates in the PVH and results in secretion of peripheral anti-inflammatory glucocorticoids. While food deprivation is well-known to increase circulating glucocorticoids, activating AgRP neurons does not significantly elevate plasma corticosterone (Steculorum et al., 2016), even though a subset of AgRP neurons densely innervate the PVH. Because it is unlikely that AgRP neurons are influencing these anti-inflammatory pathways, it is plausible that AgRP neurons are instead reducing inflammation through the inhibition of proinflammatory signals. In fact, both the PVH (Elmqvist and Saper, 1996; Elmqvist et al., 1996; Ericsson et al., 1994; Fulwiler and Saper, 1984; Moga et al., 1990; Sagar et al., 1995) and the PBN (Herbert et al., 1990; Mascarucci et al., 1998) have already been implicated in the central nervous system proinflammatory response originating from the NTS. Catecholaminergic neurons from the NTS directly target PVH neurons to activate the HPA axis, while glutamatergic signaling by NTS neurons in the PBN initiates visceral reflexes and transmits immune-sensory information to forebrain structures (Goehler et al., 2000; Herbert et al., 1990). Because AgRP neurons are inhibitory, it is possible that they block proinflammatory outputs from these pathways

We found that our circuit manipulations failed to reduce edema to the same degree as food deprivation. An intact immune system is critical for survival. Because of this, there are multiple

redundant pathways to ensure the detection of threats (Goehler et al., 2000). Here we identified two pro-inflammatory pathways, NTS→PVH and NTS→PBN, that are likely interrupted by AgRP activity. However, food deprivation is a complex full body condition that influences multiple systems outside the AgRP circuit. Alternate immune organs and pathways could be influenced by the severe level of food deprivation leading to a breakdown of multiple pathways of the pro-inflammatory response to CFA that are not captured in our AgRP neuronal activation model of hunger.

We found a parallel of AgRP→PBN to reduce injury-induced edema and inflammatory pain behavior and affect. It will be imperative for future work to determine whether the same or different PBN neurons mediate these two distinct but likely related functions. The PBN is believed to send immunosensory input to the CeA (Ericsson et al., 1994; Elmquist et al., 1996; Tkacs and Li, 1999) to integrate sensory information with an emotional context to produce the appropriate autonomic response (Roozendaal et al., 1990; LeDoux, 1995). The CeA could be the downstream target of these PBN neurons to enact both responses: decreased edema and fear.

Since we were unable to find specific cell types within the AgRP hunger pathway reducing inflammation, we questioned how inflammatory signals could be interacting with the central nervous system. The vagus nerve is a major pathway for bilateral communication between the periphery and central nervous system (Berthoud and Neuhuber, 2000; Goehler et al., 2000; Yuan and Silberstein, 2016). We next evaluated if the vagus nerve was critical for hunger to reduce CFA-induced paw inflammation.

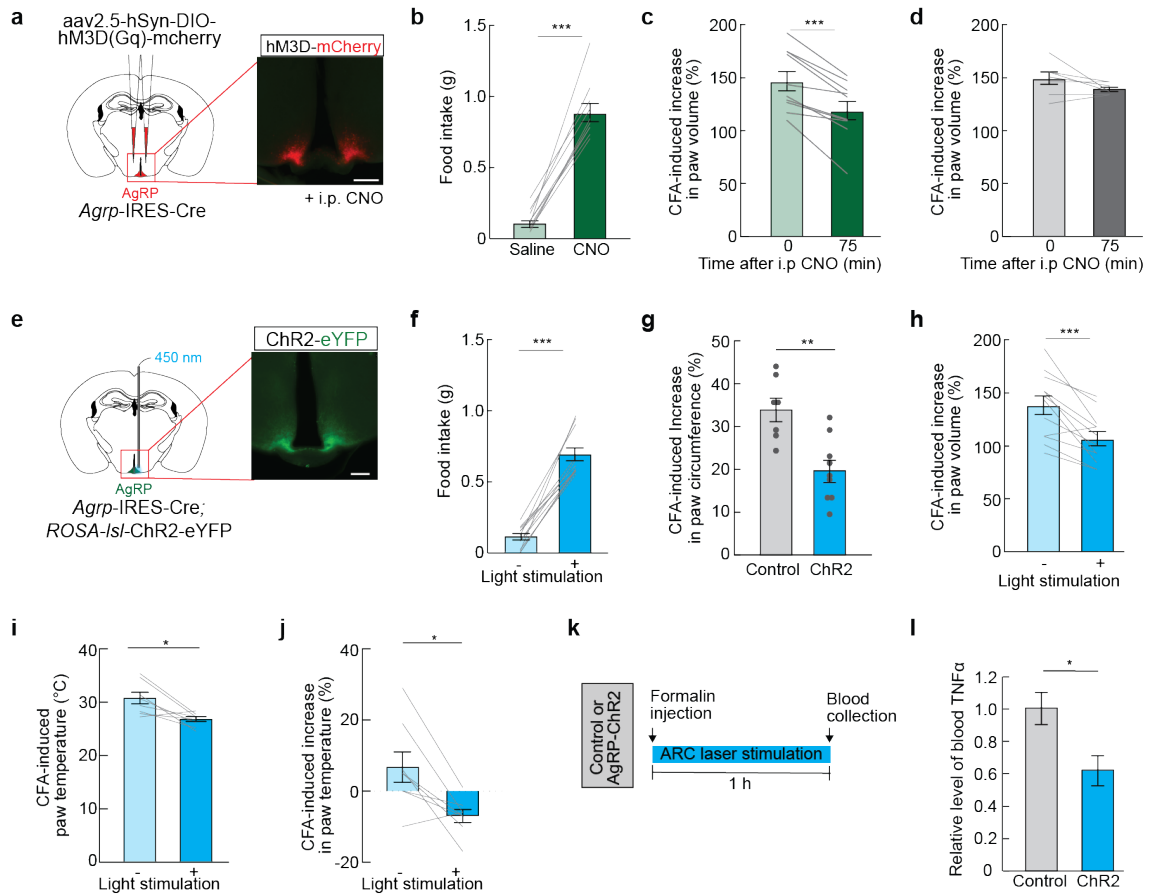


**Figure 4.1 | AgRP neuron activity reduces peripheral paw inflammation.**

(a) Schematic and representative image of Cre-dependent hM3D-mCherry expression in *AgRP-IRES-cre* mice, scale bar, 200  $\mu$ m. (b) 60 min food intake measurement following saline or 1 mg/kg CNO administration in ad libitum fed *AgRP* hM3D-expressing (n=10) mice (paired t-test, p<0.001). (c) Increase in paw volume 24 h after CFA injection in ad libitum fed *AgRP* hM3D-expressing (n=12) mice before and 75 min after 1 mg/kg CNO administration (paired t-test, p<0.001). (d) Increase in paw volume 24 h after CFA injection in ad libitum fed *AgRP* mCherry-expressing (n=7) mice before and 75 min after 1 mg/kg administration of CNO (paired t-test, p=0.153). (e) Schematic and representative image of Cre-dependent ChR2-eYFP expression in *Ai32 x AgRP-IRES-Cre* mice with an optical fiber over the ARC to selectively activate *AgRP* neurons, scale bar, 200  $\mu$ m. (f) 60 min food intake measurements without (-) and with (+) optogenetic stimulation in ad libitum fed *AgRP* ChR2-expressing (n=12) mice (paired t-test, p<0.001). (g) Increase in paw circumference

24 h after CFA injection in ad libitum fed control (n=7) and AgRP ChR2-expressing (n=9) mice (unpaired t-test,  $p < 0.01$ ). (h) Increase in paw volume 24 h after CFA injection in ad libitum fed AgRP ChR2-expressing (n=12) mice before (-) and after (+) 60 min of optogenetic stimulation (paired t-test,  $p < 0.001$ ). (i) Paw temperature 24 h after CFA injection of ad libitum fed AgRP ChR2-expressing mice (n=8) before (-) and after (+) 1 h of optogenetic stimulation (paired t-test,  $p = 0.010$ ). (j) Percent change in paw temperature before (-) and after (+) 1 h of optogenetic stimulation (paired t-test,  $p = 0.010$ ). (k) Experimental timeline: Control or AgRP ChR2-expressing mice were injected with formalin and given laser stimulation for 1 h before blood collection. (l) Relative levels of blood TNF $\alpha$  following 1 h of laser stimulation to control (n=6) or AgRP ChR2-expressing (n=6) mice (unpaired t-tests,  $p < 0.05$ ). Data are expressed as mean  $\pm$  SEM, t-tests: \* $p < 0.05$ , \*\* $p < 0.01$ , \*\*\* $p < 0.001$ .

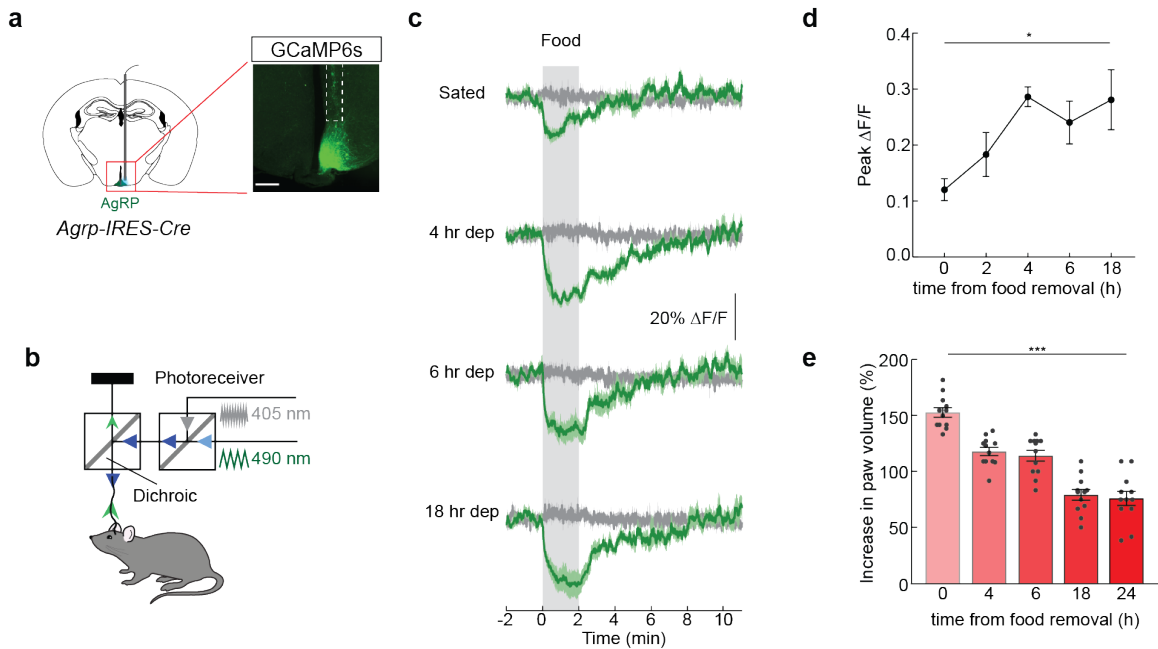


**Figure 4.2 | AgRP activity peaks after 4 hours of food deprivation, however, 18 hours of food deprivation maximally reduces CFA-induced edema.**

(a) Representative image showing GCaMP6s expression in AgRP neurons of AgRP-IRES-Cre mice. (b) Schematic showing the dual-wavelength fiber photometry setup used to monitor AgRP neuron activity during food deprivation. (c) Calcium-dependent (mean, green; SEM, green shading) and calcium-independent (mean, gray; SEM, gray shading) change in fluorescence ( $\Delta F/F$ ) in AgRP neurons in response to a food pellet at increasing hours of food deprivation (one-way repeated measures ANOVA,  $p=0.0211$ ). (d) Peak calcium-dependent  $\Delta F/F$  in response to a food pellet at increasing hours of food deprivation. (e) Increase in paw volume at various time points after food removal in mice ( $n=12$ ) injected with CFA (one-way repeated measures ANOVA,  $p<0.001$ ). Data is expressed as mean + SEM, t-tests: \* $p<0.05$ , \*\*\* $p<0.001$ .

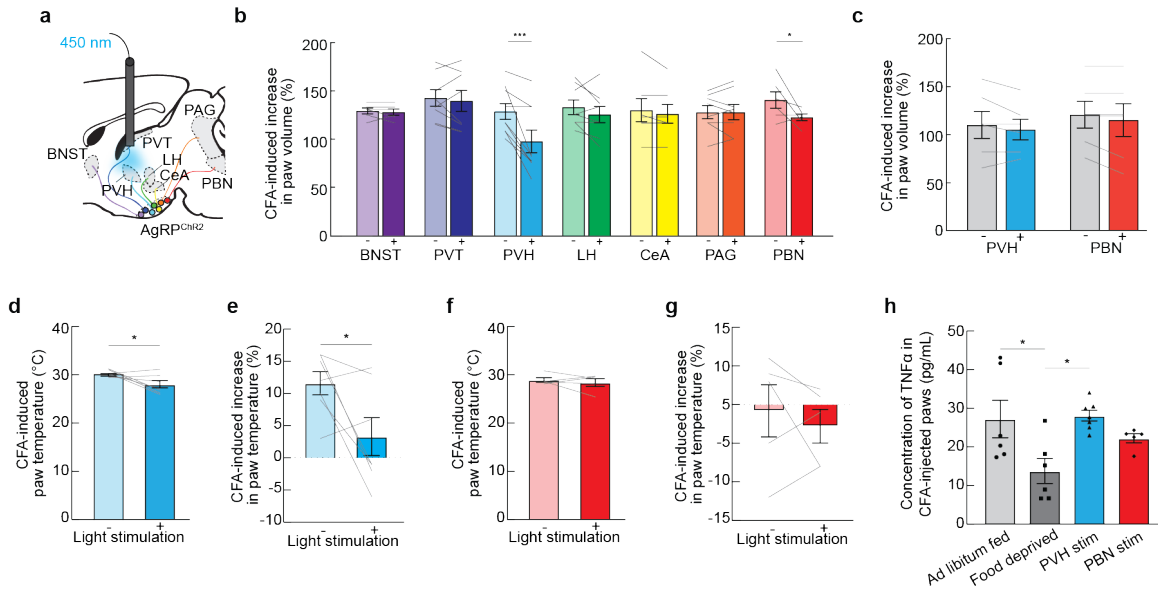


**Figure 4.3 | AgRP→PVH and AgRP→PBN neuron activity suppresses CFA-induced paw inflammation.**

(a) Diagram of the major AgRP projection subpopulations analyzed. Delivery of light to individual axon target fields of ChR2 expressing AgRP neurons (PVH shown here) allows for selective activation of discrete AgRP neuron projection subpopulations. (b) Increase in paw volume 24 h after a CFA injection in mice before (-) and after (+) 1 h of optogenetic stimulation of AgRP neuron projection subpopulations (n=8-9/group, two-way mixed effects ANOVA, Holm-Sidak post hoc, PVH p<0.001, PBN p=0.045, all other structures p=ns). (c) Increase in paw volume 24 h after a CFA injection of mice before (-) or after (+) 1 h of light exposure to AgRP neuron projection subpopulations (PVH, PBN) with control expression of tdTomato (n=6/group, two-way mixed effects ANOVA, p=0.863). (d) Paw temperature 24 h after CFA injection in mice (n=6) before (-) and after (+) 1 h of optogenetic stimulation of AgRP neuron projections in the PVH (paired t-test, p=0.044). (e) Percent change in paw temperature before (-) and after (+) 1 h of optogenetic stimulation of AgRP neuron projections in the PVH (n=6) (paired t-test, p=0.049). (f) Paw temperature 24 h after CFA injection in mice (n=5) before (-) and after (+) 1 h of optogenetic stimulation of AgRP neuron projections in the PBN (paired t-test, p=0.563). (g) Percent change in paw temperature before (-) and after (+) 1 h of optogenetic stimulation of AgRP neuron projections in the PBN (n=5) (paired t-

test,  $p=0.521$ ). (h) Concentration of TNF $\alpha$  detected in paws 24 h after CFA injection in ad libitum fed ( $n=6$ ), food deprived ( $n=6$ ), AgRP $\rightarrow$ PVH optogenetic stimulation ( $n=6$ ) and AgRP $\rightarrow$ PBN optogenetic stimulation ( $n=5$ ) mice (one-way ANOVA,  $p=0.012$ ). Data are expressed as mean  $\pm$  SEM, t-test and post-hoc comparisons: \* $p<0.05$ , \*\*\* $p<0.001$ .

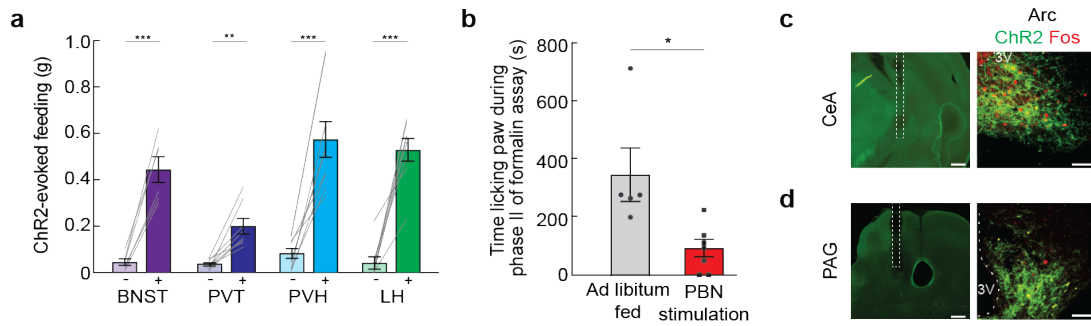


**Figure 4.4 | Axon targets were confirmed through feeding assays, pain assays, and histology.**

(a) ChR2-evoked feeding before (-) and after (+) 1 h stimulation of AgRP→BNST, PVT, PVH, and LH axon targets (paired t-tests,  $p=0.002$  for PVT,  $p<0.001$  for all other structures). (b) Time spent licking during formalin assay in ad libitum fed ( $n=5$ ) and AgRP→PBN stimulated mice ( $n=7$ ) (unpaired t-test,  $p=0.012$ ). (c) Fiber placement over the CeA, scale bar = 400 μm, and fos activation in the ARC after 1 h of AgRP→CeA axonal stimulation, scale bar = 100 μm. (d) Fiber placement over the PAG, scale bar = 400 μm, and Fos activation in the ARC after 1 h of AgRP→PAG axonal stimulation, scale bar = 100 μm. Data are expressed as mean  $\pm$  SEM, t-test and post-hoc comparisons: \* $p<0.05$ .

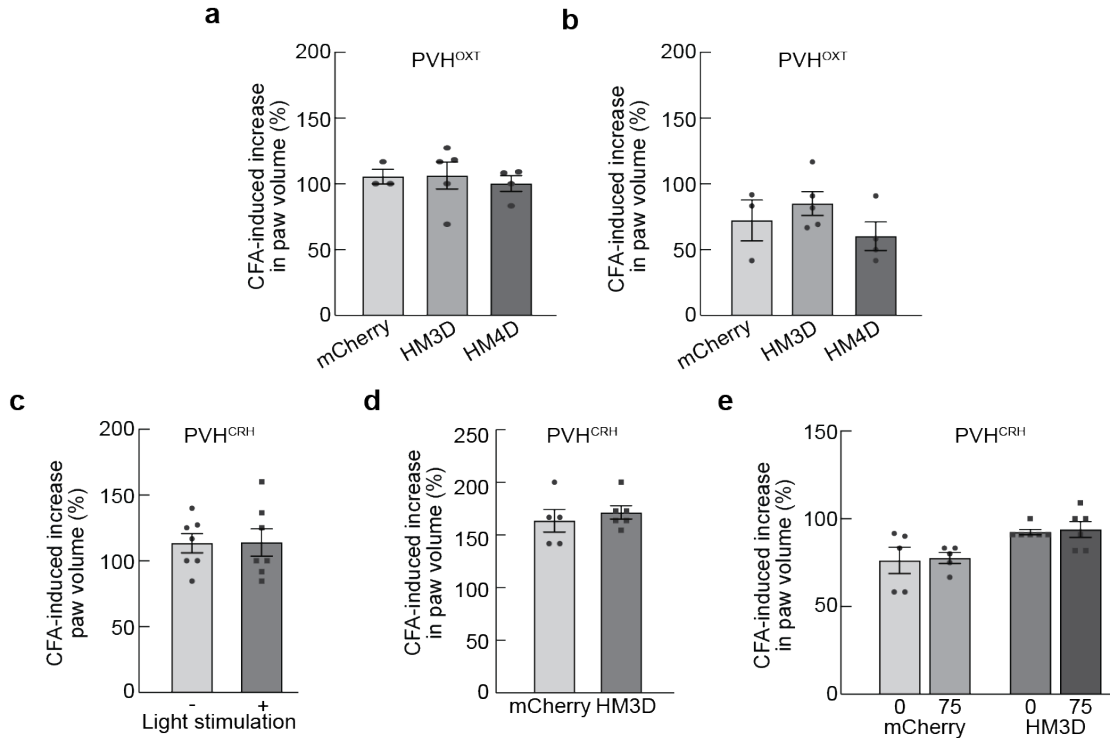


**Figure 4.5 | Manipulations of PVH<sup>OXT</sup> and PVH<sup>CRH</sup> neurons had no effect on CFA-induced paw volume.**

(a) Increase in paw volume after CFA injection in *OXT-IRES-cre* mice expressing PVH<sup>mCherry</sup> (n=3), PVH<sup>HM3D</sup> (n=5), or PVH<sup>HM4D</sup> (n=4) 75 minutes after 1mg/kg CNO administration (one-way ANOVA, main effect of virus p=0.862). (b) Increase in paw volume after CFA injection and 24 h food deprivation in *OXT-IRES-cre* mice expressing PVH<sup>mCherry</sup> (n=3), PVH<sup>HM3D</sup> (n=5), or PVH<sup>HM4D</sup> (n=4) 75 minutes after 1mg/kg CNO administration (one-way ANOVA, main effect of virus p=0.298). (c) Increase in paw volume after CFA injection in Ai32 x *CRH-IRES-cre* mice (n=7) before (-) and after (+) 60 min of optogenetic stimulation (paired t-test, p=0.920). (d) Increase in paw volume after CFA injection in *CRH-IRES-cre* mice expressing PVH<sup>mCherry</sup> (n=5) or PVH<sup>HM3D</sup> (n=6) 75 minutes after 1mg/kg CNO administration (unpaired t-test, p=0.528). (e) Increase in paw volume after CFA injection and 24 h food deprivation in *CRH-IRES-cre* mice expressing PVH<sup>mCherry</sup> (n=5) or PVH<sup>HM3D</sup> (n=6) before (0) and after (75) 1mg/kg CNO administration (paired t-tests, p=0.901, p=0.695). Data expressed as mean ± SEM.

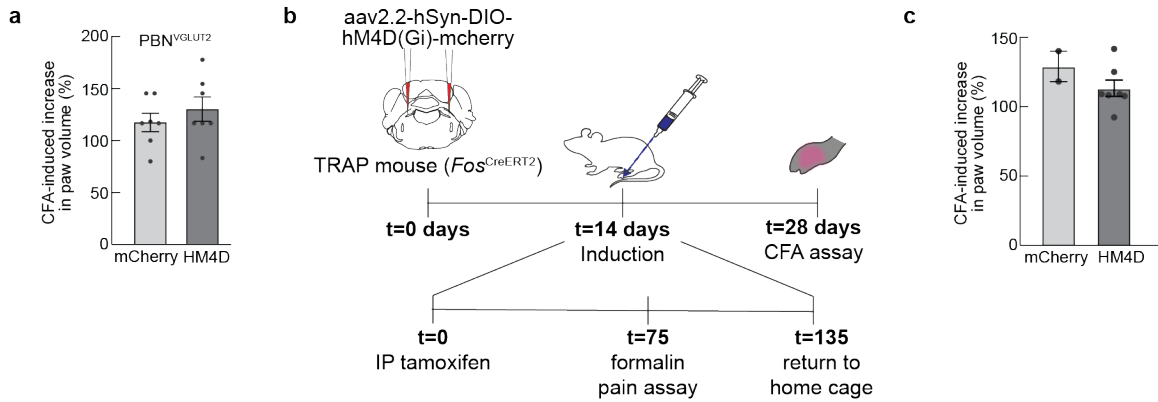


**Figure 4.6 | Manipulations of PBN populations capable of reducing inflammatory pain had no effect on CFA-induced paw volume.**

(a) Increase in paw volume after CFA injection in *VGlut2*-IRES-cre mice expressing PBN<sup>mCherry</sup> (n=7) or PBN<sup>HM4D</sup> (n=7) 75 minutes after 1mg/kg CNO administration (unpaired t-test, p=0.407). (b) Schematic for strategy to express HM4D in “PBN pain neurons” using Fos Trap mice. (c) Increase in paw volume after CFA injection in Fos Trap mice expressing PBN<sup>mCherry</sup> (n=2) or PBN<sup>HM4D</sup> (n=7) 75 minutes after 1mg/kg CNO administration (unpaired t-test, p=0.249). Data expressed as mean ± SEM.

## **CHAPTER 5: HUNGER USES THE EFFERENT PATHWAY OF THE VAGUS NERVE TO REDUCE PERIPHERAL INFLAMMATION**

The vagus nerve, also known as cranial nerve 10, is critical for communication between the periphery and central nervous system. The vagus transmits sensory information from peripheral organs to the brain and returns motor output to regulate heart rate, respiration, gut motility, and endocrine signaling among other things (Berthoud and Neuhuber, 2000; Yuan and Silberstein, 2016). To carry out these dual functions, the vagus nerve is composed of two signaling pathways: the afferent and efferent pathways. Vagal afferents detect interoceptive stimuli such as pain, pressure, nutrient levels, and inflammation through chemosensors and mechanosensors (Berthoud and Neuhuber, 2000). This information is transmitted to the brain, integrated among different structures, and returned to the periphery through vagal efferents (Craig, 2003). The vagus nerve allows for bidirectional communication and control of physiological functions to be tailored to the organism's mood, environment, and physiology at any given moment.

Both vagal pathways are composed of bipolar cells with cell bodies located in the nodose ganglion. The afferent pathway collects sensory information in the periphery and transmits it to the NTS and area postrema. Second order sensory neurons in the NTS carry information to other regions of the brain including the PBN, the hypothalamus, and motor nuclei in the medulla (Berthoud and Neuhuber, 2000). The central nervous system then returns information to the periphery via vagal efferents in the dorsal motor nucleus (DMX) (Yuan and Silberstein, 2016). The afferent pathway is primarily composed of glutamatergic neurons expressing the transient receptor potential cation channel subfamily V member 1 (TRPV1), while most efferent neurons are cholinergic (Berthoud and Neuhuber, 2000; Yuan and Silberstein, 2016). Together these two branches of the vagus nerve communicate and integrate information to elicit physiological changes to adapt to acute and chronic stimuli within the organism and in its surrounding environment.

Due to the vagus nerve's branching, chemosensation, and bidirectional communication, it is a key player in immunosensory detection and integration with the central nervous system. The

vagus nerve has afferent endings surrounding all major organs allowing for immediate recognition of inflammatory signals (Goehler et al., 2000; Pavlov and Tracey, 2012). The vagus nerve is also surrounded by dendritic cells. Dendritic cells are immunochemosensors located throughout the body. They detect pathogenic threats through TOLL-like receptors or by engulfing pathogenic particles. Once activated, dendritic cells release proinflammatory molecules include cytokines and chemokines that activate the vagus nerve (Sousa et al., 1999). The vagus nerve expresses many different types of immunoreceptors that allows the nerve to be responsive to inflammatory molecules. In fact, the cytokines can induce *fos* activation in vagal neurons (Goehler et al., 2000). Since the vagus nerve is poised so well for immune-to-brain communication, it is likely that the vagus is playing a role in anti-inflammatory effect of hunger.

#### **Subdiaphragmatic vagotomy disrupts the anti-inflammatory effect of hunger.**

The vagus nerve is known to influence the immune system by bridging the periphery with the central nervous system through the inflammatory reflex (Bonaz et al., 2017; Goehler et al., 2000; Pavlov and Tracey, 2012; Pavlov et al., 2003b). The inflammatory reflex initiates neural, endocrine, and behavioral responses to immune threats as an immediate innate defense mechanism to reestablish homeostasis (Bonaz et al., 2016, 2017). To understand if vagal signaling is responsible for the attenuation of CFA-induced paw inflammation during food deprivation, we performed a bilateral subdiaphragmatic vagotomy (VGX) as previously described (Alhadeff et al., 2019) (Figure 5.1a). This procedure destroys both the afferent and efferent connections of the vagus nerve preventing communication between the gut and the central nervous system. Importantly, this type of vagotomy leaves connections to the cardiac and respiratory systems intact. VGX and sham-operated mice both had a large inflammatory response to CFA resulting in similar increases in paw volume. However, after food deprivation, sham-operated mice had significantly smaller paws compared to VGX mice. Food deprivation failed to reduce the paws of VGX mice to the same extent as sham-operated mice (Figure 5.1b). This suggests that hunger is incapable of its full anti-inflammatory effect without vagal signaling.

## **Pharmacological blockade of all vagal output pathways disrupts the anti-inflammatory effect of hunger.**

We verified this result by pharmacologically blocking the inflammatory outputs of the vagus nerve. The vagus nerve communicates between the central nervous system and inflammatory pathways through adrenergic, corticosterone, and cholinergic signaling pathways (Bonaz et al., 2017) (Figure 5.2a, adapted from Bonaz et al., 2017). We tested the influence of each of these pathways on the relationship between hunger and inflammation. First, we looked at the HPA. Vagal afferents can influence immune responses through interaction with the HPA. In fact, VGX rats fail to show the proinflammatory response to a model of septic shock typically initiated by the HPA (Goehler et al., 1997; Watkins et al., 1995). Further, vagal afferents can activate the NTS in response to inflammatory cytokines leading to a release of anti-inflammatory glucocorticoids from the HPA to balance the immune response (Bonaz et al., 2017). To test the role of the HPA, we used corticotropin releasing factor (CRF) antagonists to prevent the output from the HPA and therefore render vagal communication ineffective. Systemic treatment with a CRF1 antagonist, antalarmin, and CRF2 antagonist, astressin 2B, had no effect on paw volume measurements compared to controls (Figure 5.2b). The vago-parasympathetic reflex uses acetylcholine as a modifier of the immune system. Specifically, the release of acetylcholine on to  $\alpha 7$  nicotinic acetylcholine receptors (nAChRs) on macrophages causes a reduction in the release of pro-inflammatory cytokines (Jonge and Ulloa, 2007; Wang et al., 2003). To test the role of the vago-parasympathetic reflex on the anti-inflammatory effect of hunger, we blocked all nAChRs using the antagonist mecamylamine during hunger. Mice systemically treated with mecamylamine had no difference in paw size compared to controls (Figure 5.2c). We also specifically tested the role of  $\alpha 7$  nAChR with the antagonist methyllycaconitine (MLA). Mice systemically treated with MLA also had no difference in paw size compared to controls during food deprivation (Figure 5.2d.) The vagus can also connect the immune-to-brain axis through the vago-sympathetic reflex. Through the vago-sympathetic reflex, the vagus nerve activates the spleen to reduce TNF $\alpha$  production through adrenergic signaling to T-cells (Bonaz et al., 2017; Rosas-Ballina et al., 2011). To test the role of

the vago-sympathetic reflex in food deprivation, we blocked beta adrenergic signaling using propranolol and SR59230A. Antagonism of beta adrenergic signaling had no effect on paw volume in food deprivation compared to controls (Figure 5.2e). We also tested the vago-sympathetic reflex by removing the spleen and therefore removing the output of vagal nerve activation. Splenectomy mice failed to show a difference in paw volume compared to sham mice during ad libitum or food deprived conditions (Figure 5.2f).

Pharmacological blockade of each output path of the vagus nerve had no effect on paw inflammation just like our pharmacological manipulations previously (see Figure 3.6). With redundancy and complexity in mind, we next tried to block all three pharmacological outputs from the vagus by administering a cocktail of adrenergic, corticosterone, and cholinergic antagonists. Simultaneous blockade of these three signaling pathways during food deprivation failed to reduce CFA-induced paw volume to the same extent as control treated mice (Figure 5.2g), recapitulating the effect of surgical VGX. Together these data suggest that food deprivation is partially working through the vagus nerve to reduce CFA-induced edema. Completely eliminating vagal signaling to and from the central nervous system either through surgical removal or pharmacological antagonism during food deprivation prevents the full attenuation of CFA-induced paw volume by food deprivation.

### **Hunger influences CFA-induced inflammation through the efferent vagus nerve.**

The VGX and pharmacology studies revealed a role for the vagus nerve in reducing inflammation during hunger, however, it did not tell us which direction of communication is responsible. Since the afferent and efferent pathways of the vagus nerve serve different functions, we sought to determine a directionality to the vagus nerve's influence on CFA-induced inflammation during hunger. To do this we used an afferent pathway specific vagotomy technique. Capsaicin is a neurotoxin that can ablate afferent fibers of the vagus nerve through binding of TRPV1 receptors (Berthoud, Patterson, Willing, Mueller, & Neuhuber, 1997; Hölzer, 1991, Prechtel & Powley, 1990; Sengupta & Gebhart, 1994). After administration of capsaicin, mice will no longer have afferent

signaling from the periphery through the vagus to the brain but will still have brain to periphery signaling through efferent fibers (Figure 5.3a). We verified that the capsaicin vagotomy (CAPS) ablated the afferent fibers through a cholecystokinin (CCK) feeding assay, hot plate assay and formalin pain assay. Administration of the satiation hormone CCK prevents food deprived animals from immediately eating chow. While CCK caused sham mice to eat very little chow, CAPS mice ate significantly more chow during the 30-minute assay (Figure 5.3b). CAPS mice also had a significantly longer latency to react on the hot plate than sham mice (Figure 5.3c). Interestingly, CAPS mice also had differences in paw licking during the inflammatory phase of the formalin pain assay. CAPS mice spent significantly less time licking their paw in response to the inflammatory pain compared to sham mice (Figure 5.3d). Through these three assays, we were confident that our CAPS model was successful at ablating the majority of vagal afferent neurons. To evaluate the role of the afferent vagus in inflammation, we measured CFA-induced inflammation to in ad libitum fed and food deprived animals. Both capsaicin and control treated mice had an increase in paw volume after a CFA injection while ad libitum fed showing that the immune response to injury was still intact. Interestingly, both groups also had a similar decrease in paw volume after food deprivation suggesting that the afferent vagus is not mediating the anti-inflammatory effect of hunger (Figure 5.3e). This shows that gut to the brain communication via the afferent fibers is not necessary. The different phenotypes between the VGX and CAPS models leads us to propose that efferent vagal fibers are mediating the anti-inflammatory effect of hunger.

While we have not directly tested the role of efferent vagal fibers in our CFA model, we wanted to see if there are differences in the activation of each pathway during hunger. To do this we looked at *fos* staining in the brainstem at structures where each path integrates with the central nervous system. The afferent pathway projects on to NTS neurons while the efferent pathway projects from the DMX (Berthoud and Neuhuber, 2000). These two brain regions are in proximity of each other but have different expression profiles. The main identifier for NTS neurons is CCK, while DMX neurons express choline acetyltransferase (ChAT). It is well known that NTS neurons are activated by feeding. D'Agostino et al. (2016) showed that NTS<sup>CCK</sup> neurons express the

immediate early gene *fos* after consuming nutrients but not when fasted (Figure 5.4a, 5.4b; adapted from D'Agostino et al., 2016) Conversely, preliminary data shows that DMX<sup>ChAT</sup> neurons become active during food deprivation as evident by *fos* staining (Figure 5.4c). Together with our VGX and pharmacology studies, this suggests that the efferent fibers are the critical pathway in the vagus nerve to reduce CFA-induced inflammation during hunger.

## **Discussion**

The vagus nerve has already been implicated in bridging the central nervous system with the immune system. The vagus nerve is well poised to serve as an immunosensory organ because it branches throughout the body and, thus, can have immediate detection of acute threats (Goehler et al., 2000). In fact, the vagus nerve expresses immunoreceptors that respond to the presence of cytokines and chemokines in the lymph and vascular systems (Goehler et al., 1997, 1999). Further, cytokines activate vagal sensory neurons as indicated by staining for the immediate early gene *fos* (Goehler et al., 2000). Our work shows that AgRP neurons can influence injury-induced edema responses mediated by the vagus likely through inhibition of the PVH and PBN. This finding corroborates two locations already known to be involved in central nervous system inflammatory pathways. When an immune threat is detected by the vagus nerve, excitatory inputs are transmitted to NTS. There is a parallel and redundant pro-inflammatory pathway from the NTS to both the PVH (Ericsson et al 1994, Sagar et al. 1995, Elmquist et al 1996, Fulwiler and Saper 1984, Moga et al 1990, Elmquist and Saper 1996) and the PBN (Herbert et al 1990, Schaffar et al., 1997, Mascarucci et al 1998). Both pathways are dependent on the vagus as subdiaphragmatic vagotomies prevents neuronal activation (Wan et al., 1994; Gaykema et al., 1995; Kapcala et al., 1996). We suggest that AgRP neurons can block these pathways at the PVH and PBN ultimately prevent pro-inflammatory signaling and changing the output of the vagus through efferent fibers to suppress injury-induced edema.

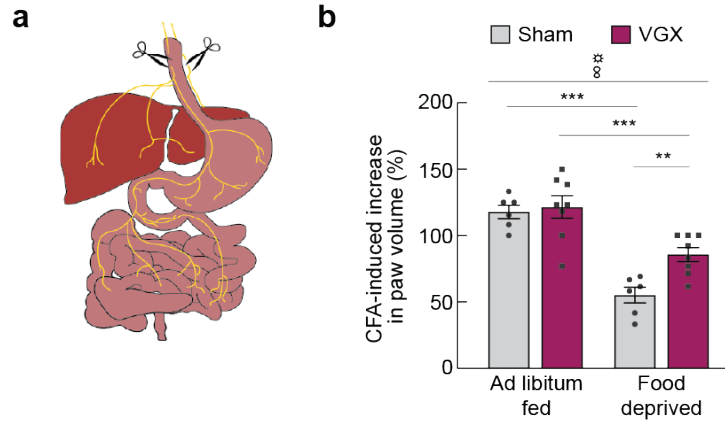


**Figure 5.1 | Mechanical destruction of both vagal pathways attenuates the suppression of CFA-induced paw inflammation during food deprivation.**

(a) Diagram of sub-diaphragmatic vagotomy procedure. (b) Increase in paw volume after CFA injection of sham- (n=11) and VGX- (n=13) operated mice during ad libitum fed and food deprived states (two-way ANOVA, main effect of operation  $p=0.049$ ; main effect of state:  $p<0.001$ ). Data expressed as mean  $\pm$  SEM; post-hoc comparisons: \*\* $p<0.01$ , \*\*\* $p<0.001$ ; two-way ANOVA interaction:  $\infty p<0.05$ ; ANOVA main effect:  $\odot p<0.05$ .

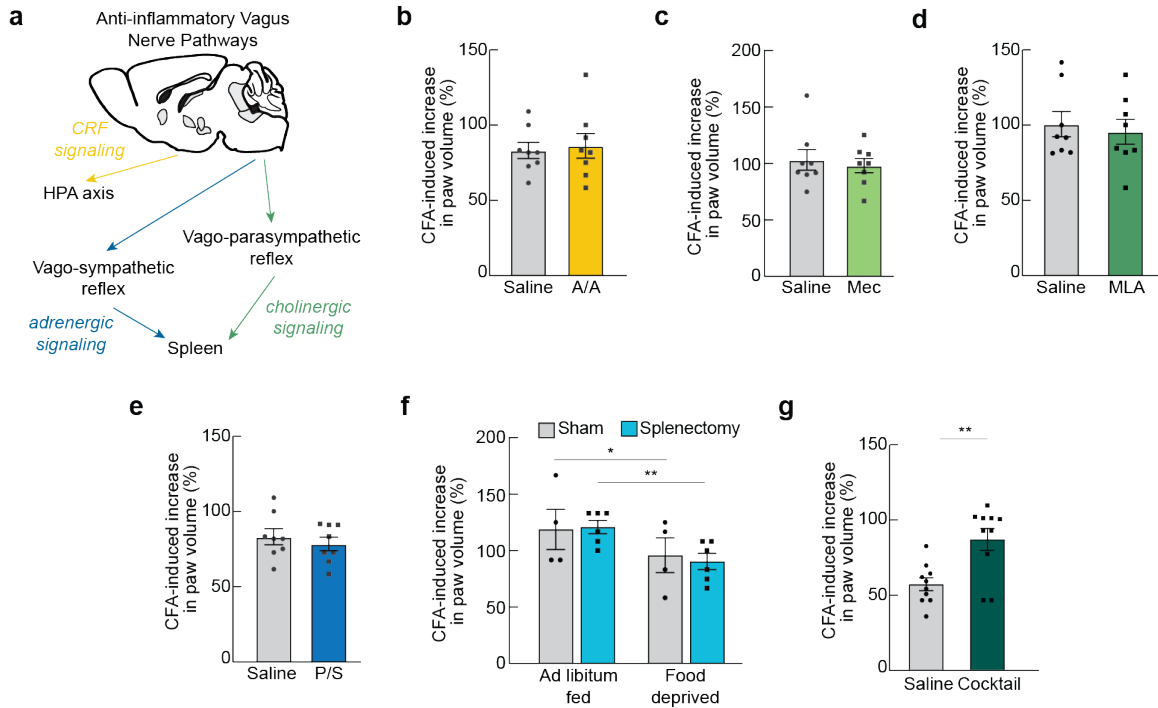


**Figure 5.2 | Pharmacological blockade of anti-inflammatory vagal outputs attenuates the anti-inflammatory effect of hunger.**

(a) Diagram of anti-inflammatory vagal pathways adapted from Bonaz et al. 2017. (b) Increase in paw volume of mice injected with CFA, food deprived and treated with saline (n=8) or 30mg/kg antalarmin and 15µg/kg astressin 2B (A/A) (n=8) to block CRF signaling (unpaired t-test, p=0.756). (c) Increase in paw volume of mice injected with CFA, food deprived and treated with saline (n=8) or 5mg/kg mecamlamine (Mec) (n=8) to block nAChRs (unpaired t-test, p=0.659). (d) Increase in paw volume of mice injected with CFA, food deprived and treated with saline (n=8) or 5mg/kg methyllycaconitine (MLA) (n=8) to block α7 nAChRs (unpaired t-test, p=0.677). (e) Increase in paw volume of mice injected with CFA, food deprived and treated with saline (n=8) or 10mg/kg propranolol and 5mg/kg SR59230A (P/S) (n=8) to block adrenergic signaling (unpaired t-test, p=0.506). (f) Increase in paw volume of mice injected with CFA in sham- (n=4) and splenectomy- (n=6) operated mice during ad libitum fed and food deprived states (two-way ANOVA, main effect of operation p=0.909; main effect of state: p<0.001). (g) Increase in paw volume of mice injected with CFA, food deprived and treated with saline (n=8) or a cocktail of A/A, Mec, and P/S (n=8) to

block all vagal signaling (unpaired t-test,  $p=0.002$ ). Data expressed as mean  $\pm$  SEM; t-test and post-hoc comparisons: \* $p<0.05$ , \*\* $p<0.01$

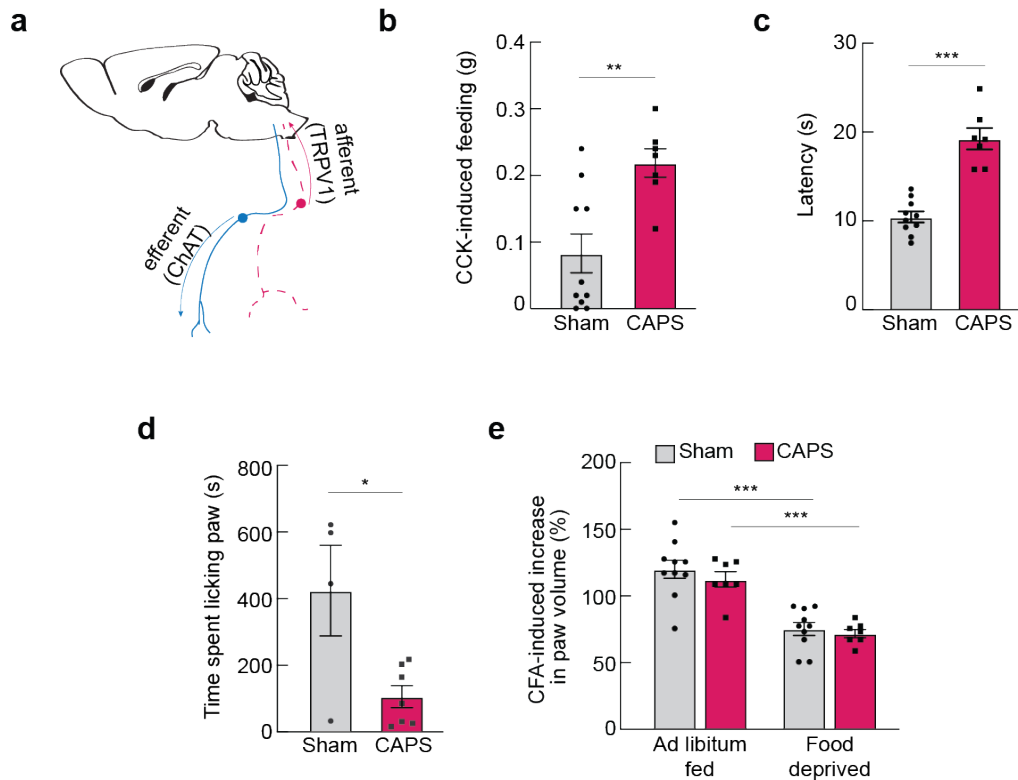
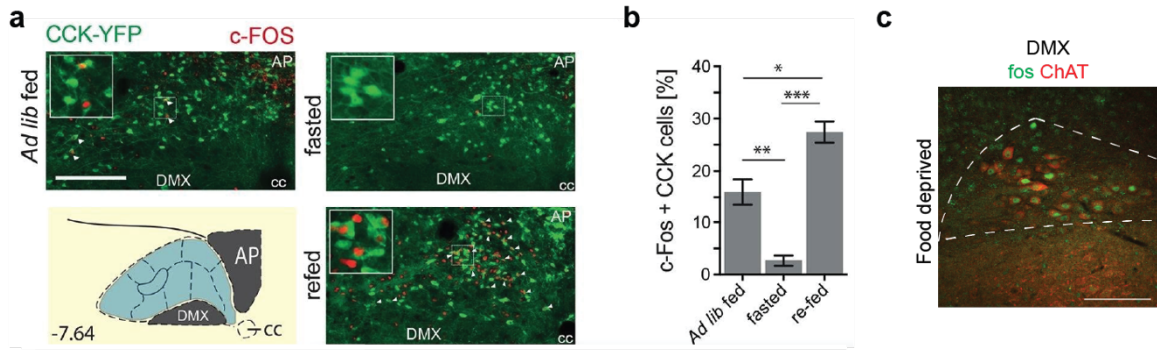


**Figure 5.3 | The afferent vagal pathway is not required for the anti-inflammatory effect of hunger.**

(a) Diagram of vagal pathways ablated by systemic treatment with capsaicin. (b) CCK-induced feeding in sham- (n=10) or capsaicin- (n=8) treated (CAPS) mice after 24 h food deprivation (unpaired t-test,  $p=0.004$ ). (c) Latency to paw withdraw of sham- (n=10) or capsaicin- (n=8) treated mice on 52°C hot plate (unpaired t-test,  $p<0.001$ ). (d) Time spent licking paw during phase II of formalin pain assay in sham- (n=4) and CAPS- treated mice (n=7) (unpaired t-test,  $p=0.040$ ). (e) Increase in paw volume after CFA injection in sham- (n=8) or capsaicin- (n=10) treated mice in ad libitum fed and food deprived states (two-way ANOVA, main effect of treatment  $p=0.435$ ; main effect of state:  $p<0.001$ ). Data expressed as mean  $\pm$  SEM; t-test and post-hoc comparisons: \* $p<0.05$ , \*\* $p<0.01$ , \*\*\* $p<0.001$ .



Adapted from D'Agostino et al. 2016

**Figure 5.4 | Hunger is likely working through the efferent pathway to reduce inflammation.**

(a) Representative *fos* labeling in the NTS of CCK reporter mice during ad libitum fed, fasted or fasted then re-fed mice (white arrows denote colocalized neurons, scale bar = 200  $\mu$ m) (adapted from D'Agostino et al., 2016). (b) Quantification of *fos* positive NTS<sup>CCK</sup> neurons (n=3-4) (one way ANOVA,  $p < 0.001$ ) (adapted from D'Agostino et al., 2016) (c) Representative *fos* activation (green) in *ChAT* positive (red) DMX neurons of mice ad libitum fed or 24 h food deprived (scale bar = 100  $\mu$ m).

## CHAPTER 6: METHODS FOR INFLAMMATION EXPERIMENTS

### Collaborators

Michelle L. Klima<sup>1,2</sup>, Kayla A. Kruger<sup>1</sup>, Nitsan Goldstein<sup>1,2</sup>, Santiago Pulido<sup>1</sup>, Aloysius Y. T. Low<sup>1</sup>, Charles-Antoine Assenmacher<sup>3</sup>, Amber L. Alhadeff<sup>2,4\*</sup>, J. Nicholas Betley<sup>1,2\*</sup>

1. Department of Biology, University of Pennsylvania, Philadelphia, PA 19104
2. Department of Neuroscience, University of Pennsylvania, Philadelphia, PA 19104
3. Comparative Pathology Core, Department of Pathobiology, University of Pennsylvania School of Veterinary Medicine, Philadelphia, PA 19104
4. Monell Chemical Senses Center, Philadelphia, PA 19104, USA

### Acknowledgements

We thank Jamie Carty, Ella Cho and Claudia Pichardo for assistance with experiments. We thank Dr. Brent Helliker for use of his infrared thermal camera. We thank Heather Collins of the University of Pennsylvania Diabetes Research Center Radioimmunoassay & Biomarkers Core for completion of the radioimmunoassay who is supported by P30-DK19525 and S10-OD025098. KAK is supported by the Center for Undergraduate Research & Fellowships at the University of Pennsylvania. NG is supported by the National Science Foundation Graduate Research (DGE-1845298). CAA is supported by the Abramson Cancer Center Support Grant (P30 CA016520) and instrumentation used by an NIH Shared Instrumentation Grant (210 OD023465-01A1). ALA is supported by the Monell Chemical Senses Center, NIH (DP2AT011965), the Klingenstein-Simons Fellowship Award, the American Heart Association (857082) and the Penn Institute for Diabetes, Obesity, and Metabolism. JNB is supported by the University of Pennsylvania School of Arts and Sciences, the American Diabetes Association (118IBS116), the American Heart Association (AHA 17SDG33400158), the Whitehall Foundation, the Klingenstein-Simons Fellowship Award and the NIH (1R01DK114104).

## STAR Methods

### EXPERIMENTAL MODEL AND SUBJECT DETAILS

Mice were group housed on a 12 h light/12 h dark cycle with ad libitum access to food (Purina Rodent Chow, 5001) and water unless otherwise noted. Vivarium rooms are controlled between 21.5 and 22.3 degrees Celsius with maintained with negative pressure between -191.6 to 109.5 Pascal. Group housed adult male and female mice (at least 8 weeks old) were used for experimentation. *Agrp*-IRES-Cre (Jackson Labs 012899, *Agrp*<sup>tm1(cre)Lowl/J</sup>) (Tong et al., 2008), *Crh*-IRES-cre (Jackson Labs 012704, B6(Cg)-Crhtm1(cre)Zjh/J), *Oxt*-IRES-cre (Jackson Labs 024234, B6;129S-Oxttm1.1(cre)Dolsn/J), *Vglut2*-IRES-cre (Jackson Labs 016963, Slc17a6tm2(cre)Lowl/J), Ai32 (Jackson Labs 012569, B6;129S-Gt(ROSA)26Sor<sup>tm32(CAG-COP4\*H134R/EYFP)Hze/J</sup>) (Madisen et al., 2012), Ai9 (Jackson Labs 007909, B6.Cg-GT(ROSA)26Sortm9(CAG-tdTomato)Hze/J) (Madisen et al., 2012), TRAP2 (*Fostm2.1(icre/ERT2)Luo/J*)(Allen et al., 2017), CD1 (Charles River 022) and C57BL6 (Jackson Labs 000664) mice were used for experimentation. All mice were habituated to handling and experimental conditions prior to experiments. We performed experiments in both male and female subjects and did not observe any trends or significant sex differences. Thus, to ensure our studies were appropriately powered and to minimize the number of subjects who had to undergo painful procedures, we combined males and females for analyses in all experiments. All procedures were approved by the University of Pennsylvania Institutional Animal Care and Use Committee.

### METHOD DETAILS

#### Recombinant Adeno-Associated Virus (rAAV) Constructs:

The following Cre-dependent rAAV vectors were used: AAV1-Syn-Flex-GCaMP6s-WPRE-SV40 (titer: 4.216e13 GC/mL), AAV5.Ef1a.doublefloxed-hChr2(H134R)-WfP-wPRE-HGHpA (titer: 1x10<sup>13</sup> vg/mL, Addgene 20298), AAV5.hSyn.DIO.hM3D(Gq).mcherry (titer: 7x10<sup>12</sup> vg/mL, Addgene 44361), AAV8.hSyn.DIO.mcherry (titer: 1x10<sup>13</sup> vg/mL, Addgene 50459). These viruses were

purchased from Addgene. Flex, Cre-dependent flip-excision switch. GCaMP, Genetically encoded calcium indicator resulting from a fusion of GFP, M13 and Calmodulin. WPRE, woodchuck hepatitis virus response element. ChR2, channelrhodopsin-2. hSyn, human Synapsin 1 promoter. DIO, double-floxed inverse orientation. hM3, human M3 muscarinic receptor.

### **Viral Injections, Fiber Optic and Cannula Placement:**

Bilateral viral injections and unilateral implantation of ferrule-capped optical fibers (200- $\mu$ m core, NA 0.37 for optogenetic stimulation) were performed as previously described (Alhadeff et al., 2018). For somatic stimulation of AgRP neurons, *AgRP-IRES-Cre* mice were crossed with Ai32 mice to express ChR2 in AgRP neurons. Mice were anesthetized with isoflurane (1.5-3%), given ketoprofen (5 mg/kg) and bupivacaine (2 mg/kg) analgesia and placed into a stereotaxic device (Stoelting). An optical fiber was placed over the arcuate hypothalamic nucleus (ARC) at bregma -1.35 mm, midline  $\pm$ 0.25 mm, skull surface -5.8 mm. For axonal stimulation of AgRP neurons, a rAAV encoding Cre-dependent ChR2 was bilaterally injected into the ARC of *AgRP-IRES-Cre* mice using the aforementioned ARC injection coordinates (150 nl per site, bilaterally). Optical fibers were implanted unilaterally according to the following coordinates: BNST: bregma +0.85 mm, midline  $\pm$ 0.82 mm, skull surface -3.8 mm; PVH: bregma -0.5 mm, midline  $\pm$ 0.2 mm, skull surface -5.4 mm; PVT: bregma -1.0 mm, midline  $\pm$ 0.0 mm, skull surface -2.7 mm; LH: bregma -1.0 mm, midline  $\pm$ 0.9 mm, skull surface -5.4 mm; CeA: bregma -1.15 mm, midline  $\pm$ 2.4 mm, skull surface -4.25 mm; ARC: bregma -1.35 mm, midline  $\pm$ 0.25 mm, skull surface -5.8 mm; PAG: bregma -4.4 mm, midline  $\pm$ 0.6 mm, skull surface -2.8 mm; lateral PBN: bregma -5.8 mm, midline  $\pm$ 1.2 mm, skull surface -3.7 mm. Fibers were secured to the skull with bone screws and dental cement. Mice were given at least 3 weeks for recovery and transgene expression. For fiber photometry (FP) experiments, unilateral injections of a virus designed to express GCaMP6s for AgRP neurons were performed in the arcuate hypothalamic nucleus (ARC, 300 $\mu$ L total) according to the coordinates above. A ferrule-capped optical fiber (400- $\mu$ m core, NA 0.48, Doric, MF2.5, 400/430-0.48) was implanted 0.2 mm above the injection site and secured to the skull with Metabond cement (Parkell, S380) and dental cement (Lang Dental Manufacturing, Ortho-jet BCA Liquid, B1306 and Jet Tooth

Shade Powder, 143069). For chemogenetic inhibition of AgRP neurons, PVH<sup>OXT</sup>, PVH<sup>CRH</sup>, PBN<sup>VGLUT2</sup>, and PBN FosTrap pain neurons, the appropriate transgenic cre mouse was bilaterally injected (300nl/hemisphere) with Cre-dependent rAAV encoding inhibitory Designer Receptors Exclusively Activated by Designer Drugs (DREADDs, HM4D) or Cre-dependent rAAV encoding excitatory Designer Receptors Exclusively Activated by Designer Drugs (DREADDs, HM3D). Fiber placements and viral expression were verified post-mortem.

#### **Complete Subdiaphragmatic Vagotomy:**

Mice were maintained on a liquid diet (Ensure Plus Vanilla, Abbott, 53642) for at least 3 days prior to surgery to promote survival and recovery. Mice were anesthetized with isoflurane (1.5%–3%) and treated with subcutaneous meloxicam (5 mg/kg), bupivacaine (2 mg/kg) and buprenorphine SR (1 mg/kg) analgesia. An abdominal midline incision was made through skin and muscle. The stomach was laparotomized to expose the esophagus, and the dorsal and ventral vagal trunks were then exposed by gently teasing them apart from the esophagus. The vagal trunks were resected and cauterized. Control mice received a sham surgery that consisted of all surgical procedures except for the resection and cauterization of the vagus nerve. Functional verification of vagotomy was confirmed by examining CCK induced anorexia (see below). Histological verification of vagotomy was confirmed using an i.p. injection of 0.1% Fluoro-Gold and examining Fluoro-Gold presence in the dorsal motor nucleus of the vagus (DMX) 5 days post-injection.

#### **Capsaicin-Induced Vagotomy:**

4-week-old mice were treated with varying 3 doses of capsaicin for 2 days to ablate the afferent vagal pathway. Mice were pretreated with an i.p. injection of 0.3mg/kg atropine 30 minutes before each capsaicin dose. Mice were maintained at 1.5-3% isoflurane 10 minutes prior to capsaicin treatment and for 30 minutes post injection. On day 1, mice received 8mg/kg capsaicin in the morning and 15mg/kg in the evening. On day 2, mice received a second 15mg/kg dose of capsaicin. Mice were given 4 weeks to recover from the procedure before being used for experiments. Vagal afferent ablation was verified by examining CCK induced anorexia, and pain measurements.

**Splenectomy:**

Mice were anesthetized with isoflurane (1.5%–3%) and treated with subcutaneous meloxicam (5 mg/kg), bupivacaine (2 mg/kg) and buprenorphine SR (1 mg/kg) analgesia. An abdominal midline incision was made through skin and muscle. The stomach was laparotomized to expose the spleen. The spleen was resected and cauterized. Control mice received a sham surgery that consisted of all surgical procedures except for the resection and cauterization of the spleen.

**FosTrap “pain neuron” capture:**

Trap2 mice with bilaterally injections of HM4D were i.p. injected with 50mg/kg of 4-hydroxytamoxifen (dissolved in ethanol and diluted in corn oil, and subsequent removal of ethanol by evaporation). Mice then underwent a formalin pain assay (described below).

**General Experimental Design:**

For each experiment, our subject numbers were determined by our pilot studies, laboratory publications, and power analyses [power=0.8, significance level=0.05, effect sizes=10-30%]. For within-subject behavioral analyses, all mice received all experimental conditions. For between-subject analyses, mice were randomly assigned to experimental condition. For all behavioral experiments, virus expression, fiber placements, and/or cannula placements were verified post-mortem, and any mice with viral expression or implants outside of the area of interest were excluded from all analyses.

**Induction of Peripheral Inflammation by Noxious Chemical Stimuli:**

To induce inflammation mice were injected subcutaneously in the dorsal hind paw with 20  $\mu$ l of 2% formalin or saline (control). To induce longer-term inflammation, mice were injected subcutaneously in the plantar hind paw with 30  $\mu$ L of 1:1 ratio of Complete Freund's Adjuvant (CFA) and saline. Doses and volumes of chemicals were based on previous work from our lab and others' (Alhadeff et al., 2018; Carey et al., 2017; Hamm and Lyeth, 1984; Hunskaar and Hole, 1987; Marchand et al., 2005).

**In Vivo Photostimulation:**

Photostimulation of AgRP neurons was performed as previously described, with 10 ms pulses at 20 Hz for 1 s, repeated every 4 s (Aponte et al., 2011). The output beam from a diode laser (450 nm, Opto Engine) was controlled by a microcontroller (Arduino Uno) running a pulse generation script. The laser was coupled to a multimode optical fiber (200  $\mu\text{m}$  core, NA 0.37, Doric) with a 1.25 mm OD zirconium ferrule (Kientech) and mating sleeve that allowed delivery of light to the brain by coupling to the implanted ferrule-capped optical fiber in the mouse. Power was set to ensure delivery of at least 2 mW/mm<sup>2</sup> to AgRP soma and at least 5 mW/mm<sup>2</sup> to the center of the AgRP neuron projection fields using the following software: <https://web.stanford.edu/group/dlab/cgi-bin/graph/chart.php>.

**Photostimulation-induced food intake measurements:**

To functionally verify our AgRP neuron stimulation, we measured 1 h AgRP neuron stimulation-evoked food intake as previously described (Aponte et al., 2011). Briefly, at least one week following ARC fiber optic implant and 3 weeks following AgRP axonal subpopulation fiber optic implant, *Agrp-IRES-Cre* x *Ai32* mice were allowed to habituate for at least one hour to a chamber with ad libitum access to chow and water. Following the habituation period, food intake was measured for 1 h to establish a pre-stimulation baseline. Photostimulation was performed during the next hour as described above. After each hour, food intake was measured. Mice that consumed <0.55 g of chow during 1 h of AgRP neuron stimulation were excluded from experiments.

**Chemogenetic-induced food intake measurements:**

To functionally verify our AgRP neuron activation via chemogenetic activation, we measured 1 h AgRP neuron CNO-evoked food intake in a similar manner as for stimulation-evoked food intake (Krashes et al., 2011). Briefly, at least three weeks following ARC HM3D injections, *Agrp-IRES-Cre* mice were i.p. injected with CNO (1 mg/kg) or saline and allowed to habituate for fifteen minutes to a chamber with access to water. Chow was then added to the chamber and food intake was measured after 1 h. Feeding assays were performed in a counterbalanced manner so that each

mouse received both a CNO and saline injection on different days. Mice that consumed <0.55 g of chow during 1 h of AgRP neuron chemogenetic activation were excluded from experiments.

#### **Food Deprivation/Restriction:**

For 24 h food deprivation, mice were placed in a cage with alpha dry bedding and ad libitum access to water, but no food, 24 h prior to experimentation. For chronic food restriction, mice were weighed at the same time each day and given chow once daily (1.5–3.0 g) after experimentation to maintain 85%–90% of their starting body weight.

#### *Effect of AgRP Neuron Stimulation on Food Intake.*

Mice were allowed to habituate for at least one hour to a chamber with a lined floor and ad libitum access to chow and water. Following the habituation period, food intake was measured for 1 h to establish a prestimulation baseline. Photostimulation was performed during the next hour. After each hour, food intake was measured. For somatic AgRP neuron stimulation, only mice that consumed > 0.6 g of chow were included in experiments, see Figure 4.1f. Food intake evoked by stimulation of each AgRP neuron projection subpopulation was measured and reported in Figure 4.4a.

#### *Effect of AgRP Neuron Activation on Food Intake.*

Mice were allowed to habituate for 15 min after an i.p. injection of saline or CNO (1mg/kg) to a chamber with a lined floor and ad libitum access to water. Following the habituation period, food intake was measured for 1 h. CNO and saline trials were counterbalanced across mouse so that each mouse received both conditions over the course of a week. Only mice that consumed > 0.6 g of chow were included in experiments, see Figure 4.1b.

#### *Effect of CCK on Food Intake.*

Sham or capsaicin-treated mice were overnight food deprived and given i.p. injections of CCK (10 mg/kg in saline). Food intake was measured after 30 min.

## QUANTIFICATION OF INFLAMMATION

### Paw Volume Measurements:

Mice were anaesthetized with 1.5-3% isoflurane for a baseline paw volume measurement as well as for inflammation-induced paw volume measurements. The plethysmometer (Ugo Basile, Italy, 37140) water cell was filled with a saline solution to create a visible meniscus. Before each trial, the plethysmometer was calibrated with a 0.5 mL calibrating weight. The anesthetized mouse was then positioned so that the paw was submerged in the solution up to the ankle joint and the volume was recorded. Both paws were measured and recorded for all animals. Paw measurements were taken by experimenters blinded to the experimental conditions. Mice were kept in their home cages in the intervening time between paw measurements. Mice who had a raw CFA-induced paw volume less than 0.25 were eliminated from experiments to ensure all mice had sufficient inflammation to make comparisons. To analyze the data, paw volume measurements taken after the CFA injection were compared to their original paw volume pre-injection using the following equation:

$$\frac{\text{paw measurement} - \text{baseline paw measurement}}{\text{baseline paw measurement}} \times 100$$
 to obtain a percent increase from baseline paw volume.

### Paw Circumference Measurements:

Mice were anaesthetized with 1.5-3% isoflurane for a baseline paw circumference measurement as well as for inflammation-induced paw circumference measurements. A thin string was tied and marked around the middle of the paw, ensuring all digits were included in the measurement. Marked strings were measured by experimenters blinded to experimental condition. Mice were kept in their home cages in the intervening time between injection and paw measurement.

### Paw Temperature Measurements:

Mice were lightly anesthetized with 1.5-3% isoflurane. Mice were positioned so that their paw was flat on a cardboard surface. Using an FLIR T450sc Professional Thermal Camera, paws were imaged with the temperature sensor positioned in the center of the paw and the corresponding temperature was recorded.

**Paw TNF $\alpha$  measurements:**

Mice were heavily sedated using isoflurane prior to sample collection. Hindpaws were cut at the patella, flash frozen on dry ice in 2 mL tubes, and stored at -80°C. Immediately before the ELISA, hindpaw samples were crushed and placed in 2mL tubes with 3 mm zirconium beads and 1 mL of lysis buffer (Invitrogen, FNN0071), and PMSF protease inhibitor (0.5 mM). Samples were shaken in a microtube homogenizer at 3 times at 400 rpm for 30 seconds each time. 100  $\mu$ L of the resulting supernatant were collected for the ELISA and not diluted further. TNF- $\alpha$  concentration was measured using a mouse Quantikine ELISA Kit (R&D Systems, Minneapolis, MN). The sensitivity of this assay is 7 pg/mL.

**Histopathology Analysis:**

Animals were anesthetized with 3% isoflurane and the legs were removed at the hip joint. Paws were rinsed in cold PBS then post-fixed in 10% formalin for 72 h on a shaker at room temperature. Paws were then stored in 50% EtOH. After fixation, the entire legs were decalcified in 15% formic acid for 12h and two sections at the level of the tarsus, going through the footpad, were obtained and processed for paraffin embedding, sectioning and staining with hematoxylin and eosin. The slides were evaluated semi-quantitatively by board certified veterinary pathologists, blinded to the experimental group distribution.

For immunohistochemistry, 5  $\mu$ m thick paraffin sections were mounted on ProbeOn™ slides (Thermo Fisher Scientific). The immunostaining procedure was performed using a Leica BOND RXm automated platform combined with the Bond Polymer Refine Detection kit (Leica #DS9800). Briefly, after dewaxing and rehydration, sections were pretreated with the epitope retrieval BOND ER2 high pH buffer (Leica #AR9640) for 20 minutes at 98°C. Endogenous peroxidase was inactivated with 3% H<sub>2</sub>O<sub>2</sub> for 10 minutes at room temperature (RT). Nonspecific tissue-antibody interactions were blocked with Leica PowerVision IHC/ISH Super Blocking solution (PV6122) for 30 minutes at RT. The same blocking solution also served as diluent for the primary antibody. Rat monoclonal primary antibody against CD45-LCA (BD Biosciences; #553076) was used at a

concentration of 1:300 and incubated on the sections for 45 minutes at RT. A biotin-free polymeric IHC detection system consisting of HRP conjugated goat anti-rat IgG (Vector Laboratories MP-7444) was then applied for 25 minutes at RT. Immunoreactivity was revealed with the diaminobenzidine (DAB) chromogen reaction. Slides were finally counterstained in hematoxylin, dehydrated in an ethanol series, cleared in xylene, and permanently mounted with a resinous mounting medium (Thermo Scientific ClearVue™ coverslipper). Pooled sections of murine lymphoid tissues, including the cervical and mesenteric lymph nodes and the spleen, served as positive controls. Negative controls were obtained either by omission of the CD45-LCA antibody or replacement with an irrelevant isotype-matched rat monoclonal antibody.

The IHC slides were scanned at 20X magnification using a Leica Aperio AT2 slide scanner (Leica Biosystems, Inc., Buffalo Grove, IL) and image acquisition and analysis was performed with ImageScope (Leica Biosystems, Inc., Buffalo Grove, IL). A single positive pixel count algorithm was generated to quantify the area of CD45-LCA positivity, while the total area of tissue on the slide was measured using a Genie algorithm.

#### *Effect of Food Deprivation on Formalin-Induced Peripheral Inflammation*

Food was removed 24 h prior to formalin injection. Ad libitum fed mice served as controls. Paw volume and paw circumference were measured 60-min post-injection.

#### *Effect of Food Restriction on Formalin-Induced Peripheral Inflammation*

Mice were maintained at 85-90% BW for 1 week prior to receiving a CFA paw injection. Paws were measured 3 h, 24 h, 48 h, 72 h, and 168 h after the injection while still maintained on the restrictive diet.

#### *Effect of Food Deprivation on CFA-Induced Peripheral Inflammation*

Ad libitum fed mice were injected with CFA and placed back into their home cage with water but no food for 24 h. Ad libitum fed mice served as controls. Mouse BW, sex, and age were noted for

all animals. Paw volume, circumference, and temperature were measured 24 h post-CFA injection. Hindpaws were harvested after all measurements for use in histopathology analysis or TNF $\alpha$  measurements.

#### *Effect of Refeeding on CFA-Induced Peripheral Inflammation*

Paw volume was measured before CFA injection and 24 h post injection. Mice were then food deprived for 24 h and paw volume measured again. Ad libitum access to food was returned and paw volume was remeasured.

#### *Effect of NSAIDs on CFA-Induced Peripheral Inflammation*

Ad libitum fed and food deprived mice received a subcutaneous injection of 10% ethanol in saline, ketoprofen (30 mg/kg) (Costa et al., 2020; Girard et al., 2008), or ketorolac (30 mg/kg) (Russo et al., 2017; Shin et al., 2006) 24 h after CFA injection. Doses were picked for their potent analgesic and anti-inflammatory effects. Paw volume was measured 1 h post i.p. injection.

#### *Effect of AgRP Neuron Activation on CFA-Induced Peripheral Inflammation*

Mice received i.p. injection of CNO (1 mg/kg) to activate AgRP neurons 24 h after CFA injection. Paw volume was measured 75 min after CNO administration.

#### *Effect of Corticosterone Signaling on CFA-Induced Peripheral Inflammation.*

Mice received i.p. injections of 10mg/kg corticosterone (Carter et al., 2013) or vehicle 24 h after CFA injection. Paw volume was measured 1 h after corticosterone administration.

Mice were food deprived for 24 h and received I.p. injections of 25m/kg RU486 (Masson et al., 2010) after CFA injection. Paw volume was measured 1 h after RU486 administration.

24 h after CFA paw injections, Mice were placed in restraint tubes for 1 h. Paw volume was measured before and after the restraint stress.

#### *Effect of Neurokinin Signaling on CFA-Induced Peripheral Inflammation.*

Mice received i.p. injections of 5mg/kg L-733-060 (Bang et al., 2003) or saline 24 h after CFA injection. Paw volume was measured 1 h after L-733-060 administration.

Mice were food deprived for 24 h and received i.p. injections of 5ug/kg substance P (Growcott and Shaw, 1979) or saline after CFA injection. Paw volume was measured 1 h after substance P administration.

*Effect of Opioid Signaling on CFA-Induced Peripheral Inflammation.*

Mice received subcutaneous injections of 0.1mg/kg buprenorphine (Cho et al., 2019) or saline 24 h after CFA injection. Paw volume was measured 1 h after buprenorphine administration.

Mice were food deprived for 24 h and received i.p. injections of 10mg/kg naloxone (Nakagawa et al., 1995) or saline after CFA injection. Paw volume was measured 1 h after naloxone administration.

*Effect of Oxytocin Signaling on CFA-Induced Peripheral Inflammation.*

Mice were food deprived for 24 h and received i.p. injections of 1mg/kg oxytocin (İşeri et al., 2005) or saline after CFA injection. Paw volume was measured 1 h after oxytocin administration.

*Effect of Leptin Signaling on CFA-Induced Peripheral Inflammation.*

Mice were food deprived for 24 h and received injections of 1mg/kg leptin (Zhou et al., 2021) or saline after CFA injection. Paw volume was measured 1 h after leptin administration.

*Effect of Ghrelin Signaling on CFA-Induced Peripheral Inflammation.*

Mice received i.p. injections of 1mg/kg ghrelin (Egecioglu et al., 2010) or saline 24 h after CFA injection. Paw volume was measured 1 h after ghrelin administration.

*Effect of Serotonin Signaling on CFA-Induced Peripheral Inflammation.*

Mice were food deprived for 24 h and received i.p. injections of 1mg/kg serotonin (Souza et al., 2013) or saline after CFA injection. Paw volume was measured 1 h after serotonin administration.

*Effect of the Microbiome on CFA-Induced Peripheral Inflammation.*

To deplete the gastrointestinal microbiota, mice were treated with a combination of ampicillin, vancomycin, metronidazole, and kanamycin at a concentration of 1 gram each per liter of drinking water (Virtue et al., 2019). After 10 days of antibiotic treatment, mice were injected with CFA. Following paw measurements 24 h after injection, mice were food deprived and paws were remeasured.

*Effect of AgRP Neuron Stimulation on CFA-Induced Peripheral Inflammation*

Mice received a CFA paw injection. Mice received optogenetic stimulation of AgRP neurons for 1 h. Paw volume and temperature were measured prior to CFA injection, 24 h post-CFA injection, and 1 h after stimulation.

*Effect of AgRP Subpopulations on CFA-Induced Peripheral Inflammation*

Mice received a CFA paw injection. Mice received optogenetic stimulation of AgRP target subpopulations for 1 h. Paw volume and temperature were measured prior to CFA injection, 24 h post-CFA injection, and 1 h after stimulation.

*Effect of PVH Subpopulations on CFA-Induced Peripheral Inflammation*

Mice with mCherry, HM3D, or HM4D expression in PVH<sup>OXT</sup> neurons received CNO (1mg/kg) 24 h after a CFA paw injection. Paw volume was measured 75 min after CNO administration. Mice were then food deprived for 24 h and retreated with CNO. Paw volume was measured 75 min after CNO administration.

24 h after CFA injection, mice received optogenetic stimulation of PVH<sup>CRH</sup> neurons for 1 h. Paw volume was measured 1 h after stimulation.

Mice with mCherry, HM3D, and HM4D expression in PVH<sup>CRH</sup> neurons received CNO (1mg/kg) 24 h after a CFA paw injection. Paw volume was measured 75 min after CNO administration. Mice

were then food deprived for 24 h and retreated with CNO. Paw volume was measured 75 min after CNO administration.

*Effect of PBN Subpopulations on CFA-Induced Peripheral Inflammation.*

Mice with mCherry or HM4D expression in PBN<sup>VGLUT2</sup> neurons received CNO (1mg/kg) 24 h after a CFA paw injection. Paw volume was measured 75 min after CNO administration.

Mice with mCherry or HM4D expression in PBN Fos Trap pain neurons received CNO (1mg/kg) 24 h after a CFA paw injection. Paw volume was measured 75 min after CNO administration.

*Effect of the Vagus Nerve on CFA-Induced Peripheral Inflammation.*

Sham- and VGX-operated mice were injected with CFA. 24 h later paws were measured, and mice were subsequently food deprived. Paws were measured again 24 h after food deprivation.

Sham- and CAPS-treated mice were injected with CFA. 24 h later paws were measured, and mice were subsequently food deprived. Paws were measured again 24 h after food deprivation.

*Effect of CRF signaling on CFA-Induced Peripheral Inflammation.*

Mice were food deprived for 24 h and received i.p. injections of 30mg/kg antalarmin and 15ug/kg Arestressin 2B or vehicle after CFA injection. Paw volume was measured 1 h after administration of CRF antagonists.

*Effect of Cholinergic Signaling on CFA-Induced Peripheral Inflammation.*

Mice were food deprived for 24 h and received i.p. injections of 5mg/kg mecamyllamine or saline after CFA injection. Paw volume was measured 1 h after mecamyllamine administration.

Mice were food deprived for 24 h and received i.p. injections of 5mg/kg methyllycaconitine or saline after CFA injection. Paw volume was measured 1 h after methyllycaconitine administration.

*Effect of Adrenergic Signaling on CFA-Induced Peripheral Inflammation.*

Mice were food deprived for 24 h and received I.p. injections of 10mg/kg propranolol and 5mg/kg SR59230A or vehicle after CFA injection. Paw volume was measured 1 h after administration of adrenergic antagonists.

*Effect of the Spleen on CFA-Induced Peripheral Inflammation.*

Sham- and splenectomy-operated mice were injected with CFA. 24 h later paws were measured, and mice were subsequently food deprived. Paws were measured again 24 h after food deprivation.

*Effect of the Vagal-Immune Pathway on CFA-Induced Peripheral Inflammation.*

Mice were food deprived for 24 h and received I.p. injections of a mixture of 30mg/kg antalarmin, 15ug/kg Astressin 2B, 5mg/kg mecamlamine, 10mg/kg propranolol and 5mg/kg SR59230A or vehicle after CFA injection. Paw volume was measured 1 h after administration of adrenergic antagonists.

**Dual-wavelength Fiber Photometry**

Dual-wavelength FP was performed as we and others have previously described (Lerner et al., 2015; Su et al., 2017; Zalocusky et al., 2016). Two excitation wavelengths were used: 490 and 405 nm. 490 nm excites calcium-dependent fluorescence from GCaMP6 protein, providing a measure of AgRP neuron activity. 405 nm excites calcium-independent fluorescence from GCaMP6 protein and serves as a control for movement and bleaching artifacts. Excitation light intensities were modulated at different frequencies (211 and 566 Hz for 490 and 405 nm, respectively) to avoid contamination from overhead lights (120 Hz and harmonics) and cross-talk between excitation lights. Excitation lights were generated through fiber-coupled LEDs (Thorlabs, M470F3 for 490 nm and M405F1 for 405 nm) and modulated by a real-time amplifier (Tucker-Davis Technology, RZ5P). Excitation lights were passed through bandpass filters (Thorlabs, MF469-35 for 490 nm and FB405-10 for 405 nm) before being collimated and combined by a 425-nm long-pass dichroic mirror (Thorlabs, DMLP425). The combined excitation light was sent into a patch cord made of a 400- $\mu$ m core, NA 0.48, low-fluorescence optical fiber (Doric, MFP\_400/430/1100-0.48\_1.5\_FCM-MF). The patch cord was connected to an implanted fiber contained in a 2.5-mm diameter ferrule via an

interconnector (Thorlabs, ADAF2). GCaMP6 emission fluorescence signals were collected through the same patch cord, collimated, passed through a GFP emission filter (Thorlabs, MF525-39), and focused onto a femtowatt photoreceiver (Newport, Model 2151, gain set to AC LOW) using a lens (Edmund Optics, 62-561). The emission lights were converted to electrical signals, sampled at 1017 Hz, and demodulated by the RZ5P real-time processor. The FP experiments were controlled by Synapse software (Tucker-Davis Technology). Synchronized infra-red cameras (Ailipu Technology, ELP-USB100W05MT-DL36) controlled by Synapse were used to video-record mice during FP experiments. Prior to experimentation, mice were habituated to experimental procedures. All FP experiments occurred in each individual's home cage with the lid removed. Baseline GCaMP6 fluorescence signals were set to similar levels by adjusting the output power of 490 and 405-nm LEDs. To achieve maximum sensitivity of signals, the 490-nm signal was set to occupy 50% of the detection range of the photoreceiver (20-100 mW at the tip of the fiber accounting for variations in GCaMP6 expressions and optical fiber positions over AgRP neurons). The 405-nm signal was set to occupy 5% of the detection range (2-10 mW output power at the tip of the fiber) to avoid saturating the detector. Baseline GCaMP6 fluorescence was recorded prior to a stimulus (5 min), and post-stimulus fluorescence was compared to baseline fluorescence as described below.

### **Fiber Photometry Data Analysis**

Demodulated data were exported from Synapse to MATLAB (MathWorks) using a script provided by Tucker-Davis Technology. The 490- and 405-nm signals were independently processed and normalized to baseline signals to determine  $DF/F$ , where  $DF/F = (F - F_{\text{baseline}}) / F_{\text{baseline}}$  and  $F_{\text{baseline}}$  is the median of pre-stimulus signal. No isosbestic normalization was introduced. Data were down-sampled to 1 Hz in MATLAB. The subsequent processing of FP data was performed in MATLAB and Excel. Mean  $DF/F$  was calculated by integrating  $DF/F$  over a period of time and then dividing by the integration time. Minimum and maximum  $DF/F$  were calculated by taking the averaged 10 s mean  $DF/F$  for each mouse at the average minimum or maximum of each recording.

### **Fiber Photometry Recordings During Food Intake**

At least 1 week following surgery, mice were food-restricted and screened for their neural response to chow refeeding. Baseline calcium activity was recorded for 5 min, and for 10 min following presentation of chow. Mice that had < 20% DF/F (AgRP neurons) or < 10% DF/F (POMC, DAT neurons or DA signal) were excluded from experiments. Further, to eliminate movement and bleaching artifacts and ensure that changes in DF/F were not due to a loose fiber connection, FP recordings with more than 15% change in the 405-nm signal were excluded from analyses.

#### *Effect of Food Deprivation on Neural Activity*

Ad libitum fed mice were removed from their home cage without access to chow towards the end of their light cycle. FP recordings were performed at various time points at the end of the light cycle through the dark cycle to evaluate changes to AgRP neural activity as the animal became hungry.

### **Inflammatory Pain Measurements (Formalin Test):**

Mice were placed in a clear enclosure for a 10 min habituation period. Mice were subcutaneously injected in the dorsal hindpaw with 2% formalin (20  $\mu$ l). Mice were monitored for time spent licking paw, and number of lick bouts, for 1 h post-injection by researchers blinded to experimental condition. All sessions were video-recorded. The time spent paw licking was recorded for 1 h and analyzed during the inflammatory phase (15-45) pain responses.

#### *Effect of AgRP $\rightarrow$ PBN stimulation on Inflammatory Pain.*

Mice received optogenetic stimulation of AgRP  $\rightarrow$  PBN neurons mice received beginning 10 min prior to formalin injection and lasting throughout the formalin test. Paw licking was recorded for 1 h post formalin injection. The inflammatory phase of the formalin assay (15-45 m) was presented.

#### *Effect of Capsaicin-Induced Vagotomy on Inflammatory Pain.*

Sham- and capsaicin-treated mice were injected with formalin in the dorsal hindpaw. Paw licking was recorded for 1 h post formalin injection. The inflammatory phase of the formalin assay (15-45 m) was presented.

#### **Thermal Pain Measurements (Hotplate Test):**

A cast iron plate with plexiglass walls was placed on a hotplate and heated to 52°C. Mice were placed on the hotplate and latency to withdraw the paw was recorded by researchers blinded to experimental condition.

#### *Effect of Capsaicin-Induced Vagotomy on Thermal Pain.*

Sham- and capsaicin-treated mice were tested on the hotplate. Latency to withdraw paw were recorded.

#### **Immunohistochemistry and Imaging:**

Mice were transcardially perfused with 0.1 M phosphate buffered saline (PBS) followed by 4% paraformaldehyde (PFA). Brains were removed and post-fixed for 4 h in PFA and then washed overnight in PBS. Coronal brain sections were cut (150  $\mu$ m sections) on a vibratome or cryostat and stored in PBS. Brain sections were incubated overnight at 4°C with primary antibodies diluted in PBS, 1% BSA and 0.1% Triton X-100. Antibodies used: rabbit anti-cFos (1:5,000, Cell Signaling, 2250), sheep anti-GFP (1:2000, AbD Serotec 4745-1051), goat anti-ChAT (1:2000, Millipore, AB144P). Sections were washed 3 times and incubated with species appropriate and minimally cross-reactive fluorophore-conjugated secondary antibodies (1:500, Jackson ImmunoResearch) for 2 h at room temperature. Sections were washed twice with PBS and mounted and coverslipped with Fluorogel. Epifluorescence images were taken on a Leica stereoscope to verify fiber placements, cannula placements, and to obtain low magnification images. Confocal micrographs were taken on a Leica SPE laser scanning microscope using a 20X, 0.75 NA objective for visualization of Fos immunoreactivity.

#### **STATISTICAL ANALYSES**

Data were expressed as means  $\pm$  SEMs in figures and text. Paired or unpaired two-tailed t-tests and Pearson regressions were performed as appropriate. One-way, two-way, and repeated measures ANOVA were used to make comparisons across more than two groups using Prism. Test, statistics, significance levels, and sample sizes for each experiment are listed in Supplementary Table 1. ns  $p > 0.05$ , t-tests and post-hoc comparisons: \* $p < 0.05$ , \*\* $p < 0.01$ , \*\*\* $p < 0.001$ ; interaction:  $\infty p < 0.05$ ,  $\infty\infty p < 0.01$ ,  $\infty\infty\infty p < 0.001$ ; main effect (group, state or drug):  $\odot < 0.05$ ,  $\odot\odot p < 0.01$ ,  $\odot\odot\odot p < 0.001$ .

## CHAPTER 7: GENERAL DISCUSSION

We have uncovered the ability of a central circuit activated by food deprivation to reduce inflammatory pain and inflammation (Table 7.1). We demonstrate that hunger specifically reduces inflammatory pain behavior, leaving intact the response to more acute threats like mechanical and thermal pain. Hunger also reduces peripheral paw inflammation by reducing swelling, temperature, and TNF $\alpha$  levels at the injury site. Hunger activated AgRP neurons ramify throughout the brain to influence behavior and physiology to prioritize food consumption. After interrogation of each AgRP subpopulation we found that one axonal target reduced pain behavior, AgRP $\rightarrow$ PBN, while two regions reduced inflammation, AgRP $\rightarrow$ PVH & PBN. NPY sensitive glutamatergic neurons in the PBN are critical for the reduction in inflammatory pain behavior. Our investigation of neuron populations responsible for reducing inflammation within the PVH and PBN were unsuccessful, however, we found that the efferent pathway of the vagus nerve is likely bridging the CNS with the periphery to reduce inflammation. Taken together, these findings reveal a central neural target that can inhibit pain behavior and peripheral inflammation, providing new insight into how food deprivation can influence non-feeding related behaviors and physiology.

### **Why does food deprivation influence pain and peripheral inflammation?**

While inflammation is an adaptive response to injury, long-term inflammation and associated pain can become maladaptive and prevent basic actions necessary for survival. When faced with a homeostatic challenge such as food deprivation, neural circuits prioritize the most salient need. We found a prime example of this as hunger, through AgRP $\rightarrow$ PBN neuron signaling, inhibits responses to inflammatory pain (Alhadeff et al., 2018). It has become apparent that AgRP neurons have a more complex relationship with hunger than just food intake. In fact, AgRP neurons and their axonal target subpopulations have been broadly implicated in a hierarchical prioritization of behavior, as their activity influences other survival needs. AgRP neuron activation yields a dire hunger state that can shift biological need. With artificial AgRP activation, sleep, fear/anxiety, and aggression are all altered (Burnett et al., 2016; Dietrich et al., 2015; Goldstein et al., 2018; Jikomes

et al., 2016; Padilla et al., 2016) (Figure 7.1). AgRP neurons encourage a wake state, inhibiting the drive to sleep presumably to ensure the capability of taking advantage of any feeding opportunity (Goldstein et al., 2018). Anxiety and fear behavior are attenuated while risk taking behavior is promoted during AgRP activation to avoid the fear of predation or injury from preventing the animal to forage for food (Burnett et al., 2016; Jikomes et al., 2016; Padilla et al., 2016). Thus, an emerging concept in the neurobiology of homeostasis suggests that need-sensing neurons, such as AgRP neurons, use multiple mechanisms to inhibit competing behavioral drives.

While AgRP neuron stimulation is well known to influence behavior, the current work describes physiological changes that are driven by activity in AgRP neurons. Specifically, we show that AgRP neuron stimulation attenuates inflammation following paw injections of noxious chemicals in part by reducing pro-inflammatory cytokines. Previous studies have shown that AgRP neuron activity can also influence metabolism (Krashes et al., 2011), glucose homeostasis (Könner et al., 2007; Steculorum et al., 2016) and autonomic nerve activity (Bell et al., 2017). These widespread effects of activity in approximately 10,000 AgRP neurons highlight the pivotal role of AgRP neurons in influencing both physiology and behavior (Betley et al., 2013).

How do so few neurons influence so much biology? The anatomical configuration of AgRP circuits lends to a logic that promotes parallel, segregated, and distinct functional consequences. For example, AgRP neuron projections to the BNST, PVT, PVH, and LH drive food intake (Betley et al., 2013), and similar projections (to the anterior BNST and LH) mediate effects on glucose homeostasis (Steculorum et al., 2016). In contrast, AgRP projections that do not directly drive food intake filter noxious environmental and physiological stimuli to indirectly enable food intake (Alhadeff et al., 2018; Essner et al., 2017; Padilla et al., 2016; Wu et al., 2012a). In addition to our previous work demonstrating a role for AgRP→PBN signaling in behavioral responses to pain (Alhadeff et al., 2018), here we identify a neural circuit architecture that attenuates peripheral inflammation. It will be imperative for future work to determine the exact mechanism of how this central signal is rapidly relayed to the periphery to reduce inflammation.

While it is known that the central nervous system has bidirectional communication with the immune system, these findings provide new neuron populations, AgRP→PVH and AgRP→PBN, that are capable of reducing localized injury-induced edema. By developing an understanding of how central and peripheral signals interact to inhibit inflammation, these experiments provide novel targets for the development of analgesic and anti-inflammatory therapies.

**The insular cortex is poised to be the hub that integrates inflammation and hunger cues to prioritize feeding behaviors in formalin and CFA-models of inflammation.**

Through this dissertation, we have investigated the role of AgRP projections in reducing pain and inflammation at various subpopulations which include brainstem, midbrain, and forebrain structures. However, we did not look beyond these regions to other areas that are known to integrate interoceptive information. AgRP neurons are interoceptive cells that sense nutrients and hormones in the body to determine the appropriate metabolic response. It is well established that interoception requires integration by the cortex to enact the appropriate response to the peripheral cues (Craig, 2003). The insular cortex is of particular importance as imaging studies have shown context dependent activation for gustation behaviors in both rodents and primates (Frank et al., 2013; Small et al., 2003; Veldhuizen et al., 2011). The insular cortex is able to use gustatory cues to predict when satiation will be accomplished and anticipate the appropriate responses (Livneh et al., 2020). To achieve gustatory awareness, the insular cortex combines information from all organ systems and cues to create the proper physiological and behavioral output. For example, cardiac fluctuations, stomach distention, and nutrients detection trigger changes to the activity in the insular cortex (Frank et al., 2012; Herbert et al., 2012; Wang et al., 2008). It is thought that disordered eating causes changes to insular function ultimately disrupting interoceptive capabilities. In fact, anorexia nervosa patients have significantly higher insular cortex activation in response to food cues, yet lower activation after consuming appetitive foods than healthy control subjects (Nunn et al., 2011). This difference in activation suggests a disruption of the integration between internal feeding signals and reward cues leading to disordered eating. Ultimately, anorexia nervosa patients

are incapable of correctly detecting gustatory cues and therefore produce the appropriate response to consumption. The insular cortex has also been implicated in inflammatory signaling. Imaging studies have shown that systemic immune challenges activate the insular cortex, while lesion studies have shown that it is required for pairing immune signals with conditioning cues (Harrison et al., 2009; Ramírez-Amaya et al., 1996, 1998). Importantly, the insular cortex can also have a direct effect on immune output in response to immune challenges. Inhibition of immune-reactive neurons in the insular cortex significantly reduced the immune response to colitis (Koren et al., 2021). Complementary to our work, Koren et al. (2021) have provided another example of how the central nervous system can actively change immune responses to a targeted organ. This leads us to question whether the insular cortex is a steppingstone for our presented AgRP mediated anti-inflammatory mechanism.

AgRP neurons do, in fact, interact with circuits that project to the insular cortex. Livneh et al. (2017) used multiple tracing approaches to identify a circuit that starts with AgRP neurons and ends at the insular cortex. Using a combination of retrograde and anterograde tracing, they found a four-structure pathway way: AgRP→PVT→basal lateral amygdala (BLA) → insular cortex (Livneh et al., 2017). While the primary pathway from AgRP→insular cortex found in this work does not include the AgRP axon targets we found implicated in inflammation, these researchers did find staining in the PBN and PVH suggesting a connection to this pathway. PVH neurons were found projecting to the BLA while PBN neurons were found through retrograde tracing from the insular cortex (Livneh et al., 2017). This suggests that there may be some influence of these two structures along the pathway to interoceptive processing. PVH and PBN neurons become active during immune challenges (Buller et al., 2004; Elander et al., 2009; Ericsson et al., 1994; Goehler et al., 2001; Hare et al., 1995; Marvel et al., 2004). Together with our data, we suspect that AgRP neurons are able to influence peripheral inflammation through the insular cortex which then causes a reduction of pro-inflammatory signaling through the efferent pathway of the vagus nerve (Figure 7.2).

**Interoception and competing biological drives provide a unique entry point to develop therapeutics for chronic inflammatory diseases.**

The running theme throughout this dissertation has been focused on understanding how biological drives can outcompete other behaviors and physiologic needs, likely through interoception. This method of prioritizing one behavior over another is a unique method of potential therapeutic value. Many chronic inflammatory diseases, especially autoimmune diseases, arise from a disorder of one system that disrupts homeostasis across many systems. For instance, obesity is classically considered as a disorder of over-consumption. However, the physiological reality of this disease is much more complex. Obese individuals fail to have interoceptive responses to cues other than gustatory related functions (Herbert and Pollatos, 2014). Obesity is also compounded with high levels of inflammation, cardiac disease, respiratory dysfunction, and psychiatric disorders (Khaodhjar et al., 1999; Pi-Sunyer, 1999). Clearly a broad spectrum of diseases, like obesity, may benefit from treatment approaches that establishes interoception, and ultimately homeostasis, across multiple systems.

**Table 7.1 | Summary of key experimental findings to identify the pathway that hunger functions through to reduce inflammatory pain and inflammation.**

	Formalin Pain Assay	Paw volume	Temperature	TNF $\alpha$
Hunger	↓↓↓	↓↓↓	↓↓↓	↓↓↓
Arc <sup>AgRP</sup> activation	↓↓	↓↓	↓↓	↓↓
Arc <sup>AgRP</sup> → PVH	×	↓↓↓	↓↓	×
Arc <sup>AgRP</sup> → PBN	↓↓↓	↓	×	×
Subdiaphragmatic Vagotomy	?	↓	?	?
Capsaicin Vagotomy	↓↓↓	×	×	?
×=no effect, ↓= minor effect, ↓↓= medium effect, ↓↓↓= strong effect, ?=not tested				

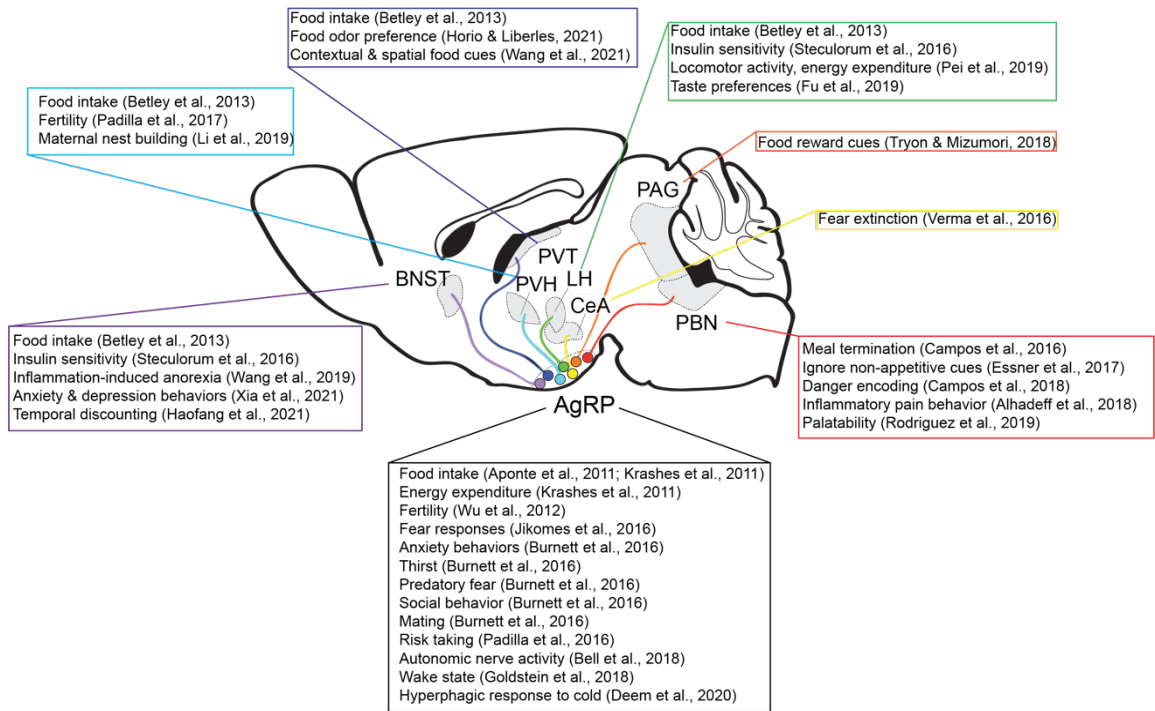


**Figure 7.1 | AgRP neurons have various effects on behavior and physiology to prioritize food intake.**

Diagram of how AgRP neurons projecting throughout the brain to influence many aspects of behavior, metabolism, and physiology.

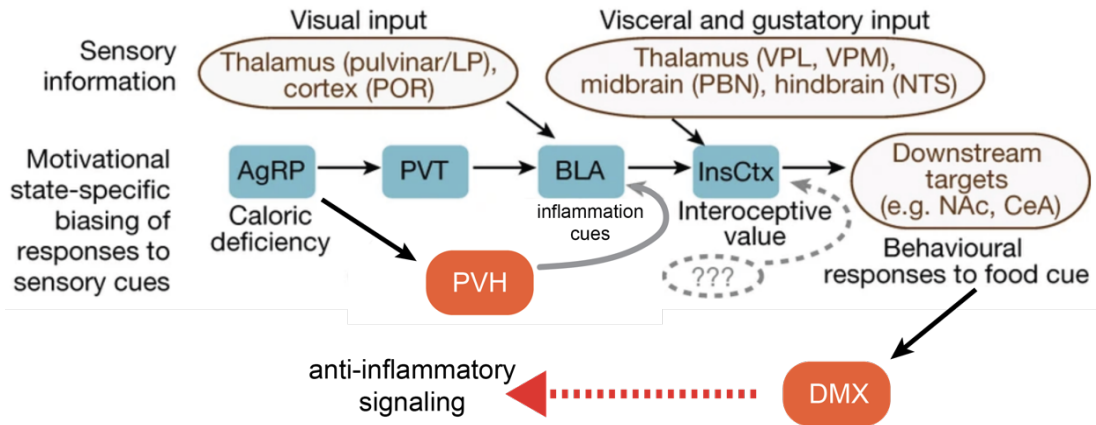


**Figure 7.2 | Proposed circuit for AgRP influence on inflammation through the insular cortex and out of the DMX (adapted from Livneh et al., 2017).**

Livneh et al. (2017) found that AgRP neurons connect with the insular cortex (InsCTX) through the PVT and BLA to allow for interoception of gustation. Our work suggests additional influence from the PVH to change the inflammatory signaling to the insular cortex and ultimately lead to an anti-inflammatory output from the DMX.

## **APPENDIX A: BRIEF REVIEW OF THE ANATOMY AND FUNCTIONS OF THE PVH**

The hypothalamus is a dense structure containing over eleven different subnuclei located on the ventral surface of the brain bisected by the third ventricle. These nuclei are defined by their location within the hypothalamus: medial to lateral as defined by the third ventricle and rostral to caudal as defined by anterior, tuberal, and mammillary respectively (Figure A.1.1a, adapted from Nesan and Kurrasch, 2016). The hypothalamus has two major output systems: the autonomic and neuroendocrine systems. Through both systems, the hypothalamus integrates stimuli from the periphery to release the appropriate behavioral and physiological response to maintain homeostasis among all systems. The location of the subnuclei dictates the function of each structure. Periventricular structures, bordering the third ventricle, respond to hormones, factors, and neurotransmitters circulating in cerebrospinal fluid or the blood stream and interact with the neuroendocrine system. Structures in the medial zone are large nuclei with receiving sensory inputs and communicating amongst hypothalamic nuclei to coordinate adaptive behavior. The lateral hypothalamus has dense connections between hypothalamic nuclei and out to cortical structures allowing for global central nervous system integration of signals (Berthoud, 2002). Berthoud (2002) created a simplified map of the hypothalamus with primary functions associated with each substructure, however, it should be noted that the behaviors and outputs of each are not as specific as this figure suggests (Figure A1.1b). The hypothalamus has reciprocal connections between the limbic system structures, the brainstem, the thalamus, the basal ganglia, the retina, and the cortex. Efferent projections are also found from the hypothalamus to the pituitary gland and motor centers (Lechan and Toni, 2016). Given the complexity of the hypothalamus as a whole, this miniature review will be focused on the paraventricular hypothalamus since it has been implicated in this dissertation to mediate the anti-inflammatory effect of hunger.

### **Anatomy of the PVH**

The PVH has two different cellular structures: the magnocellular and parvocellular level. The magnocellular level contains large cell bodies in the medial wings of the structure, while the

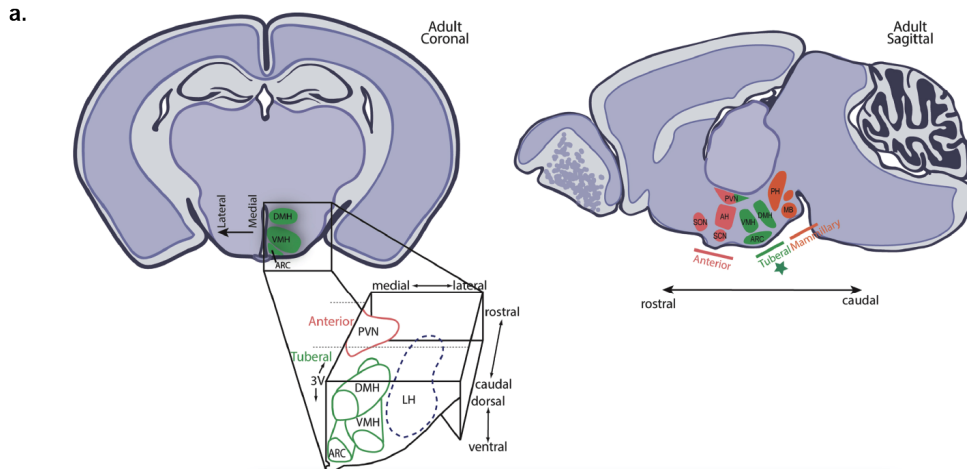
parvocellular level contains small to medium size neurons lining the third ventricle. The PVH has efferent connections throughout the central nervous system including other hypothalamic structures, the pituitary gland, and the spinal cord. The PVH communicates directly with the median eminence through thyrotropin-releasing hormone (TRH), CRH, enkephalin, somatostatin, and vasoactive intestinal peptide neurons parvocellular neurons (Kawano et al., 1991, Lechan and Toni, 2016). TRH and CRH initiate the hypothalamic-pituitary-thyroid axis and HPA axis (Qin et al., 2018). Parvocellular neurons also project to the DMX and spinal cord to initiate autonomic responses (Swanson and Kuypers, 1980). Magnocellular neurons project to the pituitary gland and secrete arginine vasopressin and oxytocin to regulate feeding, fluid balance, and sex-specific behaviors (Qin et al., 2018; Swanson and Kuypers, 1980). The afferent projections to the PVN are also directed to specific sublevels. The ventrolateral medulla projects to the parvocellular level and vasopressin magnocellular neurons. The NTS and locus coeruleus project only to parvocellular neurons. AgRP neurons from the arcuate nucleus project to OXT magnocellular neurons and can lead to obesity phenotypes when disrupted (Qin et al., 2018).

### **Stress & inflammation**

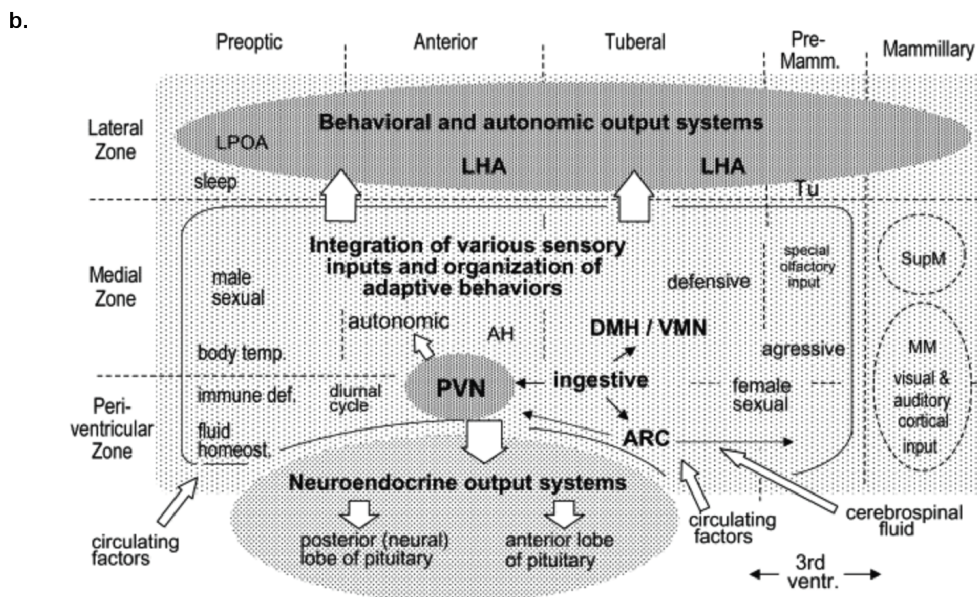
PVN CRH neurons interact in the HPA stress axis. CRH neurons integrate neural input from limbic structures and hormonal signals such as glucocorticoids and cytokines. CRH is then released to the pituitary gland to eventually stimulate the release of more glucocorticoids from the adrenal cortex. Glucocorticoids elicit the effects of stress on the body influencing things like metabolism and heart rate, but also initiates immune cell migration to start local immune reactions. The PVH is key in the maintenance of feedback loops for the HPA axis as it can detect levels of circulating glucocorticoids and adjust its output accordingly (Webster et al., 2002). PVH neurons also adjust their reactivity to HPA axis outputs based on the time course of stress. For instance, the number of angiotensin receptors increases on PVH neurons after extreme stress situations priming the system for activation in future stressful environments (Armando et al., 2007; Ferguson et al., 2008; Saavedra and Benicky, 2009).

## Metabolism

The ARC has reciprocal connections to the PVH. The PVH is primarily a feeding cessation structure receiving input from POMC neurons onto MC4R. These MC4R neurons then project to the DMX and brainstem to carry out the appropriate autonomic signals to prevent food intake (Garfield et al., 2015). Additionally, PVH<sup>OXT</sup> neurons can sense leptin and boost satiation signaling in the NTS to promote anabolic metabolism (Perello and Raino, 2013; Sutton et al., 2014). PVH<sup>MC4R</sup> can also be inhibited by AgRP to promote feeding behavior exemplifying the balance between opposing forces throughout the autonomic nervous system (Qin et al., 2018). The PVH contains four receptor types that promote satiation: Oxt, glucagon like peptide 1 receptors (Glp1r), Crh, and Mc4r (Figure A1.2). Chronic activation of PVH<sup>Glp1r</sup> and PVH<sup>Mc4r</sup> caused a significant increase in food intake leading to obesity phenotypes, while PVH<sup>Oxt</sup> and PVH<sup>Crh</sup> had no effect on food consumption or body weight (Li et al., 2019a).



Adapted from Nesan and Kurrasch, 2016



Adapted from Berthoud (2002)

**Figure A1.1 | The PVH is composed of multiple subnuclei with varying functions related to autonomic and neuroendocrine systems.**

(a) Coronal (left) and sagittal (right) of the mouse hypothalamus with labels for different subnuclei defined by their anatomical location (adapted from Nesan and Kurrasch, 2016). (b) Depiction of anatomical organization of the hypothalamus with general function labelled for each structure. ventromedial hypothalamic nucleus (VMH), dorsomedial hypothalamic nucleus (DMH), lateral hypothalamus (LH/LHA), suprachiasmatic nucleus (SCN), supraoptic nucleus (SON), anterior

hypothalamic nucleus (AH), posterior hypothalamic nucleus (PH), the mammillary body (MB/MM),  
supramammillary nucleus (SupM), lateral preoptic area (LPOA).

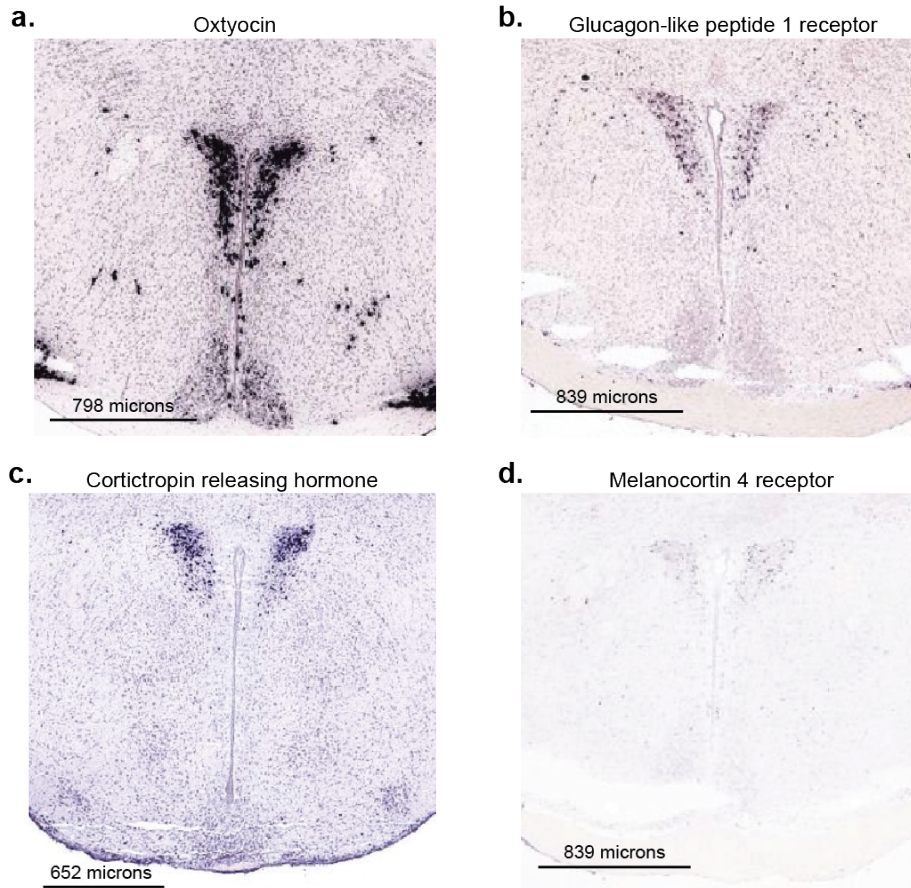


**Figure A1.2 | Examples of satiety inducing molecular markers in the PVH.**

(a) Oxytocin has very dense expression throughout the PVH. (b) Glucagon-like peptide 1 receptor is concentrated to the magnocellular layers of the PVH. (c) Corticotropin releasing hormone is expressed densely in the magnocellular layers of the PVH. (d) Melanocortin 4 receptor is present in the magnocellular level of the PVH. Images adapted from Allen Brain Explorer, <https://mouse.brain-map.org>.

## **APPENDIX B: BRIEF REVIEW OF THE ANATOMY AND FUNCTION OF THE SUB REGIONS OF THE PBN**

The PBN is large heterogeneous structure in the pontine nucleus. It surrounds the superior cerebellar peduncles as they run between the brainstem and cerebellum. As a part of the brainstem, the PBN is responsible for many autonomic functions(Hurley et al., 1991; Saper and Stornetta, 2015) and acts as a relay station for visceral and sensory signals for higher order processing(Saper and Loewy, 2016). The PBN is a complex structure that can be broken down into three main regions: the medial PBN, lateral PBN, and Kölliker Fuse nucleus. Some of the well characterized functions of the PBN include gustation(Biondolillo et al., 2009; Norgren, 1983; Norgren and Pfaffmann, 1975), thermoregulation(Geerling et al., 2016; Nakamura, 2011), breathing(Song et al., 2012; Yokota et al., 2007), appetite(Campos et al., 2016; Wu et al., 2012a), pain(Coizet et al., 2010; Han et al., 2015), osmotic regulation(Geerling and Loewy, 2007; Ryan et al., 2017), immune challenges(Buller et al., 2004), sleep(Gnadt and Pegram, 1986), and arousal (Kaur et al., 2013; Muindi et al., 2016). Each function can be associated with a specific region of the PBN (Figure B.1).

### **Anatomy of the PBN**

#### *The Medial PBN*

The medial PBN (mPBN) is located ventral to the peduncles and has been well implicated in gustatory sensation. The medial PBN responds to stimuli at the anterior and posterior portions of the tongue. Taste information is transmitted to the nucleus tractus solitarii (NTS) through the facial and glossopharyngeal nerves. The NTS then projects to the mPBN. The mPBN transmits gustatory information to many brain regions including the thalamus, lateral hypothalamus, substantia innominata, central nucleus of the amygdala, bed nucleus of stria terminalis, and the gustatory cortex. The thalamus acts as the major hub for sensory information and is responsible for transmitting the majority of taste information to the gustatory cortex. All other projection targets of the mPBN have reciprocal connections back to the mPBN. These feedback loops allow for signal

modulation(Norgren, 1983). The mPBN is also responsible for sleep and arousal behavior. Lesions of the mPBN reduce wakefulness by 40%(Fuller et al., 2011). Activation of the entire PBN leads to increased wakefulness and decreased sleep behavior. Activation of the projections from the PBN to the preoptic area and basal forebrain or the lateral hypothalamus are sufficient in producing this change in sleep. Inactivation of the mPBN increases rapid eye movement sleep(Kaur et al., 2013).

#### *The Kölliker Fuse nucleus.*

The Kölliker-Fuse nucleus (KF) is ventral and lateral to the peduncles and mPBN. It is responsible for respiration and breathing rhythm. The NTS receives cardio-respiratory information from baroreceptors in cardiac tissue and transmits this information to the KF(Michelini and Bonagamba, 1988). The KF then projects to the Phrenic nucleus in the ventral horn of the spinal cord and the rostral ventral respiratory group in the medulla. Together, these projections control the muscle groups required to maintain a steady breathing rhythm and heart rate. The KF also projects to the amygdala and lateral hypothalamus. The KF is made up of VGlut2 positive glutamatergic neurons that release glutamate onto all these structures(Yokota et al., 2007).

#### *The Lateral PBN.*

The lateral PBN (IPBN) is composed of many subregions: external lateral, lateral crescent, dorsal lateral, central lateral, internal lateral, and ventral lateral. Each subregion can be defined by its function. Related to cardiac and breathing rhythm, the external and dorsal IPBN responds to sodium fluctuations. The NTS receives cardiac and vasodilation information from baroreceptors(Michelini and Bonagamba, 1988) which is directly related to sodium levels in the system. When the body is deprived of sodium, neurons in the external IPBN are activated. When salt is detected, the dorsal and external IPBN neurons are activated by both the NTS and the area postrema(Geerling and Loewy, 2007). The ventral parts of the IPBN, the lateral crescent and external IPBN, are responsible for sleep and arousal. As stated previously, activation of the entire PBN can decrease sleep behavior. However, the mPBN is associated with normal wake behavior and the IPBN with arousal. Lesioning of the ventral IPBN greatly increased the latency to wake from repetitive CO<sub>2</sub> arousals(Kaur et al., 2013). Alternatively, activating the ventral IPBN caused rats to awaken from

anesthesia(Muindi et al., 2016). The IPBN also receives thermal information from the skin to regulate body temperature. Thermoregulation is monitored by two parts of the IPBN: warm responding neurons are in the lateral crescent and cool responsive neurons in the dorsal external IPBN. These neuron populations promote heat dissipation and thermogenesis, respectively(Geerling et al., 2016). Meal termination and appetite responsive neurons are found in the external IPBN. Calcitonin gene related protein (CGRP) expressing neurons in the external IPBN receives excitatory projections from the NTS and inhibitory projections from the arcuate nucleus of the hypothalamus. These inputs balance CGRP neuron firing during different nutritional needs states to modulate feeding behavior(Campos et al., 2016; Wu et al., 2012a). Generally, the dorsal IPBN responds to threat stimuli including noxious, visceral, and immune challenge stimuli(Campos et al., 2018; Palmiter, 2018). Pain stimuli are transmitted to the external IPBN through the spinoparabrachial pathway. Lamina I neurons of the spinal cord transmit nociceptive information to the lateral crescent and external IPBN. This information is then sent to the central amygdala and ventromedial hypothalamus(Bester et al., 1997; Buritova et al., 1998). Immune challenges also activate the IPBN. An immune challenge is triggered by systemic proinflammatory cytokines. Under this condition, the NTS and ventrolateral medulla activate the external IPBN. These neurons then project to the central amygdala and bed nucleus stria terminalis (Buller et al., 2004).

### **Molecular markers**

It is believed that most afferent projections from the PBN are glutamatergic(Saper and Stornetta, 2015). In fact, in situ hybridization (ISH) data shows vesicular glutamate transport 2 densely distributed throughout the PBN (Figure B.2A). Within this excitatory structure, there are also GABAergic neurons as seen with glutamate decarboxylase 2 ISH data (Figure B.2B). There are many markers that define the regions of the PBN as well. For example, calcitonin gene related protein (CGRP) is highly expressed in the external IPBN (Figure A.2C). CGRP positive PBN neurons play a role in threat detection and appetite. There are hundreds more markers within the

PBN emphasizing the heterogeneity of this structure. A few have been particularly important in creating mouse lines to target the IPBN(Palmiter, 2018) (Table B.1).

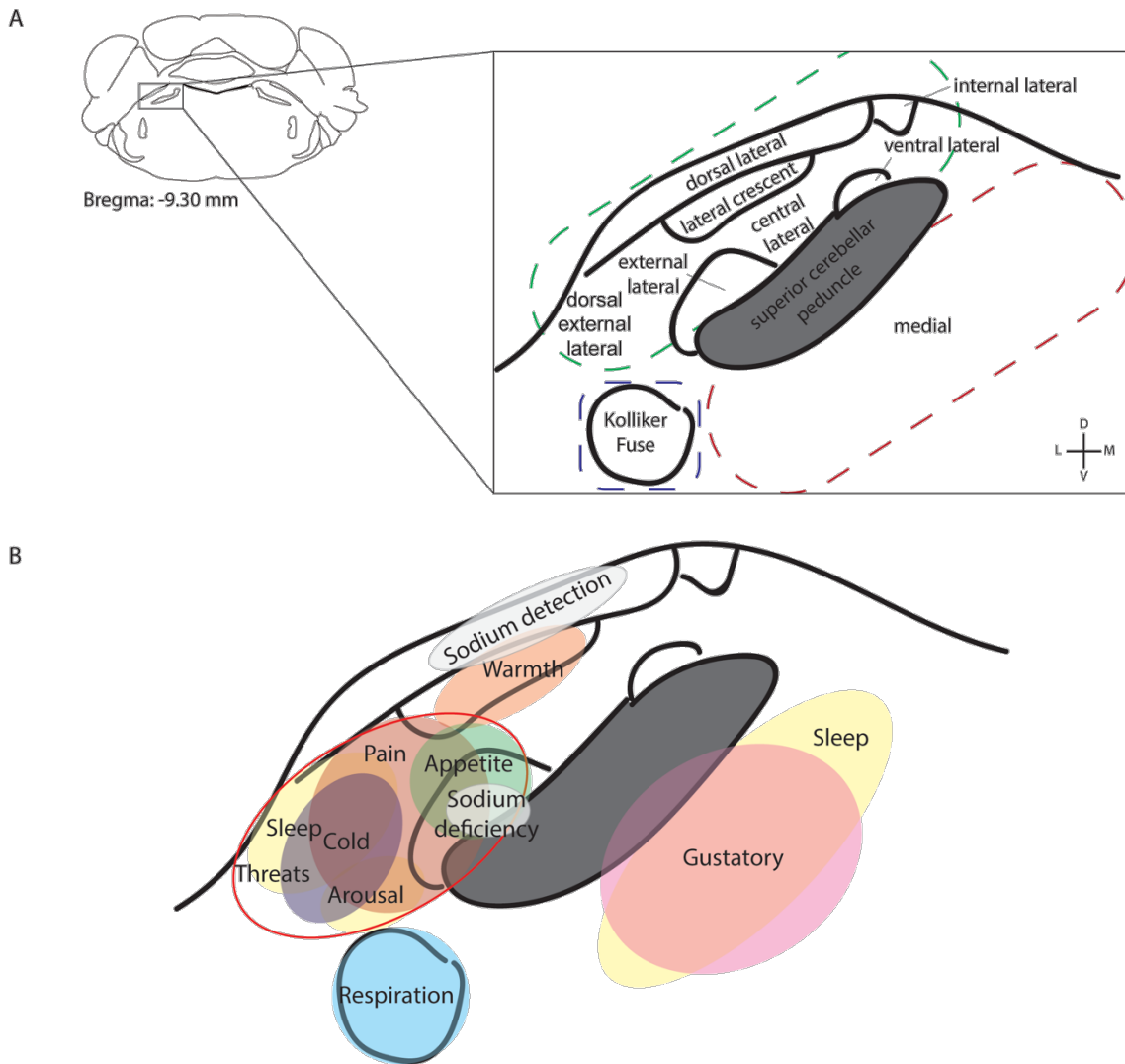


**Figure B2.1 | Anatomy and functions of the parabrachial nucleus.**

A. The parabrachial nucleus (PBN) can be divided into three main subregions: the medial PBN (red), the Kölliker Fuse nucleus (blue), and the lateral PBN (green). The lateral PBN can be further broken down into smaller subregions. B. The different subregions of the PBN are responsible for different functions. The medial PBN is responsible for sleep (Fuller et al., 2011; Kaur et al., 2013) and gustatory (Norgren and Pfaffmann, 1975) information. The Kölliker Fuse controls breathing rhythm (Yokota et al., 2007). The lateral PBN has a wide range of functions including: sleep & arousal (Kaur et al., 2013; Muindi et al., 2016), thermoregulation (Geerling et al., 2016), pain and threat responses (Bester et al., 1997; Buritova et al., 1998; Campos et al., 2018), appetite

control(Campos et al., 2016; Wu et al., 2012a), and osmoregulation(Geerling and Loewy, 2007).

Figure adapted from Buller et al., Journal of Neuroimmunology, 2004.

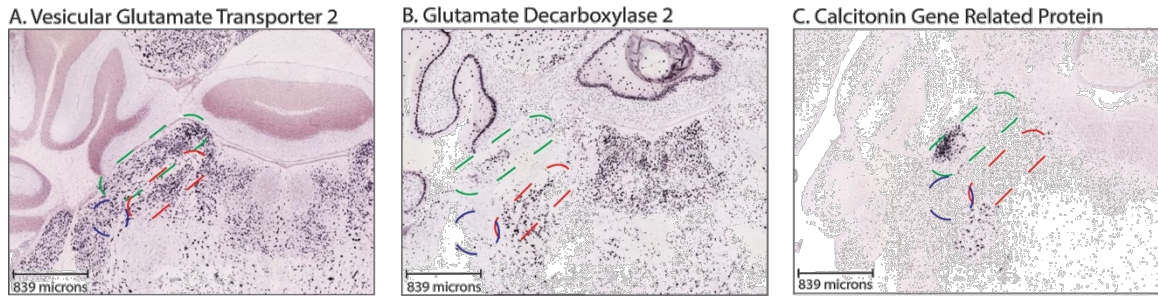


**Figure B2.2 | Examples of molecular markers in the PBN.**

A. Vesicular glutamate transport 2 is highly expressed throughout the PBN. B. Glutamate decarboxylase 2 is expressed in the medial and lateral PBN. C. Calcitonin gene related protein is densely expressed in the external lateral PBN. D. Dopamine Beta Hydroxylase is densely expressed in the medial PBN. Images adapted from Allen Brain Explorer, <http://mouse.brain-map.org>.

**Table B2.1 | Subset of parabrachial nucleus genetic markers.**

Molecular Marker	Parabrachial Nucleus subregion(s)
Foxp2	Central lateral
Lmx1b	External lateral
Cholecystokinin	Medial & dorsal lateral
Corticotropin releasing hormone	Dorsal lateral
Neurotensin	External lateral
Prodynorphin	Central lateral
PACAP	Lateral
Glycine receptor 3	Lateral
Tachykinin 1	Internal & external lateral
GABA A	Lateral & medial
Proenkephalin	Lateral & medial
Bombesin like receptor 3	Internal
Corticotropin releasing protein receptor 1	Internal
Leptin receptor	Internal
Mu opioid receptor	Central
Neuropeptide Y 1 receptor	Central & external lateral
Oxytocin receptor	Ventral lateral
G protein coupled 88	Dorsal lateral
Tachykinin receptor 1	Internal ventral lateral
Cerebellin 4	Central lateral
a5 nAChR	External lateral
Lymphocyte antigen 6 locus h	Lateral
a7 nAChR	Central

## BIBLIOGRAPHY

- Abella, V., Scotece, M., Conde, J., Pino, J., Gonzalez-Gay, M.A., Gómez-Reino, J.J., Mera, A., Lago, F., Gómez, R., and Gualillo, O. (2017). Leptin in the interplay of inflammation, metabolism and immune system disorders. *Nat Rev Rheumatol* 13, 100–109.
- Ahern, G.P. (2011). 5-HT and the immune system. *Curr Opin Pharmacol* 11, 29–33.
- Alhadeff, A.L., Su, Z., Hernandez, E., Klima, M.L., Phillips, S.Z., Holland, R.A., Guo, C., Hantman, A.W., Jonghe, B.C.D., and Betley, J.N. (2018). A Neural Circuit for the Suppression of Pain by a Competing Need State. *Cell* 173, 140-152.e15.
- Alhadeff, A.L., Goldstein, N., Park, O., Klima, M.L., Vargas, A., and Betley, J.N. (2019). Natural and Drug Rewards Engage Distinct Pathways that Converge on Coordinated Hypothalamic and Reward Circuits. *Neuron* 103, 891-908.e6.
- Al-Hasani, H., and Joost, H.-G. (2005). Nutrition-/diet-induced changes in gene expression in white adipose tissue. *Best Pract Res Clin En* 19, 589–603.
- Allen, W.E., DeNardo, L.A., Chen, M.Z., Liu, C.D., Loh, K.M., Fenno, L.E., Ramakrishnan, C., Deisseroth, K., and Luo, L. (2017). Thirst-associated preoptic neurons encode an aversive motivational drive. *Science* 357, 1149–1155.
- Anastasio, T.J. (2017). Editorial: Computational and Experimental Approaches in Multi-target Pharmacology. *Front Pharmacol* 8, 443.
- Aponte, Y., Atasoy, D., and Sternson, S.M. (2011). AGRP neurons are sufficient to orchestrate feeding behavior rapidly and without training. *Nat Neurosci* 14, 351–355.
- Armando, I., Volpi, S., Aguilera, G., and Saavedra, J.M. (2007). Angiotensin II AT1 receptor blockade prevents the hypothalamic corticotropin-releasing factor response to isolation stress. *Brain Res* 1142, 92–99.
- ASAM (2016). Opioid Addiction: 2016 Facts & Figures.
- Baganz, N.L., and Blakely, R.D. (2013). A Dialogue between the Immune System and Brain, Spoken in the Language of Serotonin. *Acs Chem Neurosci* 4, 48–63.
- Bang, R., Sass, G., Kiemer, A.K., Vollmar, A.M., Neuhuber, W.L., and Tiegs, G. (2003). Neurokinin-1 Receptor Antagonists CP-96,345 and L-733,060 Protect Mice from Cytokine-Mediated Liver Injury. *J Pharmacol Exp Ther* 305, 31–39.
- Bell, B.B., Harlan, S.M., Morgan, D.A., Guo, D.-F., and Rahmouni, K. (2017). Differential contribution of POMC and AgRP neurons to the regulation of regional autonomic nerve activity by leptin. *Mol Metab* 8, 1–12.
- Benarroch, E.E. (1993). The Central Autonomic Network: Functional Organization, Dysfunction, and Perspective. *Mayo Clinic Proceedings* 68.

- Berntson, G.G., and Khalsa, S.S. (2021). Neural Circuits of Interoception. *Trends Neurosci* 44, 17–28.
- Berthoud, H.-R. (2002). Multiple neural systems controlling food intake and body weight. *Neurosci Biobehav Rev* 26, 393–428.
- Berthoud, H.-R., and Neuhuber, W.L. (2000). Functional and chemical anatomy of the afferent vagal system. *Autonomic Neurosci* 85, 1–17.
- Besse, D., Weil-Fugazza, J., Lombard, M.-C., Butler, S.H., and Besson, J.-M. (1992). Monoarthritis induces complex changes in  $\mu$ -,  $\delta$ - and  $\kappa$ -opioid binding sites in the superficial dorsal horn of the rat spinal cord. *Eur J Pharmacol* 223, 123–131.
- Bester, H., Matsumoto, N., Besson, J., and Bernard, J. (1997). Further evidence for the involvement of the spinoparabrachial pathway in nociceptive processes: A c-Fos study in the rat. *J Comp Neurol* 383, 439–458.
- Betley, J.N., Cao, Z.F., Ritola, K.D., and Sternson, S.M. (2013). Parallel, redundant circuit organization for homeostatic control of feeding behavior. *Cell* 155, 1337–1350.
- Betley, J.N., Xu, S., Cao, Z.F.H.F., Gong, R., Magnus, C.J., Yu, Y., and Sternson, S.M. (2015). Neurons for hunger and thirst transmit a negative-valence teaching signal. *Nature* 521, 180–185.
- Billiau, A., and Matthys, P. (2001). Modes of action of Freund's adjuvants in experimental models of autoimmune diseases. *Journal of Leukocyte Biology* 70, 849–860.
- Biondolillo, J.W., Williams, L.A., and King, M.S. (2009). Blocking Glutamate Receptors in the Waist Area of the Parabrachial Nucleus Decreases Taste Reactivity Behaviors in Conscious Rats. *Chem Senses* 34, 221–230.
- Bonaz, B., Sinniger, V., and Pellissier, S. (2016). Anti-inflammatory properties of the vagus nerve: potential therapeutic implications of vagus nerve stimulation. *J Physiology* 594, 5781–5790.
- Bonaz, B., Sinniger, V., and Pellissier, S. (2017). The Vagus Nerve in the Neuro-Immune Axis: Implications in the Pathology of the Gastrointestinal Tract. *Front Immunol* 8, 1452.
- Brandhorst, S., Choi, I.Y., Wei, M., Cheng, C.W., Sedrakyan, S., Navarrete, G., Dubeau, L., Yap, L.P., Park, R., Vinciguerra, M., et al. (2015). A Periodic Diet that Mimics Fasting Promotes Multi-System Regeneration, Enhanced Cognitive Performance, and Healthspan. *Cell Metab* 22, 86–99.
- Broberger, C., Johansen, J., Johansson, C., Schalling, M., and Hökfelt, T. (1998). The neuropeptide Y/agouti gene-related protein (AGRP) brain circuitry in normal, anorectic, and monosodium glutamate-treated mice. *Proc National Acad Sci* 95, 15043–15048.
- Buller, K.M., Allen, T., Wilson, L.D., Munro, F., and Day, T.A. (2004). A critical role for the parabrachial nucleus in generating central nervous system responses elicited by a systemic immune challenge. *Journal of Neuroimmunology* 152, 20–32.
- Buritova, J., Besson, J., and Bernard, J. (1998). Involvement of the spinoparabrachial pathway in inflammatory nociceptive processes: A c-Fos protein study in the awake rat. *Journal of Comparative Neurology* 397, 10–28.

- Burnett, C.J., Li, C., Webber, E., Tsaousidou, E., Xue, S.Y., Brüning, J.C., and Krashes, M.J. (2016). Hunger-Driven Motivational State Competition. *Neuron* 92, 187–201.
- Campos, C., Bowen, A., Roman, C., and Nature, P.-R. (2018). Encoding of danger by parabrachial CGRP neurons.
- Campos, C.A., Bowen, A.J., Schwartz, M.W., and Palmiter, R.D. (2016). Parabrachial CGRP Neurons Control Meal Termination. *Cell Metabolism* 23, 811–820.
- Carey, L.M., Gutierrez, T., Deng, L., Lee, W.-H., Mackie, K., and Hohmann, A.G. (2017). Inflammatory and Neuropathic Nociception is Preserved in GPR55 Knockout Mice. *Sci Rep-Uk* 7, 944.
- Carmel, P.W. (1980). Surgical Syndromes of the Hypothalamus. *Neurosurgery* 27, 133–159.
- Carter, B.S., Hamilton, D.E., and Thompson, R.C. (2013). Acute and chronic glucocorticoid treatments regulate astrocyte-enriched mRNAs in multiple brain regions in vivo. *Front Neurosci-Switz* 7, 139.
- Carter, C.S., Kenkel, W.M., MacLean, E.L., Wilson, S.R., Perkeybile, A.M., Yee, J.R., Ferris, C.F., Nazarloo, H.P., Porges, S.W., Davis, J.M., et al. (2020). Is Oxytocin “Nature’s Medicine”? *Pharmacol Rev* 72, 829–861.
- Cho, C., Michailidis, V., Lecker, I., Collymore, C., Hanwell, D., Loka, M., Danesh, M., Pham, C., Urban, P., Bonin, R.P., et al. (2019). Evaluating analgesic efficacy and administration route following craniotomy in mice using the grimace scale. *Sci Rep-Uk* 9, 359.
- Coizet, V., Dommett, E.J., Klop, E.M., Redgrave, P., and Overton, P.G. (2010). The parabrachial nucleus is a critical link in the transmission of short latency nociceptive information to midbrain dopaminergic neurons. *Neuroscience* 168, 263–272.
- Cook, C.D., and Nickerson, M.D. (2005). Nociceptive Sensitivity and Opioid Antinociception and Antihyperalgesia in Freund’s Adjuvant-Induced Arthritic Male and Female Rats. *J Pharmacol Exp Ther* 313, 449–459.
- Corder, G., Ahanonu, B., Grewe, B.F., Wang, D., Schnitzer, M.J., and Scherrer, G. (2019). An amygdalar neural ensemble that encodes the unpleasantness of pain. *Science* 363, 276–281.
- Costa, S.K.P.F., Muscara, M.N., Allain, T., Dallazen, J., Gonzaga, L., Buret, A.G., Vaughan, D.J., Fowler, C.J., Nucci, G. de, and Wallace, J.L. (2020). Enhanced Analgesic Effects and Gastrointestinal Safety of a Novel, Hydrogen Sulfide-Releasing Anti-Inflammatory Drug (ATB-352): A Role for Endogenous Cannabinoids. *Antioxid Redox Sign* 33, 1003–1009.
- Cowley, M.A., Smith, R.G., Diano, S., Tschöp, M., Pronchuk, N., Grove, K.L., Strasburger, C.J., Bidlingmaier, M., Esterman, M., Heiman, M.L., et al. (2003). The Distribution and Mechanism of Action of Ghrelin in the CNS Demonstrates a Novel Hypothalamic Circuit Regulating Energy Homeostasis. *Neuron* 37, 649–661.
- Craig, A. (Bud) (2003). Interoception: the sense of the physiological condition of the body. *Curr Opin Neurobiol* 13, 500–505.

- Culbert, K.M., Racine, S.E., and Klump, K.L. (2016). Hormonal Factors and Disturbances in Eating Disorders. *Curr Psychiat Rep* 18, 65.
- D'Agostino, G., Lyons, D.J., Cristiano, C., Burke, L.K., Madara, J.C., Campbell, J.N., Garcia, A.P., Land, B.B., Lowell, B.B., Dileone, R.J., et al. (2016). Appetite controlled by a cholecystokinin nucleus of the solitary tract to hypothalamus neurocircuit. *Elife* 5, e12225.
- Dandona, P., Mohanty, P., Ghanim, H., Aljada, A., Browne, R., Hamouda, W., Prabhala, A., Afzal, A., and Garg, R. (2001). The Suppressive Effect of Dietary Restriction and Weight Loss in the Obese on the Generation of Reactive Oxygen Species by Leukocytes, Lipid Peroxidation, and Protein Carbonylation. *J Clin Endocrinol Metabolism* 86, 355–362.
- Deem, J., Faber, C.L., Pedersen, C., Phan, B.A., Larsen, S.A., Ogimoto, K., Nelson, J.T., Damian, V., Tran, M.A., Palmiter, R.D., et al. (2020). Cold-induced hyperphagia requires AgRP-neuron activation in mice. *Elife* 9, e58764.
- Dietrich, M., Zimmer, M., Bober, J., and Horvath, T. (2015). Hypothalamic AgRP neurons drive stereotypic behaviors beyond feeding.
- Doyle, H.H., and Murphy, A.Z. (2017). Sex differences in innate immunity and its impact on opioid pharmacology. *J Neurosci Res* 95, 487–499.
- Egecioglu, E., Jerlhag, E., Salomé, N., Skibicka, K.P., Haage, D., Bohlooly-Y, M., Andersson, D., Bjursell, M., Perrissoud, D., Engel, J.A., et al. (2010). PRECLINICAL STUDY: FULL ARTICLE: Ghrelin increases intake of rewarding food in rodents. *Addict Biol* 15, 304–311.
- Eisenstein, T.K. (2019). The Role of Opioid Receptors in Immune System Function. *Front Immunol* 10, 2904.
- Elander, L., Engstrom, L., Ruud, J., Mackerlova, L., Jakobsson, P.-J., Engblom, D., Nilsberth, C., and Blomqvist, A. (2009). Inducible Prostaglandin E2 Synthesis Interacts in a Temporally Supplementary Sequence with Constitutive Prostaglandin-Synthesizing Enzymes in Creating the Hypothalamic-Pituitary-Adrenal Axis Response to Immune Challenge. *J Neurosci* 29, 1404–1413.
- Elmquist, J.K., and Saper, C.B. (1996). Activation of neurons projecting to the paraventricular hypothalamic nucleus by intravenous lipopolysaccharide. *J Comp Neurol* 374, 315–331.
- Elmquist, J.K., Scammell, T.E., Jacobson, C.D., and Saper, C.B. (1996). Distribution of fos-like immunoreactivity in the rat brain following intravenous lipopolysaccharide administration. *J Comp Neurol* 371, 85–103.
- Ericsson, A., Kovacs, K., and Sawchenko, P. (1994). A functional anatomical analysis of central pathways subserving the effects of interleukin-1 on stress-related neuroendocrine neurons. *J Neurosci* 14, 897–913.
- Essner, R.A., Smith, A.G., Jamnik, A.A., Ryba, A.R., Trutner, Z.D., and Carter, M.E. (2017). AgRP Neurons Can Increase Food Intake during Conditions of Appetite Suppression and Inhibit Anorexigenic Parabrachial Neurons. *J Neurosci* 37, 8678–8687.

Ferguson, A.V., Latchford, K.J., and Samson, W.K. (2008). The paraventricular nucleus of the hypothalamus – a potential target for integrative treatment of autonomic dysfunction. *Expert Opin Ther Tar* 12, 717–727.

Fontana, L., Meyer, T.E., Klein, S., and Holloszy, J.O. (2004). Long-term calorie restriction is highly effective in reducing the risk for atherosclerosis in humans. *P Natl Acad Sci Usa* 101, 6659–6663.

Franceschi, C., and Campisi, J. (2014). Chronic Inflammation (Inflammaging) and Its Potential Contribution to Age-Associated Diseases. *Journals Gerontology Ser* 69, S4–S9.

Frank, S., Linder, K., Kullmann, S., Heni, M., Ketterer, C., Çavuşoğlu, M., Krzeminski, A., Fritsche, A., Häring, H.-U., Preissl, H., et al. (2012). Fat intake modulates cerebral blood flow in homeostatic and gustatory brain areas in humans. *Am J Clin Nutrition* 95, 1342–1349.

Frank, S., Kullmann, S., and Veit, R. (2013). Food related processes in the insular cortex. *Front Hum Neurosci* 7, 499.

Fu, O., Iwai, Y., Narukawa, M., Ishikawa, A.W., Ishii, K.K., Murata, K., Yoshimura, Y., Touhara, K., Misaka, T., Minokoshi, Y., et al. (2019). Hypothalamic neuronal circuits regulating hunger-induced taste modification. *Nat Commun* 10, 4560.

Fuller, P.M., Fuller, P., Sherman, D., Pedersen, N.P., Saper, C.B., and Lu, J. (2011). Reassessment of the structural basis of the ascending arousal system. *The Journal of Comparative Neurology* 519, 933–956.

Fulwiler, C.E., and Saper, C.B. (1984). Subnuclear organization of the efferent connections of the parabrachial nucleus in the rat. *Brain Res Rev* 7, 229–259.

Garfield, A.S., Li, C., Madara, J.C., Shah, B.P., Webber, E., Steger, J.S., Campbell, J.N., Gavrilova, O., Lee, C.E., Olson, D.P., et al. (2015). A neural basis for melanocortin-4 receptor-regulated appetite. *Nat Neurosci* 18, 863–871.

Gaskin, D., and Pain, R.-P. of (2012). The economic costs of pain in the United States.

Geerling, J.C., and Loewy, A.D. (2007). Sodium deprivation and salt intake activate separate neuronal subpopulations in the nucleus of the solitary tract and the parabrachial complex. *Journal of Comparative Neurology* 504, 379–403.

Geerling, J.C., Kim, M., Mahoney, C.E., Abbott, S.B., Agostinelli, L.J., Garfield, A.S., Krashes, M.J., Lowell, B.B., and Scammell, T.E. (2016). Genetic identity of thermosensory relay neurons in the lateral parabrachial nucleus. *American Journal of Physiology-Regulatory, Integrative and Comparative Physiology* 310, R41–R54.

Gershon, M.D., and Tack, J. (2007). The Serotonin Signaling System: From Basic Understanding To Drug Development for Functional GI Disorders. *Gastroenterology* 132, 397–414.

Gibbons, C.H. (2019). Chapter 27 Basics of autonomic nervous system function. *Handb Clin Neurology* 160, 407–418.

- Girard, P., Verniers, D., Coppé, M.-C., Pansart, Y., and Gillardin, J.-M. (2008). Nefopam and ketoprofen synergy in rodent models of antinociception. *Eur J Pharmacol* 584, 263–271.
- Gnadt, J.W., and Pegram, V.G. (1986). Cholinergic brainstem mechanisms of REM sleep in the rat. *Brain Research* 384, 29–41.
- Goehler, L.E., Relton, J.K., Dripps, D., Kiechle, R., Tartaglia, N., Maier, S.F., and Watkins, L.R. (1997). Vagal Paraganglia Bind Biotinylated Interleukin-1 Receptor Antagonist: A Possible Mechanism for Immune-to-Brain Communication. *Brain Res Bull* 43, 357–364.
- Goehler, L.E., Gaykema, R.P.A., Hansen, M.K., Anderson, K., Maier, S.F., and Watkins, L.R. (2000). Vagal immune-to-brain communication: a visceral chemosensory pathway. *Autonomic Neurosci* 85, 49–59.
- Goehler, L.E., Gaykema, R.P.A., Hansen, M.K., Kleiner, J.L., Maier, S.F., and Watkins, L.R. (2001). Staphylococcal enterotoxin B induces fever, brain c-Fos expression, and serum corticosterone in rats. *Am J Physiology-Regulatory Integr Comp Physiology* 280, R1434–R1439.
- Golbidi, S., Daiber, A., Korac, B., Li, H., Essop, M.F., and Laher, I. (2017). Health Benefits of Fasting and Caloric Restriction. *Curr Diabetes Rep* 17, 123.
- Goldstein, N., Levine, B.J., Loy, K.A., Duke, W.L., Meyerson, O.S., Jamnik, A.A., and Carter, M.E. (2018). Hypothalamic Neurons that Regulate Feeding Can Influence Sleep/Wake States Based on Homeostatic Need. *Curr Biol* 28, 3736-3747.e3.
- Gonidakis, S., Finkel, S.E., and Longo, V.D. (2010). Genome-wide screen identifies *Escherichia coli* TCA-cycle-related mutants with extended chronological lifespan dependent on acetate metabolism and the hypoxia-inducible transcription factor ArcA. *Aging Cell* 9, 868–881.
- Goodrick, C.L., Ingram, D.K., Reynolds, M.A., Freeman, J.R., and Cider, N. (1990). Effects of intermittent feeding upon body weight and lifespan in inbred mice: interaction of genotype and age. *Mech Ageing Dev* 55, 69–87.
- Gordon, J., and Barnes, N.M. (2003). Lymphocytes transport serotonin and dopamine: agony or ecstasy? *Trends Immunol* 24, 438–443.
- Gouin, J.-P., Carter, C.S., Pournajafi-Nazarloo, H., Glaser, R., Malarkey, W.B., Loving, T.J., Stowell, J., and Kiecolt-Glaser, J.K. (2010). Marital behavior, oxytocin, vasopressin, and wound healing. *Psychoneuroendocrinol* 35, 1082–1090.
- Gropp, E., Shanabrough, M., Borok, E., Xu, A.W., Janoschek, R., Buch, T., Plum, L., Balthasar, N., Hampel, B., Waisman, A., et al. (2005). Agouti-related peptide-expressing neurons are mandatory for feeding. *Nat Neurosci* 8, 1289–1291.
- Growcott, J. W., & Shaw, J. S. (1979). Failure of substance P to produce analgesia in the mouse [proceedings]. *British journal of pharmacology*, 66(1), 129P.
- Hahn, T.M., Breininger, J.F., Baskin, D.G., and Schwartz, M.W. (1998). Coexpression of *Agrp* and *NPY* in fasting-activated hypothalamic neurons. *Nat Neurosci* 1, 271–272.

Hamm, R.J., and Lyeth, B.G. (1984). Nociceptive thresholds following food restriction and return to free-feeding. *Physiol Behav* 33, 499–501.

Han, S., Soleiman, M.T., Soden, M.E., Zweifel, L.S., and Palmiter, R.D. (2015). Elucidating an Affective Pain Circuit that Creates a Threat Memory. *Cell* 162, 363–374.

Hare, A.S., Clarke, G., and Tolchard, S. (1995). Bacterial Lipopolysaccharide-Induced Changes in FOS Protein Expression in the Rat Brain: Correlation with Thermoregulatory Changes and Plasma Corticosterone. *J Neuroendocrinol* 7, 791–799.

Hare, B.D., Beierle, J.A., Toufexis, D.J., Hammack, S.E., and Falls, W.A. (2014). Exercise-Associated Changes in the Corticosterone Response to Acute Restraint Stress: Evidence for Increased Adrenal Sensitivity and Reduced Corticosterone Response Duration. *Neuropsychopharmacol* 39, 1262–1269.

Harrison, N.A., Brydon, L., Walker, C., Gray, M.A., Steptoe, A., Dolan, R.J., and Critchley, H.D. (2009). Neural Origins of Human Sickness in Interoceptive Responses to Inflammation. *Biol Psychiat* 66, 415–422.

Heilbronn, L.K., and Ravussin, E. (2003). Calorie restriction and aging: review of the literature and implications for studies in humans. *Am J Clin Nutrition* 78, 361–369.

Herbert, B.M., and Pollatos, O. (2014). Attenuated interoceptive sensitivity in overweight and obese individuals. *Eat Behav* 15, 445–448.

Herbert, B.M., Muth, E.R., Pollatos, O., and Herbert, C. (2012). Interoception across Modalities: On the Relationship between Cardiac Awareness and the Sensitivity for Gastric Functions. *Plos One* 7, e36646.

Herbert, H., Moga, M.M., and Saper, C.B. (1990). Connections of the parabrachial nucleus with the nucleus of the solitary tract and the medullary reticular formation in the rat. *J Comp Neurol* 293, 540–580.

Horvath, T.L., Naftolin, F., Kalra, S.P., and Leranath, C. (1992). Neuropeptide-Y innervation of beta-endorphin-containing cells in the rat mediobasal hypothalamus: a light and electron microscopic double immunostaining analysis. *Endocrinology* 131, 2461–2467.

Horvath, T.L., Bechmann, I., Naftolin, F., Kalra, S.P., and Leranath, C. (1997). Heterogeneity in the neuropeptide Y-containing neurons of the rat arcuate nucleus: GABAergic and non-GABAergic subpopulations. *Brain Res* 756, 283–286.

Hunziker, S., and Hole, K. (1987). The formalin test in mice: dissociation between inflammatory and non-inflammatory pain. *Pain* 30, 103–114.

Hurlemann, R., and Grinevich, V. (2018). Behavioral Pharmacology of Neuropeptides: Oxytocin.

Hurley, K.M., Herbert, H., Moga, M.M., and Saper, C.B. (1991). Efferent projections of the infralimbic cortex of the rat. *J Comp Neurol* 308, 249–276.

Institute of Medicine (US) Committee on Examination of Front-of-Package Nutrition Rating Systems and Symbols; Wartella EA, Lichtenstein AH, Boon CS, editors. Front-of-Package

Nutrition Rating Systems and Symbols: Phase I Report. Washington (DC): National Academies Press (US); 2010 4, Overview of Health and Diet in America.

İşeri, S.Ö., Şener, G., Sağlam, B., Gedik, N., Ercan, F., and Yeğen, B.Ç. (2005). Oxytocin Protects Against Sepsis-Induced Multiple Organ Damage: Role of Neutrophils. *J Surg Res* 126, 73–81.

Jacobson, P.B., Morgan, S.J., Wilcox, D.M., Nguyen, P., Ratajczak, C.A., Carlson, R.P., Harris, R.R., and Nuss, M. (1999). A new spin on an old model: In vivo evaluation of disease progression by magnetic resonance imaging with respect to standard inflammatory parameters and histopathology in the adjuvant arthritic rat. *Arthritis Rheumatism* 42, 2060–2073.

Jikomes, N., Ramesh, R.N., Mandelblat-Cerf, Y., and Andermann, M.L. (2016). Preemptive Stimulation of AgRP Neurons in Fed Mice Enables Conditioned Food Seeking under Threat. *Curr Biol* 26, 2500–2507.

Johnson, J.B., Summer, W., Cutler, R.G., Martin, B., Hyun, D.-H., Dixit, V.D., Pearson, M., Nassar, M., Telljohann, R., Tellejohan, R., et al. (2007). Alternate day calorie restriction improves clinical findings and reduces markers of oxidative stress and inflammation in overweight adults with moderate asthma. *Free Radical Bio Med* 42, 665–674.

Jonge, W.J., and Ulloa, L. (2007). The alpha7 nicotinic acetylcholine receptor as a pharmacological target for inflammation. *Brit J Pharmacol* 151, 915–929.

Jonnakuty, C., and Gragnoli, C. (2008). What do we know about serotonin? *J Cell Physiol* 217, 301–306.

Kaerberlein, T.L., Smith, E.D., Tsuchiya, M., Welton, K.L., Thomas, J.H., Fields, S., Kennedy, B.K., and Kaerberlein, M. (2006). Lifespan extension in *Caenorhabditis elegans* by complete removal of food. *Aging Cell* 5, 487–494.

Kaur, S., Pedersen, N.P., Yokota, S., Hur, E.E., Fuller, P.M., Lazarus, M., Chamberlin, N.L., and Saper, C.B. (2013). Glutamatergic Signaling from the Parabrachial Nucleus Plays a Critical Role in Hypercapnic Arousal. *The Journal of Neuroscience* 33, 7627–7640.

Kawano, H., Tsuruo, Y., Bando, H., and Daikoku, S. (1991). Hypophysiotrophic TRH-producing neurons identified by combining immunohistochemistry for pro-TRH and retrograde tracing. *J Comp Neurol* 307, 531–538.

Khaodhiar, L., McCowen, K.C., and Blackburn, G.L. (1999). Obesity and its comorbid conditions. *Clin Cornerstone* 2, 17–31.

Kingsbury, M.A., and Bilbo, S.D. (2019). The inflammatory event of birth: How oxytocin signaling may guide the development of the brain and gastrointestinal system. *Front Neuroendocrin* 55, 100794.

Klampfer, L., Huang, J., Sasazuki, T., Shirasawa, S., and Augenlicht, L. (2003). Inhibition of interferon gamma signaling by the short chain fatty acid butyrate. *Mol Cancer Res Mcr* 1, 855–862.

- Klein, S.L., and Flanagan, K.L. (2016). Sex differences in immune responses. *Nat Rev Immunol* 16, 626–638.
- König, B., Bergmann, U., and König, W. (1992) Induction of inflammatory mediator release (serotonin and 12-hydroxyeicosatetraenoic acid) from human platelets by *Pseudomonas aeruginosa* glycolipid. *Infect. Immun.* 60, 3150–3155.
- Könner, A.C., Janoschek, R., Plum, L., Jordan, S.D., Rother, E., Ma, X., Xu, C., Enriori, P., Hampel, B., Barsh, G.S., et al. (2007). Insulin Action in AgRP-Expressing Neurons Is Required for Suppression of Hepatic Glucose Production. *Cell Metab* 5, 438–449.
- Koren, T., Yifa, R., Amer, M., Krot, M., Boshnak, N., Ben-Shaanan, T.L., Azulay-Debby, H., Zalayat, I., Avishai, E., Hajjo, H., et al. (2021). Insular cortex neurons encode and retrieve specific immune responses. *Cell* 184, 5902-5915.e17.
- Kovats, S., Carreras, E., and Agrawal, H. (2009). Sex Hormones and Immunity to Infection. 53–91.
- Krashes, M.J., Koda, S., Ye, C., Rogan, S.C., Adams, A.C., Cusher, D.S., Maratos-Flier, E., Roth, B.L., and Lowell, B.B. (2011). Rapid, reversible activation of AgRP neurons drives feeding behavior in mice. *J Clin Invest* 121, 1424–1428.
- Lago, F., Gómez, R., Gómez-Reino, J.J., Dieguez, C., and Gualillo, O. (2009). Adipokines as novel modulators of lipid metabolism. *Trends Biochem Sci* 34, 500–510.
- Lechan RM, Toni R. Functional Anatomy of the Hypothalamus and Pituitary. [Updated 2016 Nov 28]. In: Feingold KR, Anawalt B, Boyce A, et al., editors. Endotext [Internet]. South Dartmouth (MA): MDTText.com, Inc.; 2000-. Available from: <https://www.ncbi.nlm.nih.gov/books/NBK279126/>
- Li, C., Navarrete, J., Liang-Guallpa, J., Lu, C., Funderburk, S.C., Chang, R.B., Liberles, S.D., Olson, D.P., and Krashes, M.J. (2019a). Defined Paraventricular Hypothalamic Populations Exhibit Differential Responses to Food Contingent on Caloric State. *Cell Metab* 29, 681-694.e5.
- Li, H.E., Rossi, M.A., Watson, G.D.R., Moore, H.G., Cai, M.T., Kim, N., Vokt, K.A., Lu, D., Bartholomew, R.A., Hughes, R.N., et al. (2021a). Hypothalamic-Extended Amygdala Circuit Regulates Temporal Discounting. *J Neurosci* 41, 1928–1940.
- Li, N., Zhao, S., Zhang, Z., Zhu, Y., Gliniak, C.M., Vishvanath, L., An, Y.A., Wang, M., Deng, Y., Zhu, Q., et al. (2021b). Adiponectin preserves metabolic fitness during aging. *Elife* 10, e65108.
- Li, X.-Y., Han, Y., Zhang, W., Wang, S.-R., Wei, Y.-C., Li, S.-S., Lin, J.-K., Yan, J.-J., Chen, A.-X., Zhang, X., et al. (2019b). AGRP Neurons Project to the Medial Preoptic Area and Modulate Maternal Nest-Building. *J Neurosci* 39, 456–471.
- Liu, T., Kong, D., Shah, B.P., Ye, C., Koda, S., Saunders, A., Ding, J.B., Yang, Z., Sabatini, B.L., and Lowell, B.B. (2012). Fasting activation of AgRP neurons requires NMDA receptors and involves spinogenesis and increased excitatory tone. *Neuron* 73, 511–522.
- Livneh, Y., Ramesh, R.N., Burgess, C.R., Levandowski, K.M., Madara, J.C., Fenselau, H., Goldey, G.J., Diaz, V.E., Jikomes, N., Resch, J.M., et al. (2017). Homeostatic circuits selectively gate food cue responses in insular cortex. *Nature* 546, 611–616.

- Livneh, Y., Sugden, A.U., Madara, J.C., Essner, R.A., Flores, V.I., Sugden, L.A., Resch, J.M., Lowell, B.B., and Andermann, M.L. (2020). Estimation of Current and Future Physiological States in Insular Cortex. *Neuron* 105, 1094-1111.e10.
- Longo, V.D., and Mattson, M.P. (2014). Fasting: Molecular Mechanisms and Clinical Applications. *Cell Metab* 19, 181–192.
- Lührs, H., Gerke, T., Müller, J.G., Melcher, R., Schaubert, J., Boxberger, F., Scheppach, W., and Menzel, T. (2009). Butyrate Inhibits NF- $\kappa$ B Activation in Lamina Propria Macrophages of Patients with Ulcerative Colitis. *Scand J Gastroentero* 37, 458–466.
- Luquet, S., Perez, F.A., Hnasko, T.S., and Palmiter, R.D. (2005). NPY/AgRP Neurons Are Essential for Feeding in Adult Mice but Can Be Ablated in Neonates. *Science* 310, 683–685.
- Madisen, L., Mao, T., Koch, H., Zhuo, J., Berenyi, A., Fujisawa, S., Hsu, Y.-W.A., Garcia, A.J., Gu, X., Zanella, S., et al. (2012). A toolbox of Cre-dependent optogenetic transgenic mice for light-induced activation and silencing. *Nat Neurosci* 15, 793–802.
- Mansour, M.K., Dehelia, M., Hydoub, Y.M., Kousa, O., and Hassan, B. (2021). Oxytocin-Induced Acute Pulmonary Edema: A Case Report and Literature Review. *Cureus* 13, e15067.
- Marchand, F., Perretti, M., and McMahon, S.B. (2005). Role of the Immune system in chronic pain. *Nat Rev Neurosci* 6, 521–532.
- Marvel, F.A., Chen, C.-C., Badr, N., Gaykema, R.P.A., and Goehler, L.E. (2004). Reversible inactivation of the dorsal vagal complex blocks lipopolysaccharide-induced social withdrawal and c-Fos expression in central autonomic nuclei. *Brain Behav Immun* 18, 123–134.
- Mascarucci, P., Perego, C., Terrazzino, S., and Simoni, M.G.D. (1998). Glutamate release in the nucleus tractus solitarius induced by peripheral lipopolysaccharide and interleukin-1 $\beta$ . *Neuroscience* 86, 1285–1290.
- Masson, M.J., Collins, L.A., Carpenter, L.D., Graf, M.L., Ryan, P.M., Bourdi, M., and Pohl, L.R. (2010). Pathologic role of stressed-induced glucocorticoids in drug-induced liver injury in mice. *Biochem Bioph Res Co* 397, 453–458.
- Matarese, G., Procaccini, C., Menale, C., Kim, J.G., Kim, J.D., Diano, S., Diano, N., Rosa, V.D., Dietrich, M.O., and Horvath, T.L. (2013). Hunger-promoting hypothalamic neurons modulate effector and regulatory T-cell responses. *Proc National Acad Sci* 110, 6193–6198.
- Mattson, M.P., Longo, V.D., and Harvie, M. (2017). Impact of intermittent fasting on health and disease processes. *Ageing Res Rev* 39, 46–58.
- Maurer-Spurej, E., Pittendreigh, C., and Solomons, K. (2004). The influence of selective serotonin reuptake inhibitors on human platelet serotonin. *Thromb Haemostasis* 91, 119–128.
- Medzhitov, R. (2008). Origin and physiological roles of inflammation. *Nature* 454, 428–435.
- Mercken, E.M., Crosby, S.D., Lamming, D.W., JeBailey, L., Krzysik-Walker, S., Villareal, D.T., Capri, M., Franceschi, C., Zhang, Y., Becker, K., et al. (2013). Calorie restriction in humans

inhibits the PI3K/AKT pathway and induces a younger transcription profile. *Aging Cell* 12, 645–651.

Meydani, S.N., Das, S.K., Pieper, C.F., Lewis, M.R., Klein, S., Dixit, V.D., Gupta, A.K., Villareal, D.T., Bhapkar, M., Huang, M., et al. (2016). Long-term moderate calorie restriction inhibits inflammation without impairing cell-mediated immunity: a randomized controlled trial in non-obese humans. *Aging Albany Ny* 8, 1416–1426.

Michellini, L., and Bonagamba, L. (1988). Baroreceptor reflex modulation by vasopressin microinjected into the nucleus tractus solitarii of conscious rats. *Hypertension* 11, 175.

Millan, M.J., Czonkowski, A., Morris, B., Stein, C., Arendt, R., Huber, A., Höllt, V., and Herz, A. (1988). Inflammation of the hind limb as a model of unilateral, localized pain; influence on multiple opioid systems in the spinal cord of the rat. *Pain* 35, 299–312.

Moga, M.M., Herbert, H., Hurley, K.M., Yasui, Y., Gray, T.S., and Saper, C.B. (1990). Organization of cortical, basal forebrain, and hypothalamic afferents to the parabrachial nucleus in the rat. *J Comp Neurol* 295, 624–661.

Mössner, R., and Lesch, K.-P. (1998). Role of Serotonin in the Immune System and in Neuroimmune Interactions. *Brain Behav Immun* 12, 249–271.

Muindi, F., Kenny, J.D., Taylor, N.E., Solt, K., Wilson, M.A., Brown, E.N., and Dort, C.J. (2016). Electrical stimulation of the parabrachial nucleus induces reanimation from isoflurane general anesthesia. *Behavioural Brain Research* 306, 20–25.

Nahin, R.L., and Byers, M.R. (1994). Adjuvant-induced inflammation of rat paw is associated with altered calcitonin gene-related peptide immunoreactivity within cell bodies and peripheral endings of primary afferent neurons. *J Comp Neurol* 349, 475–485.

Nakagawa, T., Minami, M., Katsumata, S., Ienaga, Y., and Satoh, M. (1995). Suppression of naloxone-precipitated withdrawal jumps in morphine-dependent mice by stimulation of prostaglandin EP3 receptor. *Brit J Pharmacol* 116, 2661–2666.

Nakamura, K. (2011). Central circuitries for body temperature regulation and fever. *American Journal of Physiology-Regulatory, Integrative and Comparative Physiology* 301, R1207–R1228.

Nakazato, M., Murakami, N., Date, Y., Kojima, M., Matsuo, H., Kangawa, K., and Matsukura, S. (2001). A role for ghrelin in the central regulation of feeding. *Nature* 409, 194–198.

Nathan, C. (2002). Points of control in inflammation. *Nature* 420, 846–852.

National Institute of Health: The Autoimmune Diseases Coordinating Committee. (2005) *Progress in Autoimmune Diseases Research*. (NIH Publication No. 05-5140) US Dept of Health and Services, Washington DC.

Norgren, R. (1983). The gustatory system in mammals. *American Journal of Otolaryngology* 4, 234–237.

Norgren, R., and Pfaffmann, C. (1975). The pontine taste area in the rat. *Brain Research* 91, 99–117.

- Nunn, K., Frampton, I., Fuglset, T.S., Törzsök-Sonnevend, M., and Lask, B. (2011). Anorexia nervosa and the insula. *Med Hypotheses* 76, 353–357.
- Oliveira, P.G., Brenol, C.V., Edelweiss, M.I., Meurer, L., Brenol, J.C.T., and Xavier, R.M. (2007). Subcutaneous inflammation (panniculitis) in tibio-tarsal joint of rats inoculated with complete Freund's adjuvant. *Clin Exp Med* 7, 184–187.
- Padilla, S.L., Qiu, J., Soden, M.E., Sanz, E., Nestor, C.C., Barker, F.D., Quintana, A., Zweifel, L.S., Rønnekleiv, O.K., Kelly, M.J., et al. (2016). Agouti-related peptide neural circuits mediate adaptive behaviors in the starved state. *Nature Neuroscience* 19, 734–741.
- Padilla, S.L., Qiu, J., Nestor, C.C., Zhang, C., Smith, A.W., Whiddon, B.B., Rønnekleiv, O.K., Kelly, M.J., and Palmiter, R.D. (2017). AgRP to Kiss1 neuron signaling links nutritional state and fertility. *Proc National Acad Sci* 114, 2413–2418.
- Pahwa R, Goyal A, Bansal P, Jialal I. Chronic Inflammation. 2021 Sep 28. In: StatPearls [Internet]. Treasure Island (FL): StatPearls Publishing; 2022 Jan–. PMID: 29630225.
- Palmiter, R.D. (2018). The Parabrachial Nucleus: CGRP Neurons Function as a General Alarm. *Trends in Neurosciences* 41, 280–293.
- Pascual, D. W. (2004). The role of tachykinins on bacterial infections. *Front Biosci*, 9(1-3), 3209-17.
- Pavlov, V.A., and Tracey, K.J. (2012). The vagus nerve and the inflammatory reflex—linking immunity and metabolism. *Nat Rev Endocrinol* 8, 743–754.
- Pavlov, V.A., Wang, H., Czura, C.J., Friedman, S.G., and Tracey, K.J. (2003a). The Cholinergic Anti-inflammatory Pathway: A Missing Link in Neuroimmunomodulation. *Mol Med* 9, 125–134.
- Pavlov, V.A., Wang, H., Czura, C.J., Friedman, S.G., and Tracey, K.J. (2003b). The cholinergic anti-inflammatory pathway: a missing link in neuroimmunomodulation. *Mol Medicine Camb Mass* 9, 125–134.
- Pei, H., Patterson, C.M., Sutton, A.K., Burnett, K.H., Myers, M.G., and Olson, D.P. (2019). Lateral Hypothalamic Mc3R-Expressing Neurons Modulate Locomotor Activity, Energy Expenditure, and Adiposity in Male Mice. *Endocrinology* 160, 343–358.
- Perello, M., and Raino, J. (2013). Leptin Activates Oxytocin Neurons of the Hypothalamic Paraventricular Nucleus in Both Control and Diet-Induced Obese Rodents. *Plos One* 8, e59625.
- Pi-Sunyer, F.X. (1999). Comorbidities of overweight and obesity: current evidence and research issues. *Medicine Sci Sports Exerc* 31, S602.
- Pradhan, G., Samson, S.L., and Sun, Y. (2013). Ghrelin. *Curr Opin Clin Nutr* 16, 619–624.
- Qin, C., Li, J., and Tang, K. (2018). The Paraventricular Nucleus of the Hypothalamus: Development, Function, and Human Diseases. *Endocrinology* 159, 3458–3472.
- Quadt, L., Critchley, H.D., and Garfinkel, S.N. (2018). The neurobiology of interoception in health and disease. *Ann Ny Acad Sci* 1428, 112–128.

Rakhra, V., Galappaththy, S.L., Bulchandani, S., and Cabandugama, P.K. (2020). Obesity and the Western Diet: How We Got Here. *Mo Med* 117, 536–538.

Ramírez-Amaya, V., Alvarez-Borda, B., Ormsby, C.E., Martínez, R.D., Pérez-Montfort, R., and Bermúdez-Rattoni, F. (1996). Insular Cortex Lesions Impair the Acquisition of Conditioned Immunosuppression. *Brain Behav Immun* 10, 103–114.

Ramírez-Amaya, V., Alvarez-Borda, B., and Bermudez-Rattoni, F. (1998). Differential Effects of NMDA-Induced Lesions into the Insular Cortex and Amygdala on the Acquisition and Evocation of Conditioned Immunosuppression. *Brain Behav Immun* 12, 149–160.

Ratkay, L.G., Zhang, L., Tonzetich, J., and Waterfield, J.D. (1993). Complete Freund's adjuvant induces an earlier and more severe arthritis in MRL-lpr mice. *J Immunol Baltim Md* 151, 5081–5087.

Ren, K., and Dubner, R. (1999). Inflammatory Models of Pain and Hyperalgesia. *Ilar J* 40, 111–118.

Rivest, S. (2001). How circulating cytokines trigger the neural circuits that control the hypothalamic–pituitary–adrenal axis. *Psychoneuroendocrino* 26, 761–788.

Rodriguez, E., Ryu, D., Zhao, S., Han, B.-X., and Wang, F. (2019). Identifying Parabrachial Neurons Selectively Regulating Satiety for Highly Palatable Food in Mice. *Eneuro* 6, ENEURO.0252-19.2019.

Rosas-Ballina, M., Olofsson, P.S., Ochani, M., Valdés-Ferrer, S.I., Levine, Y.A., Reardon, C., Tusche, M.W., Pavlov, V.A., Andersson, U., Chavan, S., et al. (2011). Acetylcholine-Synthesizing T Cells Relay Neural Signals in a Vagus Nerve Circuit. *Science* 334, 98–101.

Rosenbaum, M., and Leibel, R.L. (2014). 20 YEARS OF LEPTIN: Role of leptin in energy homeostasis in humans. *J Endocrinol* 223, T83–T96.

Russo, R., Caro, C.D., Avallone, B., Magliocca, S., Nieddu, M., Boatto, G., Troiano, R., Cuomo, R., Cirillo, C., Avagliano, C., et al. (2017). Ketogal: A Derivative Ketorolac Molecule with Minor Ulcerogenic and Renal Toxicity. *Front Pharmacol* 08, 757.

Ryan, P.J., Ross, S.I., Campos, C.A., Derkach, V.A., and Palmiter, R.D. (2017). Oxytocin-receptor-expressing neurons in the parabrachial nucleus regulate fluid intake. *Nature Neuroscience* 20, 1722–1733.

Saavedra, J.M., and Benicky, J. (2009). Brain and peripheral angiotensin II play a major role in stress. *Ann Ny Acad Sci* 10, 185–193.

Sagar, S.M., Price, K.J., Kasting, N.W., and Sharp, F.R. (1995). Anatomic patterns of FOS immunostaining in rat brain following systemic endotoxin administration. *Brain Res Bull* 36, 381–392.

Saper, C.B., and Loewy, A.D. (2016). Commentary on: Efferent connections of the parabrachial nucleus in the rat. C.B. Saper and A.D. Loewy, *Brain Research* 197:291–317, 1980. *Brain Res* 1645, 15–17.

Saper, C.B., and Stornetta, R.L. (2015). *The Rat Nervous System (Fourth Edition)*. Section VI: Systems 629–673.

Schwartz, M.W., Woods, S.C., Porte, D., Seeley, R.J., and Baskin, D.G. (2000). Central nervous system control of food intake. *Nature* 404, 661–671.

Shaw, A.C., Goldstein, D.R., and Montgomery, R.R. (2013). Age-dependent dysregulation of innate immunity. *Nat Rev Immunol* 13, 875–887.

Shin, J.-W., Hwang, K.-S., Kim, Y.-K., Leem, J.-G., and Lee, C. (2006). Nonsteroidal Antiinflammatory Drugs Suppress Pain-Related Behaviors, but Not Referred Hyperalgesia of Visceral Pain in Mice. *Anesthesia Analgesia* 102, 195–200.

Sherrington CS (1906) *The Integrative Action of the Nervous System*, Yale University Press

Small, D.M., Gregory, M.D., Mak, Y.E., Gitelman, D., Mesulam, M.M., and Parrish, T. (2003). Dissociation of Neural Representation of Intensity and Affective Valuation in Human Gustation. *Neuron* 39, 701–711.

Song, G., Wang, H., Xu, H., and Poon, C.-S. (2012). Kölliker–Fuse neurons send collateral projections to multiple hypoxia-activated and nonactivated structures in rat brainstem and spinal cord. *Brain Struct Funct* 217, 835–858.

Sousa, C.R. e, Sher, A., and Kaye, P. (1999). The role of dendritic cells in the induction and regulation of immunity to microbial infection. *Curr Opin Immunol* 11, 392–399.

Souza, L.C., Gomes, M.G. de, Goes, A.T.R., Fabbro, L.D., Filho, C.B., Boeira, S.P., and Jesse, C.R. (2013). Evidence for the involvement of the serotonergic 5-HT1A receptors in the antidepressant-like effect caused by hesperidin in mice. *Prog Neuro-Psychopharmacology Biological Psychiatry* 40, 103–109.

Steculorum, S.M., Ruud, J., Karakasilioti, I., Backes, H., Ruud, L.E., Timper, K., Hess, M.E., Tsaousidou, E., Mauer, J., Vogt, M.C., et al. (2016). AgRP Neurons Control Systemic Insulin Sensitivity via Myostatin Expression in Brown Adipose Tissue. *Cell* 165, 125–138.

Sternson, S.M., and Eiselt, A.-K. (2015). Three Pillars for the Neural Control of Appetite. *Annu Rev Physiol* 79, 401–423.

Su, Z., Alhadeff, A.L., and Betley, J.N. (2017). Nutritive, Post-ingestive Signals Are the Primary Regulators of AgRP Neuron Activity. *Cell Reports* 21, 2724–2736.

Sutton, A.K., Pei, H., Burnett, K.H., Myers, M.G., Rhodes, C.J., and Olson, D.P. (2014). Control of Food Intake and Energy Expenditure by Nos1 Neurons of the Paraventricular Hypothalamus. *J Neurosci* 34, 15306–15318.

Suvas, S. (2017). Role of Substance P Neuropeptide in Inflammation, Wound Healing, and Tissue Homeostasis. *J Immunol* 199, 1543–1552.

Swanson, L.W., and Kuypers, H.G.J.M. (1980). The paraventricular nucleus of the hypothalamus: Cytoarchitectonic subdivisions and organization of projections to the pituitary, dorsal vagal

complex, and spinal cord as demonstrated by retrograde fluorescence double-labeling methods. *J Comp Neurol* 194, 555–570.

Takahashi, K.A., and Cone, R.D. (2005). Fasting Induces a Large, Leptin-Dependent Increase in the Intrinsic Action Potential Frequency of Orexigenic Arcuate Nucleus Neuropeptide Y/Agouti-Related Protein Neurons. *Endocrinology* 146, 1043–1047.

Taniguchi, K., and Karin, M. (2018). NF- $\kappa$ B, inflammation, immunity and cancer: coming of age. *Nat Rev Immunol* 18, 309–324.

Tong, Q., Ye, C.-P., Jones, J.E., Elmquist, J.K., and Lowell, B.B. (2008). Synaptic release of GABA by AgRP neurons is required for normal regulation of energy balance. *Nat Neurosci* 11, 998–1000.

Traba, J., and Sack, M.N. (2017). The role of caloric load and mitochondrial homeostasis in the regulation of the NLRP3 inflammasome. *Cell Mol Life Sci* 74, 1777–1791.

Traba, J., Kwarteng-Siaw, M., Okoli, T.C., Li, J., Huffstutler, R.D., Bray, A., Waclawiw, M.A., Han, K., Pelletier, M., Sauve, A.A., et al. (2015). Fasting and refeeding differentially regulate NLRP3 inflammasome activation in human subjects. *J Clin Invest* 125, 4592–4600.

Tryon, V.L., and Mizumori, S.J.Y. (2018). A Novel Role for the Periaqueductal Gray in Consummatory Behavior. *Front Behav Neurosci* 12, 178.

Vandanmagsar, B., Youm, Y.-H., Ravussin, A., Galgani, J.E., Stadler, K., Mynatt, R.L., Ravussin, E., Stephens, J.M., and Dixit, V.D. (2011). The NLRP3 inflammasome instigates obesity-induced inflammation and insulin resistance. *Nat Med* 17, 179–188.

Veldhuizen, M.G., Albrecht, J., Zelano, C., Boesveldt, S., Breslin, P., and Lundström, J.N. (2011). Identification of human gustatory cortex by activation likelihood estimation. *Hum Brain Mapp* 32, 2256–2266.

Verma, D., Wood, J., Lach, G., Herzog, H., Sperk, G., and Tasan, R. (2016). Hunger Promotes Fear Extinction by Activation of an Amygdala Microcircuit. *Neuropsychopharmacol* 41, 431–439.

Virtue, A.T., McCright, S.J., Wright, J.M., Jimenez, M.T., Mowel, W.K., Kotzin, J.J., Joannas, L., Basavappa, M.G., Spencer, S.P., Clark, M.L., et al. (2019). The gut microbiota regulates white adipose tissue inflammation and obesity via a family of microRNAs. *Sci Transl Med* 11, eaav1892.

Waldburger, J.-M., and Firestein, G.S. (2010). Regulation of Peripheral Inflammation by the Central Nervous System. *Curr Rheumatol Rep* 12, 370–378.

Walker, K., Fox, A.J., and Urban, L.A. (1999). Animal models for pain research. *Mol Med Today* 5, 319–321.

Wang, C., Zhou, W., He, Y., Yang, T., Xu, P., Yang, Y., Cai, X., Wang, J., Liu, H., Yu, M., et al. (2021). AgRP neurons trigger long-term potentiation and facilitate food seeking. *Transl Psychiat* 11, 11.

- Wang, G.-J., Tomasi, D., Backus, W., Wang, R., Telang, F., Geliebter, A., Korner, J., Bauman, A., Fowler, J.S., Thanos, P.K., et al. (2008). Gastric distention activates satiety circuitry in the human brain. *Neuroimage* 39, 1824–1831.
- Wang, H., Yu, M., Ochani, M., Amella, C.A., Tanovic, M., Susarla, S., Li, J.H., Wang, H., Yang, H., Ulloa, L., et al. (2003). Nicotinic acetylcholine receptor  $\alpha 7$  subunit is an essential regulator of inflammation. *Nature* 421, 384–388.
- Wang, J., Chen, W.-D., and Wang, Y.-D. (2020). The Relationship Between Gut Microbiota and Inflammatory Diseases: The Role of Macrophages. *Front Microbiol* 11, 1065.
- Wang, T., Hung, C.C.Y., and Randall, D.J. (2006). THE COMPARATIVE PHYSIOLOGY OF FOOD DEPRIVATION: From Feast to Famine. *Physiology* 68, 223–251.
- Wang, Y., Kim, J., Schmit, M.B., Cho, T.S., Fang, C., and Cai, H. (2019). A bed nucleus of stria terminalis microcircuit regulating inflammation-associated modulation of feeding. *Nat Commun* 10, 2769.
- Watkins, L.R., Goehler, L.E., Relton, J.K., Tartaglia, N., Silbert, L., Martin, D., and Maier, S.F. (1995). Blockade of interleukin-1 induced hyperthermia by subdiaphragmatic vagotomy: evidence for vagal mediation of immune-brain communication. *Neurosci Lett* 183, 27–31.
- Webster, J.I., Tonelli, L., and Sternberg, E.M. (2002). NEUROENDOCRINE REGULATION OF IMMUNITY\*. *Immunology* 20, 125–163.
- Wei, M., Fabrizio, P., Hu, J., Ge, H., Cheng, C., Li, L., and Longo, V.D. (2008). Life Span Extension by Calorie Restriction Depends on Rim15 and Transcription Factors Downstream of Ras/PKA, Tor, and Sch9. *Plos Genet* 4, e13.
- Wellen, K.E., and Hotamisligil, G.S. (2005). Inflammation, stress, and diabetes. *J Clin Invest* 115, 1111–1119.
- Wrann, C.D., Laue, T., Hübner, L., Kuhlmann, S., Jacobs, R., Goudeva, L., and Nave, H. (2012). Short-term and long-term leptin exposure differentially affect human natural killer cell immune functions. *Am J Physiol-Endoc M* 302, E108–E116.
- Wu, Q., Clark, M.S., and Palmiter, R.D. (2012a). Deciphering a neuronal circuit that mediates appetite. *Nature* 483, 594.
- Wu, Q., Whiddon, B.B., and Palmiter, R.D. (2012b). Ablation of neurons expressing agouti-related protein, but not melanin concentrating hormone, in leptin-deficient mice restores metabolic functions and fertility. *Proc National Acad Sci* 109, 3155–3160.
- Xia, G., Han, Y., Meng, F., He, Y., Srisai, D., Farias, M., Dang, M., Palmiter, R.D., Xu, Y., and Wu, Q. (2021). Reciprocal control of obesity and anxiety–depressive disorder via a GABA and serotonin neural circuit. *Mol Psychiatr* 1–17.
- Xiong, W., Yao, M., Zhou, R., Qu, Y., Yang, Y., Wang, Z., Song, N., Chen, H., and Qian, J. (2020). Oxytocin ameliorates ischemia/reperfusion-induced injury by inhibiting mast cell degranulation and inflammation in the rat heart. *Biomed Pharmacother* 128, 110358.

Yang, Y., Atasoy, D., Su, H.H., and Sternson, S.M. (2011). Hunger States Switch a Flip-Flop Memory Circuit via a Synaptic AMPK-Dependent Positive Feedback Loop. *Cell* 146, 992–1003.

Yokota, S., Oka, T., Tsumori, T., Nakamura, S., and Yasui, Y. (2007). Glutamatergic neurons in the Kölliker-Fuse nucleus project to the rostral ventral respiratory group and phrenic nucleus: A combined retrograde tracing and in situ hybridization study in the rat. *Neurosci Res* 59, 341–346.

Youm, Y.-H., Grant, R.W., McCabe, L.R., Albarado, D.C., Nguyen, K.Y., Ravussin, A., Pistell, P., Newman, S., Carter, R., Laque, A., et al. (2013). Canonical Nlrp3 Inflammasome Links Systemic Low-Grade Inflammation to Functional Decline in Aging. *Cell Metab* 18, 519–532.

Youm, Y.-H., Nguyen, K.Y., Grant, R.W., Goldberg, E.L., Bodogai, M., Kim, D., D'Agostino, D., Planavsky, N., Lupfer, C., Kanneganti, T.D., et al. (2015). The ketone metabolite  $\beta$ -hydroxybutyrate blocks NLRP3 inflammasome-mediated inflammatory disease. *Nat Med* 21, 263–269.

Yuan, H., and Silberstein, S.D. (2016). Vagus Nerve and Vagus Nerve Stimulation, a Comprehensive Review: Part I. Headache *J Head Face Pain* 56, 71–78.

Zhou, B., Yuan, Y., Shi, L., Hu, S., Wang, D., Yang, Y., Pan, Y., Kong, D., Shikov, A.N., Duez, P., et al. (2021). Creation of an Anti-Inflammatory, Leptin-Dependent Anti-Obesity Celastrol Mimic with Better Druggability. *Front Pharmacol* 12, 705252.